University of Montreal

First peopling of the Americas: Modelling of the palaeo-landscape and potential Upper Palaeolithic human migration routes

by

Catharina Igrejas Lopes Martins Costa

Anthropology Department

Faculty of Arts and Sciences

Thesis presented to the faculty of Graduate and Postdoctoral studies to receive the title of Master of Sciences in Anthropology

May 2023

University of Montreal

This dissertation titled

First peopling of the Americas: Modelling of the palaeo-landscape and potential Upper Palaeolithic human migration routes

Presented by

Catharina Igrejas Lopes Martins Costa

Was evaluated by members of the following jury

Katherine Cook

François Girard

Ariane Burke, Thesis Supervisor

Résumé

Le peuplement des Amériques fut le dernier grand événement migratoire de *Homo sapiens* et nous méconnaissons toujours les détails à son sujet. Des débats surgissent concernant l'environnement, les populations concernées, ainsi que les cultures impliquées. Malheureusement, des biais scientifiques persistent quant à la chronologie de cet événement et il peut donc être difficile de proposer quelque chose de nouveau. Avec ArcMap 10.7.1, nous présentons de nouveaux modèles de migrations terrestres basés sur les sentiers de moindre effort, retraçant les routes potentielles que les humains ont pu utiliser afin d'arriver en Amérique au cours du Pléistocène; nous surlignons les facteurs environnementaux, génétiques et archéologiques spécifiques qui doivent être considérés pour les modèles futurs, et nous présentons deux trajets de migration qui auraient pu avoir été utilisé pendant le Paléolithique Supérieur, élucidant par conséquent comment les humains sont arrivés pour la première fois dans le continent américain.

Mots-clés : Peuplement des Amériques ; Système d'Information Géographique; Sentier de Moindre Effort; Pléistocène

Abstract

The peopling of the Americas was the last great dispersal event of our species, *Homo sapiens*, and there is still so much we do not know about it. Debates arise concerning the environment, the populations involved, as well as the cultural or physical markers they might have left behind. Unfortunately, the debate concerning the First Peopling of North America is marked by scientific biases and it can thus be difficult to propose something new. Through ArcMap 10.7.1, we present a Least Cost model of terrestrial migrations from Asia to America, we highlight the specific environmental, genetic and archaeological factors that need to be considered in future models, and present two migration paths that could have been used during the Late Pleistocene, thus shedding light onto how humans first arrived in the American continent.

Key words: Peopling of the Americas; Geographical Information System; Pleistocene; Least cost path analysis

Ethical observation

Although the research presented here does not involve the physical analysis of human remains, nor did it involve the direct participation of any indigenous individual, genetic analyses of human remains uncovered in Siberia and Alaska are used, as well as ethnographic work done in collaboration with indigenous communities in Siberia and northern Canada. The author of this dissertation supports the inclusion of indigenous knowledge and the use of physical remains within archaeological research provided it is done ethically and with the consent of all those involved at all times.

Copyright permission was obtained for the figures presented in this research and copyright license numbers and receipts can be presented if need be.

Table of content

List of Figures and Tables

List of Abbreviations

LGM – Last Glacial Maximum

cal yr BP – calibrated years before present

PSHK Peninsula – Palaeo-Sakhalin-Hokkaido-Kuril Peninsula

EB – Eastern Beringia

CB – Central Beringia

WB – Western Beringia

BLB – Bering Land Bridge

ACC – Alaska Coastal Current

AMOC – Atlantic Meridional Overturning Current

MRCA – Most Recent Common Ancestor

mtDNA – mitochondrial DNA

aDNA – ancient DNA

GIS – Geographical Information Systems

LCP – Least Cost Path

Yana RHS – Yana Rhino Horn Site

YMAM – Yana Mass Accumulation of Mammoth

CHAR – Charcoal Accumulation Rates

PAH – Polycyclic Aromatic Hydrocarbons

Acknowledgments

Completing my Master's degree during the Covid pandemic was most definitely challenging and it is my pleasure to acknowledge and show my appreciation to those who have made this achievement possible. First and foremost, I would like to thank my thesis supervisor, Dr. Ariane Burke, without whom I would not have had the knowledge to conduct the ArcMap modelling presented in this thesis, as well as the guidance in the completion of this research project. In addition, I would like to thank the members of the reviewing committee, Katherine Cook, and François Girard.

I am grateful to have been a part of the Hominin Dispersal Research Group (HDRG) headed by Dr. Ariane Burke, whose members, including Benjamin Albouy, Samuel Seuru, Simon Paquin, Solène Boisard and Felix Marois have offered mental support as well as guidance when needed. In addition, I would not have been able to complete the models presented in this project had I not had access to the HDRG Laboratory.

I would like to acknowledge the University of Montreal's support in the form of a bursary (*Bourse de fin d'études de maîtrise des Études Supérieures et Postdoctorales*) in 2021.

Finally, I take this opportunity to show my appreciation and gratitude to my family who supported me through the last three years and my partner, Nicholas Staub, who kept me motivated, sane and grounded even in the most challenging times.

Introduction

The peopling of the Americas has been a very debated topic for the past few decades and has inspired research in a plethora of disciplines, such as (palaeo-)botany, genetics, climatology and archaeology, due to the multi-faceted aspects of human migrations. Through archaeology, it is possible to understand how humans populated northeastern North America, how they survived considerably harsher weather, and how these Upper Palaeolithic cultures spread, evolved and diverged during this process. In fact, the American continent was the last to be populated for it was only reached by *Homo sapiens* following their arrival in Northeastern Asia. Although the peopling of the Americas was a lengthy process that took place over several millennia, it is widely believed that the initial migration occurred during the Last Glacial Maximum (LGM; ca. 21.000-18.000 calibrated years before present [cal yr BP]), when global ice sheets reached maximum volume, covering most of the northern hemisphere (*cf. Chapter 3)*.

During the LGM, North America was divided in two by the merging of two ice sheets, the Cordilleran and Laurentide Ice Sheets. The former has been recorded as reaching as far south as Montana and Idaho in the United States, and as far north as the Alaskan Peninsula, whereas the latter covered most of Canada, Greenland and reaching the United States in some areas (e.g. Chicago and New York). At this time, the two ice sheets merged at the Great Divide, however parts of Alaska and the Yukon Territory remained ice-free, and it is this region that interests us here (*cf. Chapter 3*). Our research domain includes the geographical area named '*Beringia*', which used to extend as far west as the Verkhoyansk Mountain Range in Siberia and as far east as the Mackenzie River in the Yukon (Graf & Buvit 2017; Hoffecker et al. 2016; Jakobsson et al. 2017; Meyer et al. 2017). In addition, we expanded our research domain beyond Beringia to include part of Siberia (up to the Republic of Khakassia), Mongolia, China and Japan, in order to include data surrounding Lake Baikal in southern Siberia and a smaller geographical area known as the Paleo-Sakhalin-Hokkaido-Kuril (PSHK) Peninsula (*cf. Chapter 1*). The now-submerged landscape that connected Eastern Siberia (Western Beringia) to Alaska/Yukon (Eastern Beringia), will be referred to as 'Central Beringia' (Hoffecker et al. 1993; Hoffecker et al. 2020).

Until the beginning of this century, it was widely accepted that the Americas had been populated after the North American ice sheets had begun melting and a corridor between them had reopened, ca. 15.000-14.000 cal yr BP (Brubaker et al. 2005; Dalton et al. 2020; Grégoire et al. 2012; Hoffecker et al. 1993; Kennedy et al. 2010). The timing of this event coincides with the appearance of archaeological sites represented by the Clovis culture. Named after an archaeological site near Clovis, New Mexico, and identified by a specific toolset, the "Clovis (bifacial) projectile point", this culture was believed to have first appeared around 13.000 cal yr BP (Butkus 2004:172; Waters & Stafford Jr. 2007).

However, with the discovery of a few sites of greater age (*cf. Chapter V*), whether they were quickly accepted or rejected by the academic community, it was proposed that perhaps the peopling of the American continent could have taken place considerably earlier than the establishment of the Clovis people. Two important sites come to mind: Monte Verde in Chile, whose MVII occupation is widely accepted is dated ca. 14.500 cal yr BP, more than one thousand years older than the oldest Clovis site (Dillehay 1984; Dillehay et al. 2008; Dillehay et al. 2015; Meltzer 2009; Waters & Stafford Jr. 2007) and Bluefish Caves in Yukon, Canada, which is still viewed as controversial by some, has provided considerably older dates than Clovis (Bourgeon et al. 2017; Bourgeon 2018, *cf. Chapter II and V*). Sites such as these created a divide amongst American archaeologists, some of whom defended a "Clovis-First" peopling, whereas others proposed a "pre-Clovis" migration. The latter hypothesis has gained acceptance after palaeogenetic studies were published (e.g. Tamm et al. 2007 and Llamas et al. 2016; *cf. Chapter1*) presenting genetic evidence for the existence of a considerable time span since the arrival of people of northeastern Asian genetic ancestry in North and South America. These genetic data, which will be further discussed later on (*cf. Archaeological record*), led to the proposal of a new migration hypothesis, the "Beringian Standstill Hypothesis", which this research hopes to further advance.

Within this dissertation, we take a slightly different approach to the peopling of the Americas and the archaeological record. Using an extensive database created for this dissertation (*cf. Chapter 4 and* Supplementary Data 1-4) that affords a detailed and extensive understanding of the palaeo-environmental and archaeological record prior to and during the peopling of the Americas, we create a model of human dispersal across Beringia and into the New World. We aim to present possible relationships between known archaeological sites as well as shed light on the peopling of northeastern North America during the last Ice Age.

This thesis begins with a lengthy literary review (Chapter I), focusing on the palaeo-environmental record of the study region, before tackling the archaeological record, reviewing the different migration hypotheses related to the peopling of the Americas, and presenting the genetic and linguistic evidence. Chapter II reviews the use of modelling technologies and Geographical Information Systems (GIS) within the discipline and describes previous attempts at modelling the peopling of the Americas, Chapter III presents the materials and methods used to build our own model. We present our results in Chapter IV, followed by a discussion (Chapter V) that compares our results with previous research (presented in chapter II) and explores the implications of this research from within the archaeological and ethnographic discourse about human migration.

Chapter I – Literary Review

In order to gain a better understanding of the peopling of the Americas, and to properly comprehend the modelling that was done for this project, it is necessary to consider the geography and palaeoenvironmental context of the study region during the timeframe of interest (I.I), before tackling the archaeological record (I.II). The peopling of the Americas is the last great migration of our species, *Homo sapiens* (Pinotti et al. 2019). Expansion across Eurasia from Africa had occurred by 35.000 cal yr BP and the earliest evidence of human presence in the New World now dates to the Last Glacial Maximum (ca. 21.000 cal yr BP) (Bourgeon et al. 2017). Temporally speaking, therefore, we concentrate our research on the Late Pleistocene, more specifically the period ranging from 35.000 cal yr BP until 18.000 cal yr BP, a period which includes Marine Isotope Stages (MIS) 3 and 2, which includes the LGM (Hughes & Gibbard 2015; Spada & Galassi 2017; Weitzel et al. 2020).

I.I. Study region

One important factor in studying a migratory event of any scale is the geography. Understanding past landscapes and environments can be indicative of past peoples' behaviours such as movement. When it comes to the peopling of the Americas, four distinct geographical areas are centre-stage (Fig.1.1): Eastern Beringia (henceforth "EB"), which encompasses the state of Alaska in the United States of America and the Yukon Territories in Canada, west of the Mackenzie River; Central Beringia (henceforth "CB"), which can be summarized as the now-submerged Palaeolithic landscape in the Bering Strait; Western Beringia (henceforth "WB"), corresponds to Siberia east of the Verkhoyansk Mountain Range; and the Palaeo-Sakhalin-Hokkaido-Kuril ("PSHK") Peninsula, which represents the Palaeolithic peninsula encompassing the islands of the same names.

The first three geographical areas (WB, CB and EB) are more commonly known together as *Beringia*. However, due to their different present-day ecologies and archaeological record, we have decided to consider each area as separate entities yet making a whole. This project's geographical limits were extended past Beringia to include possible areas of refugia for the populations which eventually entered the Americas (*cf. I.II. Archaeological* Record). These areas consist of the PSHK Peninsula and the landscape surrounding Lake Baikal. In fact, the area surrounding the lake has been hypothesised as a possible location of genetic origin of the population that eventually reached the Americas (*cf.* palaeogenetic data in *Beringian Standstill Hypothesis*; Sikora et al. 2019; Willerslev & Meltzer 2020).

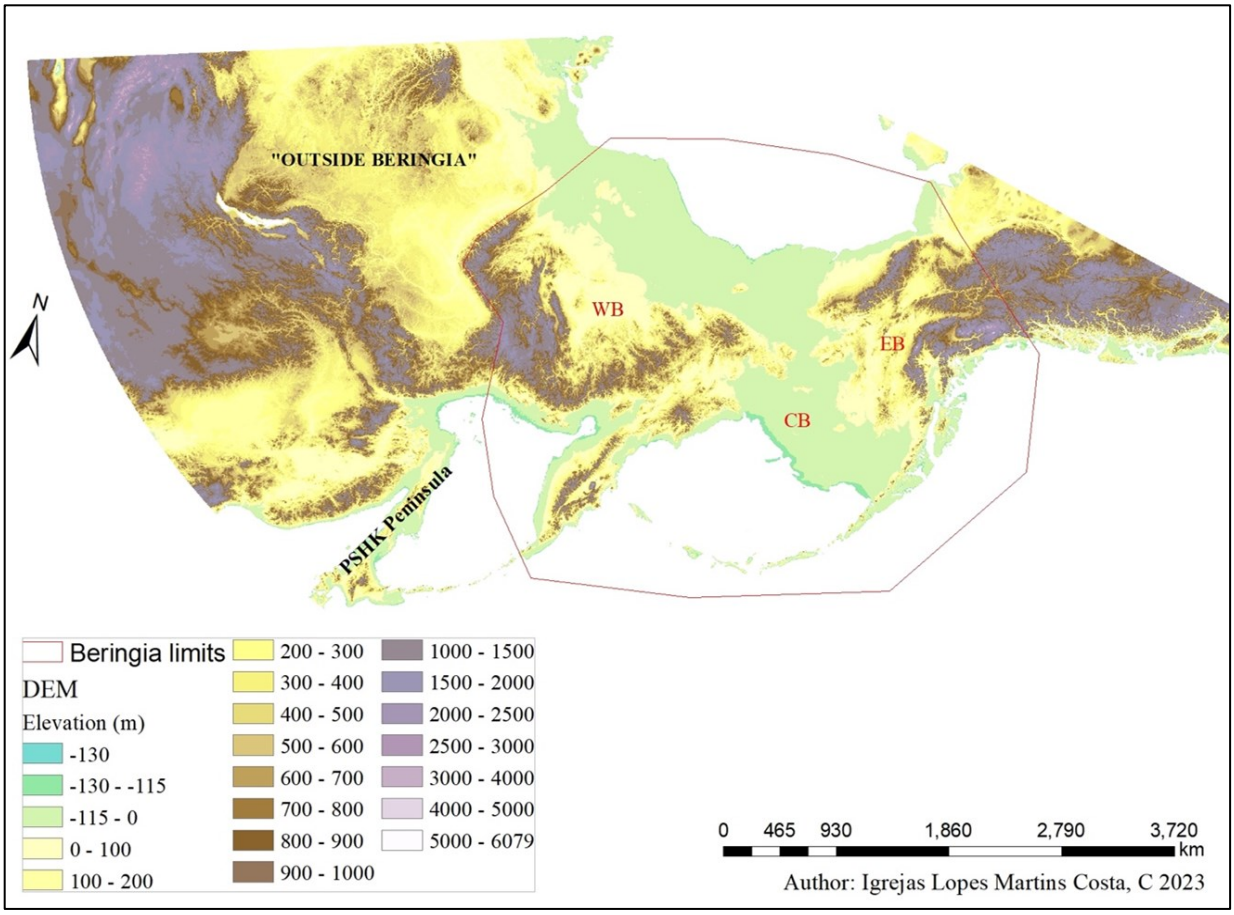

Figure 1.1 – Geographical extent of Beringia and adjacent regions pertinent to this research

I.I.I Ice sheets

During the Late Pleistocene, much of the Northern Hemisphere was covered by ice sheets. The development of ice sheets is not linear or uniform, it depends on multiple factors such as insolation, climate, changes in gravity and tectonic activity, as well as ocean circulation (Hu et al. 2010; Lambeck et al. 2002; Peltier 2004; Stabeno & Schumacher 1999). The formation of ice sheets is also a slow process, where each year, the winter's snow did not entirely melt due to moist winters and colder summers (Lambeck et al. 2002:200). In theory this process is fairly simple and understood, even though the initial creation of the ice sheets is still not yet fully comprehended. It is believed that the growth and movement of an ice sheet depend on topography as well as the location and extent of previous ice (Kleman et al. 2010). Once an extensive ice sheet is formed, it alters the landscape by creating depressions, tills, and striations in the bedrock, glacial lakes and basins, and by modifying ocean currents and circulation, consequently affecting global temperatures. These changes occur while the ice sheets are growing and expanding as well as when they begin to melt upon reaching their maximum extent (Borreggine et al. 2022; Hughes & Gibbard 2015; Kleman et al. 2010; Lambeck et al. 2002). The geographical modifications caused by the movements of the

ice sheets can be used to determine their position at a given time, although their temporality can be difficult to discern (Baranskaya et al. 2018; Bigg et al. 2008; Felzer 2001; Grosswald & Hughes 2002; Gualtieri et al. 2003). As a result, there is considerable debate as to the location and extent of the ice sheets in the study region during the LGM.

It has been hypothesized that an ice sheet in the East Siberian Sea could have joined the Barents-Kara ice sheet thus creating an extensive Arctic ice sheet (Fig. 1.2) (Felzer 2001; Grosswald & Hughes 2002). This hypothesis was first presented as an explanation for the milder temperatures recorded in the Bering Land Bridge ("BLB") during the LGM which allowed it to stay unglaciated. In this scenario the area would have been sheltered from cold Arctic winds, maintaining a warmer climate all year long; whereas the absence of an East Siberian Ice Sheet would have hypothetically reduced temperatures and suppressed vegetation:

> A 1 km thick ice sheet on the East Siberian Arctic Shelf has a significant impact on the local climate of Beringia. The presence of the East Siberian ice sheet actually warms eastern Siberia south of the ice sheet. A glacial anticyclone, characteristic of other large ice sheets in nearly all GCMs, forms over the East Siberian ice sheet during winter, causing subsidence and increased southerly advection with warming south of the ice sheet. During summer the ice sheet blocks northerly flow from the Arctic, also resulting in warming south of the ice sheet. The warmer temperatures with the ice sheet present are large enough to cause changes in the dominant vegetation that are inconsistent with existing LGM vegetation reconstructions. The milder climate with the ice sheet present favors more tundra, while with no ice sheet present, polar desert dominates (Felzer 2001:444)

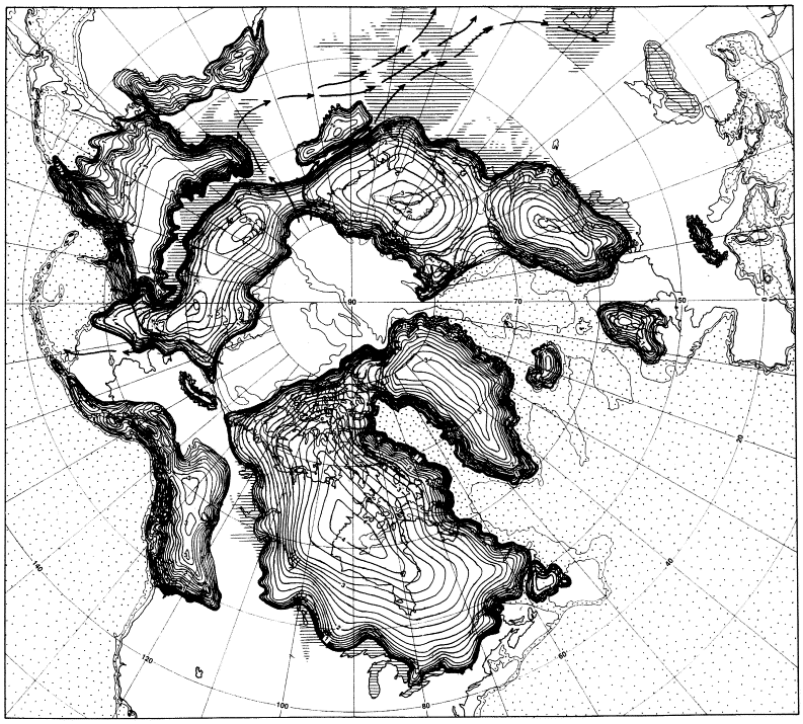

Figure 1.2 – Hypothesised extent of an Arctic ice sheet during the LGM under an 'extended' ice sheet model (Grosswald & Hughes 2002:140)

While some argue this reconstructed East Siberian ice sheet is localised solely in the East Siberian Sea, other researchers have extended it to include the Laptev and Okhotsk Seas, parts of modern-day mainland Northeastern Siberia, including the Kamchatka Peninsula, the Chukchi mountain ranges and the Yana Uplands and completely covering the East Siberian and Wrangel islands (Fig. 1.2; Bigg et al. 2008; Felzer 2001; Grosswald & Hughes 2002). In this scenario, the Bering Land Bridge (BLB, or Central Beringia [CB]) would have been completely isolated from the rest of Northeastern Asia and practically (if not completely) uninhabitable during the LGM due to a possible extension of the ice sheet on the Bering and/or Chukchi Seas, a hypothesis brought forth due to the presence of ridges in the Bering seafloor (Bigg et al. 2008; Felzer 2001; Grosswald & Hughes 2002). When calculating the ice sheet volume to determine past sea levels using a eustatic model, a 'missing ice' is proposed to account for discrepancies, an argument which could be used in favour of an extended East Siberian ice sheet (Simms et al. 2019).

Another hypothesis has been proposed whereby instead of an extended Arctic (Barents-Kara-Laptev-East Siberian-Beringian-Okhotsk) Ice Sheet (Fig. 1.2, above), a reduced ice sheet with fewer glaciated landscapes would have existed throughout Eastern Siberia and Beringia (Western and Eastern included); these would have been most likely centered around mountain chains and leaving Beringia largely unglaciated (Fig. 1.3, below) (Elias & Brigham-Grette 2013).

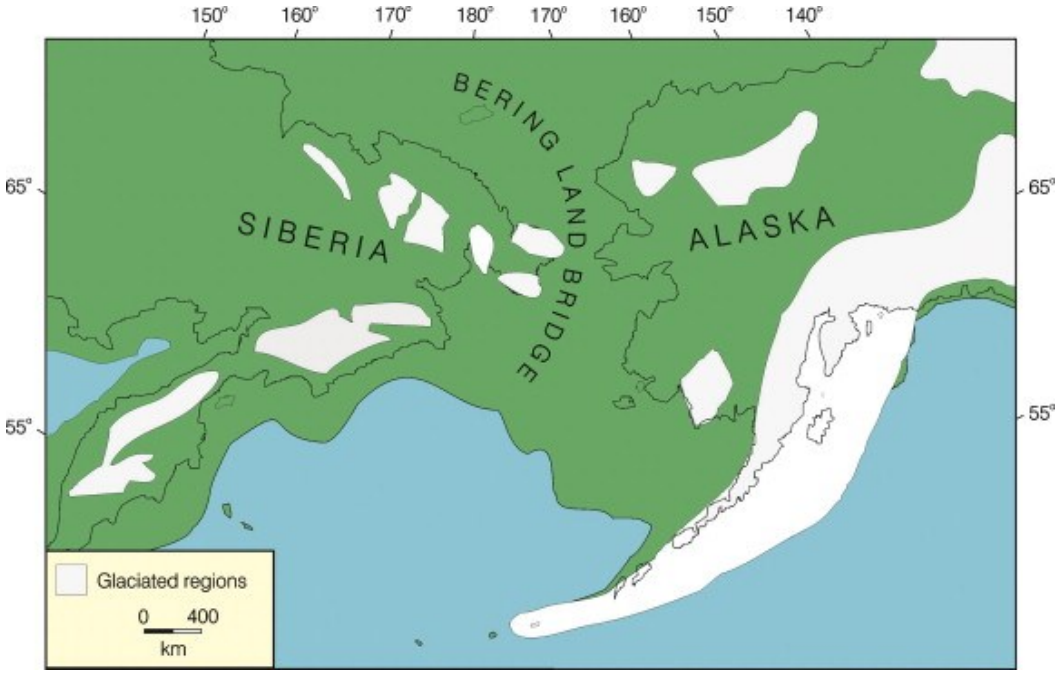

Figure 1.3 – Representation of the Beringian ice sheets during the LGM (Elias & Brigham-Grette 2013:1058)

Moraines and ridges have been presented as proof of the existence of an extended Arctic ice sheet (Fig. 1.4), where these geographical features would be representative of these ice sheets moving in the landscape (Grosswald 2001; Grosswald & Hughes 2002). This technique has been used to determine the extent of LGM glaciation in Kamchatka Peninsula (Fig. 1.5). However, some of these have been proven to be older than the LGM, such as those in the Laptev Sea, East Siberian and Wrangel Islands. In addition, dated *yedoma* (Pleistocene-dated permafrost layer) has been used to dispute the Arctic Ice Sheet model. This model does not negate the possibility of icebergs originating from the North American ice sheets circulating in the southern Bering Sea, however (Baranskaya et al. 2018; Bigg et al. 2008; Elias & Brigham-Grette 2013; Weitzel et al. 2020). In addition, Wrangel Island was unglaciated and is known to having been home to woolly mammoth populations during the Pleistocene (El Adli et al. 2017), therefore disproving the extended Arctic ice sheet. The modelling presented by Batchelor et al. (2019) supports a restricted glaciation of Beringia, even in their maximum scenarios.

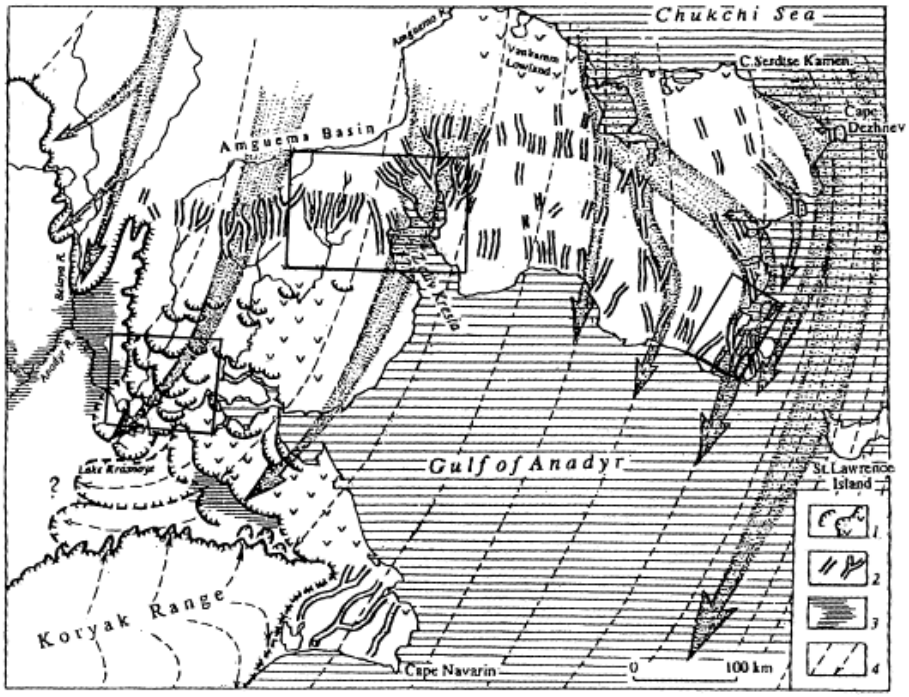

Figure 1.4 – Sketch of the location of ridges representative of a North-to-South glacial overflow across the Chukchi peninsula indicative of the presence of an ice sheet (Grosswald & Hughes 2002:134)

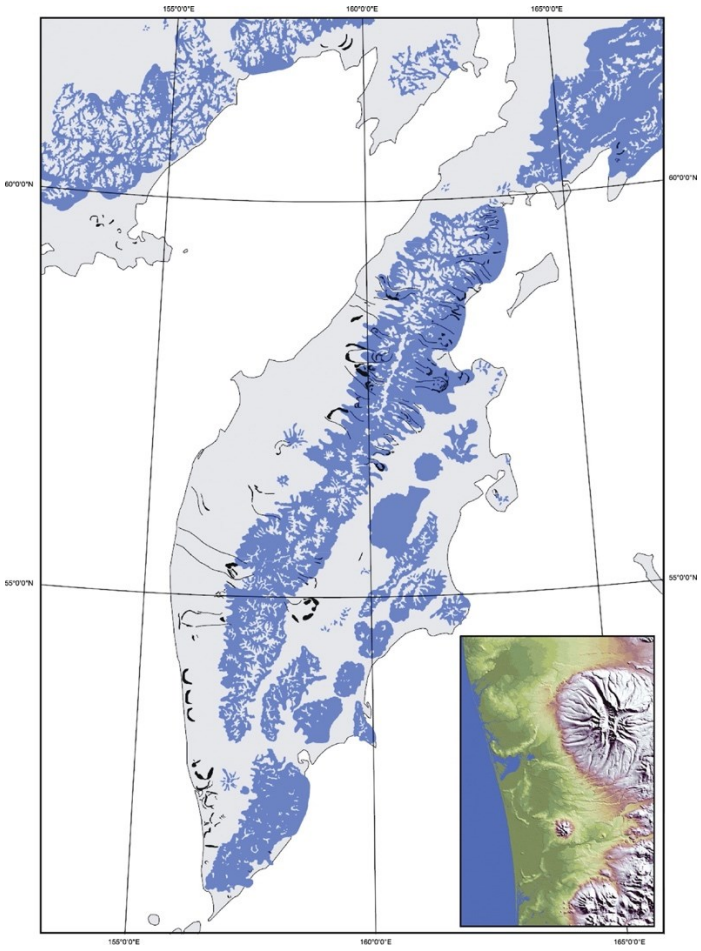

Figure 1.5 – LGM glaciation in the Kamchatka Peninsula (blue) as determined by moraines (black) (Bigg et al. 2008:565)

On the other side of the Bering Strait, the Cordilleran and Laurentide Ice Sheets (Fig. 1.6) covered most of modern-day Canada and northern United States during the LGM completely isolating Eastern Beringia from the rest of the American continent, creating the North American Ice Sheet Complex. This isolation lasted until at the earliest 14.000 cal yr BP when an opening between the two ice sheets was created (Brubaker et al. 2005; Dalton et al. 2020; Grégoire et al. 2012; Kennedy et al. 2010). (*cf: Vegetation and climate; Migration hypotheses* below).

Figure 1.6 – Reconstruction of the North American ice sheet complex at the end of the LGM (±18ka) (Dalton et al. 2020:8)

Eastern Beringia (Alaska and the Yukon Territory) remained unglaciated with multiple glacial drainage systems (e.g., Kuskokwim) marked by glacial lakes (e.g., Old Crow) during the last glaciation (Elias 2000; Kennedy et al. 2010; Reuther et al. 2019; Zazula et al. 2006). A continental climate existed in Eastern Beringia during this timeframe (Elias 2001; Zazula et al. 2006). In some areas, such as the Arctic and Atlantic North American coasts, the timing of the regression of the ice sheets is as of yet unknown (undated). In EB, it has been established that during MIS3 (stadial) and MIS2 (LGM), the southern coast of Alaska was glaciated, impeding a coastal human migration during the LGM until approximately 19.000-18.000 yr BP, while its western coast appears to have been unglaciated (Dobson et al. 2021; Fladmark 1990; Yesner et al. 2019).

Certain lakes in Western Beringia were present and unglaciated during MIS3 and LGM, therefore offering key information about the landscape. Data gathered from lakes such as Lake El'gygytgyn in Northern Chukotka inform us on an unglaciated Chukotka, and although a small area at the northern basin of Lake Baikal appeared to have been glaciated at times, it remained mostly unglaciated (Forman et al. 2007; Horiuchi et al. 2000).

I.I.II. Sea levels

In order for there to be a terrestrial migration originating in Northeastern Asia and reaching the American continent, there needs to be a physical conduit connecting the two. The present depth of the Bering Strait is approximately 50m at its shallowest and 3.500m in the deepest basin (Hu et al. 2010; Pelto et al. 2018; Stabeno & Schumacher 1999); however, during the LGM, sea levels were between 125 and 135 meters (m) lower than present-day (Ager & Phillips 2008; Batchelor et al. 2019; Clark et al. 2014; Grosswald & Hughes 2002; Hughes & Gibbard 2014; Lambeck et al. 2002; Manley 2002; Peltier 2004; Pelto et al. 2018; Rogers & Anitchtchenko 2014; Royer & Finney 2020; Simms et al. 2019, Tarasov et al. 2021). Therefore, sea levels do not need to be reduced more than 50 meters for the Chukchi and Seward Peninsulas to be connected, through a land-bridge (i.e., the Bering Land Bridge [BLB], or for the purpose of this research, Central Beringia [CB]) reuniting Western and Eastern Beringia (Fig. 1.7).

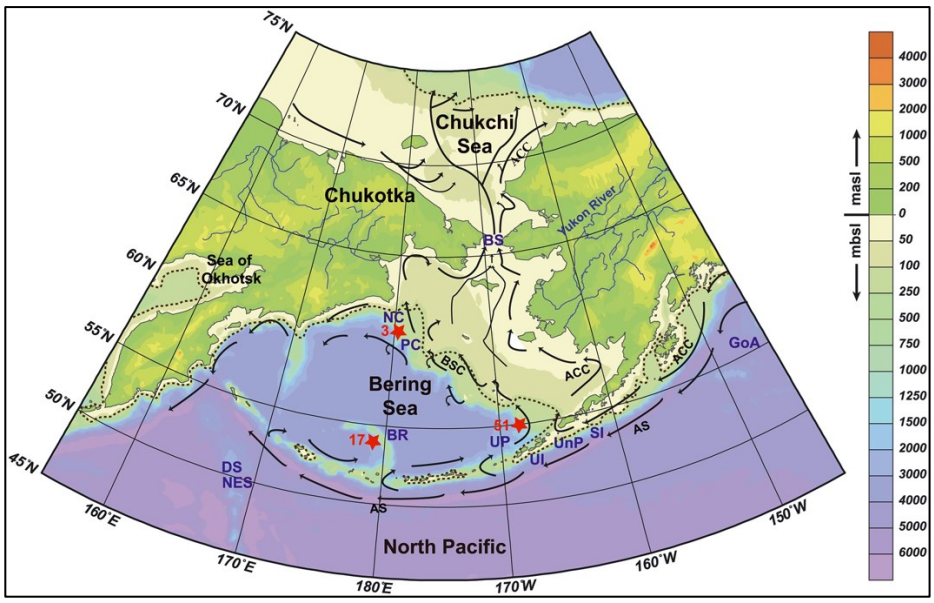

Figure 1.7 – Bathymetric and topographic map of Beringia (ACC – Alaska Coastal Current; AS – Alaskan Stream; BSC – Bering Slope Current) (Pelto et al. 2018:94)

The BLB, which can also be interpreted as an *aquaterra*, is difficult to study as it is today submerged and conducting underwater archaeological research in arctic and sub-arctic waters is complicated (Dixon & Monteleone 2014; Hoffecker et al. 2016; Rogers & Anitchtchenko 2014). Central Beringia, therefore, remains fairly unstudied. What we do know, however, is that whenever sea levels dropped 50m below present-day sea levels (Harris 2019), the BLB appears. The exposure of the BLB affects three processes: terrestrial migration of flora and fauna between Northeastern Asia and Northwestern North America (*cf: vegetation and climate*, below); aquatic migration of fauna (aquatic mammals); and ocean circulation.

During our timeframe (35.000-18.000 cal yr BP), the lowest sea levels reached in the present-day Bering Strait lie between -120 and -135m during the LGM (Ager & Phillips 2008; Batchelor et al. 2019; Clark et al. 2014; Grosswald & Hughes 2002; Hughes & Gibbard 2014; Lambeck et al. 2002; Manley 2002; Peltier 2004; Pelto et al. 2018; Rogers & Anitchtchenko 2014; Royer & Finney 2020; Simms et al. 2019, Tarasov et al. 2021). Although it is believed the BLB may have first appeared around 80.000 yr BP (Harris 2019:24; Hu et al. 2012), and again as early as 45.000 yr BP, it reached its maximum extent during the LGM (Hughes & Gibbard 2014; Vershinina et al. 2021).

The moment the BLB was completely inundated by Pacific waters entering the Chukchi Sea (Woodgate 2013) is still debated. It is believed the inundation occurred in stages as sea levels slowly started to rise. Manley (2002)[1]'s simulation of the flooding of the BLB is perhaps the simplest representation of this gradual geographical modification, showing a rapid rise between 15.000 and 14.000 cal yr BP, with the first inundations causing what appears to be 'gaps' or lakes in the landscape, occurring around 12.000 cal yr BP as sea levels rose before total submergence between 11.000 and 10.000 cal yr BP (Elias et al. 1997; Farmer et al. 2021; Harris 2019; Jakobsson et al. 2017; Pico et al. 2020; Ponkratova et al. 2021; Spada & Galassi 20017; Vershinina et al. 2021), and not around 13.000 yr BP as it had previously been argued (Clark et al. 2014). A hypothesis has been put forth suggesting a "double opening" of the BLB at 13.000 and 11.000 cal BP with stable sea levels between the two dates (Liu et al. 2015 *apud* Pico et al. 2020:2)

The determination of past sea levels is primarily based on estimates of the volume and extent of the ice sheets and thus, the volume of water in the oceans. There are two methods used to model past sea levels: the global eustatic model, also colloquially called the 'bathtub model' and the 'glacial isostatic adjustment (GIA) model'. The former method considers the growing volume of ice sheets to be inversely proportional to the lowering of sea levels (Batchelor et al. 2019; Borregine et al. 2022; Clark et al. 2014; Grosswald & Hughes 2022; Hu et al. 2010; Jakobsson et al. 2017; Lambeck et al. 2002; Peltier 2004). Modelling paleo-shorelines using this method simply requires a bathymetric map. GIA models, on the other hand, consider "sea surface variation, and the vertical displacement of the solid Earth" (Spada & Melini 2019:5058), creating a model considering the planet's ellipsoid surface (Baranskaya et al. 2018; Borregine et al. 2022; Clark et al. 2014; Dobson et al. 2020; Simms et al. 2019; Spada & Galassi 2017; Spada & Melini 2019; Zong 2015).

Creating a model of sea levels and ice sheets evolution through time requires two kinds of data, accurate representation of global ice sheets as well as a detailed representation of the Earth's viscoelasticity (Clark et al. 2014), which is physically illustrated through geographical formations like raised beaches,

[1] http://instaar.colorado.edu/groups/QGISL/bering_land_bridge/

marine terraces, basins, and marshes (Baranskaya et al. 2018). Discrepancies have been observed between the proposed sea level models (Simms et al. 2019) and the physical evidence in the study region (Baranskaya et al. 2018). It has been proposed that an extra ice sheet existed in Eastern Siberia/Central Beringia could explain this discrepancy (*cf: ice sheets*, above) through a "missing ice" explanation used in a global eustatic model, affecting sea level calculations (Grosswald & Hughes 2002:141-142; Simms et al. 2019; Spada & Galassi 2017; Zong 2015).

Focusing on the Bering Sea, the emergence of the BLB affected sea currents. In a very summarized explanation, the closure of the Bering Strait prevented the Alaska Coastal Current (ACC) from crossing the Bering Strait (Fig. 1.7, above), which consequently caused the Atlantic Meridional Overturning Circulation (AMOC) hysteresis and the activation of a Pacific Meridional Overturning Circulation (PMOC) (Daniels et al. 2021; Hu et al. 2010; Hu et al. 2012; Jakobsson et al. 2017; Meyer et al. 2016; Pico et al. 2020; Rae et al. 2020; Stabeno et al. 1999; Takahashi 2005).

The Bering Sea shelf is broad and shallow and the development of a continental climate with the appearance of the BLB during the last Ice Age allowed for near-modern temperatures to be established in the area. As sea levels rose following the LGM, more maritime climates developed throughout Beringia. This sea level rise is directly linked to the deglaciation of ice sheets, which began after the LGM around 18.000 cal yr BP (Elias et al. 1992; Daniels et al. 2021; Harris 2019; Meyer et al. 2017; Pelto et al. 2018). Although understanding the intricacies of Beringian sea-levels and ice sheets prior to and during the LGM is important to properly understand the peopling of the Americas, it is equally important to consider how they affected the vegetation and climate, which play a role in the viability of the BLB for human habitation.

I.I.III. Pleistocene vegetation and climate

Different ice sheet models have been proposed for the Beringian landscape (as mentioned above), which influence reconstructions of the vegetation and climate. In what follows, Beringian vegetation and palaeoenvironmental records are presented.

In Eastern Beringia, palynological records are often recovered from lake sediments. Sediments such as those found in northern Yukon have produced sedimentological records that reach as far back as approximately 30.000 yr BP. A 'Basal Herb Zone' covering the late MIS 3 and MIS2 periods, with a high percentage of *Artemisia*, Gramineae and Cyperaceae is indicative of a landscape containing mostly non-arboreal plants mixed with few trees and shrubs, creating a discontinuous landscape of herbaceous tundra in higher altitudes with a higher proportion of sedge-grass in lower altitudes (Cwynar & Ritchie 1980; Cwynar 1982). *Artemisia*, Gramineae and Cyperaceae are xerophyte and/or halophyte herbs, indicating

cold and/or salty environments with deep seasonal thawing (Cwynar & Ritchie 1980; Vershinina et al. 2021; Young 1982; Zazula et al. 2003; Zazula et al. 2006). *Artemisia* is found in drier and wind-sheltered steppe, tundra and loess-steppe vegetation which constitutes part of the diet of saiga antelopes (*Saiga tatarica*), woolly rhinoceros (*Coelodonta antiquitatis*), bison (*Bison* priscus) and horse (*Equus* sp.), which make up part of the megafauna found in Beringia during MIS 3 and MIS 2 (Vereshchagin & Baryshnikov 1982; Young 1982).

The pollen data suggest the existence of a 'tundra-steppe' ecosystem which could be described as "(…) a cold, dry grassland containing abundant elements that now grow in [a] tundra zone" (Hibbert 1982:155). However, paleontological studies have presented a much more diverse picture of a herb-dominated landscape which was attractive to grazing mammals and consequently to humans. This creates a 'Productivity Paradox' whereby various paleoenvironmental indicators do not provide the same indicators of habitat suitability (Yurtsev 2001). Guthrie interpreted the data as proof of the existence of what he named the 'Mammoth-Steppe', described as a mosaic of arid grassland with a mixture of herbs, with sparse trees and shrubs, associated with colder temperatures and limited snow depth (Elias 1997; Guthrie 1990). This ecosystem has no modern parallels and explains the presence of woolly mammoth (*Mammuthus primigenius*), bison (*Bison priscus*), horse (*Equus* sp.), caribou (*Rangifer tarandus*), saiga (*Saiga tatarica*) in Beringian glacial landscapes, therefore making Beringia resource-rich (Elias 1997; Felzer 2001; Gaglioti et al. 2011; Guthrie 1982; Guthrie 1990; Hughes & Gibbard 2014; ; Lozhkin & Anderson 2016; Rabassa & Ponce 2013; Yesner et al. 2019; Yurtsev 2001; Zazula et al. 2003; Zazula et al. 2006).

Furthermore, palaeoentomological data suggest that around 31.000 and 29.000 yr BP, northern and western Alaska appears to have harbored similar climates to present-day, yet with milder maximum temperatures. However, average winters in Alaska at the end of MIS 3 would have been colder than present. The same can be said during the LGM. According to beetle data gathered, trees were sparse, while tundra grasslands and moss were common (Elias 2000; Elias 2001). Furthermore, seed macrofossils recovered from arctic ground squirrel caches defend the palynological data summarized previously and is indicative of a mostly graminoid vegetation, with wetter, drier and colder temperatures (Gaglioti et al. 2011; Hughes & Gibbard 2014; Zazula et al. 2006).

Central Beringia (CB), which constitutes the now-submerged part Beringia, is at the centre of questions concerning the viability of the BLB for the peopling of the Americas. Reconstructing the vegetation of the region is difficult, however. Data recovered from sediment cores in the Chukchi Sea indicate a cold coastal environment, as evidenced by the insects and ostracods recovered, as well as pollen indicating a mesic and graminoid tundra. No definitive evidence of a steppe or grassland ecosystem were recovered from the Chukchi Sea Shelf (Elias et al. 1992; Elias et al. 1997; Zazula et al. 2003). Palynological

data from a lake core in the Seward Peninsula (Zagoskin Lake, St. Michael Island) suggest an arid, cold climate with graminoid-tundra as well as a willow-tundra, which correlates with the EB data. In fact, the environment surrounding Zagoskin Lake (Fig. 1.8, n°5) appears to have contained poplar trees (*Populus*) which is indicative of a possible forested refugia (Ager & Phillips 2008; Brubaker et al. 2005). Further south in the modern-day Bering Sea, on Pribilof Island (Fig. 1.8, bottom of image), evidence of a graminoid-focused vegetation of southern Central Beringia has also been found (Ager & Phillips 2008).

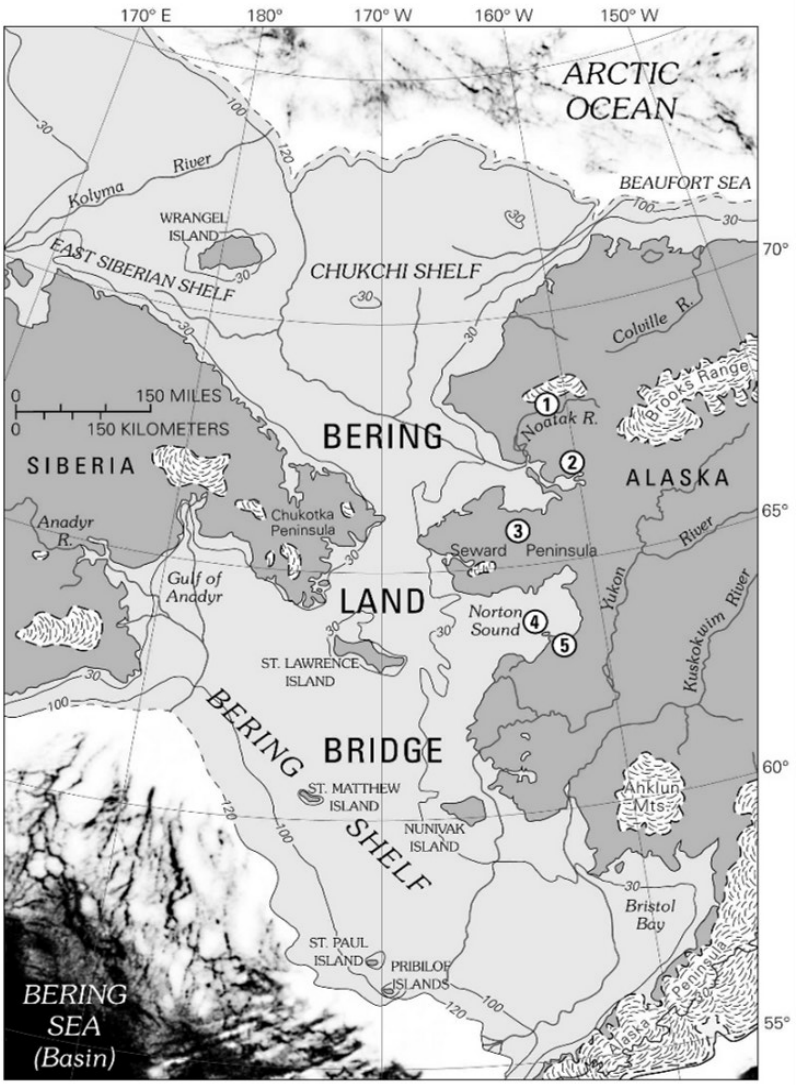

Figure 1.8 – Map of Beringia with a reconstructed LGM coastline indicating present-day islands and lakes (numbered: 1 – Kaiyak Lake, 2 – Squirrel Lake, 3 – Imuruk Lake, 4 – Core 79-121 (Norton Sound), and 5 – Zagoskin Lake (St. Michael Island)) (Ager & Phillips 2008:452)

In Western Beringia, the Kamchatka Peninsula yields evidence of both maritime and continental climates during the LGM, as suggested by the presence of *Larix* and Cyperaceae pollen in the palaeoenvironmental record. The former is found near water bodies in forest-tundra or taiga ecosystems, while the latter is more representative of herbaceous ecosystems, both data sets suggest temperatures similar to modern-day (Ponkratova et al. 2021; Weitzel et al. 2020).

In the Taimyr lowlands there is evidence for a shrub birch ecosystem, indicating higher levels of moisture, even though the lack of *Pinus* and *Alnus* pollen are representative of colder climates in the Upper Kolyma. The presence of ice wedges in the landscape could support either reconstruction. In addition, the presence of Cyperaceae, grass and herb pollens in several Western Beringian sites indicate a mixture of open, forested and herbaceous ecosystems, with overall dryer, and colder winter temperatures. The presence of these forested pollens could also indicate a forested refugia in Western Beringia (Brubaker et al. 2005; Clark et al. 2014; Hughes & Gibbard 2014; Lozhkin & Anderson 2016; Weitzel et al. 2020).

Sediment recovered from a gravity core extracted from the Academician Ridge in Lake Baikal contains grasses, shrubs and coniferous pollen, while lacking arboreal pollen during MIS2. Further southeast, pollen cores from Lake Kotokel (52.78°N, 108.12°E; 458m a.s.l.) indicates an open landscape with scattered trees and steppe and tundra herbaceous pollen during MIS 3, whereas a higher percentage of sedges and grasses – as opposed to boreal trees and shrubs – is visible during MIS2. East of the Verkhoyansk Mountain Range, at Lake Billyakh (65.28°N, 126.78°E; 340m a.s.l.) the environment evolved from cryophytic steppe to herbaceous tundra from MIS3 to MIS2. A similar, yet delayed evolution also took place near El'gygytgyn Lake (67.50°N, 172.00°E; 492m a.s.l.). Furthermore, on Sakhalin Island, traces of a forested landscape are visible in the palaeoenvironmental record, creating a sharp contrast with northern Beringia. This forested ecosystem is also visible in the Tanon quarry (59°40'N, 151°12'E; 40m a.s.l.) which documents a mixture of herbaceous and forested ecosystems during MIS3 dominated by Cyperaceae and Artemisia , representative of an herbaceous tundra (or tundra-like) ecosystem and xeric climates, as well as by *larix* pollen representative of forested ecosystems. The herbaceous pollen in the Tanon quarry continues into MIS2 (Hoffecker & Elias 2003; Hopkins et al. 1982; Horiuchi et al. 2000; Lozhkin et al. 2019; Tarasov et al. 2021). In summary, the vegetation of Western Beringia during the LGM was mostly tundra-like, where some indications of tree cover in certain locations (e.g., Sakhalin island and Tanon quarry), while in Eastern Beringia tundra vegetation appeared to have been more evenly spread out in the landscape (Rabassa & Ponce 2013:97-98).

I.II. Dispersal hypotheses

The study of the peopling of the Americas is intrinsically entangled with both the environmental and archaeological record. The paleoenvironmental record presents a detailed image of a landscape marked by the presence of some ice sheets, low sea level (from 125 to 135 meters below present-day levels) and a mixed tundra vegetation that sustained diverse fauna during the LGM. These factors are indicative of a resource-rich environment which would have been favourable to a human presence in Beringia.Palaeogenetic and paleontological evidence suggests that a wave of human dispersal originating from Central Asia reached Western Beringia by 35,000 BP and eventually crossed to Eastern Beringia. In the following, we shall review the main migration hypotheses which have attempted to answer the question of how and when humans first arrived in the Americas, as well as a quick introduction to the palaeogenetic data. At the centre of the theoretical framework of this research is a specific migration hypothesis, the *Beringian Standstill Hypothesis*, which stipulates that the source population for the first peopling of the Americas would have been genetically isolated before their entrance into North America; this process would have occurred over multiple generations.

Four conditions must be met in order for a possible migratory path to be seen as viable (Potter et al. 2017): (1) there must not be obstacles present that would have made its crossing difficult, if not impossible; (2) there must be vegetation present able to sustain human populations and the prey populations on which they depended; (3) food and fuel sources must be available; and (4) the human populations using these paths must have had the technological knowledge to surpass the obstacles and/or to extract available resources (vegetation, fauna and fuel). All of these conditions are intrinsically connected to one another and are required to ensure human survival.

I.II.I. The Ice-Free Corridor Hypothesis and the Clovis First Model

Since first being proposed in 1933 (Johnston 1933), the Ice-Free Corridor Hypothesis has gone through multiple changes as more research has been conducted to verify the chronology of deglaciation as well as the environmental viability of the land exposed between the Cordilleran and Laurentide Ice Sheets. This hypothesis proposes that the first humans to reach North America would have crossed a corridor along the Mackenzie watershed, east of the Rocky Mountain Range following their crossing of the BLB (Fig. 1.6, the dotted lines) before reaching the modern-day United States of America (Montana) (Heintzman et al. 2016; Johnston 1933; Potter et al. 2017; White et al. 1985).

As the North American ice sheets separated following the Last Glacial Maximum, a corridor would

have formed. As time passed, and the deglaciation continued, what was at first a bottleneck turned into a biogeographical corridor connecting modern-day Yukon Territory to Montana. Once a path was formed, the retreat of the ice sheets caused the appearance of proglacial lakes, i.e., lakes formed by the damming of melting glacial water by moraines. These lakes are still present nowadays, although their size has changed. In order to assess the timing and evolution of the ice sheets, the coring of these lakes is done to date vertebrates and/or flora located in the lake sediments using radiocarbon dating. The resulting dates indicate the presence of an established vegetation, which provides a minimum age for deglaciation (Dalton et al. 2020; Pedersen et al. 2016; Potter et al. 2017). Potter et al. (2017) propose an initial opening around ~14.868 cal yr BP, while Pedersen et al. (2016) propose a more complex scenario where the first opening of the corridor would have taken place around 15.000 cal yr BP but that it would be entirely open around 13.800±05 cal yr BP based on evidence that the 'British Columbia site', where grasses and sedges (indicative of steppe vegetation) only appear around ~12.000 cal yr BP (Clark et al. 2022; Pedersen et al. 2016).

The exact evolution of the deglaciation of the ice sheets and of the creation of the corridor is still debated. The most agreed upon theory is that the corridor was entirely glaciated during the LGM and that the separation of the ice sheets (and thus the expansion of the corridor) occurred subsequently either in a south-to-north (Pedersen et al. 2016; Wilson 1996) or north-to-south movement (Clark et al. 2022; Potter et al. 2017). The establishment of vegetation in the corridor is important because it informs us of when it became viable for sustaining animal and human life, and of thus a maximum age of usage by human populations to reach the rest of the continents south of the ice sheets. While some argue for a quick floral expansion (<100 years), it could take "a few hundred years" for a herbaceous tundra to be establish and probably "thousand years" for a forest to appear in the Ice-Free Corridor (Potter et al. 2017:45).

The 'Clovis First Model' is associated here to the Ice-Free Corridor Hypothesis because it was believed that the first human populations to use the corridor established the Clovis techno-culture (Becerra-Valdivia & Higham 2020; White et al. 1985). The Clovis complex is the oldest archaeological technological culture discovered in North America; it is technologically identifiable by its distinctive projectile points (Collard et al. 2010; Waters & Stafford Jr. 2007). Discovered in the 1930s, at an archaeological site located between modern-day city of Clovis and a stream channel called Blackwater Draw in the United States, Blackwater Locality 1 (Fig. 1.9, n□19), is the Clovis 'type-site'. It contained a new lithic toolset, different from previously established cultures in Eastern Asia, including fluted projectile points within a flake and blade core toolkit. This "Clovis" technology quickly spread throughout present-day United States of America into northern Mexico (Fig. 1.9; Boldurian 2008; Haynes 1995; Hoffecker et al. 1993; Jennings & Smallwood 2019; Waters & Stafford Jr. 2007).

The fact that multiple sites throughout the American continent (south of the icesheets) contained the same techno-culture was the basis of a hypothesis that portrayed the Clovis people as a mobile population that colonized an 'empty' continent in a relatively short time – perhaps in hundreds of years. Small variations within the toolkit of these sites are thought to represent local adaptations to new environments and/or cultural drift. The Clovis people are still considered as the first American population with a specific and elaborate toolkit. Three types of settlements can be attributed to the Clovis culture: camp sites – of medium and large sizes -, kill sites usually associated with megafaunal remains-, and caches. In addition, it is believed that Clovis hunter-gatherers had a seasonal mobility pattern and targeted megafauna, thus portraying them as 'big game hunters'. In fact, the recurring presence of megafaunal remains in Clovis kill sites led to the development of the hypothesis that Clovis populations were behind the extinction of American megafauna, more specifically of Proboscideans. Two chronologies are proposed for the Clovis complex: a short chronology of 12.940-12.680 cal yr BP (11.050-10.800 ^{14}C yr BP) and a longer chronology of 13.400- 12.680 cal yr BP (11.600-10.800 ^{14}C yr BP) (Becerra-Valdivia & Higham 2020; Haynes Jr. 1992; Jennings & Smallwood 2019; Miller et al. 2014; Potter et al. 2017; Waters & Stafford Jr. 2017).

Figure 1.9 – Location of Clovis and pre-Clovis sites (1 – Lange-Ferguson; 2 – Sloth Hole; 3 – Anzick; 4 – Dent; 5 – Paleo Crossing; 6 – Domebo; 7 – Lehner; 8 – Shawnee-Minisink; 9 – Murray Springs; 10 – Colby; 11 – Jake Bluff; 12 – East Wenatchee; 13 – Indian Creek; 14 – Lubbock Lake; 15 – Bonneville Estates; 16 – Kanorado; 17 – Arlington Springs; 18 – Sheriden Cave; 19 – Blackwater Draw; 20 – Cactus Hill; 21 – Wally's Beach; 22 – Union Pacific; 23 – Aubrey; 24 – Sheaman; 25 – Mill Iron; 26 – Hell Gap; 27 – Cerro Tres Tetas, Argentina; 28 – Cuevas Casa del Minero, Argentina; 29 – Piedra Museo, Argentina; 30. Fell's Cave, Chile; 31 – Monte Verde, Chile; 32 – Nenana Complex sites, Alaska; 33 – Broken Mammoth, Alaska)(Waters & Stafford Jr. 2007:1123 with permission)

The establishment of Clovis as the oldest culture in the American continent was however short-lived: the discovery of new archaeological sites containing older dates than Clovis, labelled as 'Pre-Clovis', have led to a search for new migration hypotheses. In the late 20th century, Monte Verde II, in southern Chile was discovered and excavated by Tom Dillehay (Fig. 1.9, n□31). The site surprised the archaeological community due to its exceptional preservation of organic materials indicative of the human diet (berries, algae, fish), settlement (hut floors, timbers), archaeological artefacts (wood, ivory, bone and lithics), as well as human faecal remains. This site is dated to approximately 14.500 cal yr BP (12.310±40 ^{14}C yr BP), with a possible earlier occupation estimated at a maximum age of ~18.000 cal yr BP (Becerra-Valdivia & Higham 2020; Dillehay 1984; Dillehay et al. 2008; Dillehay et al. 2015; Meltzer 2009; Politis & Prates 2019; Waters & Stafford Jr. 2007). This means that Monte Verde's occupation is either contemporary with Blackwater Locality 1 (the Clovis type-site; Fig. 1.9, n□19), which in itself hints at an earlier migration given the distance that separates the two sites, or much older. Monte Verde II therefore became the model site for the 'Pre-Clovis Model', which suggests that early humans arrived in the Americas prior to 13.000 cal yr BP.

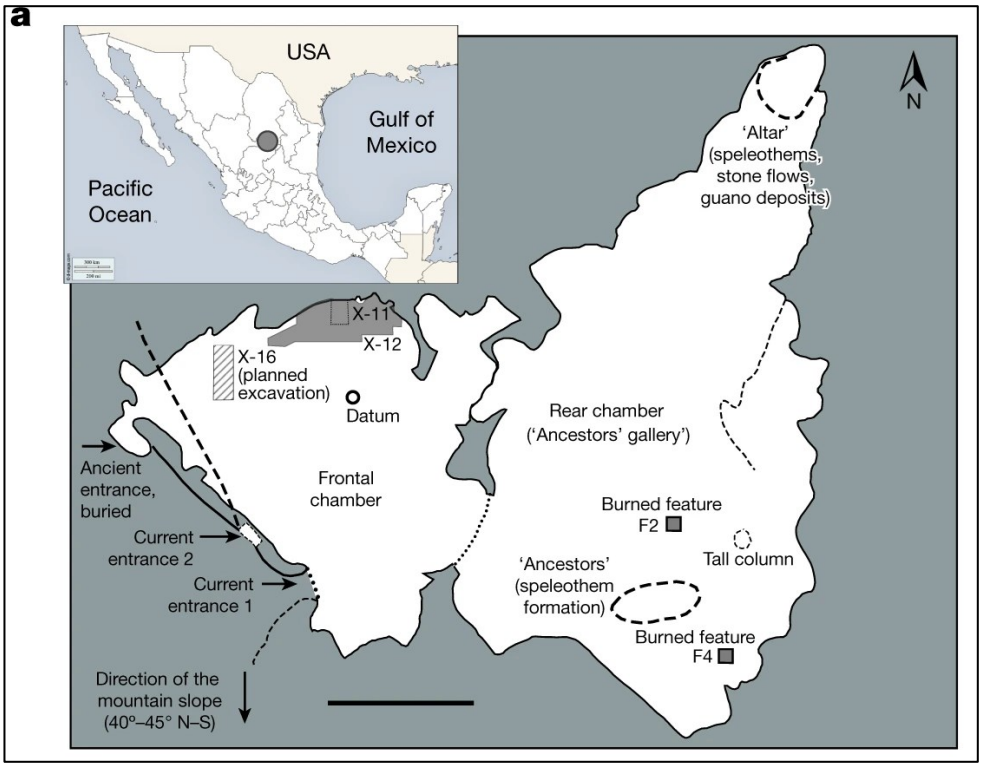

Figure 1.10 – Location of Chiquihuite Cave, Mexico (Ardelean et al. 2020:88, Figure 1a)

Other sites such as Meadowcroft Rockshelter, Gault and Cactus Hill (Becerra-Valdivia & Higham 2020), for example, have produced similar pre-Clovis ages. More significantly, however, sites dating to the LGM or earlier have recently been uncovered, two of which have been at the centre of debates within the scientific community. The first, Chiquihuite Cave, located in Zacatecas, Mexico (Fig. 1.10), has reported a pre-LGM age of 33.150-31.405 cal yr BP (Ardelean et al. 2020; Ardelean et al. 2022). The site appears to have been abandoned during the LGM and re-occupied shortly afterwards at 16.000 cal yr BP. The stone tools (Fig. 1.11) located at the site are mostly represented by debitage debris, flakes, points and some blades, with no evidence of stratigraphic displacementor of contamination, including a bifacial lanceolate preform from stratum 1223 which is dated to 27.929±82 ^{14}C yr BP. When calibrating using the IntCal 20 calibration curve, this provides an age of 30.124-29.651 (~29.887) cal yr BP. This artefact is important because it shows undeniable proof of human agency in the site and has been dubbed "the most ancient bifacial piece reported to date in the Americas" (Boëda et al. 2021:3). In addition to a wide array of radiocarbon ages, environmental DNA analyses show that the area surrounding the cave would have supported human populations. The inhabitants of this site have been proposed to represent a 'ghost' – or 'archaeologically invisible' – ancestral population unrelated to present-day Native Americans (Ardelean et al. 2020; Ardelean et al. 2022; Becerra-Valdivia & Higham 2020; Boëda et al. 2020). Some researchers reject the claim that Chiquihuite could be the oldest archaeological site in the Americas by claiming the artefacts are geofacts on the basis of published information. For example, Chatters and colleagues (2022:11-12) state that:

> Given the data presented by Ardelean et al. (2020), we do not agree with their interpretations that Chiquihuite Cave represents either a never-before-seen lithic industry or evidence of a hitherto unexpected early human occupation of the Americas. Their central assumption – that the lithics represent human-modified stone tools – is not supported by the evidence which they themselves present (Chatters et al. 2022:11-12).

However, this statement was quickly rebutted by the team who discovered the cave when they comment:

> (…) it [became] evident that [Chatters et al. 2022] failed to recognize human-made stone items in the illustrations, as well as the concise descriptions we provided in our paper, of an assemblage whose traits would not occur naturally and under the circumstances alleged by our critics" (Ardelean et al. 2022:18)

Unfortunately, it has become common practice to criticise new archaeological sites in the Americas that are considerably older than Clovis (Ardelean et al. 2022:18-19). This is seen in South American archaeological sites mentioned by Boëda and colleagues (2021).

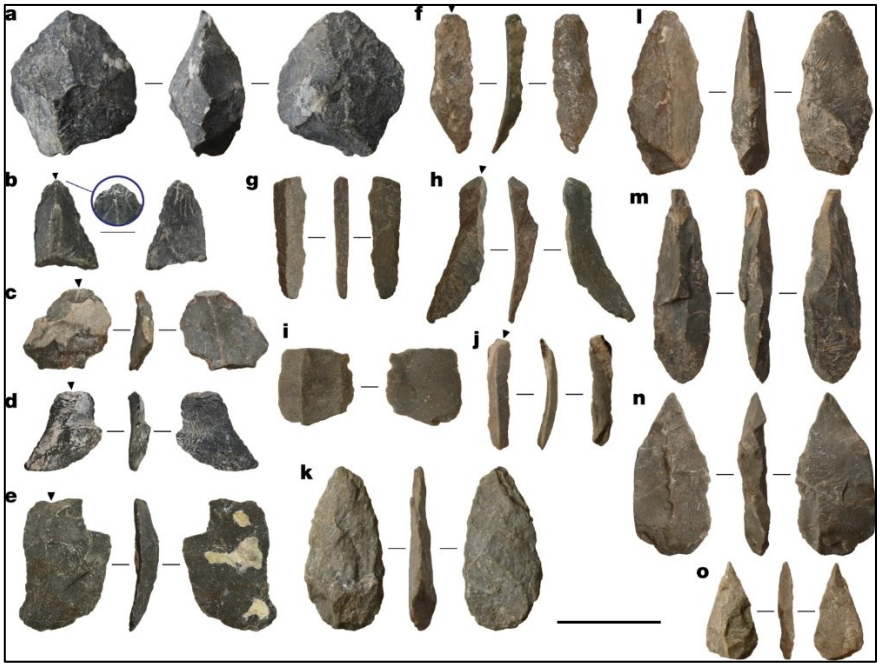

Figure 1.11 – Stone tools excavated from Chiquihuite Cave (a. Cores; b-e. Flakes; f-j. Blades; k-o. Points) (Ardelean et al. 2020:91)

The second archaeological site that has sparked debates is located in the White Sands National Monument (WHSA) in New Mexico, where human footprints were fossilized (Fig. 1.12). The importance of human footprints in an undisturbed setting is their undeniable proof of human presence. These appear to be contemporary to Pleistocene megafauna – i.e., the ground sloth (Folivora), and the mammoth (Proboscidea), amongst other species. It has been suggested the two species walked over the site at the same time due to the superposition of the two tracks (human and sloth), as well as the absence of water or sediments in between the superimposed steps. The general consensus is that these footprints show humans stalking and/or hunting sloths. The tracks represent two path directions (North/Northwest and South/Southeast), and it is also possible to spot a child's footprint; when the child was carried, a heavier footprint can be seen. (Bennett et al. 2020; Bennett et al. 2021; Bustos et al. 2018; Haynes 2022; Pigati et al. 2022). Grass seeds (ditch grass, *Ruppia* cirrhosa) embedded into the footprints, indicate an age of 22.860±32 ^{14}C yr BP and 21.130±25 ^{14}C yr BP (25.342-25.196 (~25.269) and 23.702-23.337 (~23.519) cal yr BP (Bennett et al. 2021; Pigati et al. 2022). If accepted, these older ages would indicate a pre-Clovis and pre-LGM age for the White Sands footprints. This older age is, however, still debated, and a redeposition of older sediments (and seeds) caused by erosion has been proposed, or alternatively a Clovis individual walking over a Pleistocene-aged sediment (Haynes 2022). These two hypotheses are criticised by Pigati and colleagues (2022:100) who claim "(…) these scenarios [are] not only highly improbable but realistically impossible."

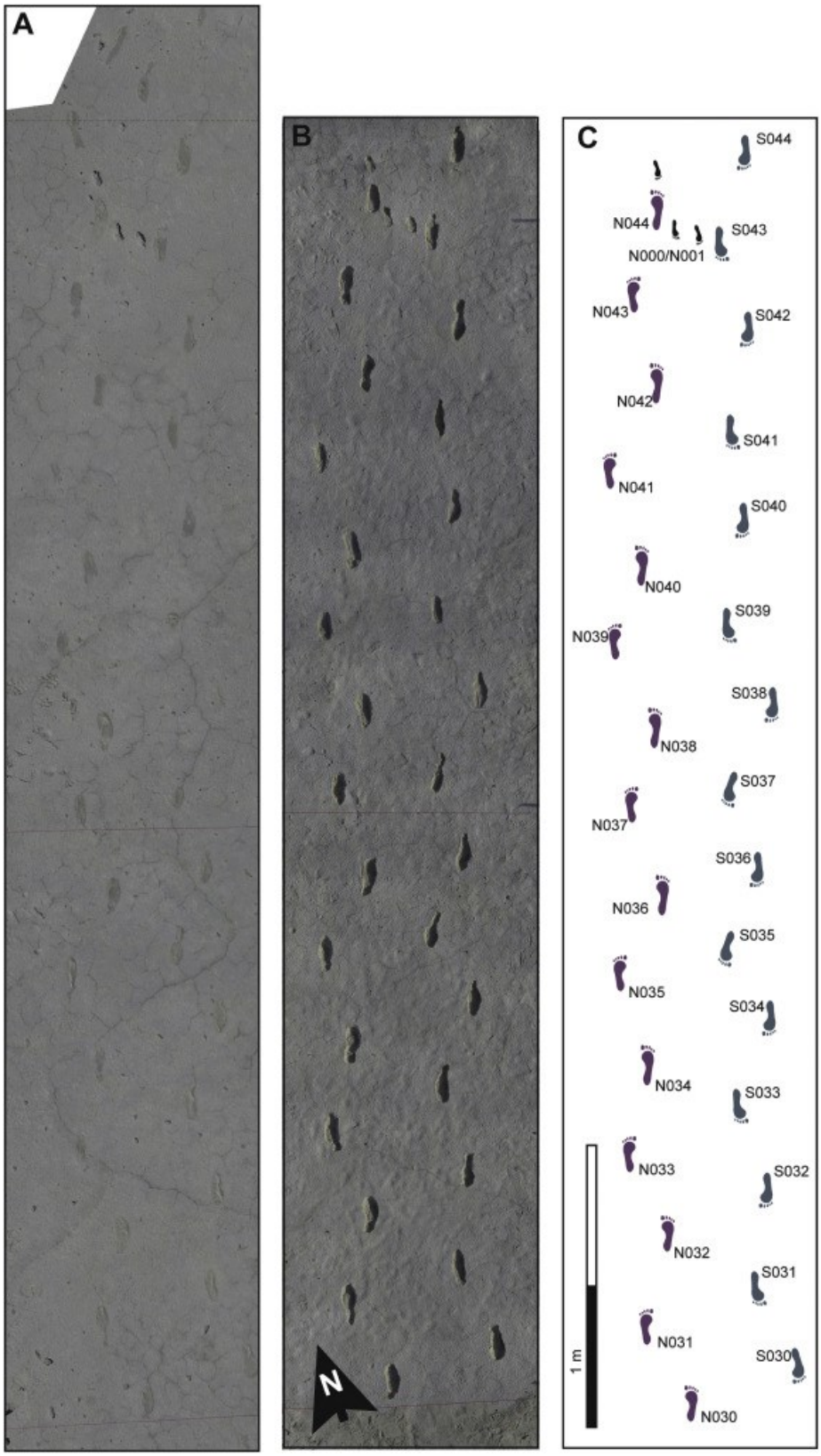

Figure 1.12 – Aerial photographs (A and B) and sketch (C) of the White Sands footprints (Bennett et al. 2020:9)

The discovery of Chiquihuite and White Sands hint strongly at a pre-Clovis date for initial peopling of the Americas. This presents a difficulty because the Ice-Free Corridor was not available prior to a ~13,000 cal BP date suggested by the Clovis-First model, as explained previously. A coastal migration has therefore been proposed.

I.II.II. Coastal Migration Hypothesis

The establishment of the 'Pre-Clovis Model' created a need for a new migration path. A 'Coastal Migration' (Fig. 1.13) path was suggested whereby humans reached the American continent prior to 13.000 cal yr BP before dispersing south of the Cordilleran and Laurentide ice sheets via the Northwestern Pacific Coast. Two important requirements for this hypothesis are an unglaciated landscape in the Alaskan and British Columbian coasts, and consequently the presence of resources (food and tools) required for the survival of human populations. A coastal migration is supported by genetic evidence, as shall be discussed further on (Becerra-Valdivia & Higham 2020; Davis & Madsen 2020; Lesnek et al. 2018; Potter et al. 2017).

Two hypotheses have been created to explain the process of a coastal migration: the 'stepping-stone hypothesis' and the 'kelp highway hypothesis'. When modelling sea level evolution in the Bering Sea, small islands that are now submerged appear, bordering the Okhotsk and Bering Sea (*cf. Chapters III and IV*). These archipelagos could have served as 'stepping-stones' for Palaeolithic hunter-gatherers travelling from Northeastern Asia into Northwestern North America. This hypothesis thus requires human populations to possess knowledge of maritime technology, i.e., fishing tools, maritime transportation, etc. Upon reaching the Alaskan coast, this population would have continued southward through the northwestern North American coast, eventually reaching the unglaciated landscape south of the Cordilleran and Laurentide ice sheets prior to the appearance of the Ice-Free Corridor (Fig. 1.13; Dobson et al. 2021).

Figure 1.13 – Map representing the sites and coastal path suggested in support of a coastal migration to the Americas (Davis & Madsen 2020:3)

Similarly, the 'Kelp Highway Hypothesis', based on both the modern-day presence of kelp forest bordering the North American Pacific coast, as well as the presence of kelp in archaeological sites bordering the Pacific coast, highlights the importance of kelp as a source of food for both humans and prey. The presence of kelp in the Monte Verde II site, located 90km from the Pacific coast, supports this hypothesis (Aguerrevere & Zurro 2021; Erlandson et al. 2015). It has been proven that bears (*Ursus arctos, Ursus americanus* and *Ursus simus*) were present in the Northwestern North American coast, on Vancouver Island, prior to the opening of the Ice-Free Corridor, around 13.000 cal yr BP (Kubiak et al. 2022), further supporting the hypothesis while highlighting the coast's ability to support human life prior to the opening of the Ice-Free Corridor.

Both proposed routes suggest a migratory pathway originating in the Palaeo-Sakhalin-Hokkaido-Kuril Peninsula (PSHK Peninsula), where a maritime culture is archaeologically known (Dobson et al. 2020; Dobson et al. 2021; Erlandson et al. 2015; Erlandson et al. 2007; Ramsey et al. 2004; Royer & Finney 2020). Further supporting this hypothesis, according to Royer and Finney (2020), reduced Alaska Coastal Current

flow caused by minimal glacial melting during the LGM would have made this an opportune time to cross the Bering Sea from Northeastern Asia into Northwestern North America, thus suggesting a possible point of origin to the source population prior to their arrival in EB.

I.II.III. Beringian Standstill Hypothesis

Advances in genetic studies make it possible to use the genetic evidence from contemporary human populations, as well as that of ancient populations whose skeletal remains have been properly preserved, to trace their ancestry. In doing so, it is important to remember that these remains continue to hold an instrumental role in indigenous life and beliefs, they must therefore be treated with respect and all scientific research should be done with the consent of their living relatives.

Two main constraints to the use of genetic data must be mentioned. Firstly, due to the Native American genocide that occurred in the Americas at the end of the 15th century and the genetic admixture with European and African populations that occurred in its' aftermath, there has been a considerable loss of genetic data within Native American populations (Llamas et al. 2016; Reich et al. 2012; Skoglund et al. 2015). Secondly, there is a gap in the LGM archaeological record in Beringia, thus raising the question as to whether the discovery of new archaeological sites would offer more insights into the genetic history of modern-day Native Americans and indigenous eastern Siberian populations (Llamas et al. 2017). However, it has been proposed that between 18.000 and 15.000 yr BP, the population size would have been relatively small, ranging from approximately 70 to 2000 individuals, which could have made them 'archaeologically invisible' (Fagundes et al. 2018:207; Gómez-Carballa et al. 2018; Llamas et al. 2016:3).

It is possible to identify the haplotypes that constitute the genetic heritage of individuals, which can in turn inform us about the genetic mutations that occurred and genetic transmissions that took place through migrations, isolation and/or new contacts. The haplotypes can be analysed and compared in order to establish genetic relationships between populations. The 'coalescent theory' states that genetic similarities should be visible in the DNA trees of two (or more) populations who share a most recent common ancestor (MRCA). As daughter populations migrate, their genetic similarities with the parent population decrease with the distance traveled as gene flow decreases and new genetic mutations are accumulated, as well as possible mixing with new populations; this is visible within the American genetic record, where genetic diversity increased as human populations first migrated south (Reich et al. 2012; Rosenberg & Nordborg 2002; Wang et al. 2007).

Paleogenetic research has been incorporated into archaeological research into the peopling of the Americas, establishing associations between different archaeological populations. The discovery of specific

haplotypes stemming from a founding population has made it possible to establish that New World populations originated in Central Asia . Further discoveries have led palaeogeneticists to propose that populations dispersing from Asia to the New World spent a considerable amount of time, i.e., between 6.000 and 9.000 years (Tamm et al. 2007; Llamas et al. 2016; Llamas et al. 2017; Llamas et al. 2020; Pinotti et al. 2019; Sun et al. 2020), isolated from neighboring populations. This isolation allowed novel genetic mutations to arise creating unique American 'sister- clades'. Tamm et al. (2007) suggest that this period of genetic isolation could have taken place in Beringia during the LGM which is the basis of the 'Beringian Standstill ' hypothesis (Becerra-Valdivia & Higham 2020; Fagundes et al. 2018; Gómez-Carballa et al. 2018; Graf & Buvit 2017; Hoffecker et al. 2016; Llamas et al. 2016; Llamas et al. 2017; Moreno-Mayar et al. 2018b; Pinotti et al. 2019; Raghavan et al. 2014; Raghavan et al. 2015; Skoglund & Reich 2016; Sun et al. 2020; Tamm et al. 2007; Willerslev & Meltzer 2021).

The analysis of genetic polymorphisms can be based on nuclear DNA, mitochondrial DNA (mtDNA), which represents the female genetic line, and the Y-chromosome, representative of the male genetic line. The importance of studying both male and female genetic lineages is that they offer more detail about the nature of the dispersal and a population's demographics. mtDNA is most often used in ancient DNA (aDNA) genome sequencing due to its higher preservation rate, cost-efficiency (it requires a smaller sample for it to be processed), as well as its ability to register mutations. On the other hand, Y-chromosome analyses need a higher sample and is only present in specific cells ("somatic male cells"), therefore reducing its preservation rate (Colombo et al. 2022; Hoffecker et al. 2016; Llamas et al. 2017; Llamas et al. 2020; Nielsen et al. 2017; Raghavan et al. 2015)

Four mtDNA haplogroups that have been identified as representing the founding Asian population which migrated into the Americas: these are haplogroups A, B, C, and D (subclades A2, B2, C1b, C1c, C1d, C4c, D1, D4h3) (Colombo et al. 2022; Hoffecker et al. 2016; Pinotti et al. 2019; Raghavan et al. 2015; Sun et al. 2020; Tamm et al. 2007; Volodko et al. 2008). Haplogroup C (C2) appears to be representative of the Last Glacial peopling of the Siberian Arctic, which would have been the first step in an Eastward migration towards the Americas (Tamm et al. 2007; Volodko et al. 2008). This haplogroup is also representative of a southward peopling of Mongolia, as represented by haplogroup C2a-M504. Interestingly, there is evidence of further genetic isolation among the populations of Chukotka and Alaska, with the appearance of sub-clades A2a, A2b and D2a1a. Further increasing the genetic diversity that existed during the peopling of the Americas, haplogroup C1 originated from southeastern Siberia, in the Amur region; as did haplogroup sub- clade D2, with the sub-clade D3 having been exposed to genetic diversity in the Altai, in Southern Siberia (Volodko et al. 2008).

Amongst the mtDNA haplogroups which were developed solely within the Americas, haplogroup D4h3a represents an American coastal migration, both within North and South American populations, most

likely representing the North-to-South coastal peopling of the Americas below the Cordilleran and Laurentide Ice sheets. This haplogroup can be traced back to Asian haplogroup D4h, thus indicating a genetic connection between the southward migrating American population and the founding population (Llamas et al. 2016; Scott et al. 2021; Skoglund & Reich 2016; Tamm et al. 2007).

An important haplogroup which has stirred up considerable debate is haplogroup X (X2a). This haplogroup is found in North America and its parent group (X2) is only found in Europe (Hoffecker et al. 2016; Llamas et al. 2016; Tamm et al. 2007). The presence of this haplogroup has been used to support a 'Solutrean migratory hypothesis', which stipulates a Late Pleistocene human migration originating in Western Europe towards Eastern North America on the basis of stone tool taxonomies (Bradley & Stanford 2010; Oppenheimer et al. 2014). This hypothesis was quickly rejected on chronological grounds (Fiedel 2022): the presence of this haplogroup in modern-day Native American DNA is an example of the admixture that occurred with the arrival of Europeans on the American continent in historical times.

One of the debates surrounding the use of genetic data to study the peopling of the Americas is whether the migration took place in one or multiple waves. The genetic data indicate the presence of one founding population, whose genetic diversity increased as the founding population migrated further south through time (Llamas et al. 2016; Pinotti et al. 2019; Raghavan et al. 2015; Skoglund et al. 2015; Skoglund & Reich 2016; Wang et al. 2007). On the other hand, on the basis of linguistic, morphological and hematological evidence, a more complex model, the 'three migratory waves model' has previously been proposed (Bonatto & Salzano 1997; Greenberg et al. 1986; Szathmay 1993; Sun et al. 2020), where a 'First American' or 'Palaeoamerican' population would have entered northwestern North America around 15.000 yr BP before two further waves of migration originating from northeastern Asia, thus explaining the distinct linguistic, genetic and cultural identities of the Eskaleut and Na-Dene populations. Through this model, it has been proposed this 'First American' or 'Palaeoamerican' population was descendant of a 'Population Y' which would in theory have carried genetic traits from eastern Asia. The third migratory wave is represented by the direct ancestors of the Na-Dene and other Native American populations. (Fagundes et al. 2018; Flegontov et al. 2019; Llamas et al. 2017; Nielsen et al. 2017; Reich et al. 2012; Scheib et al. 2018; Sikora et al. 2019; Skoglund et al. 2015; Sun et al. 2020; Willerslev & Meltzer 2021).

The Standstill hypothesis suggests that Beringian populations started to diverge from the founding population around 30.000-25.000 yr BP (Hoffecker et al. 2016; Llamas et al. 2016; Tamm et al. 2007), which would represent the last Siberian genetic influx into the Native American founding population's gene poolprior to their entrance into northwestern North America. More recently, it has also been proposed that an earlier divergence could have taken place 36.000 years ago while still maintaining gene flow with Pleistocene Asian populations (Moreno-Mayar et al. 2018a). The founding population would have then split into the Northern

and Southern branches, while still maintaining gene flow. This latest split would have taken place between 17.000 and 14.000 yr BP, which would coincide with the 'First American' model's entrance in the Americas (Moreno-Mayar et al. 2018a).

Paleontological evidence for the chronology of human dispersal in Beringia is rare. The archaeological record yields skeletal remains from seven sites in Western Beringia which provide evidence for the migration of human populations: Ust'-Ishim, Yana Rhinoceros Horn Site (RHS), Mal'ta-1, Afontova Gora-2, Kolyma1 and Upward Sun River 1. A femur found in a secondary deposit in Siberia (Omsk Oblast), colloquially dubbed 'Ust-Ishim Man', has been dated to 41.000 yr BP (uncalibrated; 43.000-46.000 cal yr BP) providing clues as to the earliest human presence in the region. The Ust'-Ishim Man's mtDNA was centered around haplogroup R and Y-chromosome haplogroup K, two haplogroups present nowadays in Eurasia, showing genetic similarities with modern Asians, while diverging from modern-day Europeans (Fu et al. 2014). In the Yana Rhinoceros Horn Site, located in Northern Siberia, two male skeletal remains dated approximately 31,000 cal BP were found belonging to mtDNA haplogroup U, also commonly found in Western Eurasia, and Y-chromosome haplogroup P1 represents a genetic ancestor of haplogroups Q and R which are found within modern Native American populations. (Raghavan et al. 2014; Sikora et al. 2019; Sun et al. 2020; Willerslev & Meltzer 2020). The 24.000 cal yr BP human remains from Mal'ta (Irkutsk Oblast) belong to the U haplogroup (mtDNA) and R haplogroup (Y-chromosome) showing clear association with modern-day Western Eurasians (eastern Europe and western Siberia) and Native Americans, yet no similarities with the Ust'-Ishim remains. Based on these two remains, it can be hypothesized that Pleistocene Siberia was initially peopled by a group represented by Ust'-Ishim, followed by (at least) a second wave with genetic ties to the Mal'ta-1 remains. The genetic similarities between MA-1 and Native American populations indicate the American founding population diverged from its MRCA after MA-1, i.e. after 24,000 cal BP. (Mao et al. 2021; Nielsen et al. 2017; Raghavan et al. 2014; Sikora et al. 2019; Skoglund & Reich 2016; Sun et al. 2020; Willerslev & Meltzer 2020).

Further adding to the complex picture of human dispersals through Western Beringia, the Afontova Gora-2 (AG-2) human remains, found in the eponymous archaeological site located in modern-day Southern Siberia (Krasnoyarsk Krai), dated to 17.000 cal BP are closely related to the MA-1 individual and a South American Native population (Karitiana) (Mao et al. 2021; Moreno-Mayar et al. 2018a; Raghavan et al. 2014; Skoglund & Reich 2016). The human remains recovered from Kolyma 1, dated to approximately 10.000 cal BP, belongs to mtDNA haplogroup G (G1b) and Y-chromosome haplogroup Q (Q1a1b), indicative of a close relationship between the Yana and Mal'ta individuals, as well as with modern-day Native Americans (Sikora et al. 2019; Willerslev & Meltzer 2020). Lastly, two children's remains, discovered in Alaska at the Upward Sun River (USR) site, dated to approximately 11.000 cal BP belong to mtDNA haplogroups C (C1) and B (B2), and appear to be closely related to Kolyma1 (Llamas et al. 2017; Sikora et al. 2019).

In summary, the human remains from Yana RHS would represent an early dispersal into Siberia (the Ancient North Siberian (ANS) population) whose descendants became the Ancestral North Eurasian population (ANE) represented by the MA-1 remains. A subsequent eastward migration is illustrated by the Kolyma 1 human remains, after which the appearance of an Ancient Beringian (AB) population associated with Upward Sun River 1 remains. The Ust'-Ishim remains most likely represent a previous population occupation in southern Siberia which was replaced by the Ancient North Siberian and/or Ancestral North Eurasian populations . The Ancient Beringian population would be ancestral to most modern-day Native Americans (Llamas et al. 2020; Moreno-Mayar et al. 2018; Sikora et al. 2019; Sun et al. 2020; Willerslev & Meltzer 2021).

While the paleontological and paleogenetic data show a source population 'homeland' originating in Siberia, there is still no direct evidence in support of the proposed "standstill population" and its location. Two geographic locations are currently proposed: southern Siberian/Altaian/Amur, (Buvit & Terry 2016) or the Palaeo-Sakhalin-Hokkaido-Kuril (PSHK) Peninsula. The PSHK is considered an LGM refugium on the basis of its favourable environment (Buvit et al. 2021). In fact, this resulted in the "out of Japan" hypothesis as an alternative to the suggestion that the founding population stemmed from a Central Beringian source, or the BLB; no definitive evidence of an 'out of Japan' homeland exists based on the archaeological record however (Scott et al. 2021).

The landscape that supported a Standstill population for thousands of years would have had to have been a viable environment, i.e., one where food and technological sources were abundant, as well as the presence of shelter and manageable climate. It has been suggested that Beringia is the location of the Standstill population due to its promising location between Asia and North America and evidence that it supported biodiversity during MIS 3 and MIS 2 (see section 1.1 above) (Bourgeon et al. 2017; Buvit & Kerry 2016; Buvit et al. 2021; Fagundes et al. 2018; Gómez-Carballa et al. 2018; Graf & Buvit 2017; Hoffecker et al. 2016; Llamas et al. 2016; Llamas et al. 2017; Moreno-Mayar et al. 2018a; Moreno-Mayar et al. 2018b; Nielsen et al. 2017; Pinotti et al. 2019; Potter et al. 2017; Raghavan et al. 2014; Raghavan et al. 2015; Skoglund & Reich 2016; Sun et al. 2020; Tamm et al. 2007; Volodko et al. 2008; Willerslev & Meltzer 2021).

As we have seen previously, multiple lines of evidence support this hypothesis (*cf: Palaeoenvironmental record*). The most concerning counterargument so far is the lack of archaeological evidence for human presence within Beringia dating to the proposed isolation period, with the exception of Western Beringia. One large constraint is the fact that most of CB is nowadays submerged, thus having potentially obscured or destroyed archaeological evidence. As yet, no underwater archaeological projects have taken place in the Bering Strait due to the complications of conducting such projects in Arctic waters (Buvit & Kerry 2016; Buvit et al. 2021; Dixon & Monteleone 2014; Hoffecker et al .2016).

It has also been proposed that the 'Standstill population' could have been located in the PSHK Peninsula. First formulated as an extension of the Coastal Migration Hypothesis, an origin in the PSHK Peninsula was proposed on the basis of evidence that the Peninsula would have been an environmental refugium during the LGM (Buvit et al. 2021). During the LGM, the PSHK would have been largely unglaciated and the maritime population living there, which is archaeologically documented, could have migrated eastward into the American continent after a period of isolation, either by following the Central Beringian coast or by 'island hopping'. The PSHK peninsula could therefore represent the location of the standstill population – but this hypothesis predicts genetic similarities between Native Americans, northeastern Asians (Siberians/Altaians) and Japanese (Jomon) populations (Buvit & Kerry 2016; Buvit et al. 2021; Buvit et al. 2022; Davis & Madsen 2020; Scott et al. 2021).

Unfortunately, the genetic makeup of populations from both sides of the northern Pacific Ocean and aDNA samples obtained from remains from Hokkaido Island establish that there is no mtDNA relationships between the Jomon and Native American populations, whereas there are some connections with modern-day Siberian populations (haplogroup N9b). Nonetheless, the Native American haplogroup D4h3a has distant mutated cousins, D4h3b and D4h2, which can be found in modern-day China (Shandong Province), Japan and Siberia (Khabarovsk Krai). Multiple analyses have been done in an attempt at understanding the Jomon genetic makeup (mtDNA, Y-chromosome and nuclear genome sequencing), as well as physical similarities (teeth – i.e., crowns and roots) in order to see a possible relationship between this Palaeolithic population and Native Americans, however, results proved the opposite. Although the haplogroup D4h3a found mostly in Native Americans does contain sister-haplogroups in indigenous populations around the Pacific Ocean (Arctic North American [D2a], Chukotkan [D4b1a2a1a], and Jomon [D4h2] populations), the genetic link is still quite distant (Scott et al. 2021). Archaeological evidence indicates that technologically, some similarities can be seen between the Jomon and the Western Stemmed Point Tradition (Native American technocomplex that follows the Clovis culture) (Becerra-Valdivia & Higham 2020; Scott et al. 2021) but chronologically the evidence is tenuous.

It has also been proposed that multiple migrations could have occurred after the period of genetic isolation. A terrestrial route further inland in Central Beringia and a coastal route could also have taken place semi-simultaneously. This double migration could originate from either Western Beringia and/or the PSHK Peninsula. These two points of origin are at the centre of the computational modelling done in this project, where we attempt to use known archaeological sites to examine possible routes of dispersal across Central Beringia into Eastern Beringia during the LGM.

I.III. The archaeological record of Beringia.

The archaeological record is at the centre of this research inasmuch as it offers the data for the computational model to be run, as well as the material record of the past people whose migration we are trying to model. Many hypotheses exist as to the 'source' location of the people who migrated into Eastern Beringia during the LGM, yet it is most likely that there was no conscious decision to migrate eastward and that through generational movements, people eventually reached new landscapes.

In a bid to present possibly different routes, we have estimated three possible 'origin' sites for our models: Yana Rhinoceros Horn Site (RHS) complex, Mal'ta, and Kashiwadai-1 located in Western Beringia (present-day Yakutia), southern Siberia (present-day Cis-Baikal) and in the PSHK Peninsula (present-day Hokkaido Island), respectively (Fig. 1.14). These three specific sites were chosen as the 'origin' point of our models because they could be representative of the migratory movements explained previously based on genetic data). Bluefish Caves (Yukon, Canada) is viewed as the ultimate 'destination' site in this research's models due to its geographical position (Fig. 1.14). These sites' material record is quickly reviewed below.

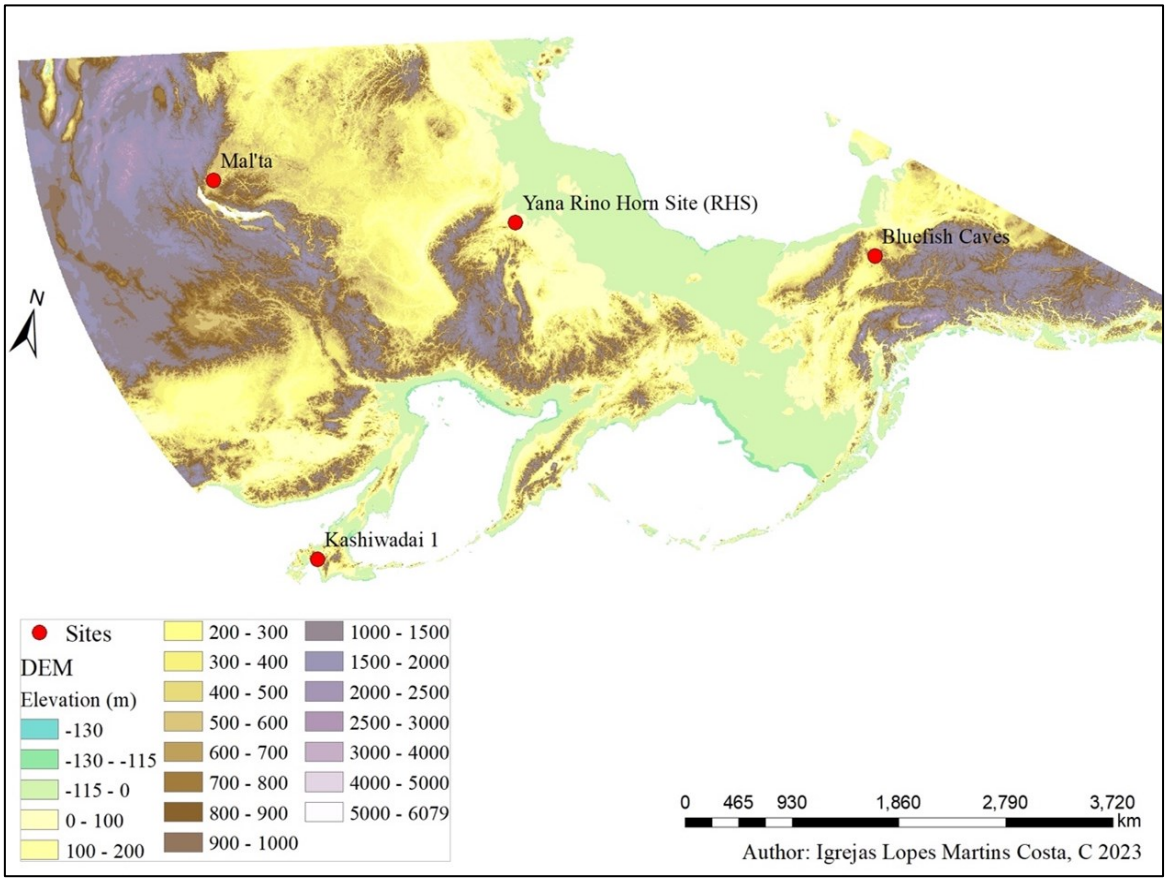

Figure 1.14 – Map illustrating the four main archaeological sites discussed in this research

The site complex of Yana RHS (Fig. 1.14) encompasses the following sites: TUMS, Northern Point (*Severnyi*), Yana B, South Point (*Yuzhnyi*), ASN, Upstream Point (*Verkhnii*) and YMAM (*Yana Mass Accumulation of Mammoth*). Due to their close proximity of a few hundred metres, they shall all be agglomerated under the name 'Yana RHS', located at 70.72N 135.42E (Hoffecker et al. 2020; Nikolskiy & Pitulko 2013; Pitulko & Pavlova 2016; Pitulko et al. 2004; Pitulko et al. 2014a). This site has also been called '*Yanskaya*' (Kuzmin 2017:214). In 1993, a woolly rhinoceros horn foreshaft was discovered on the banks of the Yana River in Arctic Siberia (WB) and in 2001 the first archaeological expedition took place. Its resemblance to those made by Clovis and the fact it was made out of rhinoceros bone, an animal that went extinct prior to the appearance of the Clovis culture first brought up the hypothesis that the inhabitants of Yana could be the ancestral population of the founding population of the Americas. It was believed human populations had not occupied the Arctic, therefore making Yana RHS the first recognized archaeological site located above the 70°N latitude. Not only was Yana RHS a unique site due to its location, but its toolkit includes both a lithic (flaked cobbles) and osseous technology (foreshafts and awls). While the lithics can be seen as 'rudimentary', this could simply mean early humans either did not have access to higher-quality lithics or the presence of easier-access and more cost-efficient cobbles. In addition, artefacts other than tools have been recovered, including beads, pendants, needles, and decorated items, mostly diadems (Fig. 1.15). Such an abundance of artefacts was unusual and representative of a society that had moved beyond survival in a harsh environment. Indeed, the artefacts from Yana RHS represented "the oldest evidence of elaborated symbolic activity" (Pitulko et al. 2012:657), with the needles most definitely being indicative of the sewing of clothes, most likely that protect against the cold environment which has been established was not too different from present-day Arctic Siberia (Bourgeon 2018; Bourgeon et al. 2017; Graf & Buvit 2017; Kuzmin & Keates 2016; Kuzmin 2017; Pitulko et al. 2004; Pitulko et al. 2012; Pitulko et al. 2014a; Pitulko et al. 2017).

*Figure 3. Personal ornaments: **A)** reindeer teeth with drilled holes; **B)** drilled canines of small carnivore (arctic fox?); **C)** ivory beads; **D)** drilled reindeer tooth; **E)** reindeer tooth with a circum cut; **F & G)** tubular beads with a circum cut decoration in the middle.*

Figure 1.15 – Photographs of the personal ornaments found at Yana RHS: A) reindeer teeth with drilled holes; B) drilled canines of small carnivores; C) ivory beads; D) drilled reindeer tooth; E) reindeer tooth with a circum cut; F & G) tubular beads with a circum cut decoration in the middle (Pitulko et al. 2012:646)

The Yana RHS site has been radiocarbon dated yielding ages spanning from ~19.514 cal yr BP to ~34.525 cal yr BP (Pitulko et al. 2014a; Pitulko & Pavlova 2016), therefore proving not only that the site had been occupied regularly, perhaps even year-round, but that it was still occupied prior to and during the LGM. This extended occupation equally informs us on human-mammoth interaction: even though the latter were intensively exploited (for their skin, meat, ivory, etc.), humans did not cause their extinction, further supporting the hypothesis that environmental conditions played a greater role in the disappearance of megafauna at the end of the Pleistocene. In fact, one of the Yana sites – YMAM – has been nicknamed 'Yana mammoth graveyard' due to the presence of at least a hundred animal remains. However, it has been proposed only one or two animals were killed a year, further supporting a sustainable hunting of megafauna. Mammoths were not the only species hunted by humans in Western Beringia: remains of other mammals such as horse, woolly rhinoceros, bison, caribou, foxes, reindeer and hare, as well as birds have been recovered from these Palaeolithic sites (Bourgeon 2018; Bourgeon & Burke 2021; Graf & Buvit 2017 Hoffecker et al. 2020; Kuzmin 2017; Nikolskiy & Pitulko 2013; Pitulko et al. 2004; Pitulko et al. 2012; Pitulko et al. 2014a; Pitulko et al. 2015; Pitulko et al. 2017; Pitulko et al. 2019).

Although the site complex is nowadays close to the mouth of the Yana River (~100km to the south),

during MIS 3 and the LGM, the site was in fact considerably further inland due to reduced sea levels . Therefore, the attractiveness of the Yana site complex's location was the unlimited material – beach gravel – for their tools, access to freshwater – which has been modelled as having its salinity values increasing as the last deglaciation takes place ranging from "less than 9" around 11.000 cal yr BP to 15-16 around 9.000-8.000 cal yr BP (Polyakova et al. 2005:220; Spielhagen et al. 2005) (freshwater salinity level is less than 7psu; Stepanova et al. 2012:566) as well as the subsequent presence of *Puccinellia* sp. grasses which would have attracted large herbivores (Ashastina et al. 2018).

Located just east of Lake Baikal, the Palaeolithic site of Mal'ta (52.83N 103.53E) (Fig. 1.14) has been termed "the main archaeological site of the Upper Paleolithic in Siberia", its "top site" (Lbova & Volkov 2016:16; Lbova 2017:10, respectively), due to its long term occupation, extensive occupation layers, presence of symbolism – mostly represented by art objects (n = >650) and ochre –, as well as human remains and dwelling structures: "No other Siberian site is comparable to Mal'ta in richness and diversity of ivory objects" (Vasil'iev 2001:365). The earliest occupation at the site has been radiocarbon dated to ~21.845-24.906 cal yr BP (OxA-7129, 19.880±160 ^{14}C yr BP and OxA-6191, 21.700 ^{14}C yr BP, respectively), a timeframe corresponding to the LGM. Younger dates are also reported but these go beyond the scope of this project and have thus been omitted. The site was discovered in the first half of the twentieth century and has been systematically studied ever since. The lithics uncovered from the site indicate a blade and bladelet industry with points, borers, end and side scrapers, as well as a pebble technology. The most important category of artefacts from this site, however, are the decorated and incised artefacts. Indeed, at the Mal'ta site, five different types of artefacts were found: personal objects which could be seen as accessories nowadays (or 'personal adornments' such as beads, pendants and bracelets, 'tiaras'); rods and other tools used to create other artefacts were also themselves decorated with carved motifs (Lbova & Volkov 2016); disks and plates, also decorated; zoomorphic sculptures which appear to represent birds, fish, snakes, otters, gophers and wolverines; and finally, anthropomorphic sculptures of different levels of complexity: even though all are dressed, some appear to have more details (in the clothes, accessories, hair and face). In addition, traces of ochre have been found in some of the anthropomorphic sculptures. All art objects were made out of ivory, tusk and horn. Most surprising yet is the discovery of pigments of various colours (red, green, dark and bright blue) in the ornamental objects (Gómez Coutouly 2018b; Hoffecker 2005; Khenzykhenova et al. 2019; Lbova 2017, 2021; Lbova & Volkov 2016, 2017; Pitul'ko & Pavlova 2016; Vasil'ev 1993). All of these data indicate a stable population settlement with established rituals and beliefs. In addition, the presence of multiple dwellings (n = 17), described as being in the shape of a horseshoe (Lbova & Volkov 2017:175), where most of the artefacts were located (Lbova & Volkov 2016), is indicative of a structured layout of their environment. The site, and others in Cis-Baikal are located close to rivers and streams leading to and from Lake Baikal (Goebel 1999).

Perhaps the most important aspect of the Mal'ta site, however, is the discovery of human remains, more specifically of two children (MA-1 and MA-2). Genomic studies on these remains have indicated the presence of the R and U haplogroups (Y and mtDNA, respectively), bringing these remains genetically close to modern-day Eastern Europeans, while also maintaining approximately 14-38% affinity with modern-day Native Americans, therefore indicating part of the genetic makeup of the founding population of the Americas prior to its genetic bottleneck is related to the two children from Mal'ta (Buvit & Terry 2016; Lbova & Volkov 2016; Rasmussen et al. 2014; Seguin-Orlando et al. 2014; Skoglund & Reich 2016; Willerslev & Raghavan 2013).

The island of Hokkaido contains a high number of archaeological sites. Among them, Kashiwadai-1 (42.82N 141.68E; Fig. 1.14) has been radiocarbon dated to the pre-LGM and LGM and its lithic assemblage is marked by flakes and microblades, as well as Yubetsu cores, also mostly made out of hard shale with few obsidian exceptions, through pressure flaking. In fact, it has been proposed this site could support the hypothesis that "the earlier wedge-shaped microblade core technology emerged in northeastern Asia, as it was securely found at the Kashiwadai 1 site" (Nakazawa & Akai 2020:130), therefore that the microblade technology originated from the PSHK Peninsula. Due to the bladelets' size and apparent incomplete appearance, these lithics have been proposed to being part of a composite industry (Iwase 2016; Izuho 2014; Gómez Coutouly 2018b; Graf 2014; Nakazawa & Akai 2020).

Through the models presented in this project, we aim to suggest possible migration paths between Western and Eastern Beringia. In the latter, one site has been at the centre of many debates surrounding the peopling of the Americas: Bluefish Caves (Fig. 1.14), located in the Yukon Territory (67.15N 140.75W), in a mostly unglaciated landscaped that was characterised by a mosaic of vegetation during the Late Pleistocene, consistent with the mammoth steppe. The site, first excavated in the late 1970s by Jacques Cinq-Mars (1979), is still viewed as controversial by many within the archaeological community largely due to the older radiocarbon dates it presented. The site includes three caves (MgVo-1, -2, -3, although the third cave is only partially excavated), located 250m above sea level overlooking the Bluefish River, where a variety of fauna remains were recovered, including fish, birds, and mammals such as horse, saiga antelope, deer, bison and mammoth. Although the majority of these remains is thought to have been brought to the caves by carnivores, the presence of stone tools and of some anthropogenically-modified bones are indicative of human presence (Bourgeon et al. 2017; Bourgeon 2018). A taphonomic analysis of the bones recovered from caves 1 and 2 (Bourgeon 2018) have revealed strong evidence of humans using the cave through the 'V'-shaped striations found on some of the recovered bones, which were subsequently radiocarbon dated to the LGM (Fig. 1.16).

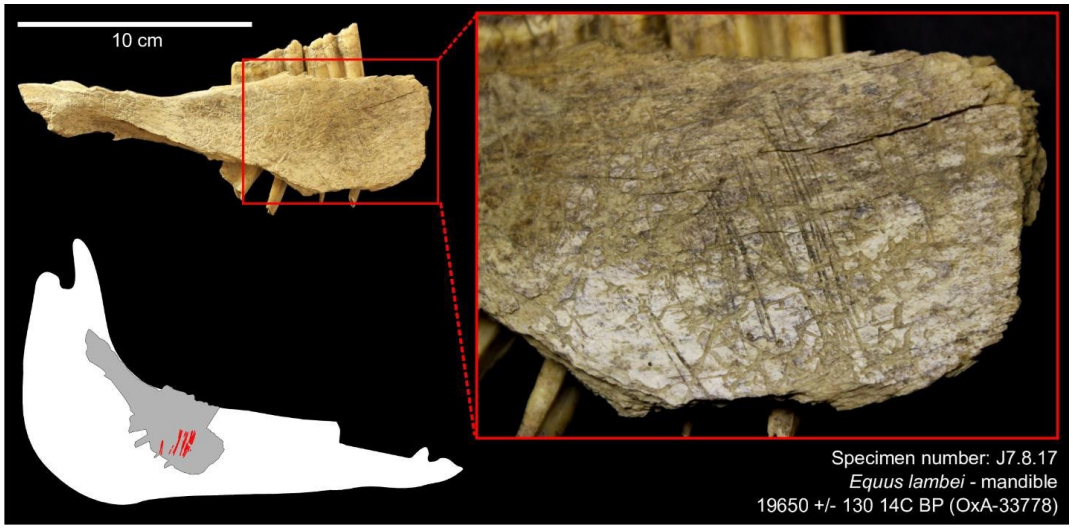

Figure 1.16 – Photographs and models of striation marks found on a horse mandible (J7.8.17) in Bluefish Caves (Bourgeon et al. 2017:7)

A possible criticism of the site is that for a Bluefish Caves lithic assemblage to be representative of an LGM Beringian population, there should be technological traits associated with accepted Western Beringian assemblages (Krasinski & Blong 2020:15). The biggest flaw with this criticism is that it disregards the substantial chronological separation that could exist between sites from either sides of the Bering Strait, with Western Beringian sites representing the older 'source' population that moved eastward over time, as well as a disregard for the ecology, lifestyle and needs of the two populations. This is what Boëda and colleagues (2022:53) have termed 'scientific ideology', where "archaeologists (…) only accept facts that conform to their perception of the archaeological record".

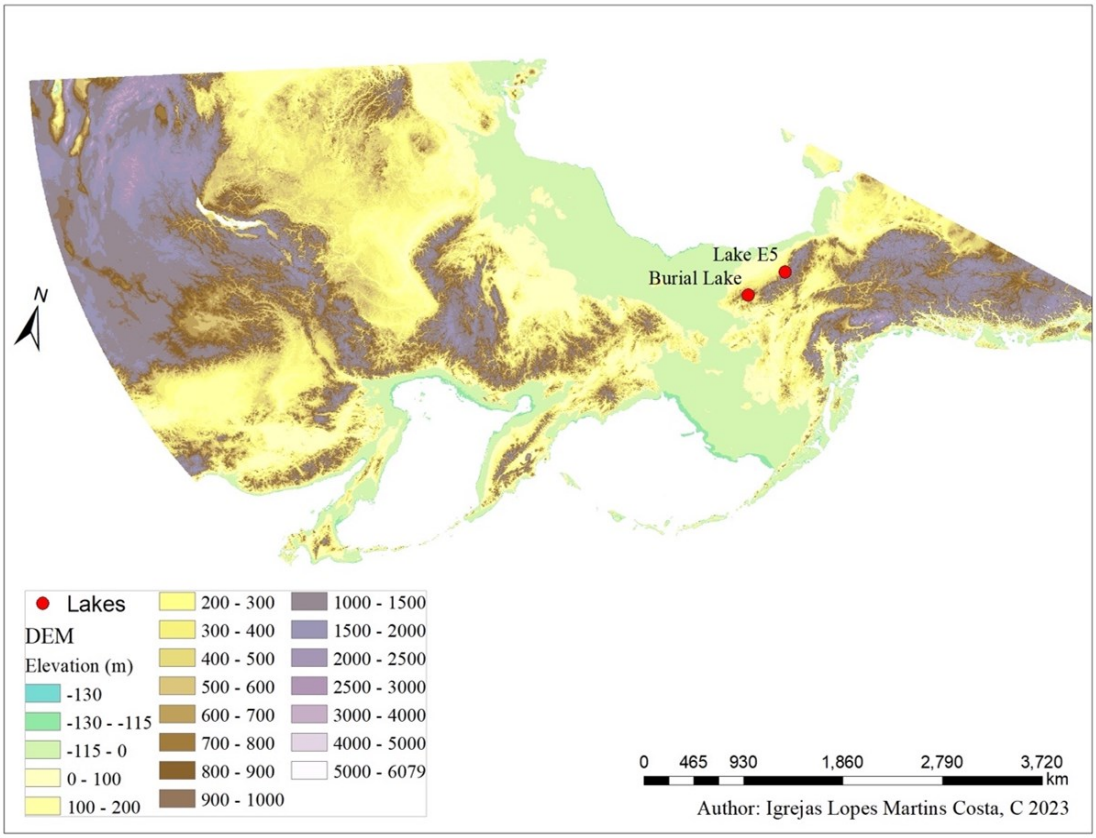

Figure 1.17 – Map illustrating the location of the two lakes' sediments reviewed in this research

Most recently, two new sites have been published representing possible evidence of human presence in Alaska's Brooks Range before and during the LGM: Lake E5 and Burial Lake (Fig. 1.17). These two sites, located at 68.64N -149.45W and 68.43N -159.17W, respectively, both use Charcoal Accumulation Rates (CHARs), Polycyclic Aromatic Hydrocarbons (PAHs) and faecal sterols (5β-stanols) to suggest a pre-LGM human presence in Alaska. The former is located on a LGM glacier, at a height of 798m above sea level, whereas the latter is located in a river basin, at a height of 460m above sea level. In order to uncover CHARs and PAHs from the site, the extraction of sediment cores is necessary. In both cases, charcoal particles were recovered in order to calculate accumulation rates and date the sites; then, sediments underwent many chemical modifications in order to extract the PAHs, which indicates the presence of burning. Finally, coprostanol and stigmastanol indices found in the sediments were analysed to created fluxes and ratios that consequently would indicate whether the faecal remains found were animal or human. To properly differentiate between species, it was established that a coprostanol:stigmastanol ratio of 0.11 is indicative of modern horses, that 0.18 is representative of mammoths (and modern elephants), whereas modern human ratios are of at least 2.22, a ratio considerably higher than other animals. One issue with the usage of this technique is that changes in diet can alter the coprostanol and stigmmastanol fluxes, however this problem

is difficult to solve archaeologically. The importance of considering the data representative of burning (CHARs and PAHs) is that because of the arid and cold environment of Beringia prior to and during the LGM, natural fires would have been limited. Another possible cause of these fires could be lightning activity, however in theory these should not be frequent in cold environments, therefore making anthropogenic burning the most likely scenario. The Lake E5 and Burial Lake data presents an age range between fire burning and human faecal remains between ~35.000 cal yr BP and ~18.000 cal yr BP, therefore implying a human sporadic occupation near the sites (Fiedel 2022; Finkenbinder et al. 2015; Goebel et al. 2022; Vachula et al. 2019; Vachula 2020; Vachula et al. 2020).

Recently, however, archaeological surveys conducted surrounding Lake E5 (Goebel et al. 2022) have shown no evidence of a human presence in the lake's shores. This was the first archaeological fieldwork conducted around the lake in an attempt to discover a Palaeolithic site. The authors still present possible alternative scenarios where either the human presence at the lake (which was shown through the biomarkers mentioned earlier) was too sporadic to be archaeologically visible, or the biomarkers generated a flawed result due to this technique still being new. Burial Lake has not yet been the subject of archaeological fieldwork. Notwithstanding the fact the faecal marker technique is still in its 'infancy', it has been used successfully elsewhere (e.g., New Zealand, Argiriadis et al. 2018). In addition to Bluefish Caves, therefore, it provides tantalizing clues of a human presence in Eastern Beringia during the LGM.

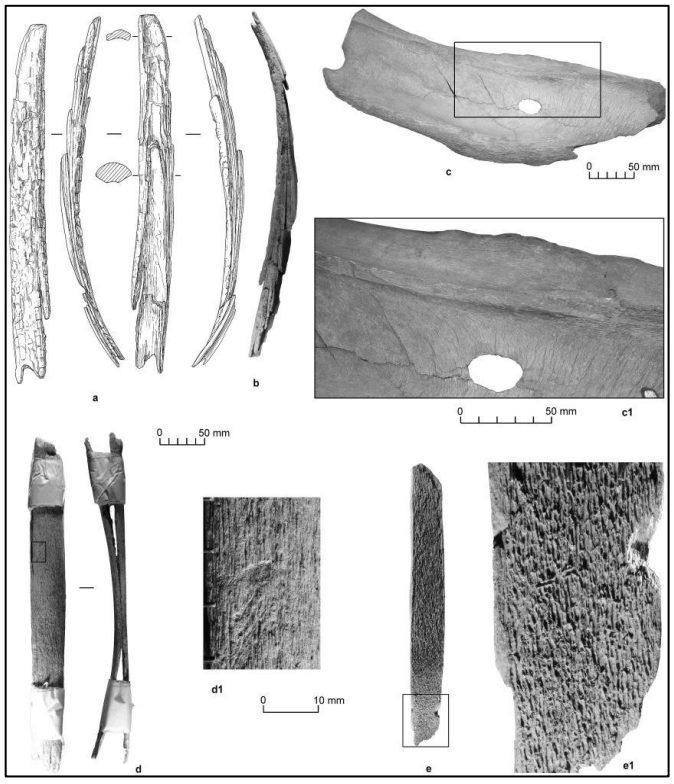

Figure 1.18 – Photographs of anthropogenically-modified mammoth bones from Ilin-Syalakh (a,b) and Wrangel Island (c,c1) and Ilin-Syalakh-34 site (d,-e1). All are attributed to MIS2 by direct radiocarbon dating: a, b – spear point/foreshaft ivory preform; c- mammoth scapula with hunting lesion; c1 is a close up for c; d, e – hunting lesions on the mammoth rib; d1 and e1 is a close up for d and e respectively (Pitulko et al. 2017:139)

The only archaeological site that is located in what used to be Central Beringia is situated on Wrangel Island. This site did not have a published name, which is why herein the site shall be known simply as 'Wrangel Island site'; in fact, it only had a description of its location being near the Mamontovaya River (Pitulko et al. 2017:137), while Kuzmin & Orlova (2004:137) gave it the basic coordinate of 71.00N 179.00E, and Pavlova & Pitulko (2020:8) mentions Wr-12, an exposure located near Mamontovaya River (71°10'N; 179°45'W). Due to its proximity to the river (Pitulko et al. 2017), and the fact it contains the same degrees as those given by Kuzmin and Orlova (2004), the coordinates for Wr-12 are the ones used for the Wrangel Island site on our database (*cf. Chapter III.I*). Even though no papers mentioning the exact coordinates, anthropogenically-modified bone are associated with the exposure (Fig. 1.18). In addition, these coordinates put the site right in the middle of the island, which for the scope of this project is enough seeing as we are looking into the peopling of the Americas on a large scale. Although no Palaeolithic archaeological site *per se* has been discovered on the island, the remains of a woolly mammoth (*Mammuthus primigenius*), a left scapula, has been found containing a hole (Fig. 1.18, #c); the bone was radiocarbon dated to ~24.728 cal yr BP (GIN-8257; 22.400±200 ^{14}C yr BP). The injury is similar to other hunting lesions found in the Yana RHS sites, thus indicating that early humans used to hunt mammoths in northern Central Beringia at the onset of the LGM, even though no lithics were found (Pavlova & Pitulko 2020; Pitulko et al. 2017).

This quick introduction of a few of the Beringian sites researched for this project had for objective a presentation of the evidence for human presence in arctic zones in and around Beringia during MIS3 and the LGM. In what follows, we will present the archaeological research conducted using GIS modelling.

Chapter II – GIS Modelling in archaeological research

This chapter examines the use of Geographical Information Systems (GIS) in Archaeology (II.I.), followed by a revision of previous archaeological models focusing on the Peopling of the Americas (II.II.) before explaining the choice of the *least cost analysis* for this project (III.III.).

II.I. GIS in Archaeology

In the second half of the twentieth century, GIS technologies were widely adopted as a means of, analyzing, manipulating and storing spatial data. Although widely used in a variety of disciplines nowadays, the ability of GISs to store spatial data, superpose different layers and manipulate environmental features has proven particularly useful in archaeological research. In fact, GIS are now widely used for archaeological surveys and excavation, allowing archaeologists to quantify and visualise archaeological data; the use of GIS technologies has revolutionized how archaeological data is stored and analysed. GIS can be used to produce predictive models, determining possible areas of interest yet unstudied, including now-submerged landscapes through the use of bathymetric and topographic data – e.g., Central Beringia during the LGM. Furthermore, qualitative data such as those obtained from oral traditions such as descriptions of geography, family ties and movement (e.g., those obtained in Indigenous Archaeology) can also be included within GIS models where appropriate (Anderson et al. 2014; Anderson & Bissett 2015; Anderson & Gillam 2017; Byrd et al. 2016; Conolly 2008; Dixon & Monteleone 2014; Egeland et al. 2010; Gustas & Supernant 2019; Howey 2011; Lewis 2020; Li et al. 2019; Raju 2006; Supernant 2017; Vogelaar 2017).

It is important to state that GIS models are theoretical constructs and should not be viewed as accurate depictions of the past landscape use, mostly because much of the past is either archaeologically invisible or has not been discovered yet. Furthermore, the choice of data presented in a GIS model is subjective, reflecting the choices made by archaeologists and as such are not unbiased. In some instances, for example, environmental factors which could have been conduits or barriers to movement (e.g., rivers, ice sheets) were left out of the modelling (as was done in Steele et al. 1996); in these cases, it is important to state the reason behind such a decision (e.g., lack of data, theoretical standpoint, etc.).

Secondly, the use of GIS technologies by archaeologists has been accused of '*environmental determinism*', in other words, the impression that past human behaviour was solely influenced or affected by the surrounding environment (Egeland et al. 2010; Hazelwood & Steele 2004; Supernant 2017; Taliaferro et al. 2010; Vogelaar 2017). Notwithstanding this criticism, by reconstructing past environments, a visual representation of barriers and/or corridors to human movements become visible.

When joined with bathymetric and/or topographic data, the spatial distribution of archaeological sites allows us to study the wide array of variables influencing human mobility, illustrating the complexity of human thought and behaviour (Klein et al. 2020; Lewis 2020; Supernant 2017; Wren et al. 2014). By reviewing the presently accepted data and by reconstructing the landscape (e.g., slope, ice sheets, vegetation, climate, etc.) and incorporating them into a GIS model, it is also possible to highlight areas that have been disregarded (Li et al. 2019), indicating possible future areas of study.

The aspect of GIS which has taken a central place in archaeology is the ability to use them to reconstruct landscapes and to create models of habitat suitability; these include statistical, predictive, cellular and agent-based models using both quantitative and qualitative data. Statistical modelling (Carrara et al. 1991; Conolly 2008; Elston & Buckland 1993), applies mathematical tools in order to create probabilistic and predictive models of site location in relation to landscape parameters (Bevan 2003).

The second, predictive modelling (Conolly 2008; Kempf 2019; Lieskovsky et al. 2013; Warren & Asch 2003), attempts to answer theoretical hypotheses under the basis that results are affected by their environment and other influencing factors; these models mostly rely on logistics such as movements and attempt to answer questions pertaining to behaviour in known and unknown landscapes. An example of such a model is the search for suitable locations of archaeological sites in Pleistocene islands off the Pacific Coast of present-day North America, where past land surfaces are reconstructed in order to create least cost path analyses determining possible routes of movements between the islands (Gustas & Supernant 2017). This research combines statistical and predictive models, where the statistical models are used in contexts to predict habitat suitability where the archaeological record presents gaps.

Cellular modelling, (Conolly 2008; Cummings 2008; van Leusen 1999) uses rasters (as indicated by their cell values) to visualize the relationship between sites and their surroundings. These models can be represented by neighbourhood calculations such as visibility, viewshed and least-cost analyses, as well as other modifications of the landscapes. However, these results can be criticised on the basis of their 'two-dimensionality'.

Lastly, agent-based modelling, (Castle & Crooks 2006; Conolly 2008; Wren et al. 2014) also reviews the relationship between archaeological sites and their environment, while adopting a dynamic approach to study how the behaviours of agents would change and/or affect other agents, their environment and ultimately, their movements (e.g., goals and behaviour). An example of such a model is the agent-based model created in order to study patterns of mobility in the Cantabrian Coast during the Late Palaeolithic/Mesolithic (Gravel-Miguel & Wren 2018). These different types of models are often used together for they inform us about different aspects of the geospatial data.

II.II. Modelling First Peopling

The use of geographical data to model past human movement and behaviour and thus to test archaeological hypotheses concerning the First Peopling of the Americas has a long history. By reducing the complexity of a continent-wide dispersal to a few key parameters, it is possible to use these models to determine which ones are instrumental to the survival of human populations as they disperse (Surovell 2003).

Indeed, the use of statistical models in studying the peopling of the Americas is exemplified by the work of Paul Martin (1967, *opud* Steele et al. 1996), who mathematically modelled the 'overkill model', which hypothesized that human appearance in the Alaskan archaeological record at the onset of the Holocene (~11.000 cal yr BP) explains the disappearance of megafauna (*cf. Chapter I, Ice Free Corridor Hypothesis and Clovis First*). Martin's model used mathematical calculations including parameters such as population growth rates, the quantity of megafauna and human migration speed; these in turn suggested quick southward human expansions and even quicker extinction of the megafauna (Mosimann & Martin 1975; Steele et al. 1996). Steele et al. (1996)'s statistical model of early human migration in North America relies on similar parameters. Neither model includes environmental reconstructions, e.g., ice sheets or vegetation. This model supports the overkill model by deeming dispersing humans as "over-exploiters" (Steele et al. 1996:226).

A correction to this model was published shortly after (Steele et al. 1998), where plant and animal fossils were used to create a vegetation reconstruction, including a representation of the ice sheets between 13.000 and 10.000 yr BP. Human behaviour also resulted in the appearance of a highly mobile and migratory population. However, these models are contradicted by the presence of radiocarbon-dated archaeological sites in South America which the simulations do not account for (Glass et al. 1999). Indeed, when conducting predictive models for the peopling of the Americas, it is always important to consider the South American archaeological data because radiocarbon ages for some of their sites are in fact older than many North American sites; this is the case of Monte Verde when the 'Clovis-First' model was first proposed (*cf: Chapter I*) (Hazelwood & Steele 2003).

Many models that tackle the peopling of the Americas, such as the ones presented above, use the concept of a 'wave-of-advance' to predict human movement in North America, which assumes that as a population spreads in the landscape, the landscape behind the 'front line' remains populated (Mosimann & Martin 1975; Steele et al. 1996; Steele et al. 1998; Wren et al. 2014), however the biggest issue with this concept is the establishment of environmental factors, such as its productivity (Salzano 2011), as well as human factors such as the wave-of-advance's width and speed, density and migrating direction; the latter of

which is most likely due to gaps in the archaeological record (Hazelwood & Steele 2004; Steele 2010). Using radiocarbon dates, as was done in Steele (2010), to estimate direction and speed of advance is problematic due to the absence of archaeological sites in large geographical areas.

These earlier attempts at modelling the spread of humans in the American continent take for granted that they crossed the BLB (or CB) and the Ice-Free Corridor, which are viewed as having a resource-rich environment (Anderson & Gillam 2000; Anderson et al. 2014; Anderson & Bissett 2015; Gustas & Supernant 2019). Lanata et al. (2008) on the other hand, include a point-of-origin in Alaska and estimate that an initial population represented by eighty people dispersing as early as 18.000 cal yr BP would not have been able to migrate south of the Cordilleran and Laurentide ice sheets if population growth was less than 2%, but would have reached northern South America by 6.000 cal yr BP if marked by a 2% population growth and the tip of South America (Tierra del Fuego) by 9.000 cal yr BP if marked by a 3% population growth and by 13.000 cal yr BP with a 5% population growth. This research suggests that to explain the dates obtained in the archaeological record, high population growth must be stipulated. It also differs from the previous two models by allowing different tempos of dispersal due to the three hypothesised bottlenecks, i.e., the northwestern North American coast west of the Cordilleran ice sheet, the ice-free corridor, and the isthmus of Panama (Lanata et al. 2008; Salzano 2011).

Another concept that can be used to model human dispersal is the 'leapfrog' concept which supposes that as a population disperses, it "leaps" forward a specified distance to occupy new regions and the landscape 'left behind' is abandoned after depleting the landscape of its resources (Anderson & Gillam 2000). One such model (Surovell 2003), with an established point-of-origin south of the Cordilleran and Laurentide ice sheets and an initial population size of fifty, attempted to model at which moment humans would begin moving inland. This model was conducted as a means of understanding how the Monte Verde population was established prior to known Clovis sites (which are younger in age). In this model's optimal scenario, assuming population growth of 0.5% and a leapfrog distance of 1000km, Monte Verde is not reached before an inland dispersal in present-day United States (2267 years after first entry) and entry into South America (after 1500 years).

Other research has modelled dispersals via a coastal route by joining LIDAR data and GIS modelling. An example of such a use resulted in areas-of-interest being identified off Quadra Island, British Columbia (Vogelaar 2017). In a similar study, least cost paths are proposed between islands off the British Columbian coast during the Late Glacial period after modelling ancient shorelines (Fig. 2.1) (Gustas & Supernant 2019). None of the models described above (Anderson & Gillam 2000; Anderson et al. 2014; Anderson & Bissett 2015; Glass et al. 1999; Mosimann & Martin 1975; Steele et al. 1996; Steele et al. 1998; Steele 2010) use a 'point-of-origin' in northeastern Asia or attempt to model patterns of mobility

within Beringia, where the Standstill Population is thought to have existed. This is where this project diverges from previous models of the peopling of the Americas.

II.III. Least cost path analysis

A least-cost path (LCP) analysis focuses on human movements within a landscape and allows archaeologists to bridge both chronological and geographical gaps in their data. As implied by the name, the LCP proposes the most cost-effective pathway between points under the assumption that humans would favour less challenging routes – in terms of energy costs – when moving across the landscape. This GIS tool is often used when studying ancient roads, determining where to place new roads, and modelling animal or human migrations, to name a few examples. Conducting surveys is a good means of determining the accuracy of the LCP (Anderson & Gillam 2000; Anderson et al. 2014; Beyin et al. 2019; Egeland et al. 2010; Field et al. 2007; Gustas & Supernant 2017; Gustas & Supernant 2019; Herzog 2020; Lewis 2020). However, it is important to highlight the tool's limitations, such as its inability to include multiple barriers simultaneously in different raster/polygon files, and its assumption of perfect knowledge of a landscape (i.e., assuming humans had a 'bird's eye' view which is not realistic especially in the case of initial dispersals). In addition, LCP analysis assumes that subsequent generations would have the same decision-making process as their ancestors (Beyin et al. 2019; Howey 2011; Wren et al. 2014). Nevertheless, it has been proposed that LCPs should be viewed as 'corridors' or 'highways' that reflect basic rules guiding human mobility :

> The super-highways that emerge from our models are both the least-calorically costly and most 'attractive' paths, while also corresponding most closely to known early archaeological sites. This concordance demonstrates that while there were a range of routes available to facilitate the rapid and efficient movement of people throughout the continent, people likely chose the most optimal visually, calorically, and hydrologically most frequently. They suggest fundamental rules guiding human movement – people orient themselves using visual clues, they search for freshwater, and they minimize caloric expenditure as much as possible as they enter new regions. (Crabtree et al. 2021:8)

The use of tools such as LCP analyses are useful for tackling the issue of human mobility. On a local scale, it is possible to use them to describe possible movements between known resources, which could be used to understand a varied archaeological record (Byrd et al. 2016; Taliaferro et al. 2010), and on a larger, regional or continental scale, it is possible to use them to suggest potential dispersal routes. An example of the latter approach is the modelling of possible paths taken by humans in South Asia (Field et al. 2007). Field et al. (2007) suggests a preference for dispersal paths bordering the coast or river systems and avoiding higher altitudes, confirming a previous hypothesis that:

> (…) the first modern humans to colonize South Asia were mobile hunter-gatherers, and that these groups may have relied upon, or at least been familiar with, subsistence strategies that included coastal resources. We also assume that regions that were mountainous, at high elevation, or with steep slopes would not have been included as part of major routes of colonization. Montane environments and resources were undoubtedly important to early colonizers; however, when considering human dispersals these regions are less likely to have served as major routes, as they are more costly to hunter-gatherers in terms of energy expenditure, and less attractive in terms of the availability of game and collectable foods. (Field et al. 2007:93)

Another example of the application of LCP is to study human dispersals in a maritime landscape, such as the one conducted by Kealy and colleagues (2018) to propose migration routes from Sunda to Sahul (Wallacea) around 70 and 65.000 cal yr BP. In addition, LCP analyses can also incorporate environmental factors such as weather patterns (Kondo et al. 2018) and oral history (Supernant 2017), the latter of which can be used to re-establish old migration pathways and proving indigenous oral histories are indeed useful for the archaeological record.

Anderson & Gillam (2000) used LCP analysis to propose four scenarios for initial dispersal to the Americas following their crossing of the Ice-Free Corridor. Although the river systems are not presented in the modelled maps, the generated paths appear to follow riverine and coastal paths when faced with another more costly path, as those presented in South Asia previously (Field et al. 2007). In summary, the LCP tool represents a useful tool for understanding past patterns of human mobility, especially in the context of initial dispersal into new landscapes such as the Americas.

In our project we use rasters that portray key aspects of the paleoenvironment (slope and elevation, distance to water), and GIS tools such as viewshed and least-cost analyses to create a predictive model of human mobility within the Beringian landscape during the Late Pleistocene. We then discuss the implications of this model in terms of the archaeological hypotheses mentioned above (*cf. Chapter I, Migration hypotheses*) and in terms of human behaviour (*cf. Chapter V*).

Chapter III – Materials & Methods

In this chapter we present our GIS database (III.I), and an explanation of the project's chronological information (III.II) before describing the construction of the models from the collection of geographical information for the study region, to the creation of derived layers (slope, distance to water) and finally, application of the LCP tools (III.III). The project's workflow is presented in Supplementary Data 1.

III.I. Database

The database created for this project contains 92 archaeological sites dated to the Last Glacial period, located in Beringia and adjacent regions. The objective was to create a thorough database of all known archaeological sites with their geographical coordinates and radiocarbon ages. The database is divided into two parts, the 'SummaryData' (Supplementary Data 3), which contains the summarized version of the database, and 'DetailedData' (Supplementary Data 4) contains all of the information gathered for this database.

For a site to be included here, there had to be few requirements. Firstly, the coordinates for the site had to be published in an academic paper, as well as its elevation (in meters above sea level) Although the DEM obtained for this project does provide data on the elevation, the elevation was required in order to be able to guarantee there are no discrepancies in the model. Next, the uncalibrated radiocarbon dates for each site had to be available. Dates were then calibrated online using the OxCal programme (v. 4.4) available via the Oxford Radiocarbon Laboratory's website [https://c14.arch.ox.ac.uk/] which uses the IntCal20 calibration curve (Reimer et al. 2020). Radiocarbon dates with a large error (a standard deviation higher than 1.000 years) were deemed suspicious, but not necessarily excluded. Dates are excluded if they are improperly referenced, lack laboratory codes or are inconsistent with other dates from the same site and/or the site's stratigraphy, or if they have been rejected by another researcher for well-documented reasons. As a means of allowing the readers to properly understand the database created for this project, its 'README' document can be found within the Supplementary Data (Supplementary Data 2).

III.II. Chronology

Both uncalibrated and calibrated radiocarbon dates for each site are included in the database. The uncalibrated dates are recorded in this database because there are regular updates on the calibration curve; therefore, it is important to be able to re-calibrate the ages of archaeological sites and update the database. In 'DetailedData' (Supplementary Data 4), the uncalibrated dates ('age') and their standard deviations ('s_dev') are presented, followed by the minimum and maximum ('age_cal') ages calibrated using OxCal 4.4/IntCal20 and the mean age of the calibration ('age_calM'). The mean ages from 'age_calM' are used

to calculate the site's mean age ('age_m') in 'SummaryData'. Should the site contain only one date, then 'DetailedData''s 'age_calM' date will be the same as SummaryData's 'age_m'.

The dates are then attributed to a temporal group ('temp_group'): value '1' is a late MIS3 date, ranging from 35.000 to 23.000 cal yr BP; the value '2' is indicative of an LGM / MIS 2 date, from 22.000 to 18.000 cal yr BP. The threshold date of 23.000 cal yr BP was chosen as it marks the final Greenland interstadial event before the LGM, which coincide with GI-2.2 (Rasmussen et al. 2014). Sites falling within temporal group '1' were further classified as either stadial ('std') or interstadial ('int') following the Greenland chronology in Rasmussen et al. (2014). The Greenland Stages are indicated in the database under the column 'grnlnd_stage' in DetailedData.

III.III GIS Methods

The goal of this research is to propose possible terrestrial migratory paths for humans moving from Central Asia to the Americas during the Late Pleistocene. It also allows us to suggest patterns of mobility within Beringia, linking known archaeological sites through LCPs. Here we highlight the principal steps taken to achieve this using ArcGIS tools. As mentioned earlier, one of the main benefits of using a GIS software is the ability to overlap multiple layers of data to obtain the most accurate image. In models such as this one, subsurface mapping results can be superimposed with layers pertaining to the current surface (Cheetham 2008).

First, we assembled the different layers of geographic information that would be required for the LCP analysis. These include: an elevation model, paleoshoreline reconstruction, reconstruction of the ice sheet extent and the hydrological system. The first step was to download a topographic map. Because Last Glacial sea levels were considerably lower than present-day, a bathymetric Digital Elevation Model (DEM) was downloaded from https://www.gebco.net/, including the study domain which is contained within 99.24°N, 40.78°S, 88.41°W and 239.58°E. The coordinate system used is GCS_WGS_1984 and the projection chosen is WGS_1984_EPSG_Arctic_Regional_zone_A5. This projection was chosen because it focuses on the Arctic region as well as the totality of the project's terrestrial extent.

Two DEMs were produced using different sea levels for the LGM and MIS3. A reduced sea level of -130m was required for the LGM in accordance with the data presented in Grosswald & Hughes (2002) and Simms et al. (2019). For MIS 3 sea levels are reduced by -90m below current sea levels in accordance with Rabassa & Ponce (2013) (*cf: Chapter I, sea levels*).

Manley (2002)'s simulation adheres to the first modelling technique (Dobson et al. 2021), and so does Batchelor et al. (2019)'s ice sheet models, which are used in this project. The decision to use the global eustatic

model in these two cases could be due to the small geographical area analysed (i.e., the Bering Strait). Depending on which data is incorporated into one's research, it is possible to obtain slight differences even within the same modelling technique, which can drastically affect one's analysis (Spada & Galassi 2017:152). In the topic of the peopling of the Americas, using accurate sea level data permits the discovery of possible pathways used by early humans that are now submerged; these could have been terrestrial (BLB) or semi-aquatic pathways, where archipelagos were used during an aquatic migration (Dobson et al. 2021).

We manually selected bathymetric contours at -130 and -90m from the initial DEM (Fig.3.1) to obtain the main extent of Beringia for these two periods, as well as the larger islands surrounding its coastline. Some incredibly small islets were not included however due to the spatial scale of the bathymetric data. A mask was created to more clearly separate the Beringian landmass from the Bering Sea. Having created the landmasses for both timeframes, we then classified the DEMs by modifying the layer's symbology. Twenty classes were manually specified to highlight the palaeo-coastlines (Fig.3.2-3.3).

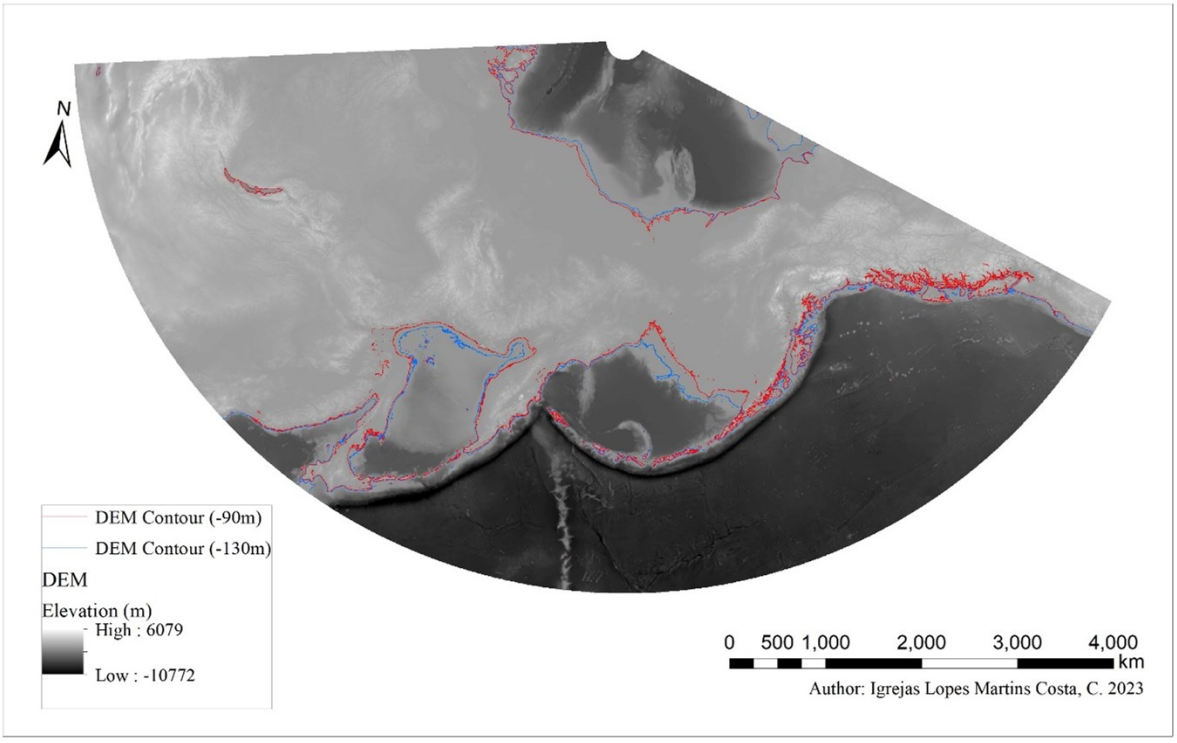

Figure 3.1 – Contour lines created with the Contour tool in ArcGIS representing our LGM (-130m, red) and MIS3 (-90m, blue) reduced sea levels

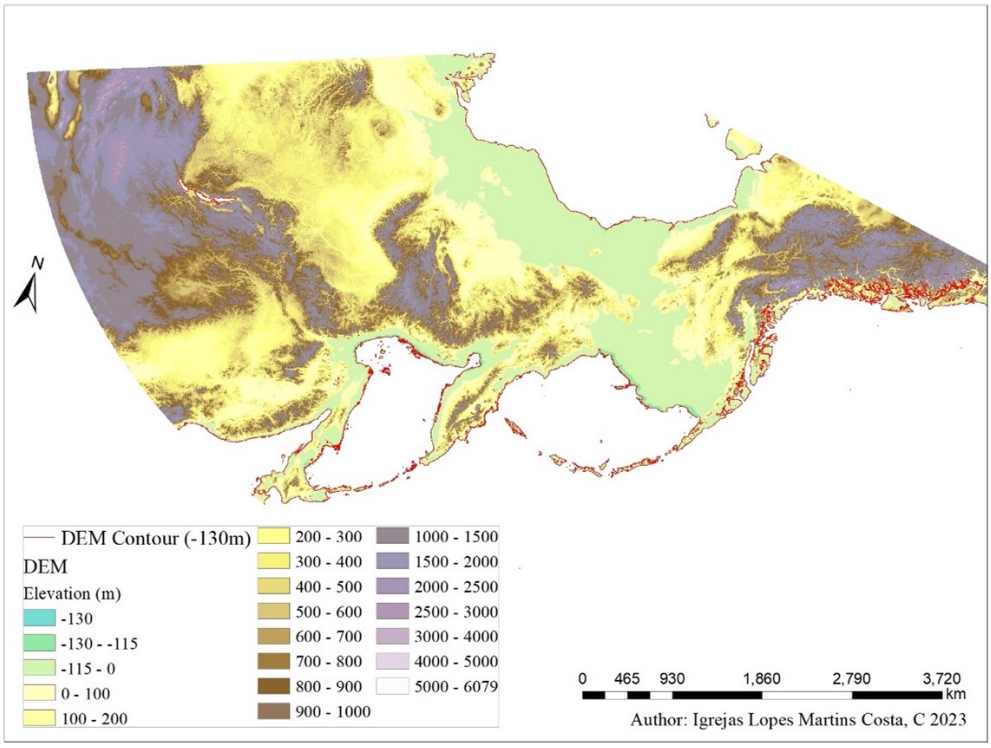

Figure 3.2 – DEM with manually specified elevations representing our LGM landmass; the -130m contour (red) highlights the coastline during the LGM's reduced sea levels

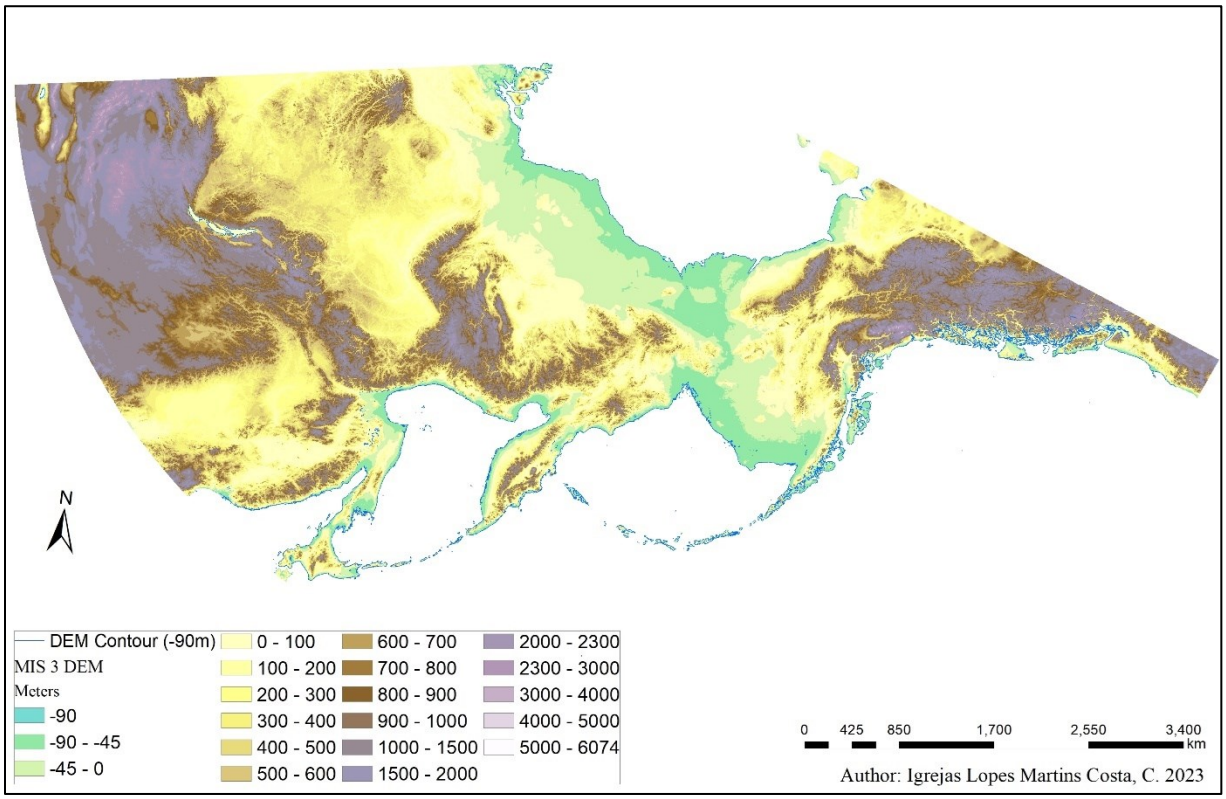

Figure 3.3 – DEM with manually specified elevations representing our MIS3 landmass; the -90m contour (blue) highlights the coastline during MIS3's reduced sea levels

The next step was to add information to the DEM, including 1) ice sheet extents and 2) the hydrological system. The extent of the ice sheets for both the LGM and MIS3 were obtained as shapefiles through Batchelor et al. 2019 (Fig. 3.4A) [https://osf.io/7jen3/]. While Ehlers et al. 2011 also provides the icesheet extents for the LGM, Batchelor et al. (2019) provide 'maximum', 'minimum' and 'best estimate' ranges for the ice sheets dating to 30.000 and 35.000 cal yr BP, which we use to represent stadial and interstadial fluctuations in the ice sheets (max and min respectively, Fig. 3.4B), in addition to an LGM 'best estimate' ice sheet extent. For this project's MIS3 maps, the 30ka BP maximum and minimum extents were used, as well as the best estimate when analysing the general MIS3 data (Fig. 3.4B).

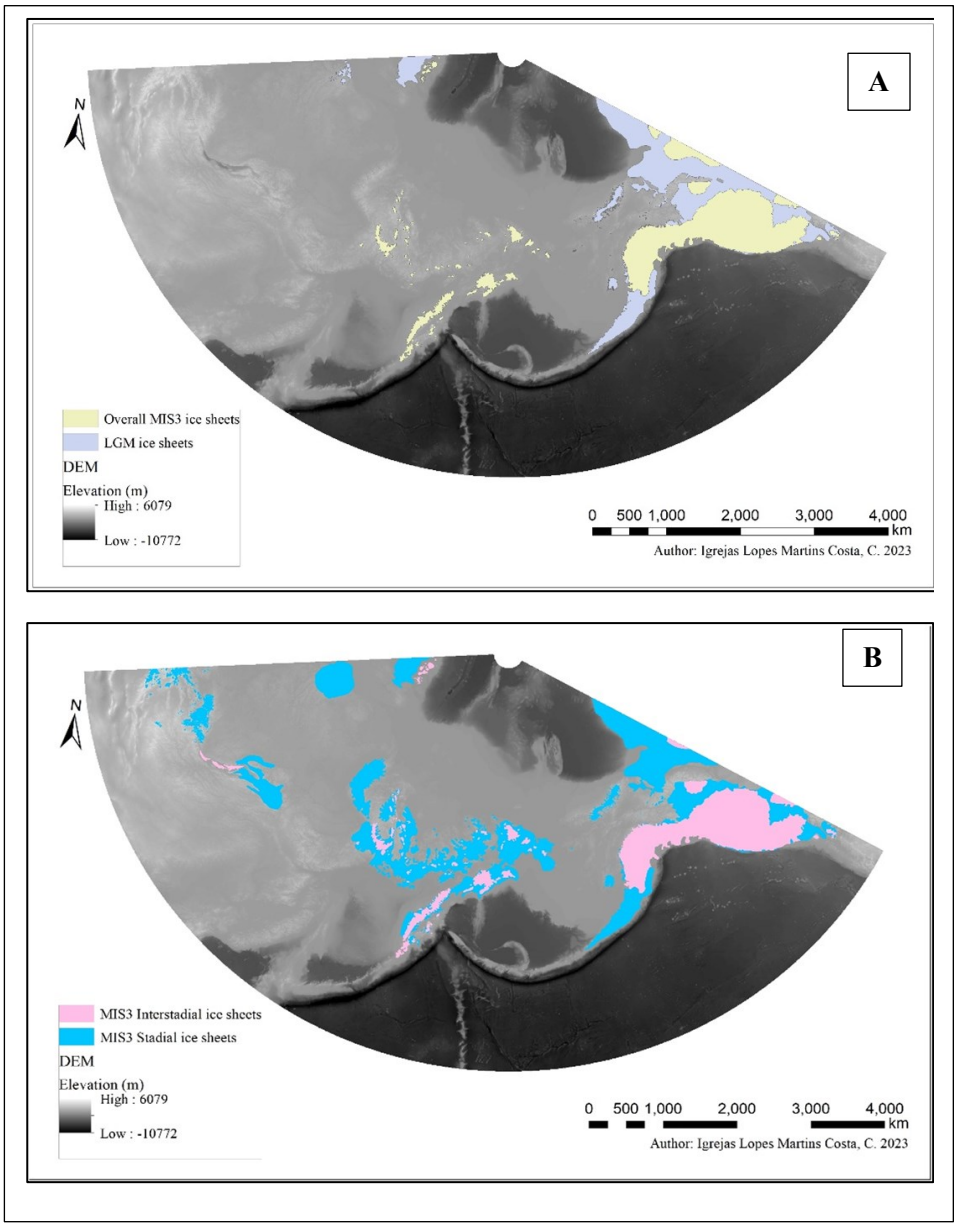

Figure 3.4 – Presentation of the modelled ice sheets used in this project: A – LGM ice sheets (lilac) and Overall MIS3 (olive green); B – MIS3 interstadial and stadial ice sheets (pink and blue, respectively) (Batchelor et al. 2019)

Although the palaeoenvironmental record (*cf. Chapter I*) includes information about the fauna and flora of Beringia, it was quickly established these data would not be included in this project's models. This is due to the complications inherent in creating distribution maps (shapefiles) for the different biotas.

Geographic parameters that are included in our models include the hydrological system and the ice sheet extents. Bond (2019) reconstructs the hydrological system in Central Beringia during the LGM based on bathymetric data. However, this reconstruction does not extend to other parts of Beringia. Therefore, we recreated the palaeo-hydrology of Beringia for both our timeframes using ArcGIS's Spatial Analyst tools, specifically the hydrology toolkit (Fig. 3.5). (*cf. Supplementary Data 1, Workflow, A*). We used to the *Con tool [Spatial Analyst]* and the SQL expression "*value>50.000*", as a means of obtaining the largest river systems possible for the project while avoiding small tributaries and creeks that will have been more affected by landform transformations we cannot control for (Pitcher et al. 2016). One aspect of our palaeo-river reconstruction is somewhat problematic, namely, we do not account for the impact of the ice sheets on local topography as it would require further modelling of the effects of ice sheets on local topography, which is beyond the scope of this project. A comparison between our hydrological reconstruction and Bond (2019)'s reconstruction (Fig. 3.5) which incorporated this information shows that there are small differences between the two layers. Although the presence of pro-glacial in various parts of Beringia during the LGM has been proven (*cf. Chapter I*; Forman et al. 2007; Horiuchi et al. 2000), we did not attempt to reconstruct the lakes due to a lack of empirical data on their Palaeolithic extents; in addition, we opted not to use Bond (2019)'s modelled lakes to avoid an inconsistency in our data: the modelled lakes and rivers are only found in Central Beringia (the now-submerged landmass).

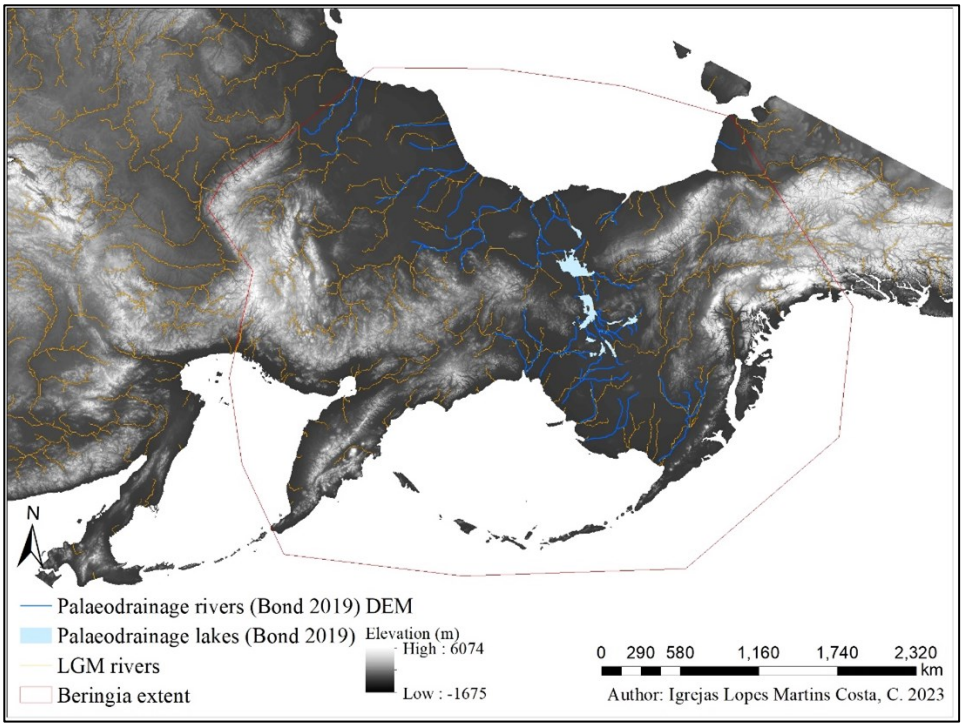

Figure 3.5 – Modelled LGM palaeo-river system (orange) in comparison with Bond (2019)'s rivers and lakes (blue royal and light blue, respectively). The extent of Bond (2019)'s reconstruction is indicated by the Beringian extent layer (dark red)

Our modelled palaeo-hydrological systems are similar for the LGM and MIS3, with slight differences, mostly due to the different sea levels (-130m for the former and -90m for the latter), as well as some diverging streams. In order to understand what these rivers represent, the stream order (*Stream Order [Spatial Analyst]*) was modelled using both the Strahler (Fig. 3.6A) and Shreve (Fig. 3.6B) methods. The former proposes a classification method whereby a stream order can only increase when two streams of the same order merge (i.e., the merging of two streams with the value '1' will create a new stream whose value is '2'); whereas the latter proposes a classification method based on magnitude whereby when two streams merge the following stream's value is the sum of the previous two values (i.e., the merging of two streams of values '1' and '2' will create a new stream whose value is '3'). The first method – Strahler – is often preferred for it is simpler and allows for a better visualization of the different types of streams present, whereas the second results in a multitude of values (Hansen 2001; Shreve 1966; Tarboton et al. 1991).

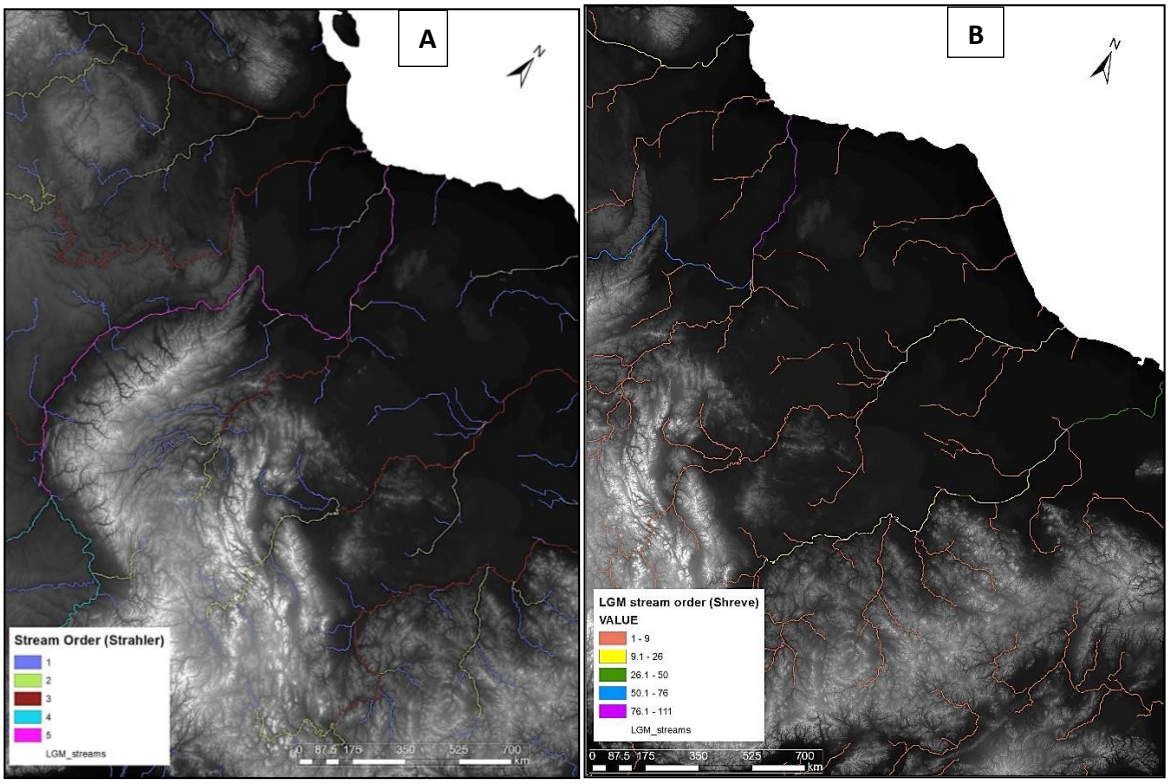

Figure 3.6 – LGM rivers ('LGM_streams') as indicated by their order methods (Strahler, A; Shreve, B). Our DEM here is zoomed in on the Verkhoyansk Mountain Range

The importance of reconstructing the hydrological system is highlighted by the fact that most of our archaeological sites are located near rivers, both with our LGM and MIS3 sites. When analyzing the totality of the MIS3 sites, with no distinction between interstadial or stadial periods, the MIS3 sites will be henceforth known as 'overall MIS3 sites', as opposed to 'Stadial/Interstadial sites' (Fig. 3.7 and 3.8).

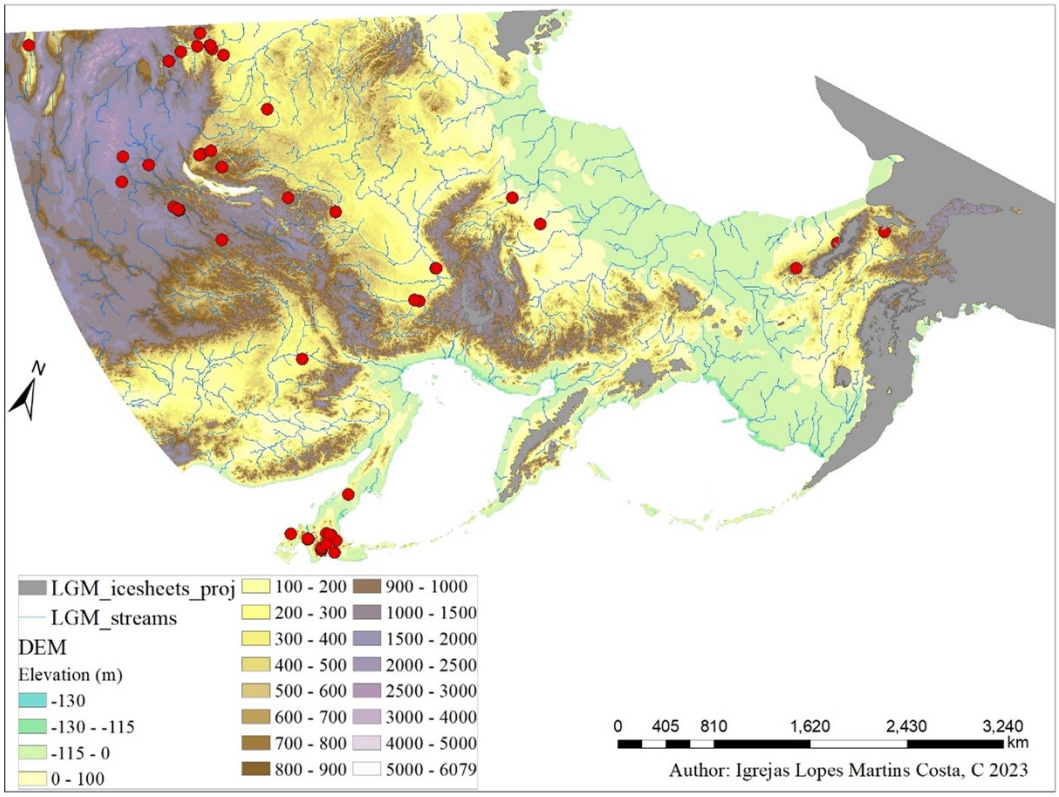

Figure 3.7 – Location of our LGM archaeological sites (red) in reference to our LGM river system

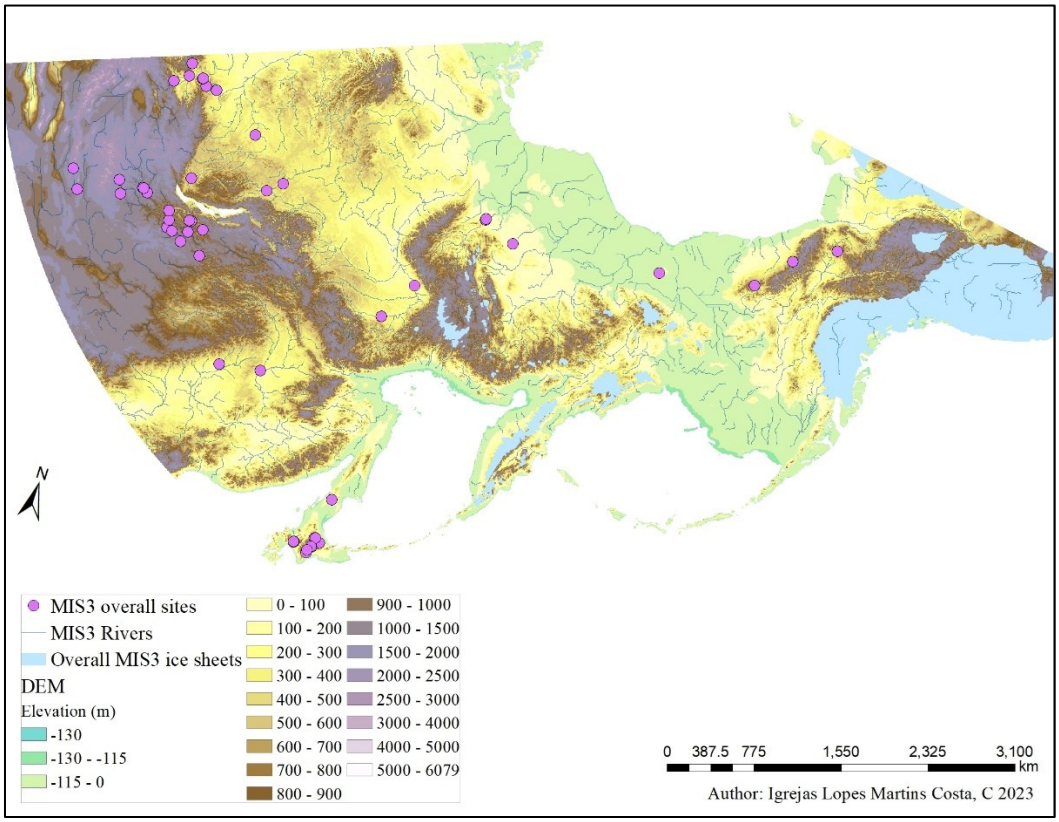

Figure 3.8 – Location of our overall MIS3 archaeological sites (purple) in reference to our MIS3 river system

In addition, Lake Baikal was removed from the DEM (LGM and MIS3 alike), rather than being incorporated into the DEM under the assumption that LCPs should not cross a lake of this size. An attempt at including the lake into the ice sheet polygons (above) was made, however, the LCP results remained the same, so we opted to remove the lake from the DEM to not confuse it with the ice sheets. Having assembled the requisite geographic information about the study region (including elevation, paleoshoreline reconstruction, ice sheet extents and hydrological reconstruction) the LCP analysis described below could begin.

III.III.I. Least Cost Path analysis

The least cost path models created for this project (*cf. Chapter IV*) use a *Weighted Sum [Spatial Analyst]* layer and the *Cost Connectivity [Spatial Analyst]* tool. The first step was to derive rasters with slope values, distance to water and distance to other archaeological sites with which to create a weighted sum raster. First, we created a slope layer based on the DEM. This slope layer is based solely on the DEM, however its output coordinate system - WGS_1984_EPSG_Arctic_Regional_zone_A5 had to be specified. Due to the fact that the slope raster is based on the DEM, it does not vary between the LGM and MIS3 the same raster was generated for both models (Fig. 3.9).

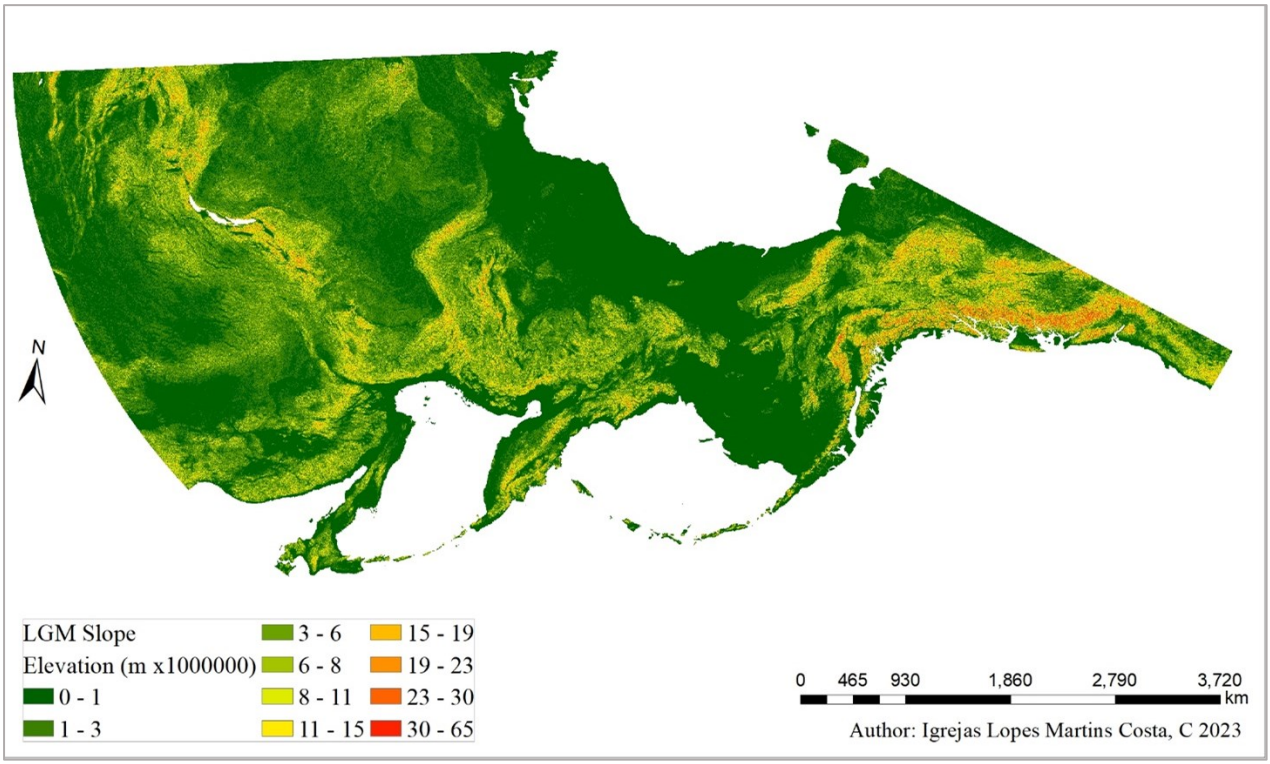

Figure 3.9 – Slope layer for the LGM

The next step was the creation of a distance-to-site layer by means of the *Euclidean Distance* tool. This tool was chosen because it allows the inclusion of a barrier raster to influence the resulting layer. This tool was run separately for the LGM and MIS3 with the corresponding ice sheets used as barriers. The *Euclidean Distance* tool calculates the closest distances from the 'input raster or feature source data'; when creating the 'distance-to-site' layer, the input raster is the table with all of the sites' details (for the LGM data, overall MIS 3 and MIS3 interstadial/stadial), thus generating a raster indicating which sites are closest to which. In addition, this tool offers the opportunity of determining a 'barrier raster', which in the case of this project are the different ice sheet rasters. The generated rasters (Fig. 3.10 and 3.11) therefore present (in yellow) the shortest distance between the sites.

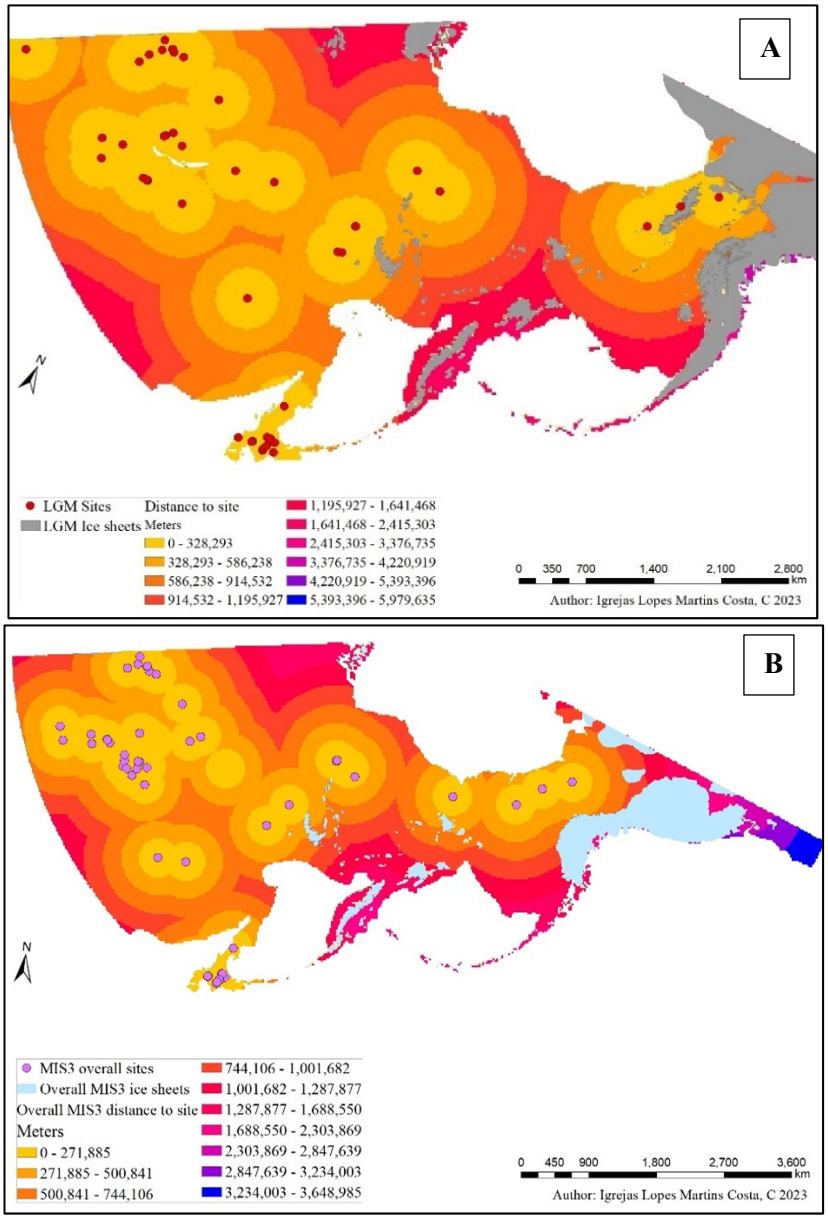

Figure 3.10 – Distance-to-site (in m) (*Euclidean Distance* tool) rasters for the LGM (A, above) and overall MIS3 (B, below)

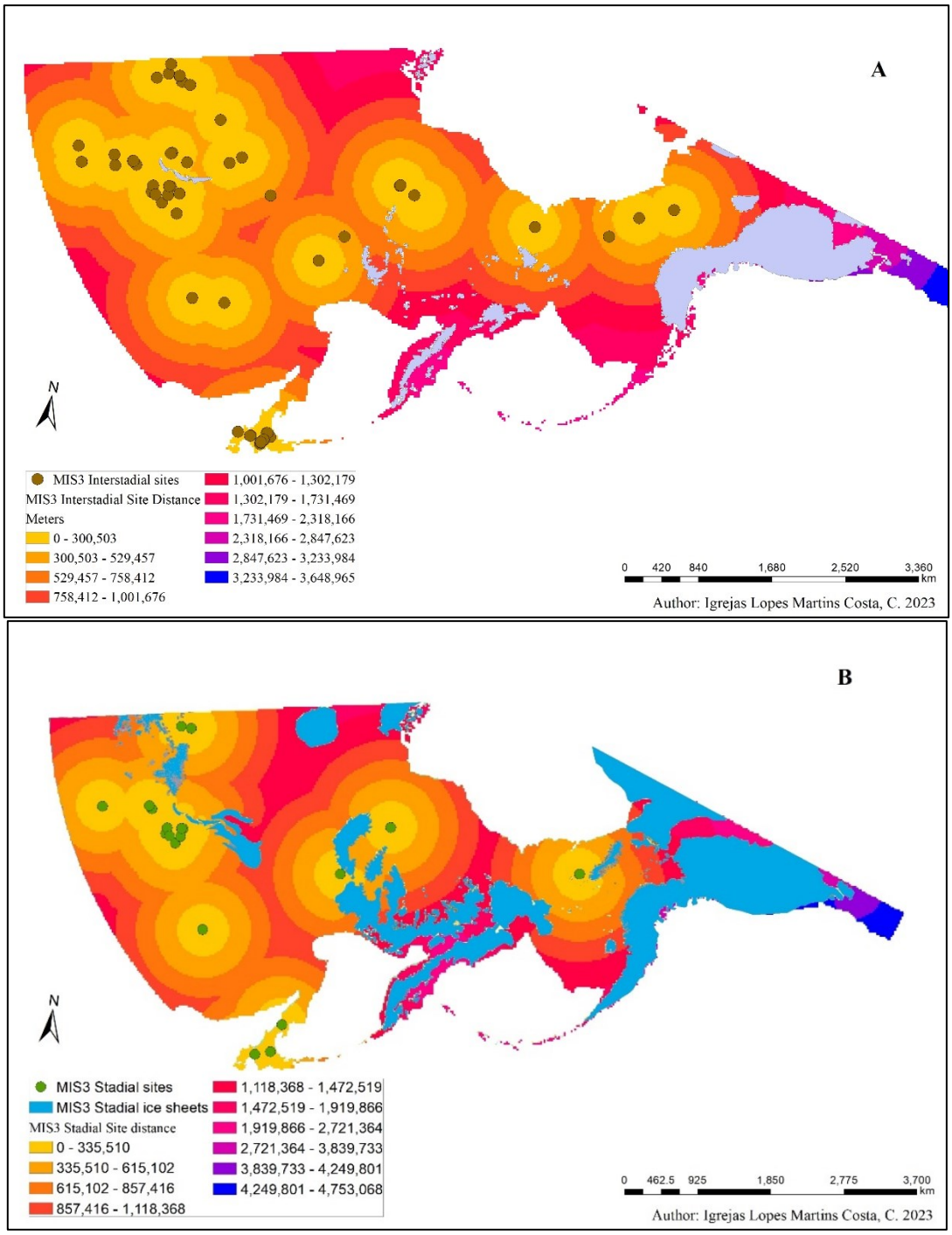

Figure 3.11 – Distance-to-site (in m) (*Euclidean Distance* tool) rasters for the MIS3 stadial (A, above) and interstadial (B, below)

While using the same tool (*Euclidean Distance*) it was also possible to create a distance-to-water (in m) layer for both the LGM (A) and MIS3 (B) (Fig. 3.12). This raster is important for it indicates the distance between each river stream. The same distance-to-water results appear for the MIS3 stadial and interstadial data for they both use the MIS3 river modelling; the results for the Overall MIS3 and LGM water-to-distance rasters are incredibly similar because the modelled river systems are basically the same. The main difference in all the distance-to-water layers are the ice sheets, for they are used as 'obstacles'.

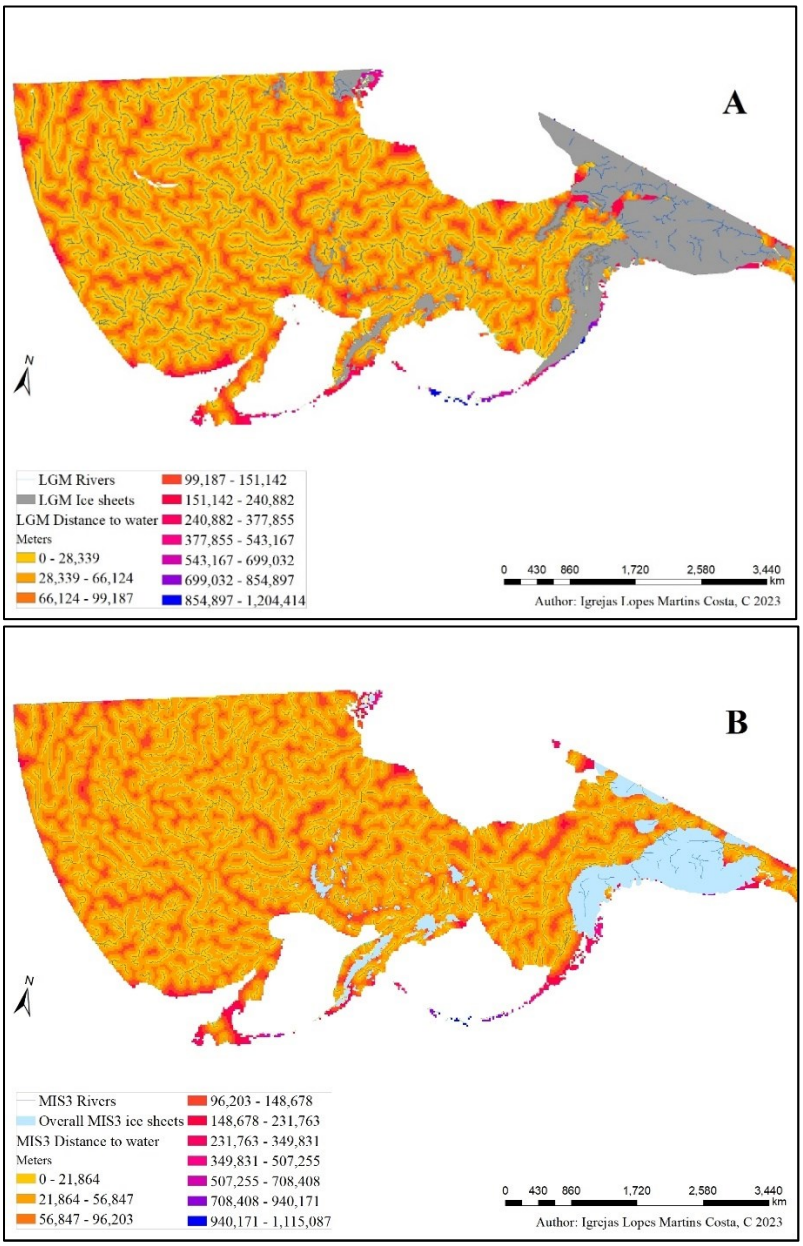

Figure 3.12 - Distance-to-water layers for the LGM (A) and overall MIS3 (B) palaeo-river systems with Batchelor et al. (2019)'s LGM and Overall MIS3 ("30ka best estimates") ice sheet reconstructions

Finally, the *Weighted Sum* tool was used to combine all of the previously mentioned layers in order to create a cost raster. An important aspect of this tool is that it is possible to specify each layer's weight, i.e., the raster's attractiveness to humans First, we used the LGM data to experiment with different weightings for the weighted cost surface (described in chapter IV, below). Once the weightings were established we proceeded with the analysis. Once a weighted surface is produced, the *Cost Connectivity [Spatial Analyst]* tool is run producing a least-cost path (LCP) between known sites, as indicated by the connectivity path, as well as the neighbouring paths, which suggest alternative routes. The results are presented in the following chapter.

A total of six LCPs (Table 1) were produced for each timeframe: one with all of the sites per timeframe where no point of origin or of destination are specified, three where a point of origin is specified (Yana RHS, Mal'ta and Kashiwadai-1), one where no point of origin or destination is specified but where experimental sites are included, and for the LGM final LCP was produced using experimental sites specifying Kashiwadai-1 as the point of origin. This was done to test the difference between the Coastal Migration Model's southern route (with the PSHK peninsula as a starting point) and a more continental based, Eastern Siberian point of origin (near lake Baikal). The sites assigned as the 'point of origin' were chosen because they are present in both temporal groups and because they are crucial to the understanding of Late Palaeolithic archaeology in their respective areas (*cf. Chapter V*). The experimental LCP with specified points of origins was not conducted for the MIS3 stadial model due to the small number of sites involved ($n = 20$).

Model	Figure	Timeframe	Point of origin	Experimental sites
1	4.4	LGM	None	None
2	4.5	LGM	Yana RHS	None
3	4.6	LGM	Mal'ta	None
4	4.7	LGM	Kashiwadai-1	None
5	4.8	LGM	None	Yes
6	4.9	LGM	Kashiwadai-1	Yes
7	4.11	Overall MIS3	None	None
8	4.12	Overall MIS3	Yana RHS	None
9	4.13	Overall MIS3	Mal'ta	None
10	4.14	Overall MIS3	Kashiwadai-1	None
11	4.15	Overall MIS3	None	Yes
12	4.17	MIS3 stadial	None	None
13	4.19	MIS3 interstadial	None	None

Table 1 – Summary table of the modelling experiments

A second set of experimental models, where random sites ('Experimental sites') were created in the now- submerged Central Beringia to compensate for a lack of archaeological survey in this region, was conducted for all timeframes. In order to generate these Experimental Sites, we had to firstly calculate the area of the now-submerged and now-exposed landmasses by first separating those two using *Raster Calculator*. By running the expression *lgm_dem_proj <= 0* , the two landmasses were separated, with the value '0' representing the distinction between land and water in the present. By *Reclassifying* the two landmasses, the two could be properly separated. Afterwards, each raster had to be transformed into polygons (*Raster to Polygon*) before being compacted (*Dissolve*) in order to each landmass be viewed as individual polygons, instead of multiple polygons joined together. Once having these two landmasses (indicating the *Exposed* and *Submerged* landmasses), it is important to *Erase* the extent of the icesheets from the 'Submerged_lgm' polygon in order to avoid generating *x* sites under the icesheets. The area for each could be calculated: 19738416.132km² for the former, and 3878972.8452km² for the latter. Then, the number of sites required for the now-submerged landmass is calculated: having 51 sites dated to the LGM in the now-exposed landmass, we calculate:

$$x = 51 / 19738416.132 * 3878972.84524 = 10.02$$

which indicates that 10 sites could be generated as *Random numbers* for the now-submerged landmass, however the minimum number allowed for this tool to work is 11 and we therefore generated 11 new sites.. In addition, the minimum allowed distance between the *x* sites was specified as 100kmin order to allow for the possibility of clusters of sites being generated (as evidenced by the proximity of Dvuglazka Rockshelter and Novoselovo-6 in Khakassia, site ID 15 and 58 respectively; or Krasny Yar 1 and Mal'ta in Irkutsk Oblast, side ID 37 and 49, respectively), but located far enough apart to include much of the now-submerged landmass. Four sites were generated in locations further south (*x*2, *x*3, *x*5 and *x*9) (Fig. 3.13).

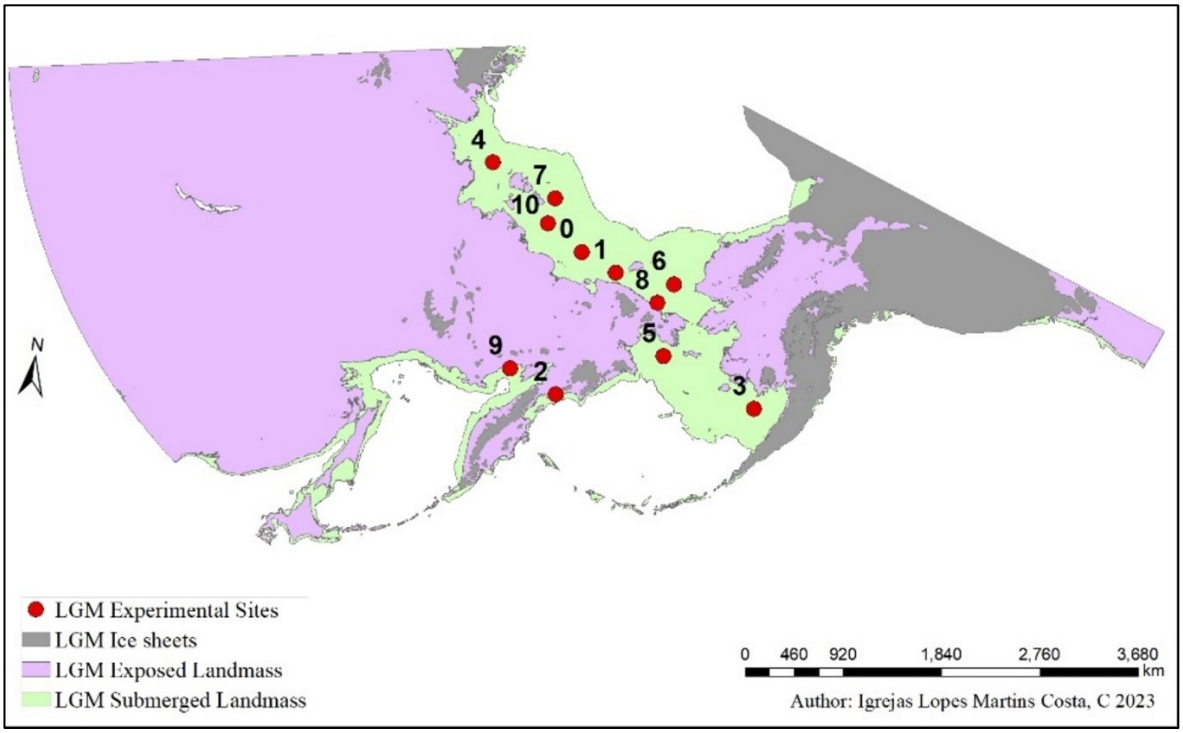

Figure 3.13 – Separation of currently exposed (lilac) and currently submerged (light green) landmasses and the LGM Experimental sites (red)

Following the merging of the Experimental and the LGM sites, LCP was modelled using the same parameters as previously, and compared with previous results in order to see if new paths were created. Following the models previously mentioned, this model was created with a cost raster constituted by a distance-to-site weighted at 1%, a slope layer weighted at 29% and a distance-to-water layer weighted at 70%.Through this method, we can test the potential impact of incomplete archaeological sampling on the LCP analysis

Next, we followed the same procedure to test the MIS3 data (Fig. 3.14). We calculated the area of the now-submerged (blue) and now-exposed (green) landmasses (19745444.4431 and 3518886.99136 km² respectively). There are sixty-one archaeological sites associated with the MIS3 (stadial and interstadial together). Thus, we were able to calculate that 11 randomly generated sites should be produced using the formula:

$$x = 61 / 19745444.4431 * 3518886.99136 = 10.87$$

The randomly generated sites are positioned equally in the northern section of the now-submerged landmass and in its southern section, although they are mostly located by the Western Beringian coast (Fig. 3.14).

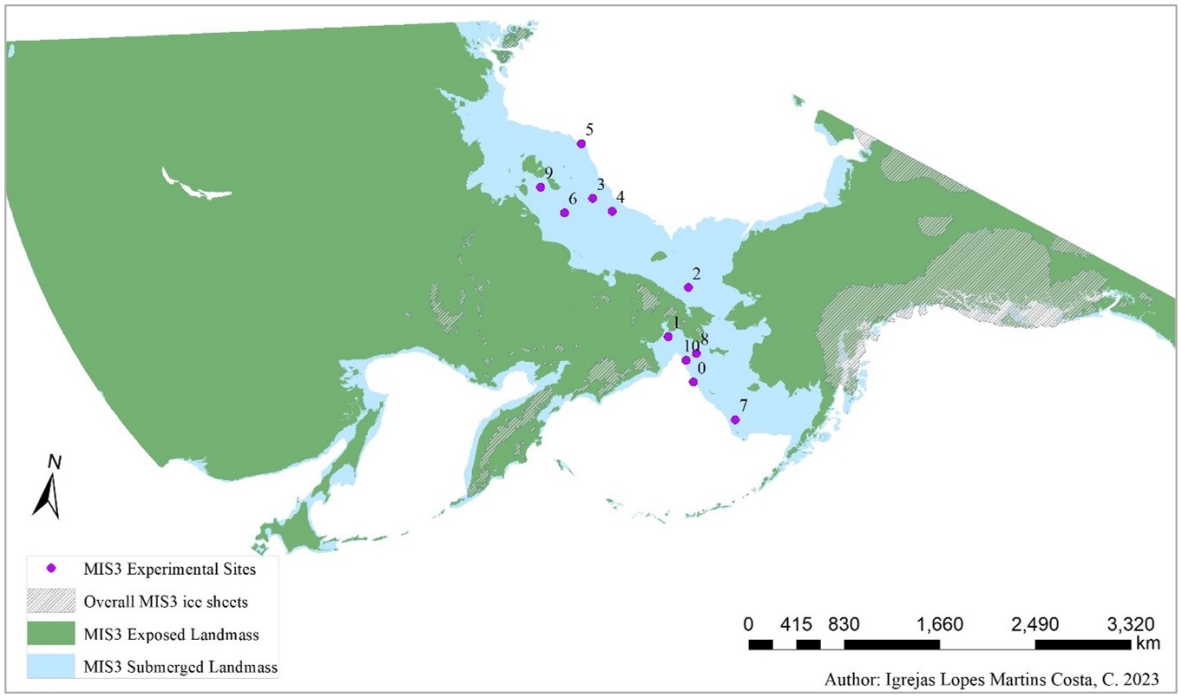

Figure 3.14 – Separation of the now-exposed (green) and now-submerged (blue) landmasses and the position of the MIS3 Experimental sites (purple)

The results of these experiments are presented in the following chapter (*cf. Chapter IV*).

Chapter IV – Results

In this chapter the results of the different modelling experiments described above (Table 1) are presented. We begin with the LGM (Temporal Group 2) because it is timeframe that best aligns with the paleogenetic data (and the "standstill hypothesis").

IV.I. Temporal group 2, LGM

This temporal group extends from 22.000 to 18.000 cal yr BP. It contains fifty-one archaeological sites, most of which are located near the Yenisei River in the Khakassia Republic (Fig. 4.1 A, *n* =11), in the PSHK Peninsula (Fig. 4.1 C; *n* =18) and surrounding Lake Baikal, in the Irkutsk Oblast and Mongolia (Fig. 4.1 D; *n*=9). The sites located in Eastern Beringia, i.e., modern-day Alaska and Yukon Territory, are few (Fig. 4.1 B; *n* =3) but remain central to this project since they provide the only evidence the BLB was crossed at this time. This temporal group provides information concerning the viability of the BLB during the LGM for early humans and the possibility that a "Standstill Population" might have existed there.

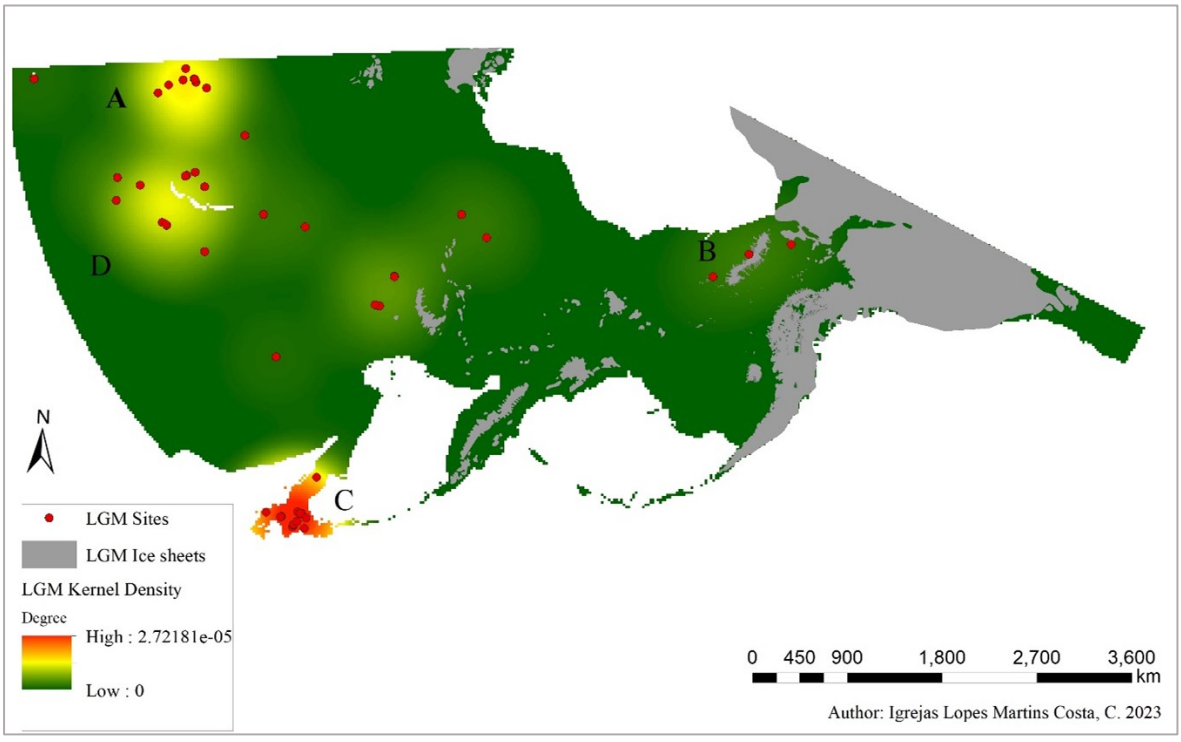

Figure 4. 1 – Map indicating the kernel density of the LGM sites present in this project's database. A – Khakassia Republic; B – Eastern Beringia; C – PSHK Peninsula; D – Cis-Baikal

We tested various combinations of weights for slope, distance-to-site and distance-to-water before selecting attributed weights of 29% for the slope, 70% for the distance-to-water and 1% for the distance-to-site layers (Fig. 4.2).

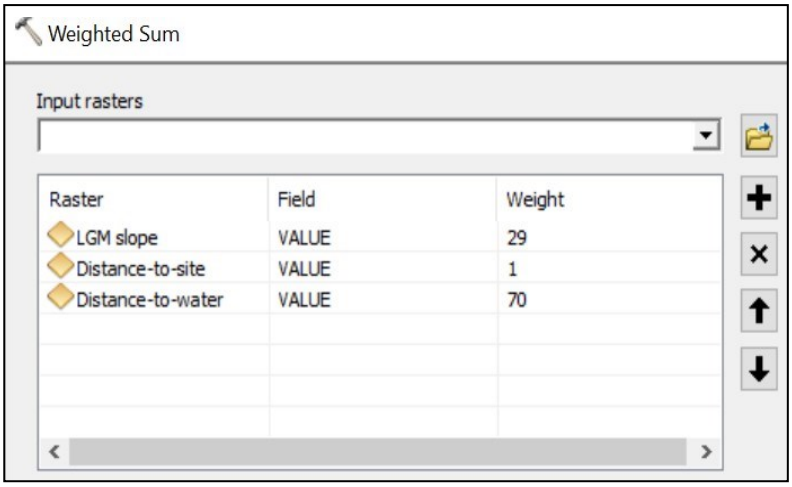

Figure 4.2 – Weighted Sum tool with the rasters and respective weights

These weights were chosen following multiple experiments; the objective was to obtain a realistic LCP path with these values. The distance-to-water raster is given a value of 70% indicating it is to be viewed as the 'preferrable' geographical feature to be considered when generating the LCP; the slope raster is given a value of 29% indicating steep slopes are to be avoided (they are not cost-efficient). The distance-to-site raster is given a symbolic 1% value as an indicator of a human factor: humans moving in the landscape are assumed to gravitate towards sites they already know. The weight of this variable is low because we are aware that gaps in the archaeological record mean only a small fraction of sites are likely to be recorded.

While modelling the least-cost path for the LGM, it was quickly noticed how important the use of a 'distance-to-water' raster is for the establishment of realistic pathways; in fact, whenever the raster was not included in the creation of a cost raster (through the *Weighted Sum* tool), or when there were no manipulations of the weights (Fig. 4.3), the resulting paths crossed mountain ranges and moved in semi-straight lines across long distances on what constitutes an uneven landscape. These results were not deemed realistic.

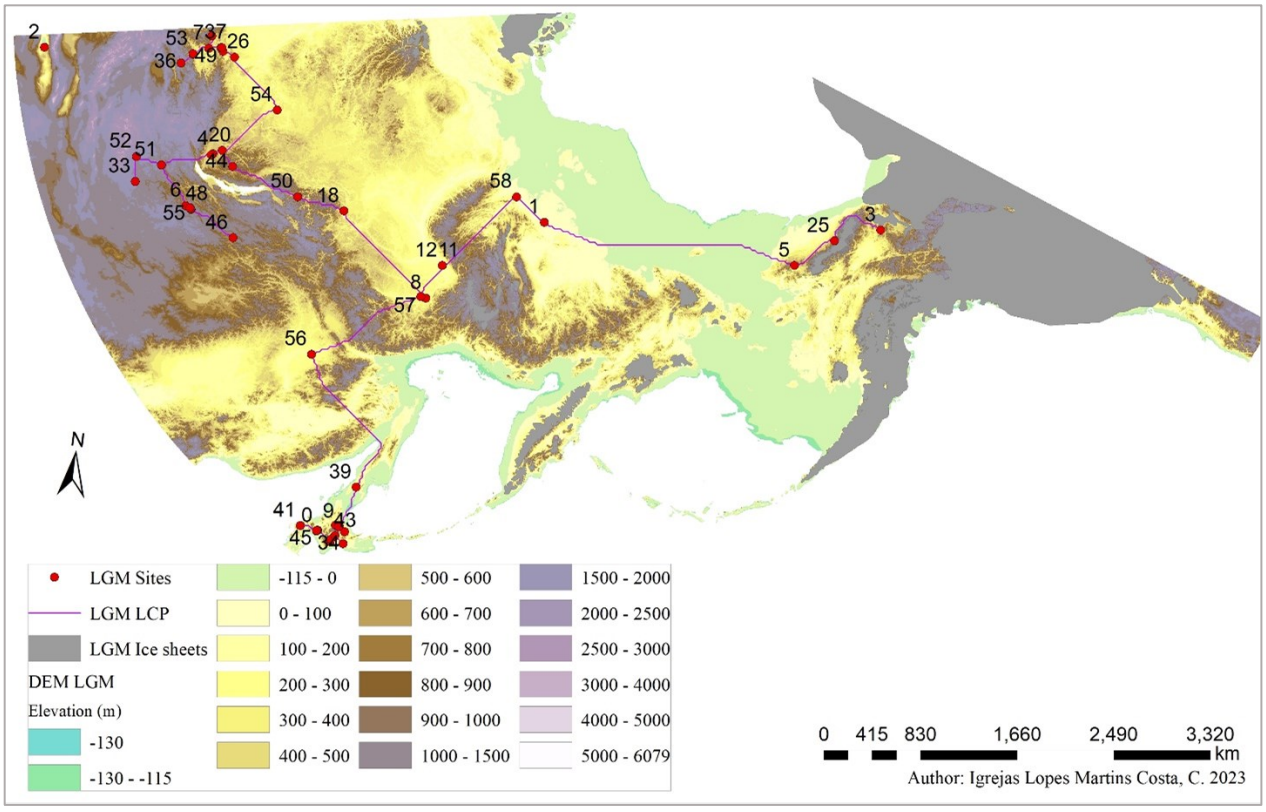

Figure 4.3 – LGM Least Cost Path generated with the distance-to-water raster but without manipulating the raster weightings. Sites present: 0. Ankarito 7; 1. Berelekh; 2. Bibi 5; 3. Bluefish Caves ; 4. Buret; 5. Burial Lake; 6. Chitkan; 7. Dvuglazka Rockshelter; 8. Ezhantsy; 9. Hattoridai 2; 10. Hokuto; 11. Ikhine I; 12. Ikhine II; 13. Kamishirataki 2; 14. Hamishirataki 5; 15. Kamishirataki 8; 16. Kashiwadai 1; 17. Kawanishi-C; 18. Khayrgas Cave; 19. Kiusu 5; 20. Krasny Yar 1; 21. Kukouminami A; 22. Kurtak-3; 23. Kurtak-4; 24. Kyushiarataki 3; 25. Lake E5; 26. Listvenka; 27. Maininskaia East; 28. Maininskaia West; 29. Malaya Siya; 30. Mal'ta; 31. Marukoyama; 32. Minamimachi 2; 33. Moil'tyn-am; 34. Nakamoto; 35. Nitto; 36. Nizhnii Idzhir-1; 37. Novoselovo-6; 38. Ochiai; 39. Ogonki 5; 40. Okushirataki 1; 41. Pirika 1; 42. Priiskovoye; 43. Shimaki; 44. Shishkino 8; 45. Shukubai-Kaso (Sankakuyama); 46. Sokhatino 4; 47. Studenoe 1; 48. Studenoe 2; 49. Tarachikha; 50. Tesa; 51. Tolbor-15; 52. Tsatsyn-Ereg 2; 53. Ui 1; 54. Ust'-Kova; 55. Ust'-Menza 2; 56. Ust'-Ulma 1; 57. Verkhne-Troitskaya; 58. Yana Rhino Horn Site (RHS)

There were no obvious differences between the paths obtained when no distance-to-water layer was used in the weighted sum raster and when it was included but the weights were not manipulated, in both cases the LCPs obtained illustrate a crossing of the Verkhoyansk Mountain Range in a steep region, where a more obvious and less costly solution would have been to use the nearby river system. This result is problematic because following the river would have been the most cost-efficient path. By adjusting the cost raster's weights to the values presented in previously (Fig. 4.2), a more realistic path (Model #1) governed by the river system is produced (Fig. 4.4, orange). The alternative path generated with Model #1 is considerably similar to the LCP with the exception of a few diversion. Therefore, we adjusted the weighting in all our models accordingly.

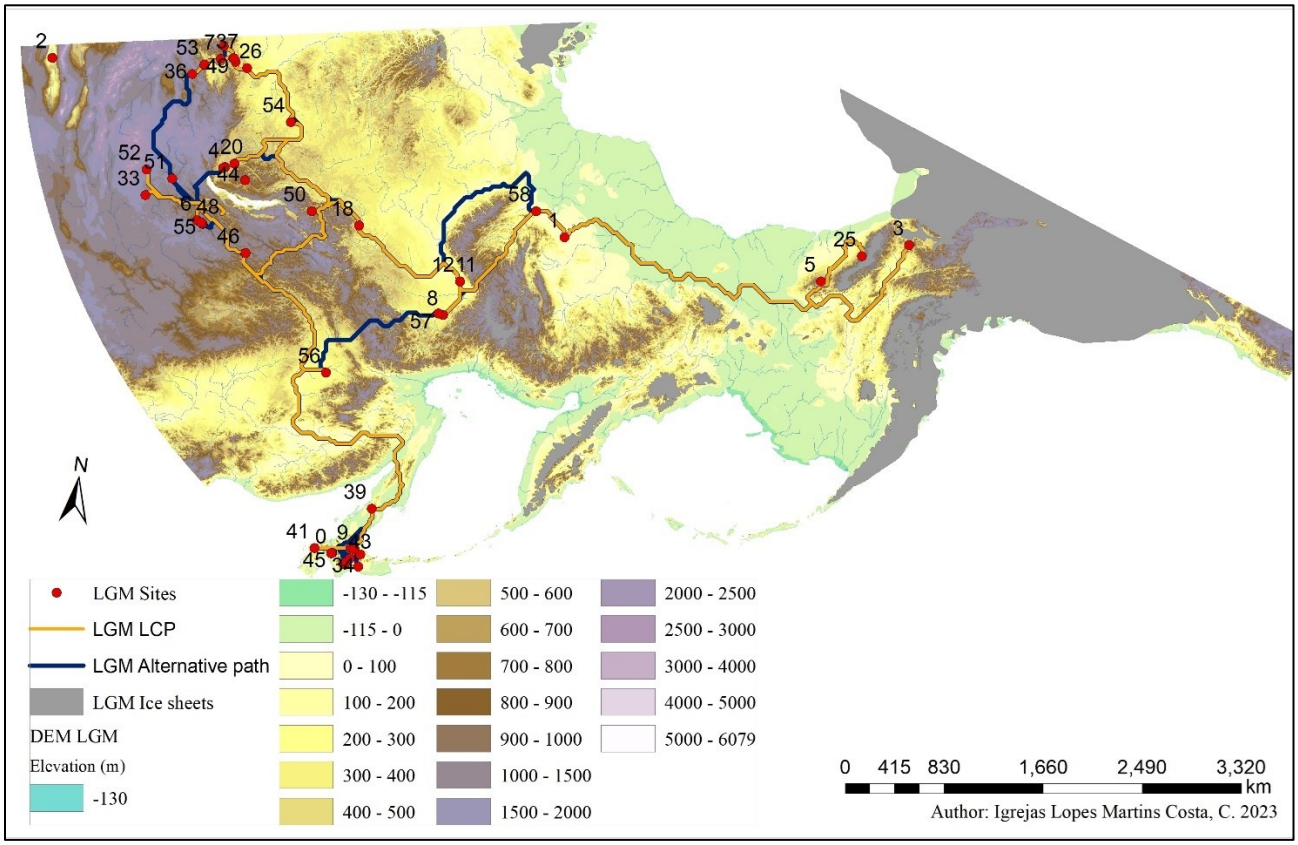

Figure 4.4 – Comparison between LCP (orange) and alternative path (dark blue) created based on the presence of a distance-to-water layer purposefully weighted at 79% (Model #1). Sites present: 0. Ankarito 7; 1. Berelekh; 2. Bibi 5; 3. Bluefish Caves ; 4. Buret; 5. Burial Lake; 6. Chitkan; 7. Dvuglazka Rockshelter; 8. Ezhantsy; 9. Hattoridai 2; 10. Hokuto; 11. Ikhine I; 12. Ikhine II; 13. Kamishirataki 2; 14. Hamishirataki 5; 15. Kamishirataki 8; 16. Kashiwadai 1; 17. Kawanishi-C; 18. Khayrgas Cave; 19. Kiusu 5; 20. Krasny Yar 1; 21. Kukouminami A; 22. Kurtak-3; 23. Kurtak-4; 24. Kyushiarataki 3; 25. Lake E5; 26. Listvenka; 27. Maininskaia East; 28. Maininskaia West; 29. Malaya Siya; 30. Mal'ta; 31. Marukoyama; 32. Minamimachi 2; 33. Moil'tyn-am; 34. Nakamoto; 35. Nitto; 36. Nizhnii Idzhir-1; 37. Novoselovo-6; 38. Ochiai; 39. Ogonki 5; 40. Okushirataki 1; 41. Pirika 1; 42. Priiskovoye; 43. Shimaki; 44. Shishkino 8; 45. Shukubai-Kaso (Sankakuyama); 46. Sokhatino 4; 47. Studenoe 1; 48. Studenoe 2; 49. Tarachikha; 50. Tesa; 51. Tolbor-15; 52. Tsatsyn-Ereg 2; 53. Ui 1; 54. Ust'-Kova; 55. Ust'-Menza 2; 56. Ust'-Ulma 1; 57. Verkhne-Troitskaya; 58. Yana Rhino Horn Site (RHS)

Next, we set out to create the different models, or experiments, described in Table 1 which are designed to test different points of origin and the possible impact of taphonomic factors (specifically the lack of survey data in Central Beringia).

In the first kind of experiment, paths were drawn following a specification of an 'origin' site (Yana, Mal'ta and Kashiwadai) while also specifying all other sites as 'destinations'. In order to do so, the 'origin site' must be isolated into its own shapefile, while the rest of the database is in another. While the workflow does not change much from the previous model, the slight difference is the usage of the 'origin' site as the input raster for the 'distance-to-site' raster and of the 'destinations' when creating the paths – i.e., through the tool *Cost Connectivity*). The results are as follows.

The LGM-Yana experiment (Model #2) uses the Yana RHS site as the *origin* point – herein called 'Yana Origin' – and all other LGM sites as the possible *destination* points – herein called ' Yana Destinations'(Fig. 4.5). When comparing the models #1 and #2 (blue and red, respectively), the LCPs generated by the Cost Connectivity tool are rather similar in Beringia – albeit with small detours. The bigger changes in routes taken can be seen West of Verkhoyansk Mountain Range.

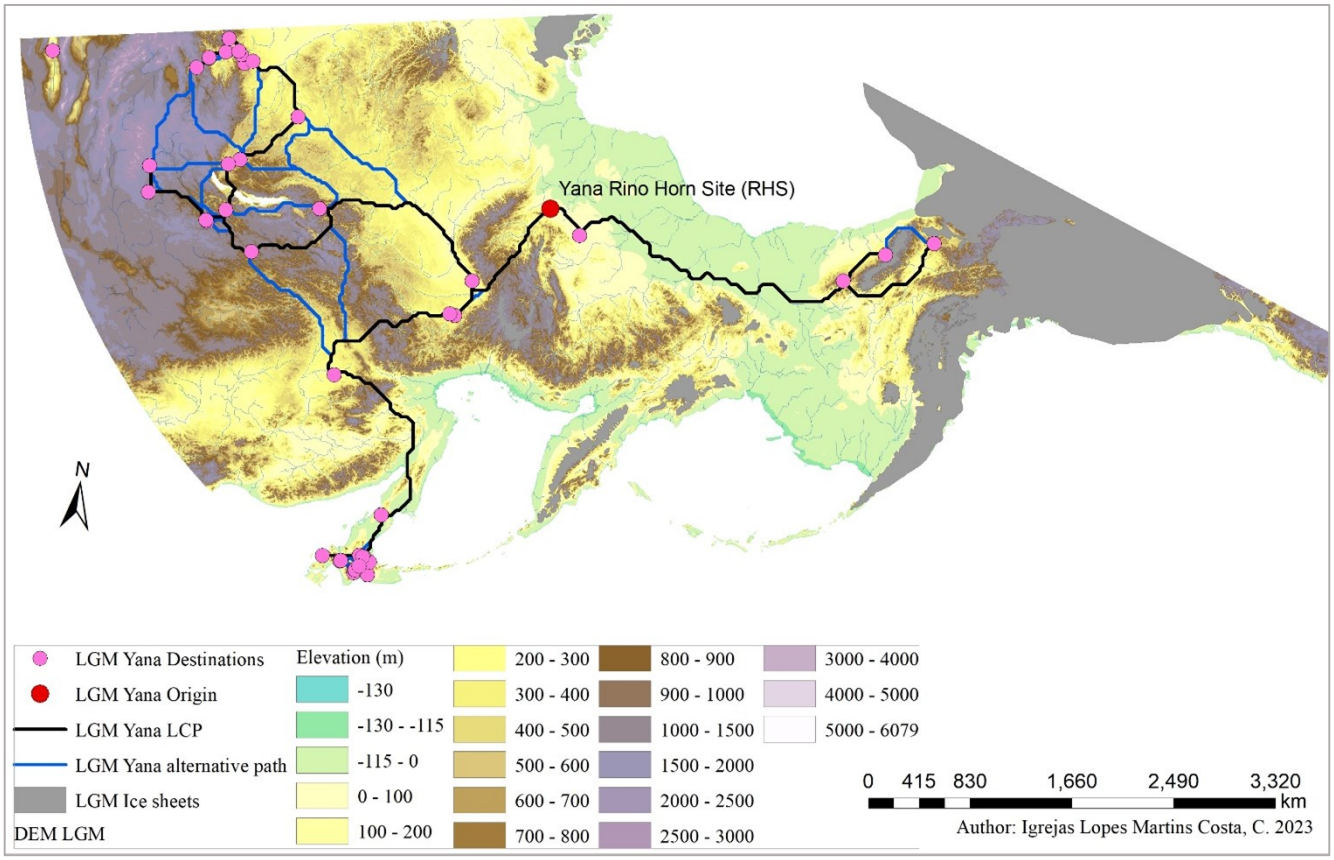

Figure 4.5 – Model #2; LCP (black) and alternative path (blue) generated upon establishing Yana as the origin point (red; 'LGM Yana Origin')

The LGM-Mal'ta experiment (Model #3) is marked by the isolation of the Mal'ta site as the point of origin ('LGM Malta Origin') and the agglomeration of all other LGM sites as the destination points, herein 'LGM Malta Destinations' (Fig. 4.6). Not much difference can be seen between originating out of Yana and Mal'ta, other than slight deviations.

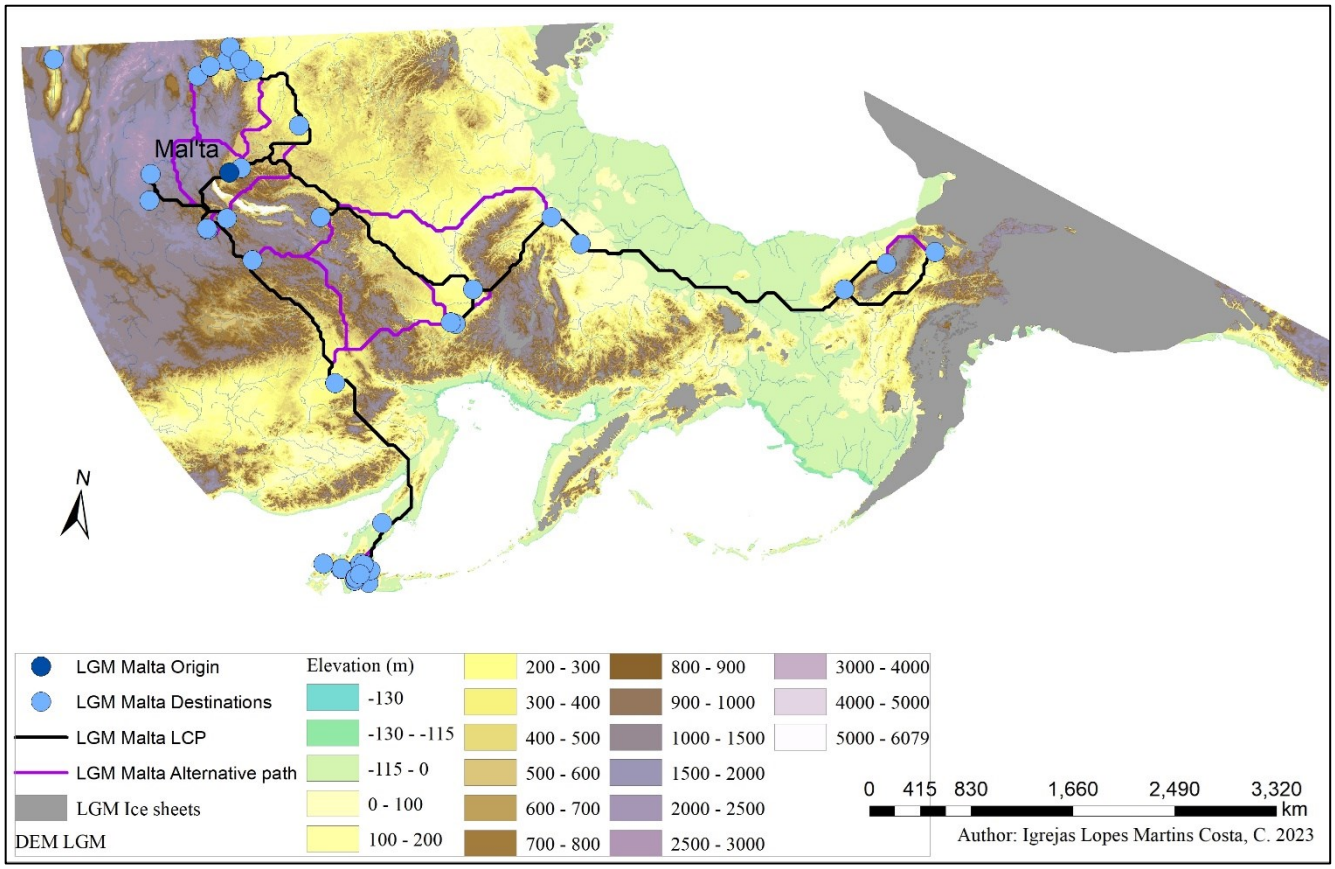

Figure 4.6 – Model #3; LCP (black) and alternative paths (purple) generated upon establishing Mal'ta as the origin point (dark blue; 'LGM Malta Origin')

The LGM-Kashiwadai 1 experiment (Model #4) is marked by the isolation of the Kashiwadai 1 site as the point of origin ('LGM Kashiwadai Origin') and the agglomeration of all other LGM sites as the destination points, herein 'LGM Kashiwadai Destinations' (Fig. 4.7). Not much difference can be seen between originating out of Yana and Mal'ta, other than slight deviations.

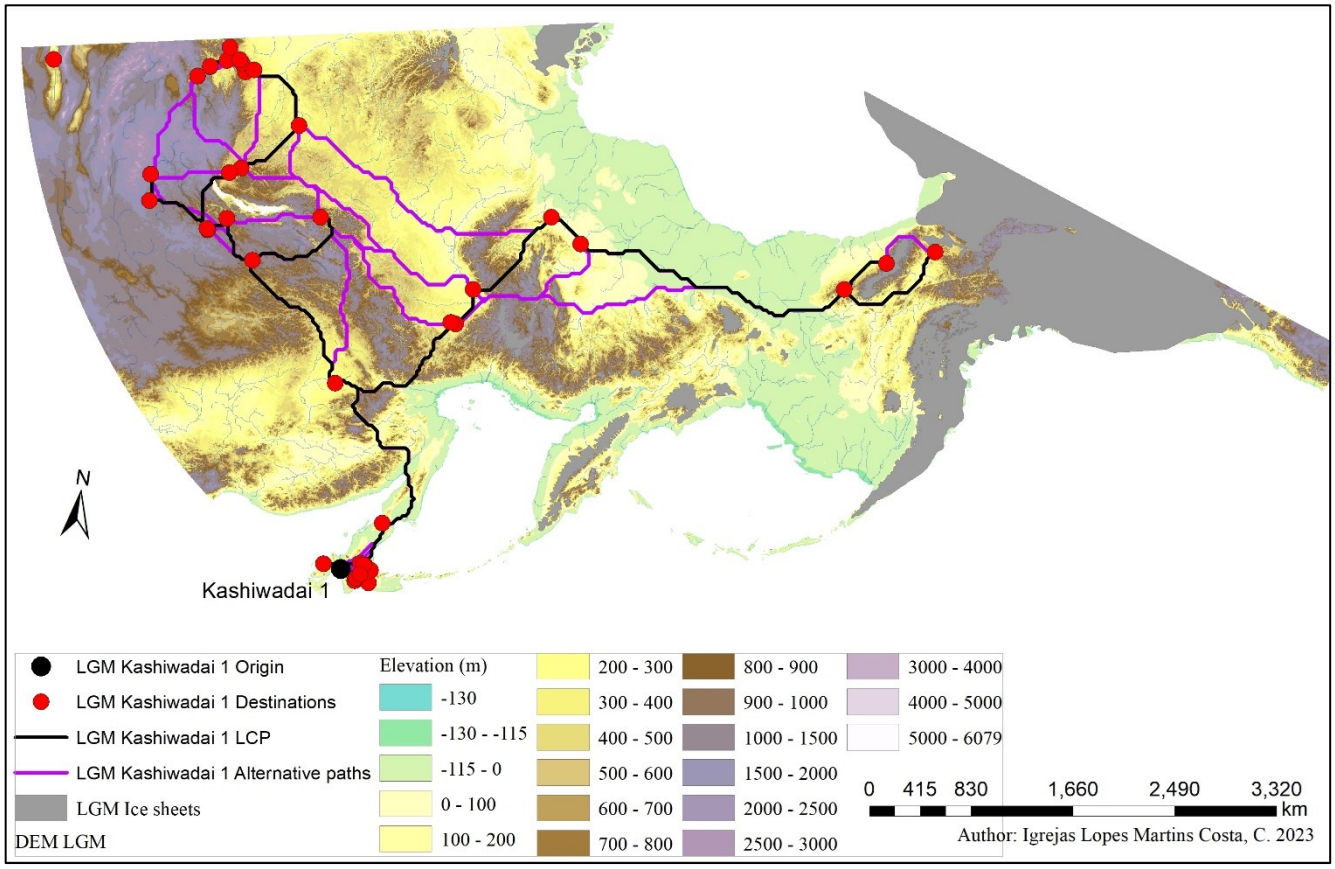

Figure 4.7 – Model #4; LCP (black) and alternative paths (purple) generated upon establishing Kashiwadai 1 as the origin point (black; 'LGM Kashiwadai 1 Origin')

Model #4 tests the proposition that the PSHK Peninsula was home to the "source" population that populated Beringia and eventually, North America. For this model we established Kashiwadai-1 (#30) as the point of origin (Fig. 4.7). The biggest difference between this model and model #1 is the generation of a route going around Lake Baikal. These paths are therefore very similar no matter their point of origin. Interestingly, the paths indicating neighbouring routes with a starting point at Kashiwadai-1 show multiple routes crossing the Verkhoyansk Mountain Range. This variety of paths could indicate the river valleys crossing the mountain range could have been preferred for human movements, or perhaps they are indicative of a bias in the archaeological record.

Following these experiments, it can be noticed that although the LCP produced in these experiments might diverge somewhat in different parts of the map, they all come together when crossing the BLB albeit with slight alterations. In addition, all models presented here propose a southern route to reach the easternmost point in Eastern Beringia thought to have been inhabited during the LGM - Bluefish caves. This leads us to wonder if this is due to a lack of archaeological sites in the now-submerged land bridge. In order to answer this question, we set out to discover whether adding experimental sites results in a different pattern (model #5).

In model (#5) the LGM sites are joined with the randomly generated Experimental sites, without establishing a point-of-origin (Fig. 4.8). This model generated multiple paths crossing the Verkhoyansk Mountain Range, as was seen with the previous model (#4). One new element of this model is the appearance of a southern coastal path connecting Verkhne-Troitskaya and the experimental sites n° 9, 2, 5 and 3. This LCP (purple) southern path, joined to WB through a branch of the alternative path (green) is interesting and could indicate the presence of two migratory paths, one following the southern CB coast, and a northern inland path joining Wrangel Island to the EB lakes. Similar paths have been generated when establishing Kashiwadai as the point of origin (Model #6; Fig. 4.9) and including the experimental sites.

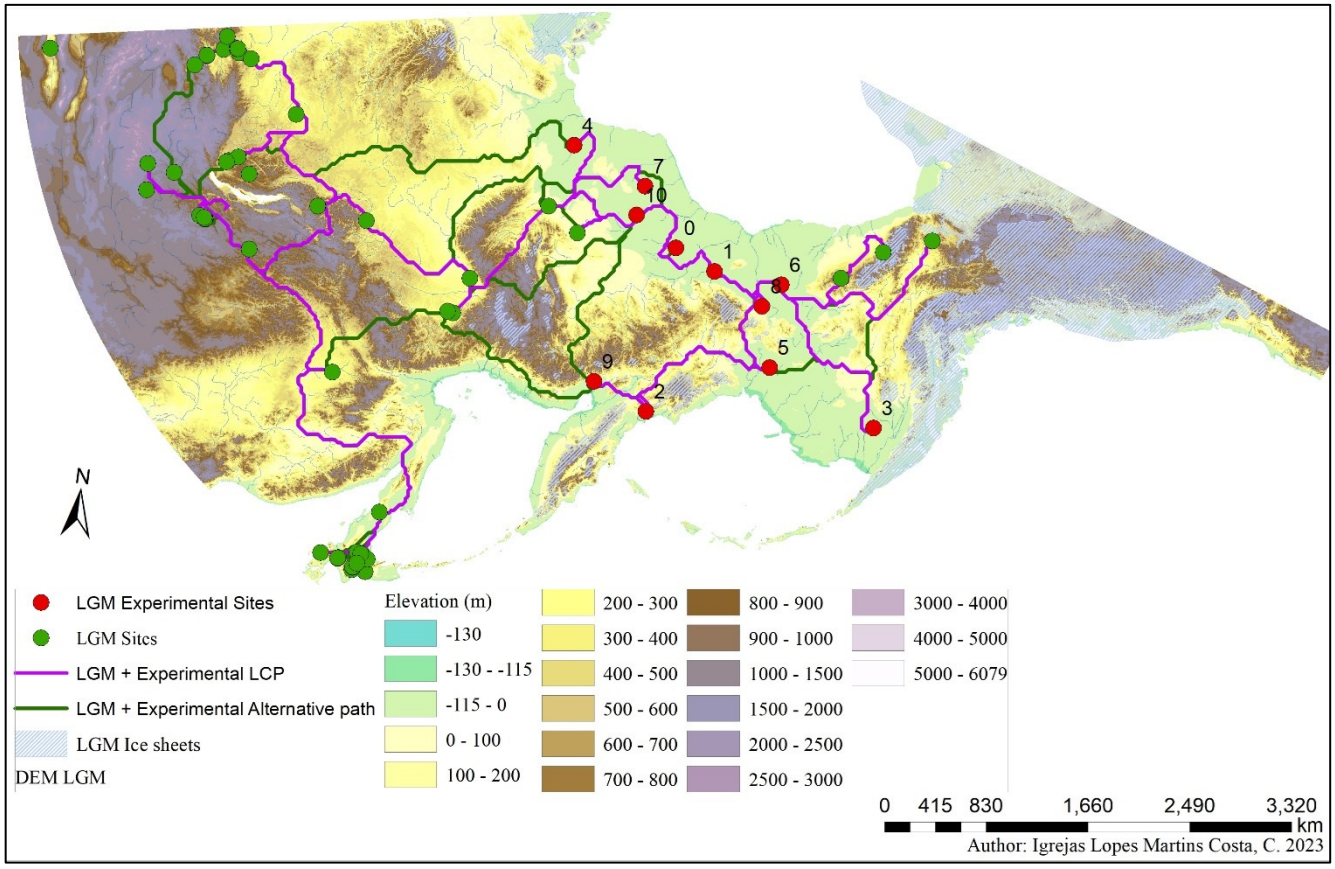

Figure 4.8 – Model #5; LCP (purple) and alternative path (green) generated upon joining both our database's LGM sites (green) and our randomly generated (*Random points*) experimental sites (red), without establishing a point of origin

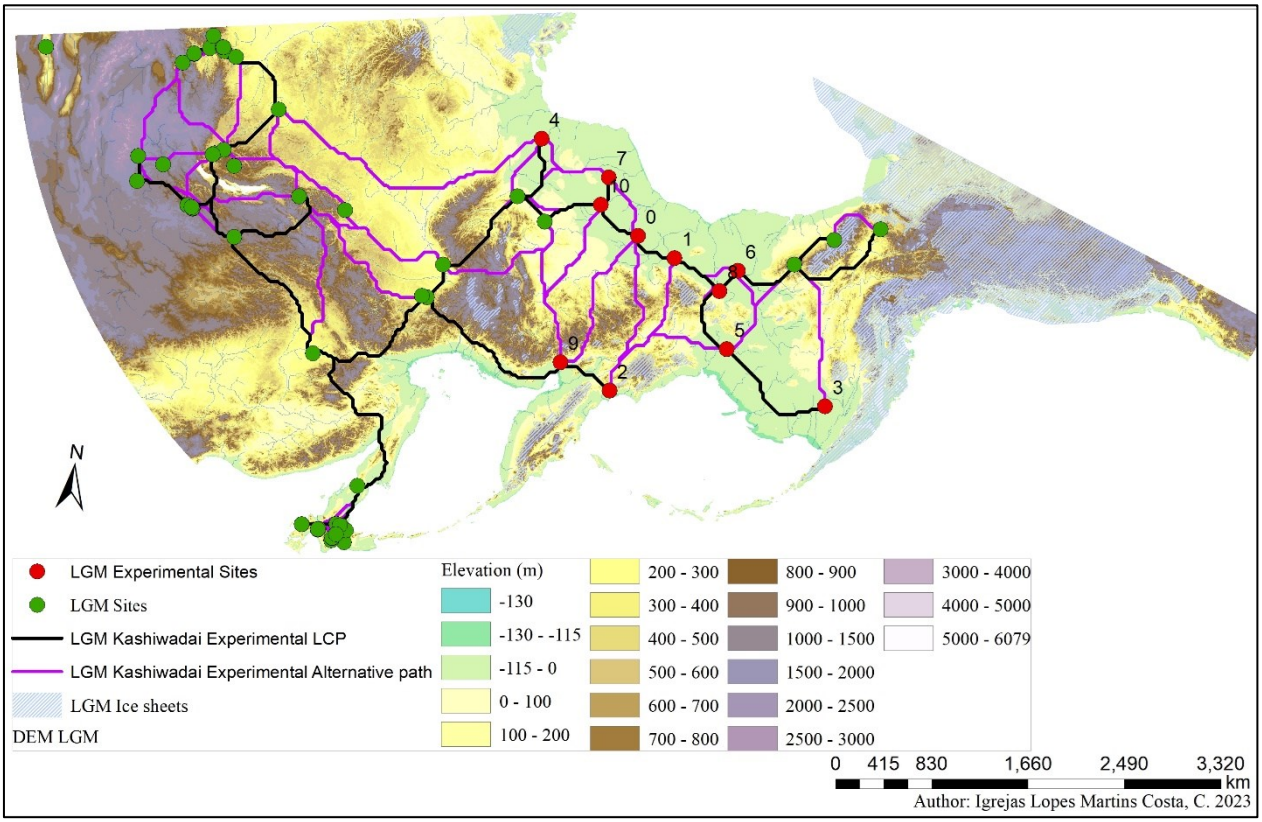

Figure 4.9 – Model #6; LCP (black) and alternative paths (purple) generated upon joining both our database's LGM sites (green) and our randomly generated sites (red), while having established Kashiwadai 1 as the point of origin.

IV.II. Temporal group 1, MIS3

Temporal group 1 ranges from 35.000 to 23.000 cal yr BP, which includes 13 stadial and interstadial events. We ran 8 experiments with this temporal group (see Table 1). The first experiment uses all MIS 3 sites ('overall MIS3 sites'), whereas the other two use the Stadial data – i.e., sites whose radiocarbon dates yielded ages corresponding to Greenland stadial stages – for models # and the Interstadial data for models #. Model # uses Batchelor et al. (2019)'s 'max' extent of the 30ka icesheets and model # uses Batchelor et al. (2019)'s 'min' extent of the 30ka icesheets.

IV.II.I Overall MIS3 sites

The overall MIS3 map contains sixty-one sites (Fig.4.10) with three distinct clusters of sites in modern-day Mongolia and Transbaikal (A), in the Khakassia Republic (B), as well as in the PSHK Peninsula (C). As opposed to the LGM (*cf: Fig. 4.1*), during the MIS3 there were more sites scattered in between the three clusters (A,B,C). We maintain the same three Eastern Beringian sites (Burial Lake, Lake E5 and Bluefish

Caves, #8, 44 and 6, respectively) despite rather tenuous evidence for their being inhabited during MIS 3 (*cf. Chapter V*). The importance of these more scattered sites is the possibility of their generating more varied LCPs throughout the experimental models.

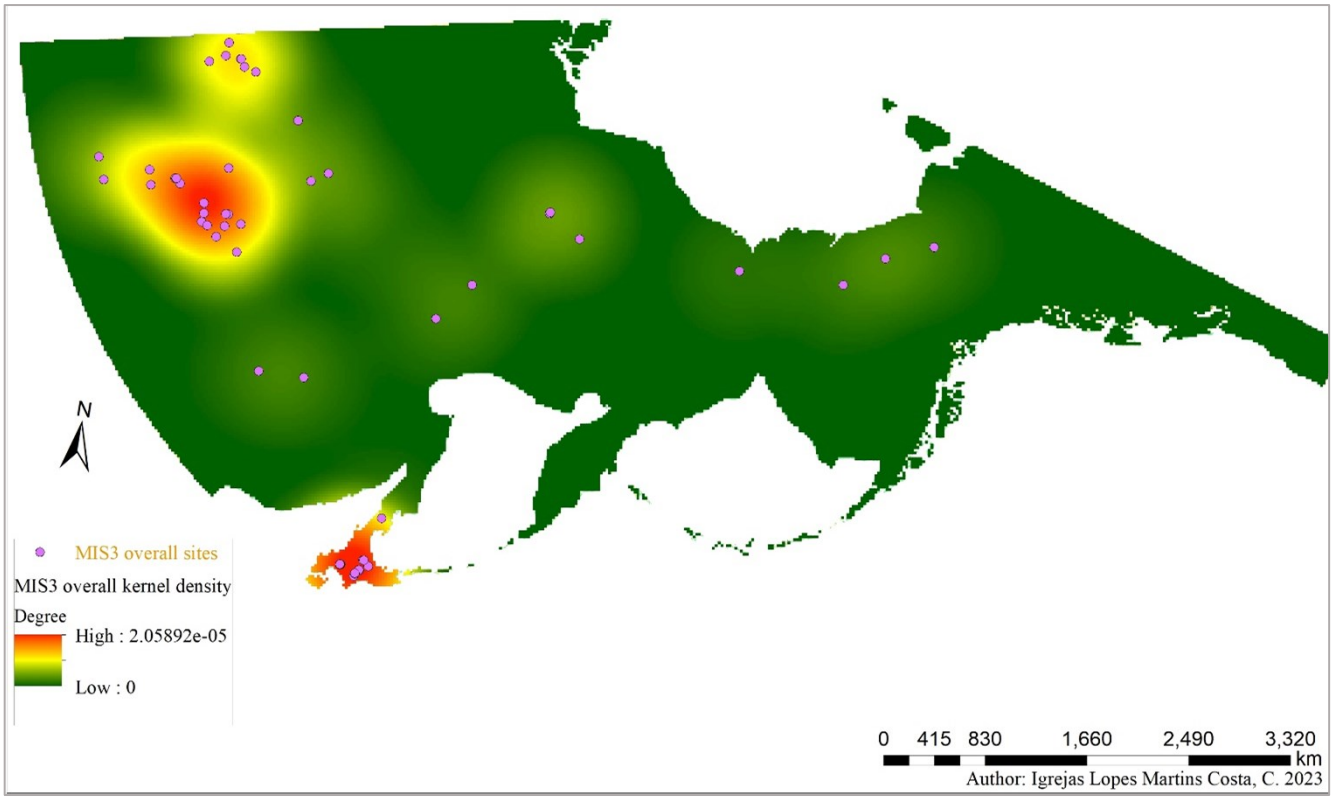

Figure 4.10 - Map indicating the kernel density of the Overall MIS3 sites present in this project's database. A – Khakassia Republic; B – Eastern Beringia; C – PSHK Peninsula; D – Cis-Baikal

By following the workflow described in chapter III, the MIS 3 experiments (Fig. 4.11) generate a model (#7) similar to the ones obtained with the LGM data with a predominantly northern path between Western and Eastern Beringia.

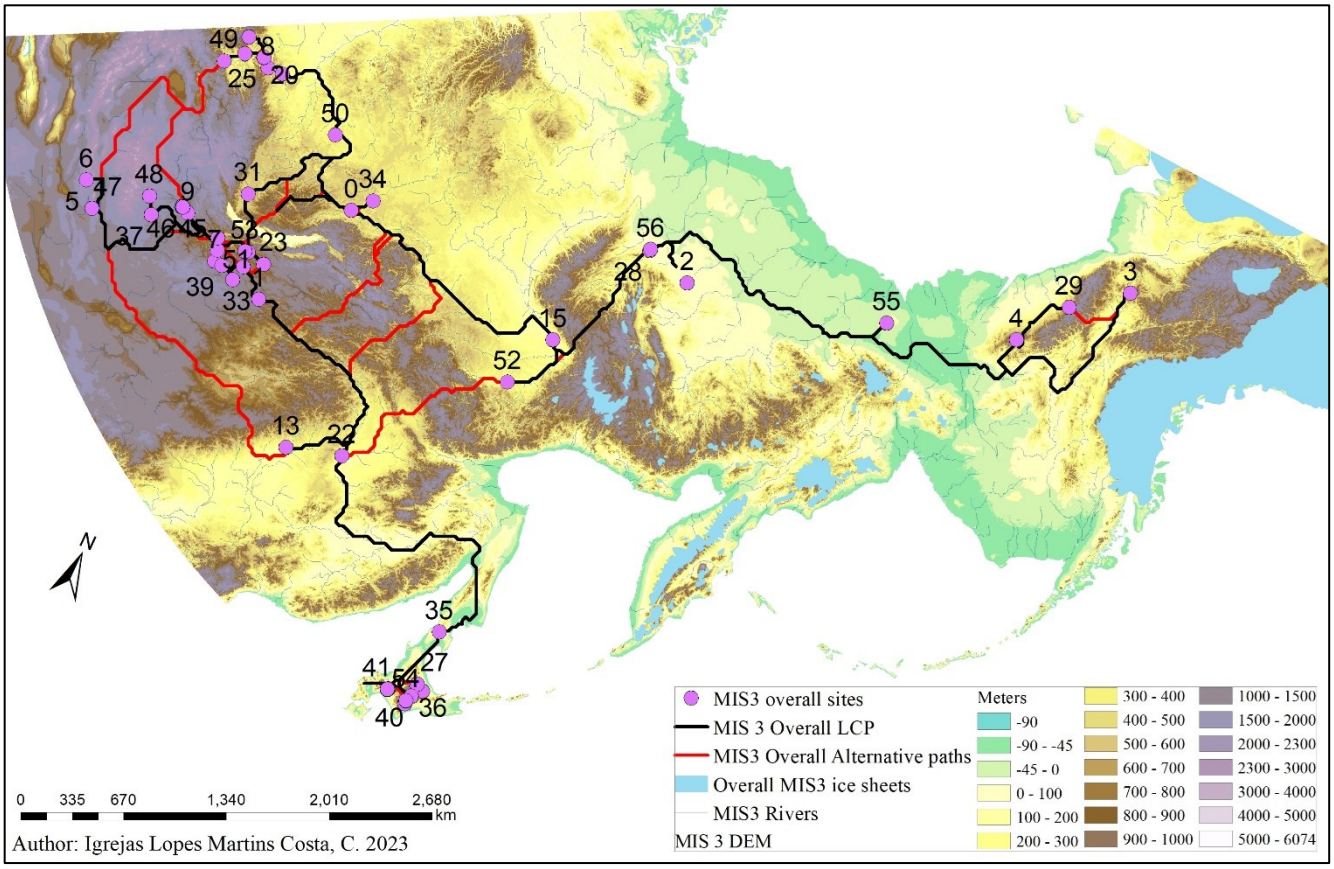

Figure 4.11 – Model #7; LCP (black) and alternative paths (red) generated with the overall MIS3 sites, without establishing a point of origin.

Models 8-10 also use the same three sites, Yana RHS, Mal'ta and Kashiwadai 1 as starting points with the overall MIS 3 data (Figs. 4.12; 4.13; 4.14). Due to the presence of more scattered sites outside of Beringia, in modern-day Siberia, the paths generated are more spread out in the landscape.

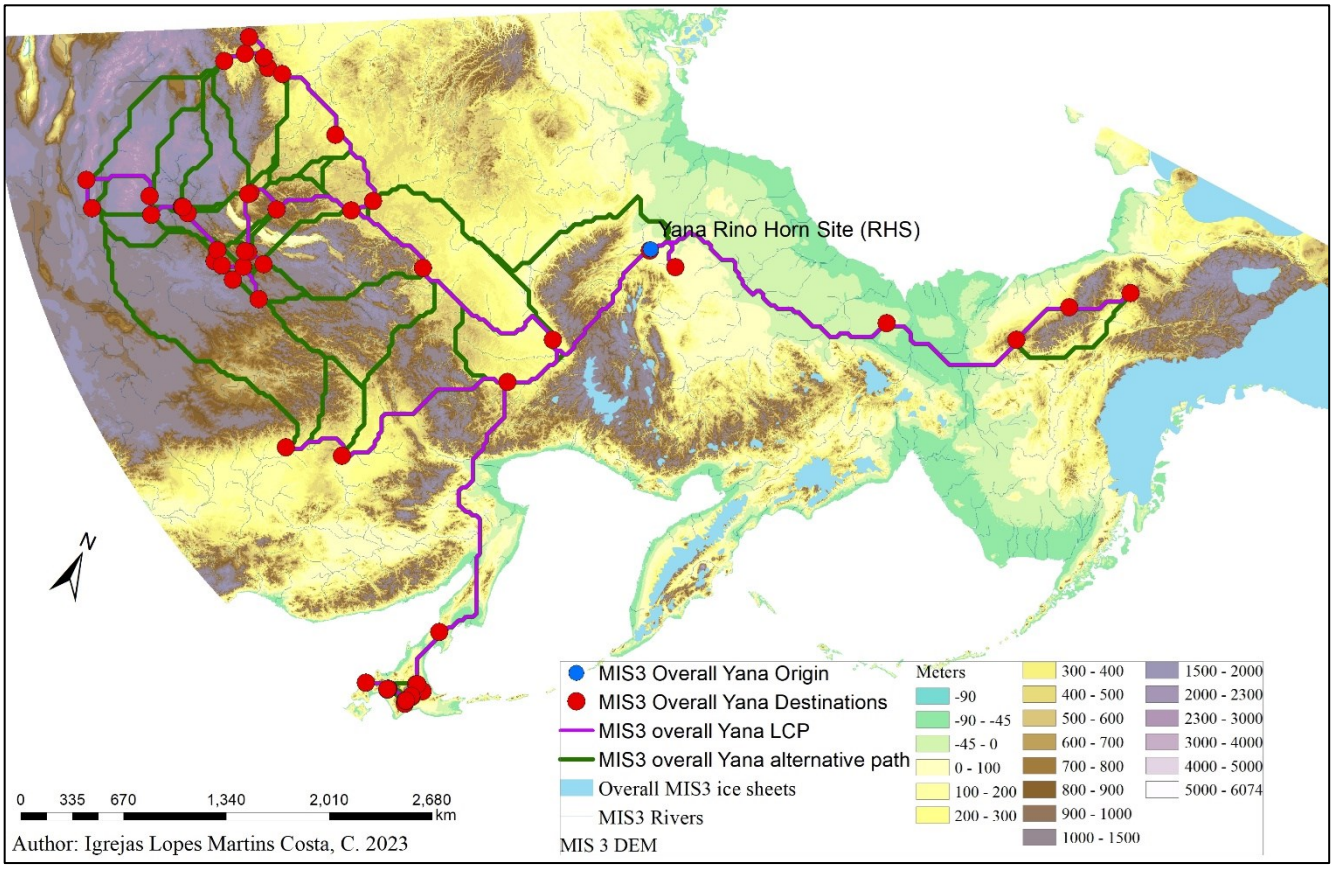

Figure 4.12 – Model #8; LCP (purple) and alternative path (green) generated with overall MIS3 sites and having established Yana RHS as the point of origin

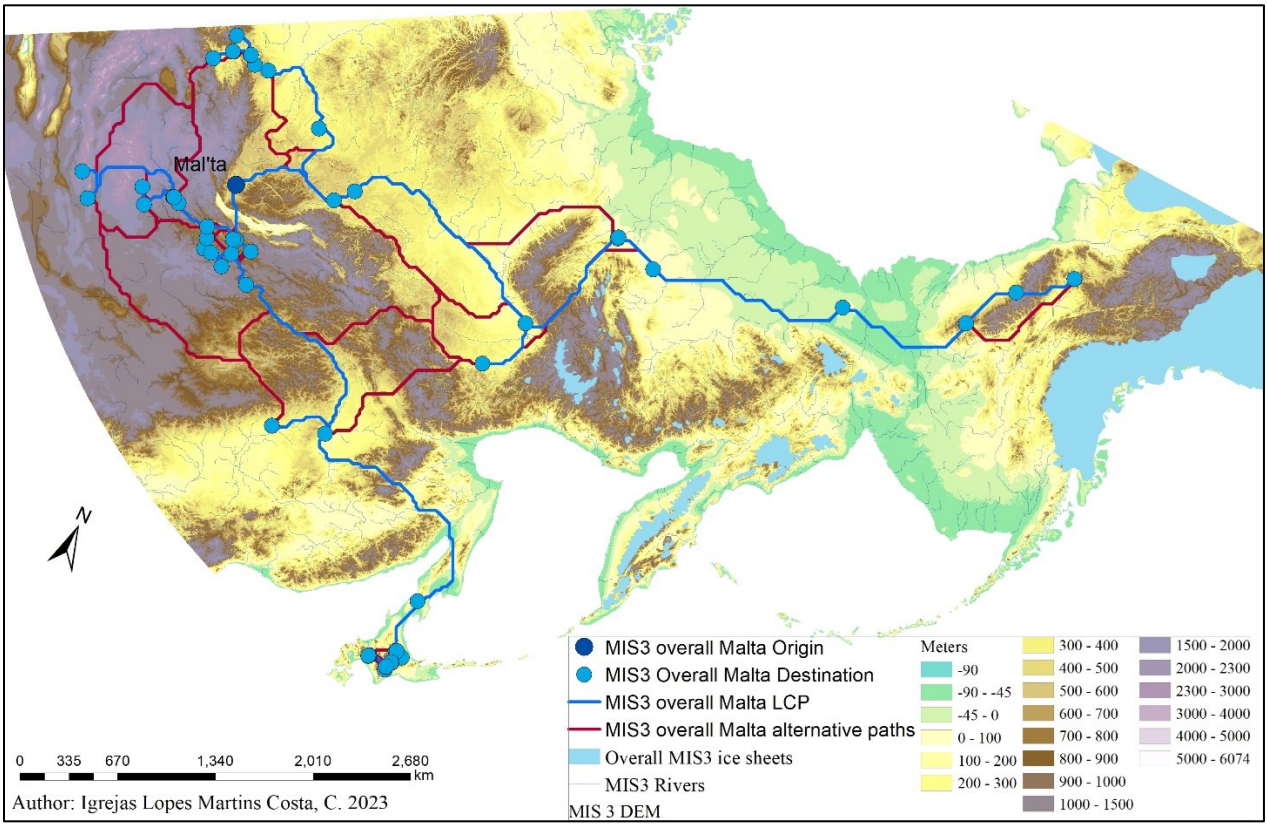

Figure 4.13 – Model #9; LCP (blue) and alternative path (red) generated with overall MIS3 sites and having established Mal'ta as the point of origin

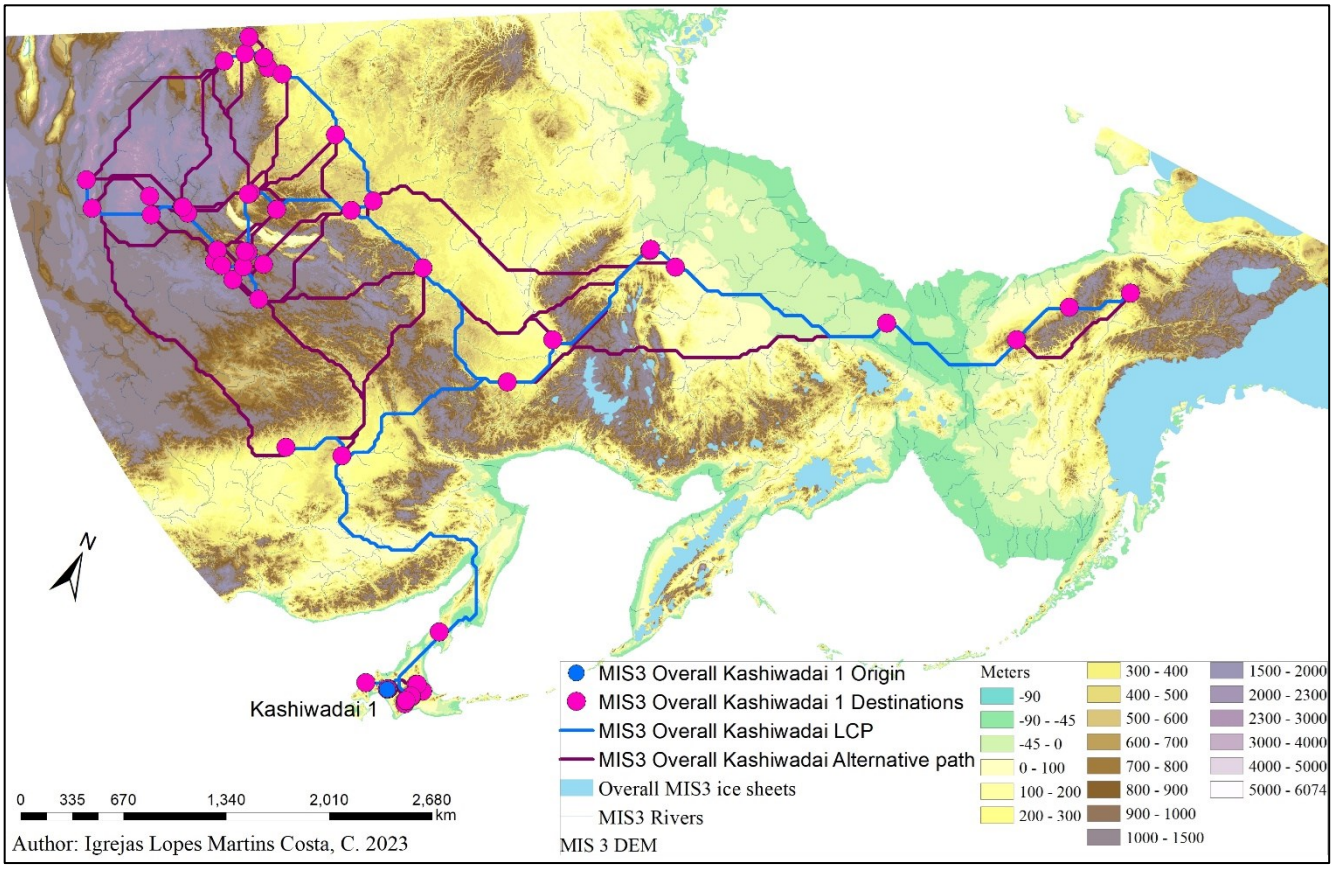

Figure 4.14 – Model #10; LCP (blue) and alternative path (dark red) generated with overall MIS3 sites and having established Kashiwadai 1 as the point of origin

These three models (8, 9 and 10) have presented similar results, albeit with small differences amongst them. Overall, the results do not appear to differ too much from the LGM models presented earlier. Following these experiments, we tested how the MIS3 overall sites would interact with randomly created experimental sites (model #11; Fig. 4.15). The model generated interesting results, where firstly an alternative path south of the Verkhoyansk Range bordering the northern Sea of Okhotsk coast until reaching the present-day Gulf of Anadyr, where the experimental site n°1 site is located. The paths created here were the first that ventured outside of the previously generated path connecting Western and Eastern Beringia passing through Wrangel Island, thus indicating possible other routes.

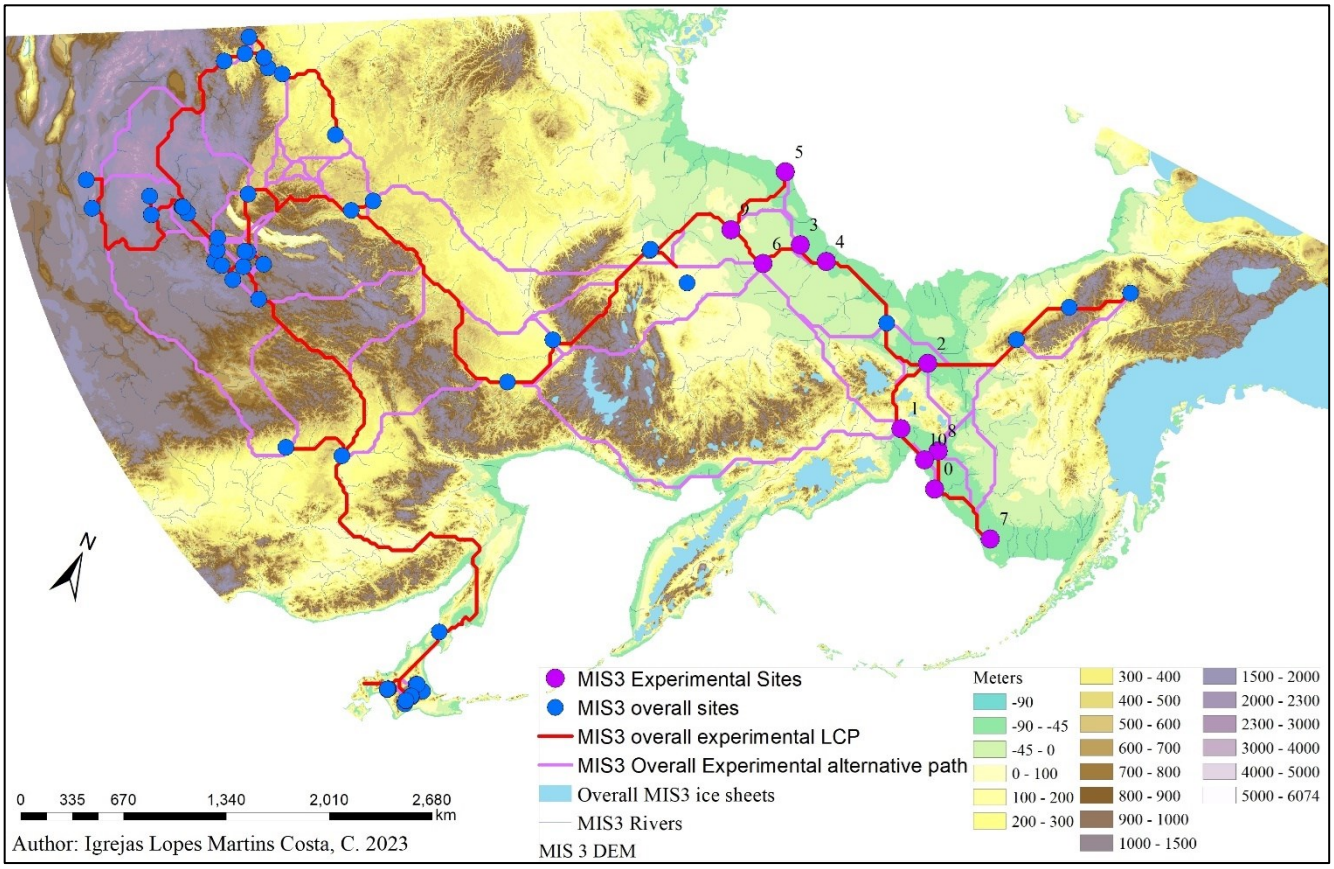

Figure 4.15 – Experimental model (#11) indicating the LCP (red) and experimental paths (pink) generated following the merging of MIS3 overall sites (blue) with the MIS3 experimental sites (purple)

It is worth noting that throughout the *overall* MIS3 models and experiments, the least-cost paths connect Lake E5 and Bluefish Caves by crossing the Brooks Range, instead of going around it. An alternative path connects Burial Lake to Bluefish caves via a path that runs the south of the Brooks Range in all models. In addition, the paths generated crossing Central Beringia usually, with the exception of the path modelled with experimental sites, prefer a direct path following the river systems through the lower altitudes of Western and Central Beringia. It is also worth noticing that the MIS3 experimental sites have also caused the generating of a different southern Beringian path across the BLB than the one generated for the LGM sites (Models #5 and 6; Fig. 4.8 and 4.9).

During MIS3, there were fluctuations between stadial and interstadial periods. Therefore, we also set out to understand how these different climate events might have affected the distribution and mobility of Beringian populations dividing sites dated to the stadial (herein 'std') and interstadial (herein 'int') Greenland stages. These two groups do not require the sites to be dated to the same sub-stage, as long as they can be attributed to a stadial or interstadial event.

IV.II.II. MIS3 Stadial sites

The MIS3 Stadial group contains twenty archaeological sites (Fig. 4.16), where the majority of the sites can be located in present-day Mongolia and Transbaikal. It has been hypothesized the reduced number of sites in this stage is caused by a reduction in population in Northeastern Asia due to the colder temperatures. However, the occupation of Yana RHS farther north is the main opposing argument to this hypothesis. This stage is joined with Batchelor et al. (2019)'s 30ka_max modelled icesheets, herein called 'MIS3 Stadial Ice sheets'.

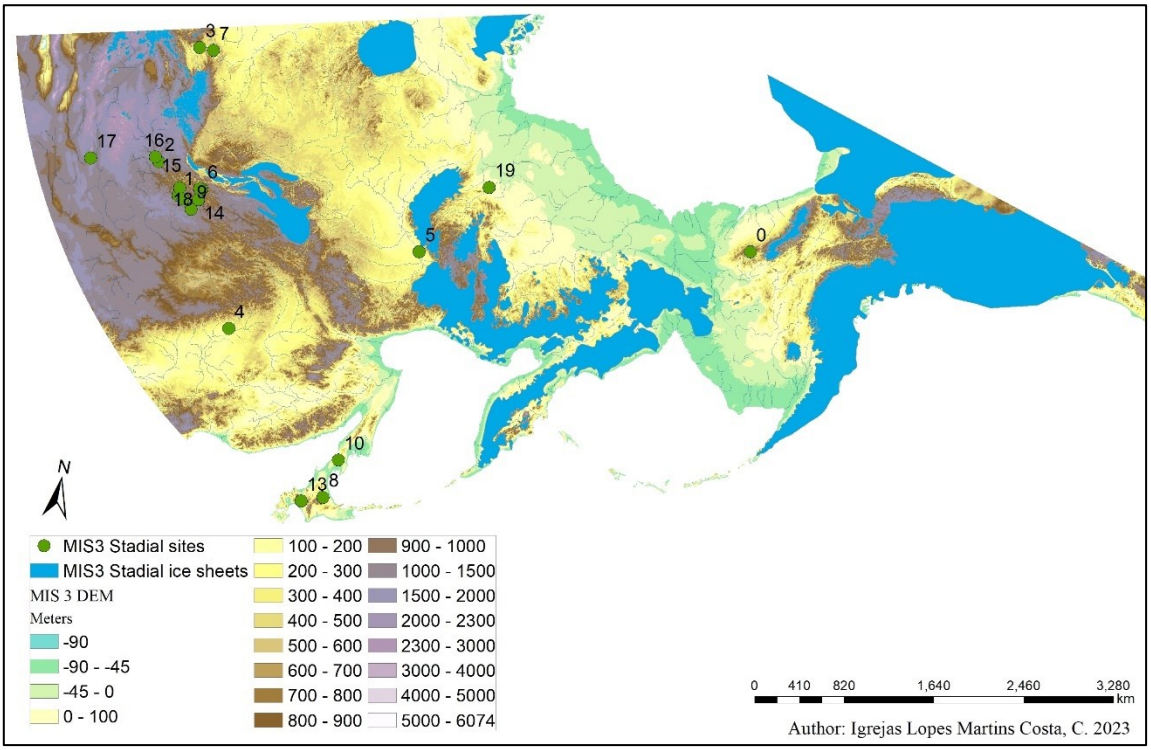

Figure 4.16 – Map indicating the location of our stadial sites. Sites present: 0. Burial Lake; 1. Chitkan; 2. Dörölj-1; 3. Dvuglazka Rockshelter; 4. Guanghetun 1; 5. Ikhine II; 6. Kamenka; 7. Kurtak-4; 8. Kyushiarataki 3; 9. Masterov Kliych; 10. Ogonki 5; 11. Podzvonkaya; 12. Priiskovoye; 13. Shukubai-kaso (Sankakuyama); 14. Tolbaga; 15. Tolbor-15; 16. Tolbor-4; 17. Tsagaan Agui; 18. Varvarina Gora; 19. Yana RHS

The least cost model generated (Model #12; Fig. 4.17) is marked by long distances following the modelled rivers due to the reduced number of sites. The path joining Yana RHS to Burial Lake is the same that was generated in previous models, however in this case, it is possible to see that not only does this path follow the river systems but also borders the icesheets.

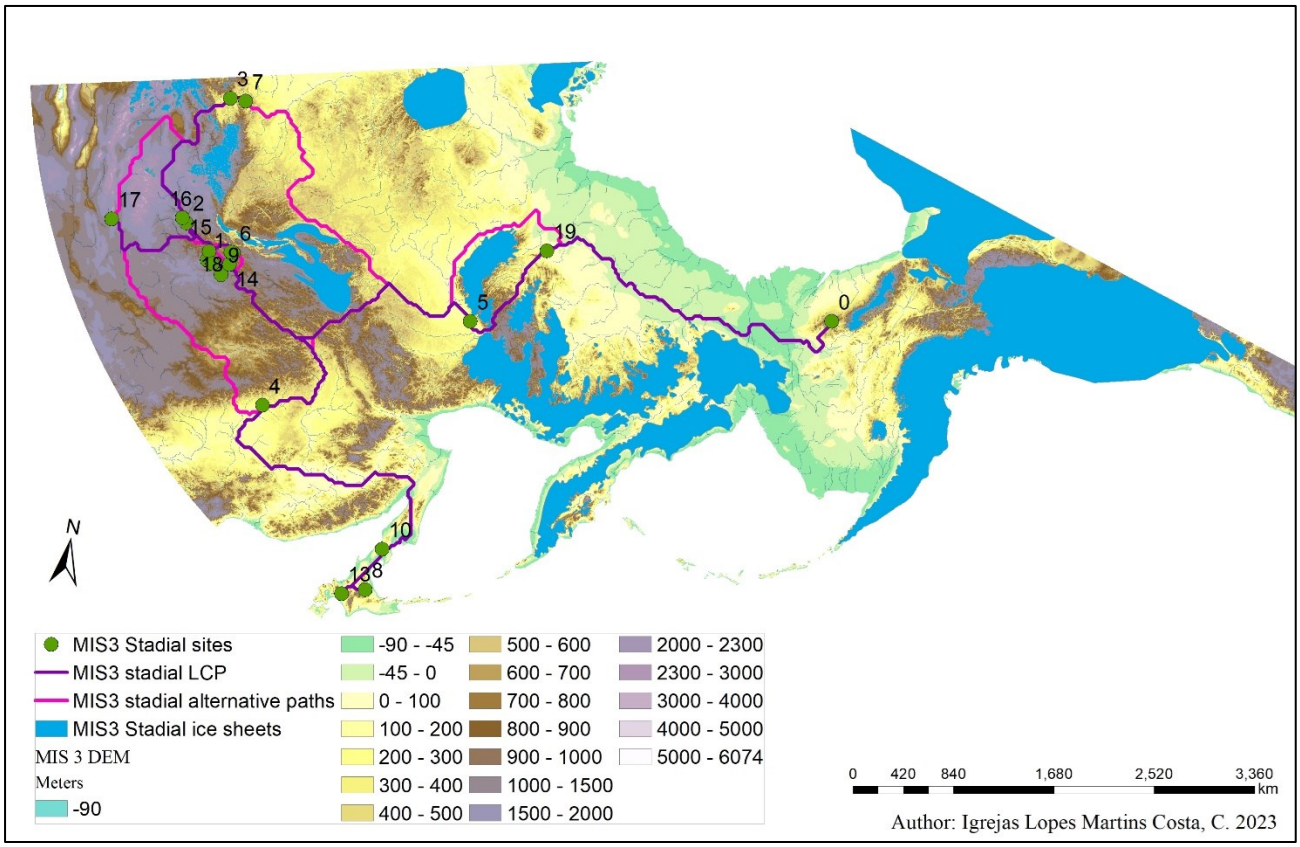

Figure 4.17 – Model #12; LCP (purple) and alternative path (pink) generated through the MIS3 Stadial sites (green)

We did not create a model with experimental sites for the stadial sites because the minimum number of random points that could be generated using the formula we established is below the threshold of the Create Ransom Points tool and would have been disproportionate relative to the current number of sites in our database.

IV.II.III. MIS 3 Interstadial sites

The MIS3 Interstadial group contains fifty-nine archaeological sites (Fig. 4.18), almost the same amount of sites as the overall MIS3 sites (*n* =61), with the exception of Ogonki-5 (#60) located in the PSHK and Tolbor-4 (#78), located in Northern Mongolia. The icesheets used in this model are obtained from Batchelor et al. (2019) for 30ka_min, herein called 'MIS3_Interstad_icesheets'. These icesheets are similar to the 'best_estimate' used in the overall MIS3 models, and should therefore result in similar paths.

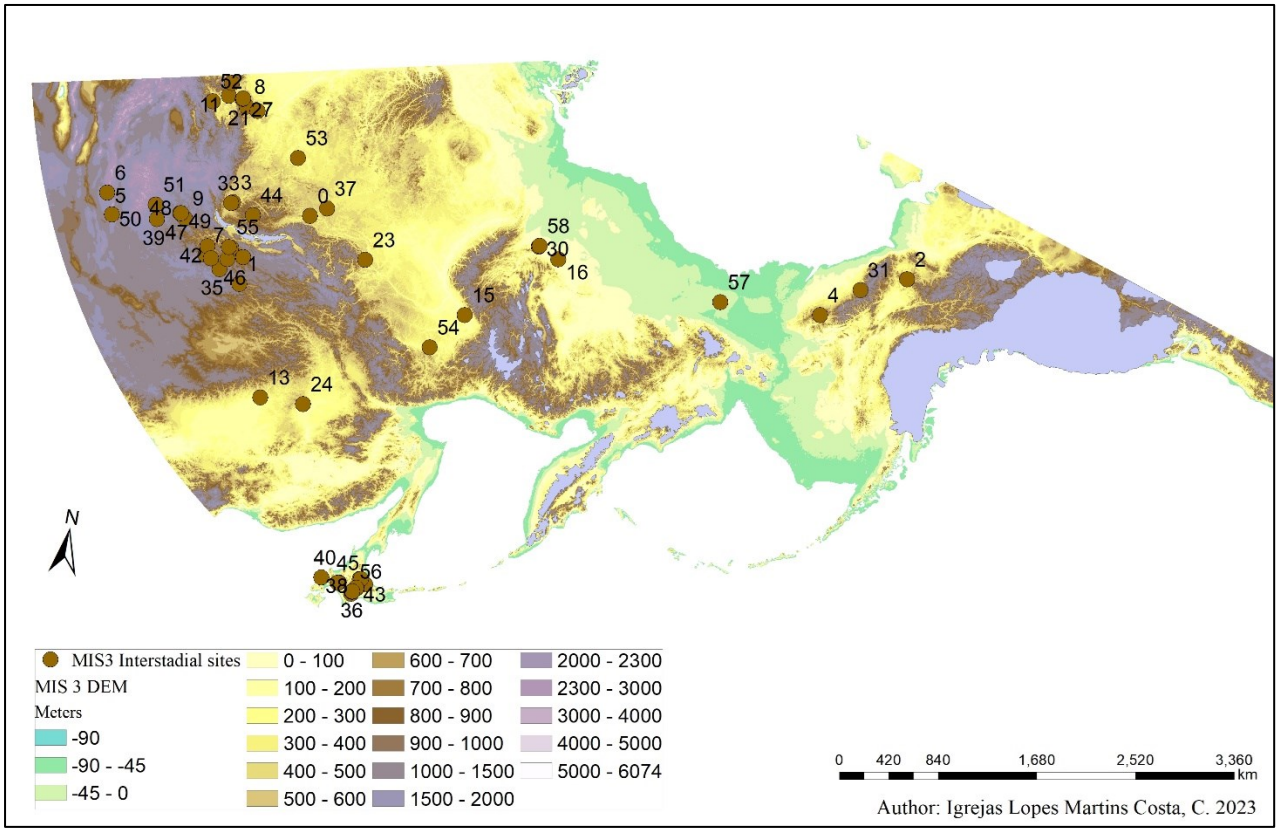

Figure 4.18 – Map indicating the location of our MIS3 interstadial sites

The LCP model (#13; Fig. 4.19) generated by the interstadial sites has resulted in similar routes to those generated by the overall MIS3 sites, although surprisingly enough, there are some slight differences.

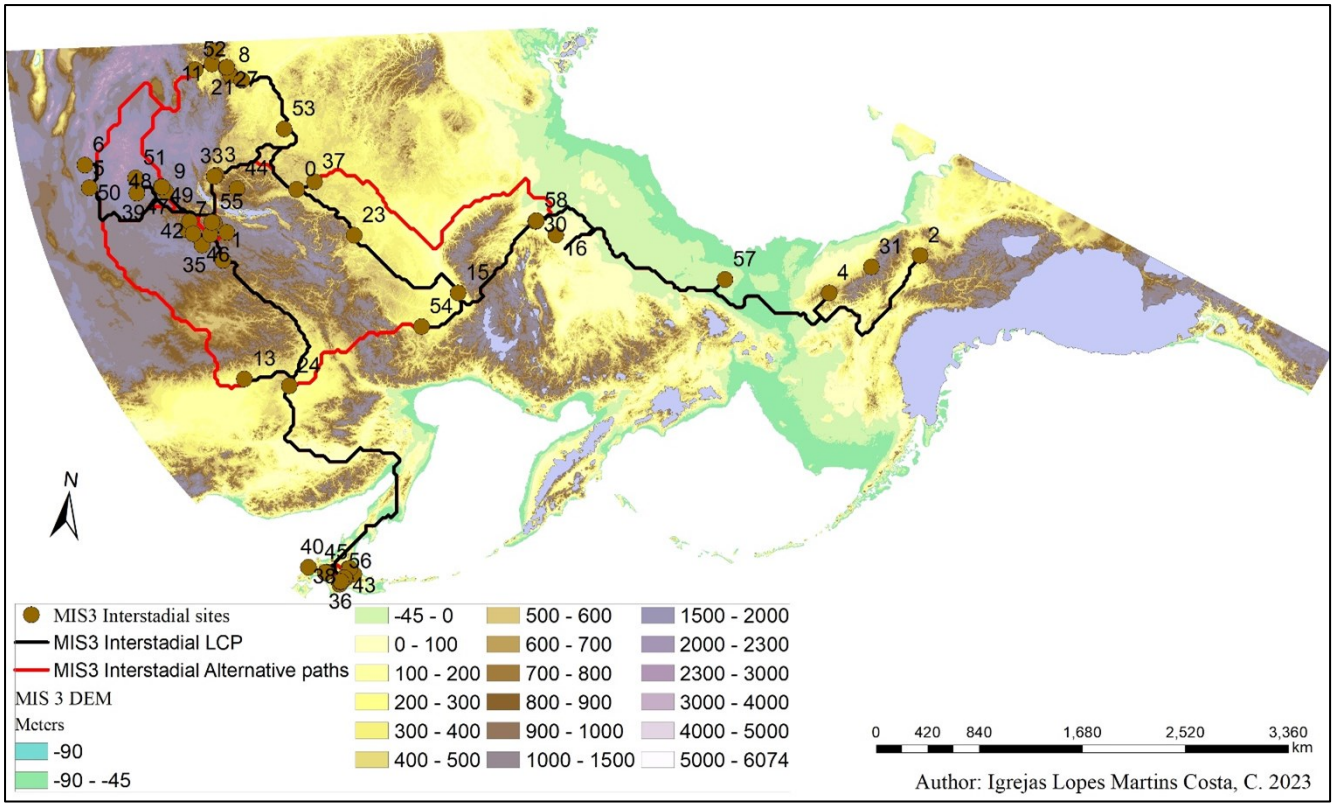

Figure 4. 19 – Model #13; LCP (black) and alternative path (red) generated with the MIS3 interstadial sites

Chapter V – Discussion

Following the presentation of the modelling results (*Chapter IV*), it is now necessary to examine what these results tell us about the Late Palaeolithic migratory event that led to the entrance of the first human population into the North American continent. The results obtained allow us to reflect on the archaeological models presented in Chapter II, allowing us to assess whether these models could indeed be representative of the past.

The results from our models suggest two possible terrestrial migration routes through the BLB. The multiple LCPs conducted within our two temporal groups all support a path further inland, crossing between Wrangel Island (to the north) and the East Siberian mountains (to the south) then continuing straight towards Burial Lake, Lake E5 and Bluefish Caves. Even when adding experimental sites, the LCP maintained the same route, albeit with some slight detours in order to reach all of the sites. This suggests that an inland route might have been the most cost-effective route when crossing Central Beringia during MIS 3 and the LGM. This hypothesis was generated in all models, regardless of the programmed point of origin.

However, when considering neighbouring paths, more specifically model #6 (with our LGM data and having categorised the site of Kashiwadai-1 as the point-of-origin), a southern route bordering the coast is also proposed. This path would support the hypothesis of a coastal model of the peopling of the Americas (Anderson & Gillam 2000; Anderson et al. 2014; Anderson & Bissett 2015; Gustas & Supernant 2019; Rybin 2014). This model is most often viewed as the only option:

> *"Movement very far inland on the Beringian landmass proper may not have been necessary or even attempted, if the numerous coastal bays and offshore islands proved to be sufficiently attractive habitats to sustain a maritime fisher-forager way of life"* (Anderson 2010:328)

This statement, however, runs counter to our results which consistently show an inland route in multiple timelines and scenarios. As we have shown in this project, an inland route around present-day Wrangel Island appears to be the most advantageous with the database presented here, when modelled in accordance with the landscape's slopes and rivers (i.e., our distance-to-water raster). It is worth highlighting that the paths generated in our projects do not have directionality defined, each path is simply the most cost-effective route between two points. Two possible sources in the West are proposed: the sites east of the Verkhoyansk mountain range (in and around the Yana site complex) and the PSHK peninsula (e.g., Kashiwadai-1). The genetic data (*cf. Chapter I*), however, does not indicate a PSHK origin; we therefore propose a population movement which originated in Yana RHS, moved southward towards Mal'ta before continuing east into Central Beringia where the 'Beringian standstill'

population could have been located during the LGM in a continental landscape with access to aquatic landscapes which would have permitted both a southward migration by the ice-free corridor as well as a coastal migration once in Eastern Beringia. Depending on the temporal group, the southern coast of CB was presented as either a corridor between the PSHK peninsula and EB (i.e., LGM and MIS3 interstadial) or as a barrier (i.e., MIS3 stadial). In addition, as mentioned earlier (*cf. Chapter I*), Kamchatka Peninsula would have consistently had some level of glaciation, further isolating the PSHK peninsula from CB; thus rendering the PSHK peninsula an unlikely point of origin.

We reconstructed a hydrological system, using it in the LCP analysis on the assumption that the Palaeolithic settlers of northeastern Asia (and therefore of Beringia) actively settled in locations near water sources. The reasons is that these locations would have provided key resources in addition to drinking water (e.g., cobbles, fauna, etc.) and because river systems could be used for transportation (either over water or ice, in winter) and as guides to navigation, (Wright 2021:437). Rivers "provide viewpoints, topographical features, and open ground that can assist travel" (Wickham-Jones 2014:695). Our LCPs tend to follow the reconstructed rivers but rarely follow the coastlines, with the exception of the three models where experimental sites were used (#5, 6, 11). Although this could be due to our use of a 21% weight on our distance-to-water layers in the modelling, we do believe these paths provide important information about likely patterns of mobility during MIS3 and 2. The addition of experimental sites indicates that taphonomic biases could be important in underestimating the importance of coastal resources, however.

Noteworthily, two main routes present themselves in our modelling: onecrosses Central Beringia approximately through Wrangel Island towards Burial Lake and the Brooks Range, and another one follows the southern coast of Central Beringia before moving northward towards Bluefish Caves. This first path is mostly presented as the 'main' route in our models, however it is possible this is due to the location of the available sites within the archaeological record; whereas the second path is presented in two scenarios: models #5, 6 and 11 which represent the neighbouring paths produced during our LGM and MIS3 overall reconstructions when using our experimental sites (*cf.* Figs. 4.8; 4.9; 4.15). The importance of considering taphonomic bias is therefore once again highlighted.

The paths generated by our models highlight questions surrounding the connectivity between the known sites as well as the distribution of possible unknown sites and land use in Central Beringia. Clusters of sites in Western Beringia (FIG XX) are well-connected by networks of paths whereas the PSHK is relatively poorly connected (FIG XX). In Central and Eastern Beringia, we lack sufficient archaeological information to confirm whether a similar situation prevailed. We suggest that the search for more archaeological data should follow the modelled paths produced for this project.

Our results support the proposition that Beringia could have been a contiguous territory occupied by human populations during MIS3 and 2. This could support the standstill hypothesis. Our results also raise the possibility that aquatic resources were important, which leaves open the possibility of a coastal migration taking place through Central Beringia prior to and during the LGM, West of the south Alaskan ice sheet (*cf.* Figs. 4.8, 4.9, 4.15).

The analysis of human remains recovered from Mal'ta (*cf.* Chapter I), near lake Baikal, dated to the LGM, confirms that the inhabitants of the site had a mixed diet, where fish and molluscs were consumed, as well as small mammals. Indeed, MA-1 contained high $\delta^{15}N$ values indicating a regular consumption of aquatic remains (±25-50%) such as freshwater fish. In addition, the importance of fish is highlighted in the archaeological record of sites around lake Baikal by the presence of figurines (Fig.5.1), such as one of fish and other riverine fauna. Similar figurines are found in the neighbouring site of Buret' (Fig. 5.2) These figurines are attributed to the LGM (Goebel 1999; Khenzykhenova et al. 2019; Lbova et al. 2020; Lbova 2021; Richards et al. 2001). Indigenous populations are knowledgeable about their history, beliefs and traditions and their participation in the interpretation of the archaeological record provides valuable information (Harris 2010). The human figurines from Buret' are represented wearing outfits similar to those worn traditionally in the area, sometimes made out of fish or seal guts. This information, as well as the presence of beads made out of fish bones in the site's archaeological record could indicate a long-standing tradition of exploiting aquatic resources in the Baikal region (Goebel 1999; Khenzykhenova et al. 2019; Lbova et al. 2020; Lbova 2021; Richards et al. 2001).

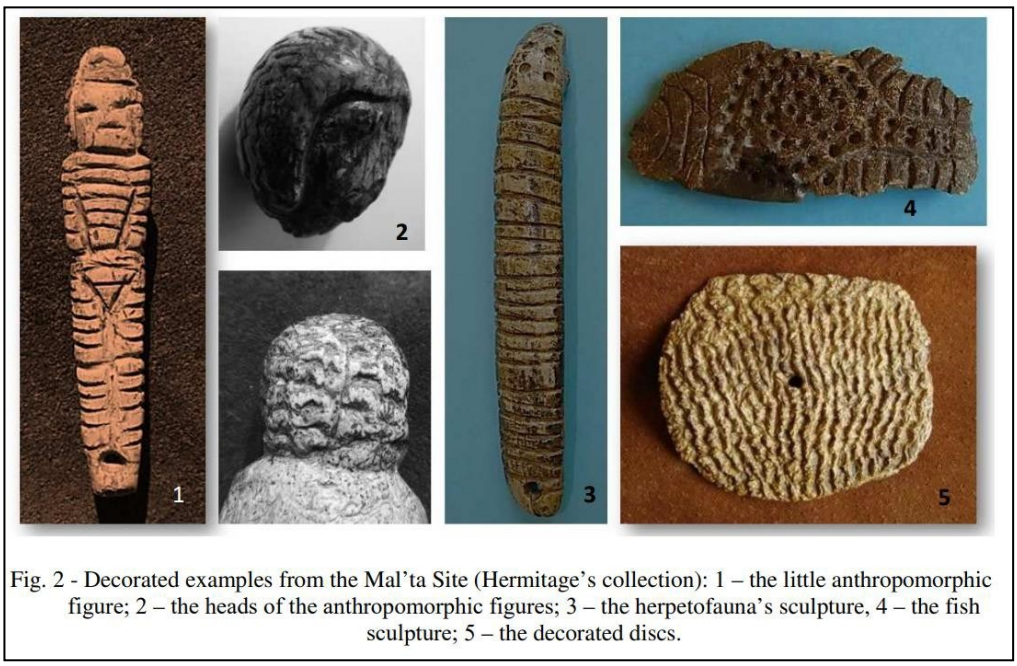

Fig. 2 - Decorated examples from the Mal'ta Site (Hermitage's collection): 1 – the little anthropomorphic figure; 2 – the heads of the anthropomorphic figures; 3 – the herpetofauna's sculpture, 4 – the fish sculpture; 5 – the decorated discs.

Figure 5.1 – Representative sample of the types of figurines found at Mal'ta, including the zoomorphic figurine of a fish (#4) (Lbova 2017:10)

Figure 5.2 – Representative sample of the types of zoomorphic figurines found at Mal'ta and Buret' (Lbova et al. 2020:9)

Ethnographic studies of indigenous populations and living oral traditions in present-day Haida Gwaii (Harris 2003) describe an early coastal migration: "In the beginning there was nothing but water and ice and a narrow trip of shoreline" (Boas 1916:883 *apud* Harris 2003:318). Oral histories, such as this one from the Heiltsuk, can be used to trace back the history and movements of indigenous populations, offering support to archaeological hypotheses. The exact timing of this dispersal is uncertain, however. Buvit and colleagues (2021) propose that the 'source' population that eventually migrated into Eastern Beringia had a mostly aquatic diet and that by passing down their technological knowledge, following generations would have been able to migrate eastward by following the Central Beringian coast; this 'source' population has been proposed to be from the PSHK Peninsula (Buvit et al. 2021). The site of Kashiwadai-1 (Hokkaido) is the oldest PSHK site (Iwase 2016; Nakazawa et al. 2005; Nakazawa & Izuho 2006; Ono et al. 2002); no artefact related to fishing has been uncovered at the site, however. The appearance of fishing in Hokkaido appears solely after the LGM, e.g., at the Taisho-3 site (dated to ±15.000 cal yr BP) (Takakura 2020).

The lack of aquatic remains or of fishing technologies in PSHK sites could be justified by the fact they are not directly on the coast, nor are they directly next to our modelled river systems. Indeed, due to reduced sea levels, the PSHK sites on our database are all located at higher altitudes that were no longer on the coast of either the Sea of Japan, Okhotsk or even the Pacific Ocean. The reconstructed palaeorivers, as we have mentioned earlier, only represent large water courses, however.

In summary, indications of a fishing technology, or of an aquatic diet, are found in sites surrounding Lake Baikal in southern Siberia, however, no evidence of fishing or of an aquatic diet can be found in the PSHK peninsula or elsewhere in Beringia prior to or during the LGM.

Ethnographic studies and the traditional knowledge of indigenous populations can also help to better understand the decisions made by hunter-gatherer societies of the past. In the case of Beringian populations, arctic populations today face similar challenges and thus, provide insights into the importance of specific landscape features and resources. The Evenki, an indigenous population living in northern Asia, can be divided into three groups: the Orochon, who are reindeer hunters, the Tungus, who are fishers, and the Murchen, who are cattle herders. These distinctions were imposed during Soviet times when indigenous communities had to pay the authorities through trade, but are also indicative of the social complexity of the Evenki (Safonova & Sántha 2016). Furthermore, the Chukchi can also be divided into two groups – the Coastal Chukchi and the Reindeer Chukchi – (Frank 2014; Grøn et al. 2008). Although determining whether these groupings were solely imposed by external factors, or whether these specialisations already existed amongst their MIS3 and LGM ancestors still remain to be determined, it is undeniable that studying present-day indigenous traditional knowledge can help archaeologists better understand past ways of life. An example of such could be the 'skylore' shared by many indigenous cultures of Siberia (Frank 2014; Grøn et al. 2008) which portrays the Milky Way as a river, thus underscoring the importance of rivers to these populations.

Further east, in present-day Yukon and Northwest Territories, members of the G'wich'in First Nation who still live a traditional lifestyle set up fish camps where they spend many months, from summer to autumn. These camps are places to reconnect, socialize and 'heal' (Proverbs 2019l; Wishart 2014). These ethnographic data highlight the importance of river systems for hunter-gatherers (and fishers) living in subarctic and arctic environments. In addition, as we have attempted to bring to light, settlements at close proximity to one another will have allowed its inhabitants meeting and sharing information. Indeed, as seen from the indigenous communities mentioned previously, there are similarities in their belief systems, ethics and even behaviours. These connections and relationships will have been formed and maintained using the neighbouring paths such as the ones modelled in this project.

Conclusion

The models presented here reflect the complexity that is the peopling of the Americas. Due to the large gaps in the archaeological record, a modelling approach is the most appropriate.

Some of the assumptions we made when designing this research include the importance of water courses in governing the movements of Beringian populations. This is defensible given archaeological and ethnographic data as well as traditional environmental knowledge (see discussion, above). The Least Cost Path analysis which we conducted, suggests the most cost-efficient routes across the Beringian Land Bridge and into the American continent during the Marine Isotope Stages 3 and 2 (or, the Last Glacial Maximum) include a north-central route, as well as a southern, more coastal route, one which had long been hypothesized to have existed. The north-central route has here been presented as a more viable path due to the presence of sites in its vicinity which were detrimental to the programming of the LCP. The difficulty with the coastal route is the lack of sites in southern Central Beringia; indeed, the path was only possible once experimental points were randomly generated. Although in theory the coastal route appear promising, the lack of archaeological data and research in the now-submerged landscape impedes us on generating viable hypotheses on this path. On the other hand, the north-central route generated for each model of this project warrants further study.

The information we generated in this project can already be used to design archaeological surveys with the goal of filling some of the gaps in our knowledge of the history of occupation of Beringia during the last Ice Age. We also hope to be use the information collected in this project for future research, adding more paleoenvironmental data in order to produce predictive models for use in archaeological expeditions in the hopes of finding more LGM or MIS3-dated archaeological sites in Eastern and/or Beringia.

References

-Adler, D.; Tushabramishvili, N. 2004. Middle Palaeolithic patterns of settlement and subsistence in the southern Caucasus. In: Conard, N.J. (eds) Settlement Dynamics of the Middle Paleolithic and Middle Stone Age. Kerns Verlag: Tubinger (chapter 5:91-132)

-Ager, T.A.; Phillips, R.L. 2008. Pollen evidence for Late Pleistocene Bering Land Bridge environments from Norton Sound, Northeastern Bering Sea, Alaska. *Artic, Antarctic, and Alpine Research* 40:451-461

-Aguerrevere, I.Z.; Zurro, D. 2021. Los retos de la sostenibilidad y la investigación en Humanidades: las algas como recurso milenario. *Vitamina Humanidades IMF-CSIC*

-Anderson, D.G.; Gillam, J.C. 2000. Paleoindian colonization of the Americas: implications from an examination of physiography, demography, and artifact distribution. *American Antiquity* 65(1):43-66

-Anderson, D.G. 2010. Human settlement in the New World: multidisciplinary approaches, the 'Beringian' Stadnstill, and the shape of things to come. In: Auerbach, B.M. (ed) Human Variation in the Americas: The Integration of Archaeology and Biological Anthropology. Center for Archaeological Investigations, Occasional Paper 38. Southern Illinois University: Carbondale (chapter 12:311-346)

-Anderson, D.G.; Bissett, T.G.; Yerka, S.J. 2014. The Late-Pleistocene and human settlement of interior North America: The role of Physiography and sea-level change. In: Graf, K.E.; Ketron, C.V.; Waters, M.R. (eds) PaleoAmerican Odyssey. Texas A&M University Press (p.183-203)

-Anderson, D.G.; Bissett, T.G. 2015. The initial colonization of North America: sea level change, shoreline movement, and great migrations. In: Frachetti, M.D.; Spengler III, R.N. (eds) Mobility and ancient society in Asia and the Americas. Springer, Cham (p.59-88)

-Antonova, Y.E.; Tashak, V.I.; Kobylkin, D.V. 2019. Palaeoenvironmental and hunting activity of the Upper Palaeolithic population in Western Transbaikalia: A case study on the Podzvonkaya Settlement, South Siberia. *International Journal of Osteoarchaeology* 30(2):131-144

-Aporta, C. 2004. Routes, trails and tracks: trail breaking among the Inuit of Igloolik. *Études Inuit* 28(2):9-38

-Ardelean, C.F.; Becerra-Valdivia, L.; Pedersen, M.W.; Schwenninger, J.-L.; Oviatt, C.G.; Macías-Quintero, J.I.; Arroyo-Cabrales, J.; Sikora, M.; Ocampo-Díaz, Y.Z.E.; Rubio-Cisneros, I.I.; Watling, J.G.; de Medeiros, V.B.; de Oliveira, P.E.; Barba-Pingarón, L.; Ortiz-Butrón, A.; Blancas-Vázquez, J.; Rivera-González, I.; Solís-Rosales, C.; Rodríguez-Ceja, M.; Gandy, D.A.; Navarro-Gutierrez, Z.; De La Rosa-Díaz, J.J.; Huerta-Arellano, V.; Marroquín-Fernández, M.B.; Martínez-Riojas, L.M.; López-Jiménez, A.; Higham, T.; Willerslev, E. 2020. Evidence of human occupation in Mexico around the Last Glacial Maximum. *Nature* 584(7819):87-92

-Ardelean, C.F.; Pedersen, M.W.; Schwenninger, J.-L.; Arroyo-Cabrales, J.; Gandy, D.A.; Sikora, M.; Macías-Quintero, J.I.; Huerta-Arellano, V.; De La Rosa-Díaz, J.J.; Ocampo-Díaz, Y.Z.E.; Rubio-Cisneros, I.I.; Barba-Pingarón, L.; Ortíz-Butrón, A.; Blancas- Vázquez J.; Solís-Rosales, C.; Rodríguez-Ceja, M.; Rivera-González, I.; Navarro-Gutiérrez, Z.; López-Jiménez, A.; Marroquín-Fernández, M.B.; Martínez-Riojas, L.M.; Willerslev, E. 2022. Chiquihuite Cave and America's hidden limestone industries: A Reply to Chatters et al. *PaleoAmerica* 8(1):17-28

-Argiriadis, E.; Battistel, D.; McWethy, D.B.; Vecchiato, M.; Kirchgeorg, T.; Kehrwald, N.M.; Whitlock, C.; Wilmshurst, J.M.; Barbante, C. 2018. Lake sediment fecal and biomass burning biomarkers provide direct evidence for prehistoric human-lit fires in New Zealand. *Scientific Reports* 8(1):1-9

-Ashastina, K.; Kuzmina, S.; Rudaya, N.; Troeva, E.; Schoch, W.H.; Römermann, C.; Reinecke, J.; Otte, V.; Savvinov, G.; Wesche, K.; Kienast, F. 2018. Woodlands and steppes: Pleistocene vegetation in Yakutia's most continental part recorded in the Batagay permafrost sequence. *Quaternary Science Reviews* 196:38-61

-Auerbach, B.M. 2018. Peopling of the New World. In: Trevathan, W. (ed) The International Encyclopedia of Biological Anthropology Wiley-Blackwell (p. 1-8)

-Batchelor, C.L.; Margold, M.; Krapp, M.; Murton, D.K.; Dalton, A.S.; Gibbard, P.L.; Stokes, C.R.; Murton, J.B.; Manica, A. 2019. The configuration of Northern Hemisphere ice sheets through the Quaternary. *Nature communications* 10(1):3713(1-10)

-Baranskaya, A.V.; Khan, N.S.; Romanenko, F.A.; Roy, K.; Peltier, W.R.; Horton, B.P. 2018. A postglacial relative sea-level database for the Russian Arctic coast. *Quaternary Science Reviews* 199:188-205

-Becerra-Valdivia, L.; Higham, T. 2020. The timing and effect of the earliest human arrivals in North America. *Nature* 584:93-97

-Bennett, M.R.; Bustos, D.; Odess, D.; Urban, T.M.; Lallensack, J.N.; Budka, M.; Santucci, V.L.; Martinez, P.; Wiseman, A.L.A.; Reynolds, S.C. 2020. Walking in mud: remarkable Pleistocene human trackways from White Sands National Park (New Mexico). *Quaternary Science Reviews* 249:106610 (1-21)

-Bennett, M.R.; Bustos, D.; Pigati, J.S.; Springer, K.B.; Urban, T.M.; Holliday, V.T.; Reynolds, S.C.; Budka, M.; Honke, J.S.; Hudson, A.M.; Fenerty, B.; Connelly, C.; Martinez, P.J.; Santucci, V.L.; Odess, D. 2021. Evidence of humans in North America during the Last Glacial Maximum. *Science* 373:1528-1531

-Bevan, A. 2003, The rural landscape of Neopalatial Kythera: a GIS perspective. *Journal of Mediterranean Archaeology* 15:217-256

-Beyin, A.; Hall, J.; Day, A. 2019. A Least Cost Path model for hominin dispersal routes out of the East Asian African Rift region (Ethiopia) into the Levant. *Journal of Archaeological Science: Reports* 23:763-772

-Bigg, G.R.; Clark, C.D.; Hughes, A.L.C. 2008. A last glacial ice sheet on the Pacific Russian coast and catastrophic change arising from coupled ice-volcanic interaction. *Earth and Planetary Science Letters* 265(3-4):559-570

-Boëda, E.; Gruhn, R.; Vilhena Vialou, A.; Aschero, C.; Vialou, D.; Pino, M., Gluchy, M.; Pérez, A.Ramos, M.P. 2020. The Chiquihuite Cave, a real novelty? Observations about the still-ignored South American Prehistory. *PaleoAmerica* 7(1):1-7

-Boëda, E.; Pérez-Balarezo, A.; Ramos, M.P. 2022. Another "Critique", same old song: A brief rebuttal to Gómez Coutouly. *PaleoAmerica* 8(1):53-61

-Boldurian, A.T. 2008. Clovis type-site, blackwater draw, New Mexico: A History 1929-2009. *North American Archaeologist* 29(1):65-89

-Bonatto, S.L.; Salzano, F.M. 1997. A single and early migration for the peopling of the Americas supported by mitochondrial DNA sequence data. *Proceedings of the National Academy of Sciences* 94(5):1866-1871

-Bond, J.D. 2019. Paleodrainage map of Beringia. *Yukon Geological Survey*. Open File 2019-2

-Borreggine, M.; Powell, E.; Pico, T.; Mitrovica, J.X.; Meadow, R.; Tryon, C. 2022. Not a bathtub: a consideration of sea-level physics for archaeological models of human migration. *Journal of Archaeological Science* 137:105507(1-11)

-Bourgeon, L. 2015. Bluefish Cave II (Yukon Territory, Canada): Taphonomic study of a bone assemblage. *PaleoAmerica* 1(1):105-108

-Bourgeon, L. 2018. Préhistoire Béringienne : étude archéologique des Grottes du Poisson-Bleu (Yukon). Ottawa : Presses de l'Université d'Ottawa + Musée canadien de l'histoire

-Bourgeon, L. 2021. Revisiting the mammoth bone modifications from Bluefish Caves (YT, Canada). *Journal of Archaeological Science: Reports* 37:102969 (1-10)

-Bourgeon, L.; Burke, A.; Higham, T. 2017. Earliest human presence in North America dated to the Last Glacial Maximum: new radiocarbon dates from Bluefish Caves, Canada. *PLoS ONE* 12(1):e0169486 (1-15)

-Bourgeon, L.; Burke, A. 2021. Horse exploitation by Beringian hunters during the Last Glacial Maximum. *Quaternary Science Reviews* 269:10714

-Bradley, B.; Stanford, D. 2010. The North Atlantic ice-edge corridor: A possible Palaeolithic route to the New World. *World Archaeology* 36(4):459-478

-Brubaker, L.B.; Anderson, P.M.; Edwards, M.E.; Lozhkin, A.V. 2005. Beringia as a glacial refugium for boreal trees and shrubs: new perspectives from mapped pollen data. *Journal of Biogeography* 32(5):833-848

-Burke, A.; Cinq-Mars, J. 1998. Paleoethological reconstruction and taphonomy of Equus lambei from the Bluefish Caves, Yukon Territory, Canada. *Arctic* 51(2):105-115

-Bustos, D.; Jakeway, K.; Urban, T.M.; Holliday, V.T.; Fenerty, B.; Raichlen, D.A.; Budka, M.; Reynolds, S.C.; Allen, B.D.; Love, D.W.; Santucci, V.L.; Odess, D.; Willey, P.; McDonald, H.G.; Bennett, M.R. 2018. Footprints preserve terminal Pleistocene hunt? Human-sloth interactions in North America. *Science Advances* 4:eaar7621 (1-6)

-Butkus, E.A. 2004. How Extensive was the Folsom Tradition in North America. *Central States Archaeological Journal* 51(3):171-175

-Buvit, I.; Terry, K. 2016. Outside Beringia: Why the Northeast Asian Upper Paleolithic Record does not support a Long Standstill Model. *PaleoAmerica* 2(4):281-285

-Buvit, I.; Izuho, M.; Terry, K.; Konstantinov, M.V.; Konstantinov, A.V. 2016. Radiocarbon dates, microblades and Late Pleistocene human migrations in the Transbaikal, Russia and the Paleo-Sakhalin-Hokkaido-Kuril Peninsula. *Quaternary International* 425:100-119

-Buvit, I.; Terry, K.; Izuho, M. 2021. Pathways along the Pacific: Using early stone tools to reconstruct coastal migratgion between Japan and the Americas. In: Carson, M.T. (ed) Palaeolandscapes in Archaeology: Lessons for the Past and Future. London:Routledge (Chapt. 4 p.39-81)

-Buvit, I.; Rasic, J.T.; Izuho, M. 2022. Archaeological evidence shows widespread human depopulation of Last Glacial Maximum Northeast Asia. *Archaeological and Anthropological Sciences* 14(7):1-11

-Byrd, B.F.; Garrard, A.N.; Brandy, P. 2016. Modeling foraging ranges and spatial organization of Late Pleistocene hunter-gatherers in the southern Levant – A least cost GIS approach. *Quaternary International* 396:62-78

-Carrara, A.; Cardinali, M.; Detti, R.; Guzzetti, F.; Pasqui, V.; Reichenbach, P. 1991. GIS techniques and statistical models in evaluating landslide hazard. *Earth Surface Processes and Landforms* 16:427-445

-Castle, C.J.E.; Crooks, A.T. 2006. Principles and concepts of agent-based modelling for developing geospatial simulations. *UCL Centre for Advanced Spatial Analysis Working Papers* 110 (p.1-61)

-Chatters, J.C.; Potter, B.A.; Prentiss, A.M.; Fiedel, S.J.; Haynes, G.; Kelly, R.L.; Kilby, J.D.; Lanoë, F.; Holland-Lulewicz, J.; Miller, D.S.; Morrow, J.E.; Perri, A.R.; Rademaker, K.M.; Reuther, J.D.; Ritchison, B.T.; Sanchez, G.; Sánchez-Morales, I.; Spivey-Faulkner, S.M.; Tune, J.W.; Haynes, C.V. 2021. Evaluating claims of early human occupation at Chiquihuite Cave, Mexico. *PaleoAmerica* 8(1):1-16

-Cheetham, P.N. 2008. Noninvasive subsurface mapping techniques, satellite and aerial imagery in landscape archaeology. In: David, B.; Thomas, J. (eds) Handbook of Landscape Archaeology. Walnut Creek: Left Coast Press (chapter 55:562-582)

-Cinq-Mars, J. 1979. Bluefish Cave 1 : A Late Pleistocene Eastern Beringian Cave deposit in the Northern Yukon. *Canadian Journal of Archaeology/Journal Canadien d'Archéologie* 3:1-32

-Cinq-Mars, J.; Morlan, R.E. 1999. Bluefish caves and Old Crow Basin: a new rapport. In: Bonnichsen, R.; Turnmire, K.L. Ice Age peoples of North America: Environments, origins, and adaptations of the first Americans. Texas A&M University Press: Center for the Study of First Americans (p.200-212)

-Clark, J.; Mitrovica, J.X.; Alder, J. 2014. Coastal paleogeography of the California-Oregon-Washington and Bering sea continental shelves during the latest Pleistocene and Holocene: implications for the archaeological record. *Journal of Archaeological Science* 52:12-23

-Clark, J.; Carlson, A.E.; Reyes, A.V.; Carlson, E.C.B.; Guillaume, L.; Milne, G.A.; Tarasov, L.; Caffee, M.; Wilcken, K.; Rood, D.H. 2022. The age of the opening of the Ice-Free Corridor and implications for the peopling of the Americas. *PNAS* 119(14):e2118558119 (1-6)

-Collard, M.; Buchanan, B.; Hamilton, M.J.; O'Brien, M.J. 2010. Spatiotemporal dynamics of the Clovis-Folsom transition. *Journal of Archaeological Science* 37(10):2513-2519thus

-Colombo, G.; Traverso, L.; Mazzocchi, L.; Grugni, V.; Rambaldi Migliore, N.; Capodiferro, M.R.; Lombardo, G.; Flores, R.; Karmin, M.; Rootsi, S.; Ferretti, L.; Olivieri, A.; Torroni, A.; Martiano, R.; Achilli, A.; Raveane, A.; Semino, O. 2022. Overview of the Americas' First Peopling from a patrilineal perspective: new evidence from the southern continent. *Genes* 13(2):220 (1-22)

-Conolly, J. 2008. Geographical Information Systems and Landscape Archaeology. In: David, B.; Thomas, J. (eds) Handbook of Landscape Archaeology. Walnut Creek: Left Coast Press (chapter 56:583-595)

-Coutouly, Y.A.G.; Holmes, C.E. 2018. The microblade industry from Swan Point cultural zone 4b: Technological and cultural implications from the earliest human occupation in Alaska. *American Antiquity* 83(4):735-752

-Crabtree, S.A.; White, D.A.; Bradshaw, C.J.A.; Saltré, F.; Williams, A.N.; Beaman, R.J.; Bird, M.I.; Ulm, S. 2021. Landscape rules predict optimal superhighways for the first peopling of Sahul. *Nature* 5:1303-1313

-Cummings, V. 2008. Virtual reality, visual envelopes, and characterizing landscape. In: David, B.; Thomas, J. (eds) Handbook of Landscape Archaeology. Walnut Creek: Left Coast Press (chapter 28:285-290)

-Cwynar, L.C.; Ritchie, J.C. 1980. Arctic steppe-tundra: A Yukon Perspective. *Science* 208(4450):1375-1377

-Cwynar, L.C. 1982. A Late-Quaternary vegetation history from Hanging Lake, Northern Yukon. *Ecological Monographs* 52(1):1-24

-Dalton, A.S.; Margold, M.; Stokes, C.R.; Tarasov, L.; Dyke, A.S.; Adams, R.S.; Allard, S.; Arends, H.E.; Atkinson, N.; Attig, J.W.; Barnett, P.J.; Barnett, R.L.; Batterson, M.; Bernatchez, P.; Borns Jr., H.W.; Breckenridge, A.; Briner, J.P.; Brouard, E.; Campbell, J.E.; Carlson, A.E.; Clague, J.J.; Curry, B.B.; Daigneault, R.-A.; Dubé-Loubert, H.; Easterbrook, D.J.; Franzi, D.A.; Friedrich, H.G.; Funder, S.; Gauthier, M.S.; Gowan, A.S.; Harris, K.L.; Hétu, B.; Hooyer, T.S.; Jennings, C.E.; Johnson, M.D.; Kehew, A.E.; Kelley, S.E.; Kerr, D.; King, E.L.; Kheldsen, K.K.; Knaeble, A.R.; Lajeunesse, P.; Lakeman, T.R.; Lamothe, M.; Larson, P.; Lavoie, M.; Loope, H.M.; Lowell, T.V.; Lusardi, B.A.; Manz, L.; McMartin, I.; Nixon, F.C.; Occhietti, S.; Parkhill, M.A.; Piper, D.J.W.; Pronk, A.G.; Richard, P.J.H.; Ridge, J.C.; Ross, M.; Roy, M.; Seaman, A.; Shaw, J.; Stea, R.R.; Teller, J.T.; Thompson, W.B.; Thorleifson, L.H.; Utting, D.J.; Veillette, J.J.; Ward, B.C.; Weddle, T.K.; Wright Jr., H.E. 2020. An updated radiocarbon-based ice margin chronology for the last deglaciation of the North American Ice Sheet Complex. *Quaternary Science Reviews* 234:106223(1-27)

-Daniels, W.C.; Russell, J.M.; Morrill, C.; Longo, W.M.; Giblin, A.E.; Holland-Stergar, P.; Welker, J.M.; Wen, X.; Hu, A.; Huang, Y. 2021. Lacustrine leaf wax hydrogen isotopes indicate strong regional climate feedbacks in Beringia since the last ice age. *Quaternary Science Reviews* 269:107130 (1-15)

-Davis, L.G.; Madsen, D.B. 2020. The coastal migration theory: Formulation and testable hypotheses. *Quaternary Science Reviews* 249:106605 (1-13)

-Dillehay, T.D.; Ramírez, C.; Pino, M.; Collins, M.B.; Rossen, J.; Pino-Navarro, J.D. 2008. Monte Verde : Seaweed, Food, Medicine and the Peopling of South America. *Science* 320 (5877):784-786

-Dillehay, T.D.; Ocampo, C.; Saavedra, J.; Sawakuchi, A.O.; Vega, R.M.; Pino, M.; Colloins, M.B.; Cummings, L.S.; Arregui, I.; Villagran, X.S.; Hartmann, G.A.; Mella, M.; González, A.; Dix, G. 2015. New Archaeological Evidence for an Early Human Presence at Monte Verde, Chile. *PLoS ONE* 10(11):e0141923

-Dillehay, T.D. 1984. A Late Ice-Age Settlement in Southern Chile. *Scientific American* 251(4):106-119

-Dillehay, T.D.; Ocampo, C.; Saavedra, J.; Sawakuchi, A.O.; Vega, R.M.; Pino, M.; Collins, M.B.; Cummings, L.S.; Arregui, I.; Villagran, X.S.; Hartmann, G.A.; Mella, M.; González, A.; Dix, G. 2015. New Archaeological Evidence for an Early Human Presence at Monte Verde, Chile. PLoS ONE 10(11):e0141923

-Dillehay, T.D.; Pino, M.; Ocampo, C. 2021. Comments on Archaeological Remains at the Monte Verde Site Complex, Chile. *PaleoAmerica* 7(1):8-13

-Dixon, E.J. 2001. Human colonization of the Americas: timing, technology and process. *Quaternary Science Reviews* 20(1-3):277-299

-Dixon, J.E.; Monteleone, K. 2014. Gateway to the Americas: Underwater archeological survey in Beringia and the North Pacific. In: Evans, A.M.; Flatman, J.C.; Flemming, N.C. (eds) Prehistoric archaeology on the continental shelf. Springer, New York NY (chapter 6: p.95-114)

-Dobson, J.E.; Spada, G.; Galassi, G. 2020. Global choke points may link sea level and human settlement at the Last Glacial Maximum. *Geographical Review* 110(4):595-620

-Dobson, J.E.; Spada, G.; Galassi, G. 2021. The Bering Transitory Archipelago: stepping stones for the first Americans. *Comptes Rendus Géosciences – Sciences de la Planète* 353(1):55-65

-Duda, P.; Zrvavy, J. 2019. Towards a global phylogeny of human populations based on genetic and linguistic data. *Modern Human Origins and Dispersals. Words, Bones, Genes, Tools: DFG Center for Advanced Studies Series I*: 331-359

-Egeland, C.P.; Nicholson, C.M.; Gasparian, B. 2010. Using GIS and Ecological variables to identify high potential areas for paleoanthropological survey: an example from Northern Armenia. *Journal of Ecological Anthropology* 14(1):89-98

-El Adli, J.J.; Fisher, D.C.; Vartanyan, S.I.; Tikhonov, A.N. 2017. Final years of life and seasons of death of woolly mammoths from Wrangel Island and mainland Chukotka, Russian Federation. *Quaternary International* 445:135-145

-Elias, S.A.; Short, S.K.; Phillips, R.L. 1992. Paleoecology of Late-Glacial peats from the Bering Land Bridge, Chukchi Sea Shelf region, Northwestern Alaska. *Quaternary Research* 38(3):371-378

-Elias, S.A.; Short, S.K.; Birks, H.H. 1997. Late Wisconsin environments of the Bering Land Bridge. *Palaeogeography, Palaeoclimatology, Palaeoecology* 136(1-4):293-308

-Elias, S.A. 2000. Late Pleistocene climates of Beringia, based on analysis of fossil beetles. *Quaternary Research* 53(2):229-235

-Elias, S.A. 2001. Mutual climatic range reconstructions of seasonal temperatures based on Late Pleistocene fossil beetle assemblages in Eastern Beringia. *Quaternary Science Reviews* 20(1-3):77-91

-Elias, S.A.; Brigham-Grette, J. 2013. Late Pleistocene glacial events in Beringia. *Encyclopedia of Quaternary Sciences* 2:191-201

-Elston, D.A.; Buckland, S.T. 1993. Statistical modelling of regional GIS data: an overview. *Ecological Modelling* 67(1):81-102

-Eren, M.I.; Buchanan, B.; O'Brien, M.J. 2015. Social learning and technological evolution during the Clovis colonization of the New World. *Journal of Human Evolution* 80:159-170

-Erlandson, J.M.; Graham, M.H.; Bourque, B.J.; Corbett, D.; Estes, J.A.; Steneck, R.S. 2007. The Kelp Highway Hypothesis : Marine Ecology, the Coastal Migration Theory, and the Peopling of the Americas. *The Journal of Island and Coastal Archaeology* 2(2):161-174

-Erlandson, J.M.; Braje, T.J. 2011. From Asia to the Americas by Boat? Paleogeography, Paleoecology and stemmed points of the Northwest Pacific. *Quaternary International* 239(1-2):28-37

-Fagundes, N.J.R.; Tagliani-Ribeiro, A.; Rubicz, R.; Tarskaia, L.; Crawford, M.H.; Salzano, F.M.; Bonatto, S.L. 2018. How strong was the bottleneck associated with the peopling of the Americas? New insights from multilocus sequence data. *Genetics and Molecular Biology* 41(1):206-214

-Farmer, J.R.; Sigman, D.M.; Granger, J.; Underwood, O.M.; Fripiat, F.; Cronin, T.M.; Martínez-García, A.; Gaug, G.H. 2021. Arctic Ocean stratification set by sea level and freshwater inputs since the last ice age. *Nature Geoscience* 14(9):684-689

-Felzer, B. 2001. Climate impacts of an ice sheet in East Siberia during the Last Glacial Maximum. *Quaternary Science Reviews* 20(1-3):437-447

-Fiedel, S.J. 2022. Initial human colonization of the Americas, redux. *Radiocarbon* 64(4):845-897

-Field, J.S.; Petraglia, M.D.; Mirazon Lahr, M. 2007. The southern dispersal hypothesis and the South Asian archaeological record: examination of dispersal routes through GIS analysis. *Journal of Anthropological Archaeology* 26(1):88-108

-Finkenbinder, M.S.; Abbott, M.B.; Finney, B.P.; Stoner, J.S.; Dorfman, J.M. 2015. A multi-proxy reconstruction of environmental change spanning the last 37.000 years from Burial Lake, Arctic Alaska. *Quaternary Science*

-Fladmark, K.R. 1990. Possible early human occupation of the Queen Charlotte Islands, British Columbia. *Canadian Journal of Archaeology/Journal Canadien d'Archéologie* 14:183-197

-Flegontov, P.; Altinisik, N.E.; Changmai, P.; Rohland, N.; Mallick, S.; Adamski, N.; Bolnick, D.A.; Broomndkhoshbacht, N.; Candilio, F.; Culleton, B.J.; Flegontova, O.; Friesen, T.M.; Jeong, C.; Harper, T.K.; Keating, D.; Kennett, D.J.; Kim, A.M.; Lamnidis, T.C.; Lawson, A.M.; Olalde, I.; Oppenheimer, J.; Potter, B.A.; Raff, J.; Sattler, R.A.; Skoglund, P.; Stewardson, K.; Vajda, E.J.; Vasilyev, S.; Veselovskya, E.; Hayes, M.G.; O'Rourke, D.H.; Krause, J.; Pinhais, R.; Reich, D.; Schiffels, S. 2019. Palaeo-Eskimo genetic ancestry and the peopling of Chukotka and North America. *Nature* 570:236-240

-Forman, S.L.; Pierson, J.; Gómez, J.; Brigham-Grette, J.; Nowaczyk, N.R.; Melles, M. 2007. Luminescence geochronology for sediments from Lake El'gygytgyn, northeast Siberia, Russia: constraining the timing and paleoenvironmental events for the past 200ka. *Journal of Paleolimnology* 37:77-88

-Francis, N. 2021. Language in the Americas: Out of Beringia (Las lenguas en América: el éxodo de Beirngia). *Lengua y migración/Language and migration* 13(2):171-191

-Frank, R.M. 2014. the skylore of the indigenous peoples of Eurasia. In: Ruggles, C.L.N. (ed) Handbook of Archaeoastronomy and Ethnoastronomy. Berlin: Springer Publishing Company (p.1679-1686)

-Fu, Q.; Li, H.; Moorjani, P.; Jay, F.; Slepchenko, S.M.; Bondarev, A.A.; Johnson, P.L.F.; Aximu-Petri, A.; Prüfer, K.; de Filippo, C.; Meyer, M.; Zwyns, N.; Salazar-García, D.C.; Kuzmin, Y.V.; Keates, S.G.; Kosintsev, P.A.; Razhev, D.I.; Richards, M.P.; Peristov, N.V.; Lachmann, M.; Douka, K.; Higham, T.F.G.; Slatkin, M.; Hublin, J.-J.; Reich, D.; Kelso, J.; Viola, T.B.; Pääbo, S. 2014. Genome sequence of a 45.000-year-old modern human from western Siberia. *Nature* 514:445-450

-Gaglioti, B.V.; Barnes, B.M.; Zazula, G.D.; Beaudoin, A.B.; Wooller, M.J. 2011. Late Pleistocene paleoecology of arctic ground squirrel (*Urocitellus parryii*) caches and nests from Interior Alaska's mammoth steppe ecosystem, USA. *Quaternary Research* 76(3):373-382

-Gladyshev, S.A.; Olsen, J.W.; Tabarev, A.V.; Kuzmin, Y.V. 2010. Chronology and periodization of Upper Paleolithic sites in Mongolia. *Archaeology, Ethnology and Anthropology of Eurasia* 38(3):33-40

-Gladyshev, S.A.; Olsen, J.W.; Tabarev, A.V.; Jull, A.J.T. 2012. The Upper Paleolithic of Mongolia: Recent finds and new perspectives. *Quaternary International* 281:36-46

-Glass, C.; Steele, J.; Wheatley, D. 1999. Modelling human range expansion across a heterogeneous cost surface. In: Dingwall, L.; Exon, S.; Gaffney, V.; Laflin, S.; van Leusen, M. (eds) Archaeology in the age of the internet: CAA97: Computer applications and quantitative methods in archaeology. Proceedings of the 25th anniversary conference. Birmingham: British Archaeological Reports (p.67-72)

-Goebel, T. 1999. Pleistocene human colonization of Siberia and peopling of the Americas: an ecological approach. *Evolutionary Anthropology: Issues, News, and reviews* 8(6):208-227

-Goebel, T.; Hoffecker, J.F.; Graf, K.E.; Vachula, R.S. 2022. Archaeological reconnaissance at Lake E5 in the Brooks Range, Alaska and implications for the early human biomarker record of Beringia. *Quaternary Science Reviews* 286:107553 (1-8)

-Gómez-Carballa, A.; Pardo-Seco, J.; Brandini, S.; Achilli, A.; Perego, U.A.; Coble, M.D.; Diegoli, T.M.; Alvarez-Iglesias, V.; Martinón-Torres, F.; Olivieri, A.; Torroni, A.; Salas, A. 2018. The peopling of South America and the trans-Andean gene flow of the first settlers. *Genome Research* 28:767-779

-Gómez Coutouly, Y.A. 2018a. Apogée et déclin de la méthode Yubetsu : les débitages lamellaires par pression dans le Nord Pacifique lors du peuplement du Nouveau Monde (de la fin du Pléistocène au début de l'Holocène). *Bulletin de la Société Préhistorique française* 115(1) :7-42

-Gómez Coutouly, Y.A. 2018b. The emergence of pressure knapping microblade technology in Northeast Asia. *Radiocarbon* 60(30):821-855

-Graf, K.E. 2009. "The Good, the Bad, and the Ugly": the radiocarbon chronology of the Middle and Late Upper Paleolithic in the Enisei River valley, south-central Siberia. *Journal of Archaeological Science* 36(3):694-707

-Graf, K.E. 2014. Siberian Odyssey. In: Graf, K.E.; Ketron, C.V.; Waters, M.R. (eds) Paleoamerican Odyssey. Texas: Texas A&M University Press (chapt. 4:65-80)

-Graf, K.E.; Buvit, I. 2017. Human dispersal from Siberia to Beringia: assessing a Beringian standstill in light of the archaeological evidence. *Current Anthropology* 58 (Supplement17): S582-S603)

-Graf, K.E.; Goebel, T. 2017. The Paleolithic of eastern Beringia from western Alaska to Canadian Yukon. In: Kotlyakov, V.M.; Velichko, A.A.; Vasil'ev, S.A. (eds) Human Colonization of the Arctic: The interaction between early migration and the paleoenvironment. New York: Elsevier Academic Press (chapt. 3.3::311-338

-Gravel-Miguel, C.; Wren, C.D. 2018. Agent-based least-cost path analysis and the diffusion of Cantabrian Lower Magdalenian engraved scapulae. *Journal of Archaeological Science* 99:1-9

-Greenberg, J.H.; Turner II, C.G.; Zegura, S.L. 1986. The Settlement of the Americas: A comparison of the linguistic, dental, and genetic evidence. *Current Anthropology* 27(5):477-497

-Grégoire, L.J.; Payne, A.J.; Valdes, P.J. 2012. Deglacial rapid sea level rises caused by ice-sheet saddle collapses. *Nature* 487(7406):219-222

-Grøn, O.; Turov, M.; Klokkernes, T. 2008. Settling in the landscape – settling the land: Ideological aspects of territoriality in a Siberian hunter-gatherer society. Olofsson, A. (ed) Archaeology of Settlements and Landscapes in the North. *Vuollerim Papers on hunter-gatherer archaeology* 2:57-80

-Grosswald, M.G. 2001. The Late Weichselian Barents-Kara Ice Sheet: In defense of a maximum reconstruction. *Russian Journal of Earth Sciences* 3(6):427-452

-Grosswald, M.G.; Hughes, T.J. 2002. The Russian component of an Arctic ice sheet during the Last Glacial Maximum. *Quaternary Science Reviews* 21(1-3):121-146

-Gualtieri, L.; Vartanyan, S.; Brigham-Grette, J.; Anderson, P.M. 2003. Pleistocene raised marine deposits on Wrangel Island, northeast Siberia and implications for the presence of an East Siberian ice sheet. *Quaternary Research* 59(3):399-410

-Guan, Y.; Li, Y.; Xing, S.; Huang, L.; Cheng, L.; Zhou, Z. 2021. Stone materials discovered newly in the Upper Paleolithic sites of Gannan county, Heilongjiang Province. *Acta Anthropologica Sinica* 40(2):281-291

-Gustas, R.; Supernant, K. 2017. Least cost path analysis of early maritime movement on the Pacific Northwest Coast. *Journal of Archaeological Sciences* 78:40-56

-Gustas, R.; Supernant, K. 2019. Coastal migration into the Americas and least cost path analysis. *Journal of Anthropological Archaeology* 54;192-206

-Guthrie, R.D. 1982. Mammals of the Mammoth Steppe as Paleoenvironmental indicators. In: Hopkins, D.M.; Matthews Jr., J.V.; Schweger, C.E.; Young, S.B. (eds) Paleoecology of Beringia. New York: Academic Press (p.307-328)

-Guthrie, R.D. 1990. Frozen Fauna of the Mammoth Steppe: the Story of Blue Babe. Chicago: University of Chicago Press.

-Hansen, W.F. 2001. Identifying stream types and management implications. *Forest Ecology and Management* 143(1-3):39-46

-Harington, C.R.; Cinq-Mars, J. 2008. Bluefish Caves – Fauna and context. *Beringian Research Notes* 19:8 (1-4)

-Harington, C.R. 2011. Quaternary cave faunas of Canada: a review of the vertebrate remains. *Journal of Cave and Karst Studies* 73(3):162-180

-Harris, H.A. 2003. Remembering 12.000 years of history: oral history, indigenous knowledge and ways of knowing in Northwestern North America. PhD thesis: University of Alberta

-Harris, S.A. 2019. The relationship of sea level changes to climatic change in northeast Asia and northern North America during the last 75 ka BP. *AIMS Environmental Science* 6(1):14-40

-Harris, H. 2010. Indigenous worldviews and ways of knowing as theoretical and methodological foundations behind archaeological theory and method. In: Bruchac, M.; Hart, S.; Wobst, H.M. (eds) Indigenous Archaeologies: A Reader on Decolonization. New York: Routledge (chapter 6 p. 63-68)

-Haynes, C.V. 1992. Contributions of radiocarbon dating to the geochronology of the peopling of the New World. In: Taylor, R.E.; Long, A.; Kra, R.S. (eds) Radiocarbon After Four Decades. Springer Science + Business Media (p. 355-374)

-Haynes, C.V. 1995. Geochronology of paleoenvironmental change, Clovis type site, Blackwater Draw, New Mexico. *Geoarchaeology* 10(5):317-388

-Haynes, C.V. 2022. Evidence for humans at White Sands National Park during the Last Glacial Maximum could actually be for Clovis people ~13.000 years ago. *PaleoAmerica* 8(2):

-Haynes, G. 2022. Sites in the Americas with Possible or Probable evidence for the butchering of Proboscideans. *PaleoAmerica* 8(3):187-214

-Hazelwood, L.; Steele, J. 2003. Colonizing new landscapes: archaeological detectability of the first phase. In: Rockman, M.; Steele, J. (eds) Colonization of Unfamiliar Landscapes: the Archaeology of Adaptation. London: Routledge (chapter 12:203-22

-Hazelwood, L.; Steele, J. 2004. Spatial dynamics of human dispersals: Constraints on modelling and archaeological validation. *Journal of Archaeological Science* 31:669-679

-Heintzman, P.D.; Froese, D.; Ives, J.W.; Soares, A.E.R.; Zazula, G.D.; Letts, B.; Andrews, T.D.; Driver, J.C.; Hall, E.; Hare, P.G.; Jass, C.N.; MacKay, G.; Southon, J.R.; Stiller, M.; Woywitka, R.; Suchard, M.A.; Shapiro, B. 2016. Bison phylogeography constrains dispersal and viability of the Ice Free Corridor in western Canada. *PNAS* 113 (29):8057-8063

-Herzog, I. 2020. Spatial analysis based on cost functions. In: Gillings, M.; Hacigüzeller, P.; Lock, G. (eds) Archaeological spatial analysis: A Methodological Guide. London: Routledge (Chapter 18:333-358)

-Hibbert, D. 1982. History of the Steppe-Tundra concept. In Hopkins, D.M.; Matthews Jr., J.V.; Schweger, C.E.; Young, S.B. (eds) Paleoecology of Beringia. New York: Academic Press (p. 153-156)

-Hirasawa, Y.; Holmes, C.E. 2017. The relationship between microblades morphology and production technology in Alaska from the perspective of the Swan Point site. *Quaternary International* 442(B):104-117

-Hoffecker, J.F. 2005. A Prehistory of the North: Human settlement of the higher latitudes. New Jersey: Rutgers University Press

-Hoffecker, J.F.; Powers, W.R.; Goebel, T. 1993. The Colonization of Beringia and the Peopling of the New World. *Science* 259(5091):46-53

-Hoffecker, J.F.; Elias, S.A. 2003. Environment and Archeology in Beringia. *Evolutionary Anthropology* 12:34-49

-Hoffecker, J.F.; Elias, S.A.; O'Rourke, D.H.; Scott, G.R.; Bigelow, N.H. 2016. Beringia and the global dispersal of modern humans. *Evolutionary Anthropology: Issues, news, and reviews* 25(2):64-78

-Hoffecker, J.F.; Elias, S.A.; Potapova, O. 2020. Arctic Beringia and Native American Origins. *PaleoAmerica* 6(2):158-168

-Hopkins, D.M.; Matthews Jr., J.V.; Schweger, C.E.; Young, S.B. 1982. Paleoecology of Beringia. New York: Academia Press

-Horiuchi, K.; Minoura, K.; Hoshino, K.; Oda, T.; Nakamura, T.; Kawai, T. 2000. Palaeoenvironmental history of Lake Baikal during the last 23000 years. *Palaeogeography, Palaeoclimatology, Palaeoecology* 157(1-2):95-108

-Howey, M.C.L. 2011. Multiple pathways across past landscapes: circuit theory as a complementary geospatial method to least cost path for modeling past movement. *Journal of Archaeological Science* 38(10):2523-2535

-Hu, A.; Meehl, G.A.; Otto-Bliesner, B.L.; Waelbroeck, C.; Han, W.; Loutre, M.-F.; Lambeck, K.; Mitrovica, J.X.; Rosenbloom, N. 2010. Influence of Bering Strait flow and North Atlantic circulation on glacial sea-level changes. *Nature Geoscience* 3(2):118-121

-Hu, A.; Meehl, G.A.; Han, W.; Timmermann, A.; Otto-Bliesner, B.; Liu, Z.; Washington, W.M.; Large, W.; Abe-Ouchi, A.; Kimoto, M.; Lambeck, K.; Wu, B. 2012. Role of the Bering Strait on the hysteresis rinaof the ocean conveyor belt circulation and glacial climate stability. *Proceedings of the National Academy of Science* 109(17):6417-6422

-Hughes, P.D.; Gibbard, P.L. 2015. A stratigraphical basis for the Last Glacial Maximum (LGM). *Quaternary International* 383:174-185

-Ickert-Bond, S.M.; Murray, D.F.; DeChaine, E. 2009. Contrasting patterns of plant distribution in Beringia. *Alaska Park Science* 8(2):26-32

-Ickert-Bond, S.M.; Huettmann, F.; Loera, I.; Strecker, L.; Sekretareva, N.; Mikhailova, Y. 2013. New insights on Beringian plant distribution patterns. *Alaska Park Sciences* 12:61-69

-Ikawa-Smith, F. 2004. Humans along the Pacific Margin of Northeast Asia before the Last Glacial Maximum: Evidence for their presence and adaptations. In: Madsen, D.B. (ed) Entering America:

Northeast Asia and Beringia before the Last Glacial Maximum. Salt Lake City: University of Utah Press (Chapter 10: 285-310

-Inizan, M.-L. 2012. Pressure *Débitage* in the Old World: Forerunners, researchers, geopolitics – handing on the baton. In: Desrosiers, P.M. (ed) The emergence of pressure blade making: from origin to modern experimentation. Springer Science & Business Media (chapter 2:11-42)

-Isern, N.; Zilhão, J.; Fort, J.; Ammerman, A.J. 2017. Modeling the role of voyaging in the coastal spread of the Early Neolithic in the West Mediterranean. *Proceedings of the National Academy of Sciences of the United States of America (PNAS)*114(5):897-902

-Iwase, A. 2016. A functional analysis of the LGM microblade assemblage in Hokkaido, northern Japan: A case study of Kashiwadai 1. *Quaternary International* 425:140-157

-Izuho, M. 2014. Human technological and behavioral adaptation to landscape changes around the Last Glacial Maximum in Japan: A focus on Hokkaido. In: Graf, K.E.; Ketron, C.V.; Waters, M.R. (eds) Paleoamerican Odyssey Texas: Texas A&M University Press (chapter 3: 45-64)

-Jakobsson, M.; Pearce, C.; Cronin, T.M.; Backman, J.; Anderson, L.G.; Barrientos, N.; Björk, G.; Coxall, H.; de Boer, A.; Mayer, L.A.; Mörth, C.-M.; Nilsson, J.; Rattray, J.E.; Stranne, C.; Semiletov, I.; O'Regan, M. 2017. Post-glacial flooding of the Bering Land Bridge dated to 11 cal ka BP based on new geophysical and sediment records. *Climate of the Past* 13(8):991-1005

-Jennings, T.A.; Smallwood, A.M. 2019. The Clovis Record. *SAA Archaeological Record* 19(3):45-50

-Johnston, W.A. 1933. Quaternary geology of North America in relation to the migration of man. In: Jennes, D. (ed) The American Aborigines: Their Origin and Antiquity. Toronto: University of Toronto Press (p. 11-45)

-Kealy, S.; Louys, J.; O'Connor, S. 2018. Least-cost pathway models indicate northern human dispersals from Sunda to Sahul. *Journal of Human Evolution* 125:59-70

-Kennedy, K.E.; Froese, D.G.; Zazula, G.D.; Lauriol, B. 2010. Last Glacial Maximum age for the northwest Laurentide maximum from the Eagle River spillway and delta complex, northern Yukon. *Quaternary Science Reviews* 29(9-10):1288-1300

-Kempf, M. 2019. The application of GIS and satellite imagery in archaeological land-use reconstruction: a predictive model? *Journal of Archaeological Science: Reports* 25:116-128

-Khenzykhenova, F.; Lipnina, E.; Danukalova, G.; Shchetnikov, A.; Osipova, E.; Semenei, E.; Tumurov, E.; Lokhov, D. 2019. The area surrounding the world-famous geoarchaeological site Mal'ta (Baikal Siberia): New data on the chronology, archaeology and fauna. *Quaternary International* 509:17-29

-Klein, K.; Wegener, C.; Schmidt, I.; Rostami, M.; Ludwig, P.; Ulbrich, S.; Richter, J.; Weniger, G.-C.; Shao, Y. 2020. Human existence potential in Europe during the Last Glacial Maximum. *Quaternary International* 581:7-27

-Kleman, J.; Jansson, K.; De Angelis, H.; Stroeven, A.P.; Hättestrand, C.; Alm, G.; Glasser, N. 2010. North American Ice Sheet build-up during the last glacial cycle, 115-21kyr. *Quaternary Science Reviews* 29(17-18):2036-2051

-Klementiev, A.M. 2010. Study and reconstruction of the landscape situation from the mammal fauna of the Western Transbaikalia. *Geography and Natural Resources* 31(1):34-40

-Kondo, Y.; Sano, K.; Omori, T.; Abe-Ouchi, A.; Chan, W.-L.; Kadowaki, S.; Naganuma, M.; O'ishi, R.; Oguchi, T.; Nishiaki, Y.; Yoneda, M. 2018. Ecological niche and least-cost path analyses to estimate

optimal migration routes of Initial Upper Palaeolithic populations to Eurasia. In: Nishiaki, Y.; Akazawa, T. (eds) The Middle and Upper Paleolithic Archaeology of the Levant and Beyond. Replacement of Neanderthals by Modern Human Series. Springer, Singapore (p. 199-212)

-Krasinski, K.E.; Blong, J.C. 2020. Unresolved questions about site formation, provenience, and the impact of natural processes on bone at the Bluefish Caves, Yukon Territory. *Arctic Anthropology* 57(1):1-21

-Kubiak, C.; Grimes, V.; Van Biesen, G. Keddie, G.; Buckley, M.; MacDonald, R.; Richards, M.P. 2022. Dietary niche separation of three Late Pleistocene bear species from Vancouver Island, on the Pacific Northwest Coast of North America. *Journal of Quaternary Science* DOI: 10.1002/jqs.3451 (p.1-13)

-Kuzmin, Y.V.; Glascock, M.D.; Sato, H. 2002. Sources of Archaeological obsidian on Sakhalin Island (Russian Far East). *Journal of Archaeological Science* 29:741-749

-Kuzmin, Y.V.; Orlova, L.A. 2004. Radiocarbon chronology and environment of woolly mammoth (*Mammuthus primigenius* Blum.) in Northern Asia: results and perspectives. *Earth-Science Reviews* 68:133-169

-Kuzmin, Y.V.; Vasilevski, A.A.; Gorbunov, S.V.; Burr, G.S.; Jull, A.J.T.; Orlova, L.A.; Shubina, O.A. 2004. Chronology of prehistoric cultural complexes of Sakhalin Island (Russian Far East). *Radiocarbon* 46(1):353-362

-Kuzmin, Y.V.; Glascock, M.D. 2007. Two islands in the ocean: Prehistoric obsidian exchange between Sakhalin and Hokkaido, Northeast Asia. *The Journal of Island and Coastal Archaeology* 2(1):99-120

-Kuzmin, Y.V. 2011. The Patterns of obsidian exploitation in the late Upper Pleistocene of the Russian Far East and neighbouring Northeast Asia. *Natural Resource Environmetn and Humans* 1:67-82

-Kuzmin, Y.V.; Glascock, M.D.; Izuho, M. 2013. The geochemistry of the major sources of archaeological obsidian on Hokkaido Island (Japan): Shirataki and Oketo. *Archaeometry* 55(3):355-369

-Kuzmin, Y.V.; Keates, S.G. 2016. Siberia and neighboring regions in the Last Glacial Maximum: did people occupy northern Eurasia at that time? *Archaeological and Anthropological Sciences* 10(1):111-124

-Kuzmin, Y.V. 2017. Central Siberia (the Yenisey-Lena-Yana Region). In: Kotlyakov, V.M.; Velichko, A.A.; Vasil'ev, S.A. (eds) Human colonization of the Arctic: the interaction between early migration and the paleoenvironment. New York: Elsevier- Academic Press (chapter 2.3:211-238)

-Kuzmin, Y.V.; Kosintsev, P.A.; Stepanov, A.D.; Boeskorov, G.G.; Cruz, R.J. 2017. Chronology and faunal remains of the Khayrgas Cave (Eastern Siberia, Russia). *Radiocarbon* 59(2):575-582

-Lambeck, K.; Esat, T.M.; Potter, E.K. 2002. Links between climate and sea levels for the past three million years. *Nature* 419(6903):199-206

-Lanata, J.L.; Martino, L.; Osella, A.; Garcia-Herbst, A. 2008. Demographic conditions necessary to colonize new spaces: the case for early human dispersal in the Americas. *World Archaeology* 40(4):520-537

-Lbova, L. 2017. Technological features of decorated ivory artifacts in the "classic" collection from the Mal'ta site (Siberia, Upper Paleolithic). *Annales d'Université "Valahia" Târgoviste. Section d'Archéologie et d'Histoire* 19 (1) :7-17

-Lbova, L. 2021. The Siberian Paleolithic site of Mal'ta: a unique source for the study of childhood archaeology. *Evolutionary Human Sciences* 3(e9):1-11

-Lbova, L.; Volkov, P. 2016. Processing technology of the objects of mobile art in the Upper Paleolithic of Siberia (the Mal'ta site). *Quaternary International* 403:16-22

-Lbova, L.V.; Volkov, P.V. 2017. Pigment decoration of Palaeolithic anthropomorphous figurines from Siberia. *Rock Art Research* 34(2):169-178

-Lbova, L.; Kazakov, V.V.; Rostiazhenko, T.E. 2020. Virtual Prehistory portable art collection of Siberian Mal'ta-Buret' culture: ways of documenting, classification and representation. *Annales d'Université Valahia Targoviste. Section d'Archéologie et d'Histoire* 22(1) :7-18

-Lee, E.J.; Merriwether, D.A.; Kasparov, A.K.; Khartanovich, V.I.; Nikolskiy, P.A.; Shidlovskiy, F.K.; Gromov, A.V.; Chikisheva, T.A.; Chasnyk, V.G.; Timoshin, V.B.; Pavlova, E.Y.; Pitulko, V.V. 2018. A genetic perspective of prehistoric hunter-gatherers in the Siberian Arctic: Mitochondrial DNA analysis of human remains from 8000 years ago. *Journal of Archaeological Science: Reports* 17:943-949

-Lesnek, A.J.; Briner, J.P.; Lindqvist, C.; Baichtal, J.F.; Heaton, T"H. 2018. Deglaciation of the Pacific coastal corridor directly preceded the human colonization of the Americas. *Science Advances* 4:eaar5040(1-8)

-Lewis, J. 2020. Assessing the impact of including traversal across slope on Least cost path accuracy: a roman road case study SocArXiv doi:10.31235/osf.io/q5yad

-Li, F.; Vanwezer, N.; Boivin, N.; Gao, X.; Ott, F.; Petraglia, M.; Roberts, P. 2019. Heading north: Late Pleistocene environments and human dispersals in central and eastern Asia. *PLoS ONE* 14(5):1-22

-Lieskovsky, T.; Duraciova, R.; Karell, L. 2013. Selected mathematical principles of archaeological predictive models: Creation and validation in the GIS environment. *Interdisciplinaria Archaeologica Natural Sciences in Archaeology* 4(2):33-46

-Llamas, B.; Fehren-Schmitz, L.; Valverde, G.; Soubrier, J.; Mallick, S.; Rohland, N.; Nordenfelt, S.; Valdiosera, C.; Richards, S.M.; Rohrlach, A.; Barreto Romero, M.I.; Espinoza, I.F.; Tomasto Cagigao, E.; Watson Jiménez, L.; Makowski, K.; Leboreiro Reyna, I.S.; Lory, J.M.; Ballivian Torrez, J.A.; Rivera, M.A.; Burger, R.L.; Ceruti, M.C.; Reinhard, J.; Wells, R.S.; Politis, G.; Santoro, C.M.; Standen, V.G.; Smith, C.; Reich, D.; Ho, S.Y.W.; Cooper, A.; Haak, W. 2016. Ancient mitocondrial DNA provides high-resolution time scale of the peopling of the Americas. *Scientific Advances* 2(4):e1501385 (1-10)

-Llamas, B.; Harkins, K.M.; Fehren-Schmitz, L. 2017. Genetic studies of the peopling of the Americas: What insights do diachronic mitochondrial genome datasets provide? *Quaternary International* 444:26-35

-Llamas, B.; Rada, X.R.; Collen, E. 2020. Ancient DNA helps trace the peopling of the world. *The Biochemist* 42(1):18-22

-Llamas, B.; Rada, X.R.; Collen, E. 2020. Ancient DNA helps trace the peopling of the world. *The Biochemist* 42(1):18-22

-Lozhkin, A.V.; Anderson, P.M. 2016. About the age and habitat of the Kirgilyakh mammoth (Dima), Western Beringia. *Quaternary Science Reviews* 145:104-116

-Lozhkin, A.V.; Anderson, P.M.; Glushkova, O.Y.; Vazhenina, L.N. 2019. Late Quaternary environmetns on the far southwestern edge of Beringia. *Quaternary Science Reviews* 203:21-37

-Manley, W.F. 2002. Postglacial flooding of the Bering land bridge: A geospatial animation. http://instaar.colorado.edu/groups/QGISL/bering_land_bridge/

-Mandryk, C.A.S.; Josenhans, H.; Fedje, D.W.; Mathewes, R.W. 2001. Late Quaternary paleoenvironments of Northwestern North America : implications for inland versus coastal migration routes. *Quaternary Science Reviews* 20:301-314

-Mao, X.; Zhang, H.; Qiao, S.; Liu, Y.; Chang, F.; Xie, P.; Zhang, M.; Wang, T.; Li, M.; Cao, P.; Yang, R.; Liu, F.; Dai, Q.; Feng, X.; Ping, W.; Lei, C.; Olsen, J.W.; Bennett, E.A.; Fu, Q. 2021. The deep population history of northeastern Asia from the Late Pleistocene to the Holocene. *Cell* 184:3256-3266

-Meltzer, D.J.2009. First Peoples in a New World: Colonizing Ice Age America. Los Angeles: University of California Press

-Meyer, V.D.; Max, L.; Hefter, J.; Tiedemann, R.; Mollenhauer, G. 2016. Glacial-to-Holocene evolution of sea surface temperature and surface circulation in the subarctic northwest Pacific and the Western Bering Sea. *Paleoceanography* 31(7):916-927

-Meyer, V.D.; Hefter, J.; Lohmann, G.; Max, L.; Tiedemann, R.; Mollenhauer, G. 2017. Summer temperature evolution on the Kamchatka Peninsula, Russian Far East, during the past 20 000 years. *Climate of the Past* 13(4):359-377

-Miller, D.S.; Holliday, V.T.; Bright, J. 2014. Clovis across the continent. In: Kraf, K.E.; Ketron, C.V; Waters, M.R. (eds) Paleoamerican Odyssey. Texas: Texas A&M University Press (chapter 12: 207-220)

-Mix, A.C.; Bard, E.; Schneider, R. 2001. Environmental processes of the ice age: land, oceans, glaciers (EPILOG). *Quaternary Science Reviews* 20:627-657

-Mochanov, Y.A.; Fedoseeva, S.A. 1996. Ikhine 1 and 2. In: West, F.H. (eds) American Beginnings : The Prehistory and Palaeoecology of Beringia. Chicago: University of Chicago Press (Chapter 3:189-194)

-Moreno-Mayar, J.V.; Potter, B.A.; Vinner, L.; Steinrücken, M.; Rasmussen, S.; Terhorst, J.; Kamm, J.A.; Albrechtsen, A.; Malaspina, M.-S.; Sikora, M.; Reuther, J.D.; Irish, J.D.; Malhi, R.S.; Orlando, L.; Song, Y.S.; Nielsen, R.; Meltzer, D.J.; Willerslev, E. 2018. Terminal Pleistocene Alaskan genome reveals first founding population of Native Americans. *Nature* 553:203-207 (Moreno-Mayar et al. 2018a)

-Moreno-Mayar, J.V.; Vinner, L.; de Barros Damsgaard, P.; de la Fuente, C.; Chan, F.; Spence, J.P.; Allentoft, M.E.; Vimala, T.; Racimo, F.; Pinotti, T.; Rasmussen, S.; Margaryan, A.; Orbegozo, M.I.; Mylopotamitaki, D.; Wooller, M.; Batialle, C.; Becerra-Valdivia, L.; Chivall, D.; Comeskey, D.; Devièse, T.; Grayson, D.K.; George, L.; Harry, H.; alexandersen, V.; Primeau, C.; Erlandson, J.; Rodrigues-Carvalho, C.; Reis, S.; Bastos, M.Q.R.; Cybulski, J.; Vullo, C.; Morello, F.; Vilar, M.; Wells, S.; Gregersen, K.; Hansen, K.L.; Lynnerup, N.; Mirazón Lahr, M.; Kjaer, K.; Strauss, A.; Alfonso-Durruty, M.; Salas, A.; Schroeder, H.; Higham, T.; Malhi, R.S.; Rasic, J.T.; Souza, L.; Santos, F.R.; Malaspinas, A.-S.; Meltzer, D.J.; Willerslev, E. 2018. Early human dispersals within the Americas. *Science* 362:eaav2621 (1-11) (Moreno-Mayar et al. 2018b)

-Morlan, R.E.; Cinq-Mars, J. 1982. Ancient Beringians: Human occupation in the late Pleistocene of Alaska and the Yukon Territory. In: Hopkins, D.M.; Matthews Jr., J.V.; Schweger, C.E.; Young, S.B. (eds) Paleoecology of Beringia. New York: Academic Press (chapt. 21:353-382)

-Mosimann, J.E.; Martin, P.S. 1975. Simulating Overkill by Paleoindians: Did man hunt the giant mammals of the New World to extinction? Mathematical models show that the hypothesis is feasible. *American Scientist* 63(3):304-313

-Naganuma, T.; Igarashi, J. 2021. Parure, pigment et art mobilier du Paléolithique supérieur au Japon. *L'Anthropologie* 125 :102970(1-18)

-Nakazawa, Y.; Izuho, M.; Takakura, J.; Yamada, S. 2005. Toward an understanding of technological variability in microblade assemblages in Hokkaido, Japan. *Asian Perspectives* 44(2):276-292

-Nakazawa, Y.; Izuho, M. 2006. Stone tool assemblage variability during the Last Glacial Maximum in Hokkaido. *Current Research in the Pleistocene* 23:26-28

-Nakazawa, Y; Akai, F. 2020. The Last Glacial Maximum Microblades from Kashiwadai 1 in Hokkaido, Japan. *Lithic Technology* 45(3):127-139

-Nichols, J.; Bentz, C. 2019. Morphological complexity of language reflects the settlement history of the Americas. In: Harvati, K.; Jäger, G. (eds) New Perspectives on the Peopling of the Americas. Kerns Verlag: Tübinger (p.13-26)

-Nielsen, R.; Akey, J.M.; Jakobsson, M.; Pritchard, J.K.; Tishkoff, S.; Willerslev, E. 2017. Tracing the peopling of the world through genomics. *Nature* 541:302-310

-Nikolskiy, P.; Pitulko, V. 2013. Evidence from the Yana Palaeolithic site, Arctic Siberia, yields clues to the riddle of mammoth hunting. *Journal of Archaeological Science* 40(12):4189-4197

-Nomokonova, T.Y.; Losey, R.J.; Goriunova, O.I.; Bazaliiskii, V.I. 2014. Holocene seal imagery in the Lake Baikal region of Eastern Siberia. *Archaeology, Ethnology & Anthropology of Eurasia* 42(3):21-28

-Okladnikov, A.P. 1978. The Paleolithic of Mongolia. In Ikawa-Smith, F. (ed) Early Paleolithic in South and East Asia Berlin: De Gruyter Mouton(p.317-325)

-Ono, A.; Sato, H.; Tsutsumi, T.; Kudo, Y. 2002. Radiocarbon dates and archaeology of the Late Pleistocene in the Japanese islands. *Radiocarbon* 44(2):477-494

-Oppenheimer, S.; Bradley, B.; Stanford, D. 2014. Solutrean hypothesis: genetics, the mammoth in the room. *World Archaeology* 46(5):752-774

-Osada, N.; Kawai, Y. 2021. Exploring models of human migration to the Japanese archipelago using genome-wide genetic data. *Anthropological Science* 129(1):45-58

-Pavlova, E.Y.; Pitulko, V.V. 2020. Late Pleistocene and Early Holocene climate changes and human habitation in the arctic Western Beringia based on revision of palaeobotanical data. *Quaternary International* 549:5-25

-Pedersen, M.W.; Ruter, A.; Schweger, C.; Friebe, H.; Staff, R.A.; Kjeldsen, K.K.; Mendoza, M.L.Z.; Beaudoin, A.B.; Zutter, C.; Larsen, N.K.; Potter, B.A.; Nielsen, R.; Rainville, R.A.; Orlando, L.; Meltzer, D.J.; Kjaer, K.H.; Willerslev, E. 2016. Postglacial viability and colonization in North America's ice-free corridor. *Nature* 537:45-49

-Peltier, W.R. 2004. Global glacial isostasy and the surface of the Ice-Age Earth: The ICE-5G(VM2) Model and GRACE. *Annual Review Earth Planetary Sciences* 32:111-149

-Pelto, B.M.; Caissie, B.E.; Petsch, S.T.; Brigham-Grette, J. 2018. Oceanographic and Climatic change in the Bering Sea, Last Glacial Maximum to Holocene. *Paleoceanography and Paleoclimatology* 33(1):93-111

-Pico, T.; Mitrovica, J.X.; Mix, A.C. 2020. Sea level fingerprinting of the Bering Strait flooding history detects the source of the Younger Dryas climate event. *Science Advances* 6(9):eaay2935 (1-8)

-Pigati, J.S.; Springer, K.B.; Holliday, V.T.; Bennett, M.R.; Bustos, D.; Urban, T.M.; Reynolds, S.C.; Odess, D. 2022. Reply to « Evidence for humans at White Sands National Park during the Last Glacial

Maximum could actually be for Clovis people ~13.000 years ago » by C. Vance, Jr. *PaleoAmerica* 8(2):99-101

-Pinotti, T.; Bergström, A.; Geppert, M.; Bawn, M.; Ohasi, D.; Shi, W.; Lacerda, D.R.; Solli, A.; Norstedt, J.; Reed, K.; Dawtry, K.; González-Andrade, F.; Paz-y-Miño, C.; Revollo, S.; Cuellar, C.; Jota, M.S.; Santos Jr., J.E.; Ayub, Q.; Kivisild, T.; Sandoval, J.R.; Fujita, R.; Xue, Y.; Roewer, L.; Santos, F.R.; Tyler-Smith, C. 2019. Y Chromosome sequences reveal a short Beringian Standstill, rapid expansion, and early population structure of Native American founders. *Current Biology* 29(1):149-157

-Pitcher, L.H.; Smith, L.C.; Gleason, C.J.; Yang, K. 2016. CryoSheds: a GIS modelling framework for delineating land-ice watersheds for the Greenland Ice Sheet. *GIScience & Remote Sensing* 53:707-722

-Pitulko, V.V.; Nikolsky, P.A.; Girya, E.Y.; Basilyan, A.E.; Tumskoy, V.E.; Koulakov, S.A.; Astakhov, S.N.; Pavlova, E.Y.; Anisimov, M.A. 2004. The Yana RHS Site: Humans in the Arctic before the Last Glacial Maximum. *Science* 303(5654):52-56

-Pitulko, V.V.; Pavlova, E.Y.; Nikolskiy, P.A.; Ivanova, V.V. 2012. The oldest art of the Eurasian Arctic: personal ornaments and symbolic objects from Yana RHS, Arctic Siberia. *Antiquity* 86(333):642-659

-Pitulko, V.; Nikolskiy, P.; Basilyan, A.; Pavlova, E. 2014a. Human habitation in Arctic Western Beringia prior to the LGM. In: Graf, K.E.; Ketron, C.V.; Waters, M.R. (eds) Paleoamerican Odyssey. Texas: Texas A&M University Press (chapter 2: 13-44)

-Pitulko, V.V.; Basilyan, A.E.; Pavlova, E.Y. 2014b. The Berelekh Mammoth "Graveyard": new chronological and stratigraphical data from the 2009 field season. *Geoarchaeology: An International Journal* 29(4):277-299

-Pitulko, V.V.; Pavlova, E.Y. 2016. Geoarchaeology and Radiocarbon chronology of Stone Age Northeast Asia. Texas: Texas A&M University Press

-Pitulko, V.; Pavlova, E.; Nikolskiy, P. 2017. Revising the archaeological record of the Upper Pleistocene Arctic Siberia: Human dispersal and adaptations in MIS3 and 2. *Quaternary Science Reviews* 165:127-148

-Pitulko, V.V.; Pavlova, E.Y.; Basilyan, A.E.; Nikolskiy, P.A. 2019. Another perspective on the age and origin of the Berelyokh mammoth site – Comment to the paper published by Lozkhin and Anderson, *Quaternary Research* 89(2018):459-477. *Quatenrary Research* 91(2):910-913

-Politis, G.G.; Prates, L. 2019. The Pre-Clovis peopling of South America. *The Peopling of the Americas at the end of the Pleistocene* 19(3):40-44

-Polyakova, Y.E.; Bauch, H.A.; Klyuvitkina, T.S. 2005. Early to middle Holocene changes in Laptev Sea water masses deduced frm diatom and aquatic palynomorph assemblages. *Global and Planetary Change* 48:208-222

-Ponkratova, I.Y.; Chlachula, J.; Clausen, I. 2021. Chronology and environmental context of the early prehistoric peopling of Kamchatka, the Russian North Far East. *Quaternary Science Reviews* 252:106702(1-14)

-Potter, B.A.; Reuther, J.D.; Holliday, V.T.; Holmes, C.E.; Miller, D.S.; Schmuck, N. 2017. Early colonization of Beringia and Northern North America: Chronology, routes, and adaptive strategies. *Quaternary International* 444(B):36-55

-Potter, B.A.; Chatters, J.C.; Prentiss, A.M.; Fiedel, S.J.; Kelly, R.L.; Kilby, J.D.; Lanoë, F.; Holland-Lulewicz, J.; Miller, D.S.; Morrow, J.E.; Perri, A.R.; Rademaker, K.M.; Reuther, J.D.; Ritchison, B.T.;

Sanchez, G.; Sánchez-Morales, I.;Spivey-Faulkner, S.M.; Tune, J.W.; Haynes, C.V. 2022. Current understanding of the Earliest Human Occupations in the Americas: Evaluation of Becerra-Valdivia and Higham (2020). *PaleoAmerica* 8(1):62-76

-Proverbs, T.A. 2019. Social-ecological change in Gwich'in territory: cumulative impacts in the cultural landscape, and determinants of access to fish. Doctoral Dissertation. Victoria University

-Rabassa, J.; Ponce, J.F. 2013. The Heinrich and Dansgaard-Oeschger climatic events during Marine Isotopic Stage 3: Searching for appropriate times for human colonization of the Americas. *Quaternary International* 299:94-105

-Rae, J.W.B.; Gray, W.R.; Wills, R.C.J.; Eisenman, I.; Fitzhugh, B.; Fotheringham, M.; Littley, E.F.M.; Rafter, P.A.; Rees-Owen, R.; Ridgwell, A.; Taylor, B.; Burke, A. 2020. Overturning circulation, nutrient limitation, and warming in the Glacial North Pacific. *Science Advances* 6:eabd1654

-Raghavan, M.; Skoglund, P.; Graf, K.E.; Metspalu, M.; Albrechtsen, A.; Moltke, I.; Rasmussen, S.; Stafford, Jr.; T.W.; Orlando, L.; Metspalu, E.; Karmin, M.; Tambets, K.; Rootsi, S.; Mägi, R.; Campos, P.F.; Balanovska, E.; Balanovsky, O.; Khusnutdinova, E.; Litvinov, S.; Osipova, L.P.; Fedorova, S.A.; Voevoda, M.I.; DeGiorgio, M.; Sicheritz-Ponten, T.; Brunak, S.; Demeshchenko, S.; Kivisild, T.; Villems, R.; Nielsen, R.; Jakobsson, M.; Willerslev, E. 2014. Upper Palaeolithic Siberian genome reveals dual ancestry of native Americans. *Nature* 505:87-94

-Raghavan, M., Steinrücken, M., Harris, K., Schiffels, S., Rasmussen, S., DeGiorgio, M., Albrechtsen, A., Valdiosera, C., Ávila-Arcos, M.C., Malaspinas, A.-S., Eriksson, A., Moltke, I., Metspalu, M., Homburger, J.R., Wall, J., Cornejo, O.E., Moreno-Mayar, J.V., Korneliussen, T.S., Pierre, T., Rasmussen, M., Campos, P.F., Damgaard, P. de B., Allentoft, M.E., Lindo, J., Metspalu, E., Rodríguez-Varela, R., Mansilla, J., Henrickson, C., Seguin-Orlando, A., Malmström, H., Stafford, T., Shringarpure, S.S., Moreno-Estrada, A., Karmin, M., Tambets, K., Bergström, A., Xue, Y., Warmuth, V., Friend, A.D., Singarayer, J., Valdes, P., Balloux, F., Leboreiro, I., Vera, J.L., Rangel-Villalobos, H., Pettener, D., Luiselli, D., Davis, L.G., Heyer, E., Zollikofer, C.P.E., Ponce de León, M.S., Smith, C.I., Grimes, V., Pike, K.-A., Deal, M., Fuller, B.T., Arriaza, B., Standen, V., Luz, M.F., Ricaut, F., Guidon, N., Osipova, L., Voevoda, M.I., Posukh, O.L., Balanovsky, O., Lavryashina, M., Bogunov, Y., Khusnutdinova, E., Gubina, M., Balanovska, E., Fedorova, S., Litvinov, S., Malyarchuk, B., Derenko, M., Mosher, M.J., Archer, D., Cybulski, J., Petzelt, B., Mitchell, J., Worl, R., Norman, P.J., Parham, P., Kemp, B.M., Kivisild, T., Tyler-Smith, C., Sandhu, M.S., Crawford, M., Villems, R., Smith, D.G., Waters, M.R., Goebel, T., Johnson, J.R., Malhi, R.S., Jakobsson, M., Meltzer, D.J., Manica, A., Durbin, R., Bustamante, C.D., Song, Y.S., Nielsen, R., Willerslev, E., 2015. Genomic evidence for the Pleistocene and recent population history of Native Americans. Science 349, aab3884 (1-10) https://doi.org/10.1126/science.aab3884

-Raju, P.L.N. 2006. Fundamentals of Geographical Information System. In: Sivakumar, M.V.K.; Roy, P.S.; Harmsen, K.; Saha, S.K. (eds) Satellite Remote Sensing and GIS Applications in Agricultural Meteorology. Geneva: World Meteorological Organisation (Chapter 6:103-120)

-Ramsey, C.L.; Griffiths, P.A.; Fedje, D.W.; Wigen, R.J.; Mackie, Q. 2004. Preliminary investigation of a late Wisconinan fauna frm K1 cave, Queen Charlotte Islands (Haida Gwaii), Canada. *Quaternary Research* 62:

-Rasmussen, M.; Anzick, S.L.; Waters, M.R.; Skoglund, P.; DeGiorgio, M.; Stafford Jr., T.W.; Rasmussen, S.; Moltke, i.; Albrechtsen, A.; Doyle, S.M.; Poznik, G.D.; Gudmundsdottir, V.; Yadav, R.; Malaspinas, A.-S.; Stockton White V, S.; Allentoft, M.E.; Cornejo, O.E.; Tambets, K.; Eriksson, A.; Heintzman, P.D.; Karmin, M.; Korneliussen, T.S.; Meltzer, D.J.; Pierre, T.L.; Stenderup, J.; Saag, L.; Warmuth, V.M.; Lopes, M.C.; Malhi, R.S.; Brunak, S.; Sicheritz-Ponten, T.; Barnes, I.; Collins, M.; Orlando, L.; Balloux, F.; Manica, A.; Gupta, R.; Metspalu, M.; Bustamante, C.D.; Jakobsson, M.;

Nielsen, R.; Willerslev, E. 2014. The genome of a Late Pleistocene human from a Clovis burial site in western Montana. *Nature* 506:225-229

-Reich, D.; Patterson, N.; Campbell, D.; Tandon, A.; Mazieres, S.; Ray, N.; Parra, M.V.; Rojas, W.; Duque, C.; Mesa, N.; García, L.F.; Triana, O.; Blair, S.; Maestre, A.; Dib, J.C.; Bravi, C.M.; Bailliet, G.; Corach, D.; Tünemeier, T.; Bortolini, M.C.; Salzano, F.M.; Petzl-Erler, M.L.; Acuña-Alonzo, V.; Aguilar-Salinas, C.; Cnaizales-Quinteros, S.; Tusié-Luna, T.; Riba, L.; Rodríguez-Cruz, M.; Lopez-Alarcón, M.; Coral-Vazquez, R.; Canto-Cetina, T.; Silva-Zolezzi, I.; Fernandez-Lopez, J.C.; Contreras, A.V.; Jimenez-Sanchez, G.; Gómez-Vázquez, M.-J.; Molina, J.; Carracedo. A.; Salas, A.; Gallo, C.; Poletti, G.; Witonsky, D.B.; Alkorta-Aranburu, G.; Sukernik, R.I.; Osipova, L.; Fedorova, S.A.; Vasquez, R.; Villena, M.; Moreau, C.; Barrantes, R.; Pauls, D.; Excoffier, L.; Bedoya, G.; Rothhammer, F.; Dugoujon, J.-M.; Larrouy, G.; Klitz, W.; Labuda, D.; Kidd, J.; Kidd, K.; Di Rienzo, A.; Freimer, N.B.; Price, A.L.; Ruiz-Linares, A. 2012. Reconstructing Native American population history. *Nature* 488:370-374

-Reimer, P.J.; Austin, W.E.; Bard, E.; Bayliss, A.; Blackwell, P.G.; Ramsey, C.B; Butzin, M.; Cheng, H.; Edwards, R.L.; Friedrich, M.; Grootes, P.M. 2020. The IntCal20 Northenr Hemisphere radiocarbon age calibration curve (0-55 cal k BP). *Radiocarbon* 62(4):725-757

-Reuther, J.D.; Rogers, J.; Druckenmiller, P.; Bundtzen, T.K.; Wallace, K.; Bowman, R.; May, K.; Feathers, J.; Cherkinsky, A. 2019. Late Quaternary (>MIS3 to MIS1) stratigraphic transitions in a highland Beringian landscape along the Kuskokwim River, Alaska. *Quaternary Research* 93:139-154

-Richards, M.P.; Pettitt, P.B.; Stiner, M.C.; Trinkaus, E. 2001. Stable isotope evidence for increasing dietary breadth in the European mid-Upper Paleolithic. *Proceedings of the National Academy of Sciences* 98(11):6528-6532

-Rogers, J.; Anichtchenko, E. 2014. Arctic Ocean and Bering Sea : Maritime Archaeology. In: Smith, C. (ed) Encyclopedia of Global Archaeology. New York: Springer (495-508)

-Rosenberg, N.A.; Nordborg, M. 2002. Genealogical trees, coalescent theory and the analysis of genetic polymorphisms. *Nature* 3:380-390

-Royer, T.C.; Finney, B. 2020. An oceanographic perspective on early human migrations to the Americas. *Oceanography* 33(1):32-41

-Rybin, E.P. 2014. Tools, beads, and migrations: Specific cultural traits in the Initial Upper Paleolithic of Southern Siberia and Central Asia. *Quaternary International* 347:39-52

-Rybin, E.P.; Khatsenovich, A.M.; Gunchinsuren, B.; Olsen, J.W.; Zwyns, N. 2016. The impact of the LGM on the development of the Upper Paleolithic in Mongolia. *Quaternary International* 425:69-87in

-Safonova, T.; Sántha, I. 2016. Evenki Hunter-Gathering Style and Cultural Contact. *Senri Ethnological Studies* 94:59-79

-Salzano, F.M. 2011. The Prehistoric Colonization of the Americas: Evidence and Models. *Evolution: Education and Outreach* 4(2):199-204

-Scheib, C.L.; Hi, H.; Desai, T.; Link, V.; Kendall, C.; Dewar, G.; Griffifth, P.W.; Mörsebug, A.; Johnson, J.R.; Potter, A.; Kerr, S.L.; Endicott, P.; Lindo, J.; Haber, M.; Xue, Y.; Tyler-Smith, C.; Sandhu, M.S.; Lorenz, J.G.; Randall, T.D.; Faltyskova, Z.; Pagani, L.; Danecek, P.; O'Connell, T.C.; Martz, P.; Boraas, A.S.; Byrd, B.F.; Levanthal, A.; Cambra, R.; Williamson, R.; Lesage, L.; Holguin, B.; Ygnacio-De Soto, E.; Rosas, J.T.; Metspalu, M.; Stock, J.T.; Manica, A.; Scally, A.; Wegmann, D.; Malhi, R.S.; Kivisild, T. 2018. Ancient human parallel lineages within North America contributed to a coastal expansion. *Science* 360:1024-1027

-Scott, G.R.; O'Rourke, D.H.; Raff, J.A.; Tackney, J.C.; Hlusko, L.J.; Elias, S.A.; Bourgeon, L.; Potapova, O.; Pavlova, E.; Pitulko, V.; Hoffecker, J.F. 2021. Peopling the Americas: Not 'Out of Japan'. *PaleoAmerica* 7(4):309-332

-Seguin-Orlando, A.; Korneliussen, T.S.; Sikora, M.; Malaspinas, A.-S.; Manica, A.; Moltke, I.; Albrechtsen, A.; Ko, A.; Margaryan, A.; Moiseyev, V.; Goebel, T.; Westaway, M.; Lambert, D.; Khartanovich, V.; Wall, J.D.; Nigst, P.R.; Foley, R.A.; Mirazon Lahr, M.; Nielsen, R.; Orlando, L.; Willerslev, E. 2014. Genomic structure in Europeans dating back at least 36.200 years. *Science* 346(6123):1113-1118

-Shreve, R.L. 1966. Statistical law of stream numbers. *The Journal of Geology* 74(1):17-37

-Sicoli, M.A.; Holton, G. 2014. Lingusitic phylogenies support back-migration from Beringia to Asia. *PLoS ONE* 9(3):e91722 (1-8)

-Sikora, M.; Pitulko, V.V.; Sousa, V.C.; Allentoft, M.E.; Vinner, L.; Rasmussen, S.; Margaryan, A.; de Barros Damgaard, P.; de la Fuente, C.; Renaud, G.; Yang, M.A.; Fu, Q.; Dupanloup, I.; Giampoudakis, K.; Nogués-Bravo, D.; Rahbe, C.; Kroonen, G.; Peyrot, M.; McColl, H.; Vasilyev, S.V.; Veselovskaya, E.; Gerasimova, M.; Pavlova, E.Y.; Chasnyk, V.G.; Nikolskiy, P.A.; Gromov, A.V.; Khartanovich, V.I.; Moiseyev, V.; Grebenyuk, P.S.; Fedorchenko, A.Y.; Lebedintsev, A.I.; Slobodin, S.B.; Malyarchuk, B.A.; Martiniano, R.; Meldgaard, M.; Arppe, L.; Palo, J.U.; Sundell, T.; Mannermaa, K.; Wessman, A.; Sajantila, A.; Lahr, M.M.; Durbin, R.; Nielsen, R.; Metlzer, D.J.; Excoffier, L.; Willerslev, E. 2019. The population history of northeastern Siberia since the Pleistocene. *Nature* 570:182-188

-Simms, A.R.; Lisiecki, L.; Gebbie, G.; Whitehouse, P.L.; Clark, J.F. 2019. Balancing the last glacial maximum (LGM) sea-level budget. *Quaternary Science Reviews* 205:143-153

-Skoglund, P.; Mallick, S.; Bortolini, M.C.; Chennagiri, N.; Hünemeier, T.; Petzl-Erler, M.L.; Salzano, F.M.; Patterson, N.; Reich, D. 2015. Genetic evidence for two founding populations of the Americas. *Nature* 525:104-108

-Skoglund, P.; Reich, D. 2016. A genomic view of the peopling of the Americas. *Current Opinion in Genetics & Development* 41:27-35

-Slobodin, S.B.; Anderson, P.M.; Glushkova, O.Y.; Lozhkin, A.V. 2017. Western Beringia (Northeast Asia). In: Kotlyakov, V.M.; Velichko, A.A.; Vasil'ev, S.A. (eds) Human colonization of the Arctic: the interaction between early migration and the paleoenvironment. New York: Elsevier- Academic Press (chapter 3.1: 241-298

-Smith, H.L.; Goebel, T. 2018. Origins and spread of fluted-point technology in the Canadian Ice-Free Corridor and eastern Beringia. *PNAS* 115(16):4116-4121

-Smithers, S. 2011. Sea-level indicators. In: Hopley, D. (ed) Encyclopedia of Modern Coral Reefs: Structure, form and process. Encyclopedia of Earth Science. Dordrecht: Springer (p.878-991)

-Spada, G.; Galassi, G. 2017. Extent and dynamic Evolution of the lost land *aquaterra* since the Last Glacial Maximum. *Comptes Rendus Geoscience* 349(4):151-158

-Spada, G.; Melini, D. 2019. SELEN^4 (SELEN version 4.0): a Fortran program for solving the gravitationally and topographically self-consistent sea-level equation in glacial isostatic adjustment modeling. *Geoscientific Model Development* 12(12):5055-5075

-Spielhagen, R.F.; Erlenkeuser, H.; Siegert, C. 2005. History of freshwater runoff across the Laptev Sea (Arctic) during the last deglaciation. *Global and Planetary Change* 48(1-3):187-207

-Stabeno, P.J.; Schumacher, J.D.; Ohtani, K. 1999. The physical oceanography of the Bering Strait. In: Loughlin, T.R.; Ohtani, K. (eds) Dynamics of the Bering Sea: A summary of physical, chemical, and biological characteristics, and a synopsis of research on the Bering Sea, North Pacific Marine Science Organization (PICES). Fairbanks, Alaska:University of Alaska Sea Grant (p.1-28)

-Steele, J.; Sluckin, T.J.; Denholm, D.R.; Gamble, C.S. 1996. Simulating hunter-gatherer colonization of the Americas. In: Kamermans H.; Fennema, K. (eds) Interfacing the Past: Computer applications and quantitative methods in Archaeology CAA95:1 (*Analecta Praehistorica Leidensia* 28). Institute of Prehistory, University of Leiden, Leiden, p.223-227

-Steele, J.; Adams, J.; Sluckin, T. 1998. Modelling Paleoindian dispersals. *World Archaeology* 30(2):286-305

-Steele, J. 2010. Radiocarbon dates as data: quantitative strategies for estimating colonization front speeds and event densities. *Journal of Archaeological Science* 37(8):2017-2030

-Stepanova, A.; Taldenkova, E.; Bauch, H.A. 2012. Ostracod palaeoecology and environmental change in the Laptev and Kara seas (Siberian Arctic) during the last 18000 years. *BOREAS* 41:557-577

-Sun, J.; Ma, P.-C.; Cheng, H.-Z.; Wang, C.-Z.; Li, Y.-L.; Cui, Y.-Q.; Yao, H.-B.; Wen, S.-Q.; Wei, L.-H. 2020. Post-last glacial maximum expansion of Y-chromosome haplogroup C2a-L1373 in northern Asia and its implications for the origin of Native Americans. *American Journal of Physical Anthropology* 174:363-374

-Supernant, K. 2017. Modeling Métis mobility? Evaluating least cost paths and indigenous landscapes in the Canadian West. *Journal of Archaeological Science* 84:63-73

-Surovell, T. 2003. Simulating coastal migration in New World colonization. *Current Anthropology* 44(4):580-591

-Szathmary, E.J. 1993. mtDNA and the peopling of the Americas. *American Journal of Human Genetics* 53(4):793-799

-Takahashi, K. 2005. The Bering Sea and paleoceanography. *Deep Sea Research Part II: Topical studies in Oceanography* 52(16-18):2080-2091

-Takakura, J. 2020. Rethinking the Disappearance of microblade technology in the Terminal Pleistocene of Hokkaido, Northern Japan: looking at archaeological and palaeoenvironmental evidence. Quaternary 3(3):21(1-19)

-Taliaferro, M.S.; Schriever, B.A.; Shackley, M.S. 2010. Obsidian procurement, least cost path analysis, and social interaction in the Mimbres area of southwestern New Mexico. *Journal of Archaeological Science* 37:536-548

-Tamm, E.; Kivisild, T.; Reidla, M.; Metspalu, M.; Smith, D.G.; Mulligan, C.J.; Bravi, C.M.; Rickards, O.; Martinez-Labarga, C.; Khusnutdinova, E.K.; Fedorova, S.A.; Golubenko, M.V.; Stepanov, V.A.; Gubina, M.A.; Zhadanov, S.I.; Ossipova, L.P.; Damba, L.; Voevoda, M.I.; Dipierri, J.E.; Villems, R.; Malhi, R.S. 2007. Beringian Standstill and spread of native American founders. *PLoS ONE* 2(9):e829(1-6)

-Tarasov, P.E.; Leipe, C.; Wagner, M. 2021. Environments during the spread of anatomically modern humans across Northern Eurasia 50-10 cal kyr BP: What do we know and what would we like to know? *Quaternary International* 596:155-170

-Tarboton, D.G.; Bras, R.L.; Rodriguez-Iturbe, I. 1991. On the extraction of channel networks from digital elevation data. *Hydrological processes* 5(1):81-100

-Turner II, C.G. 2010. The Russian-American perimortem taphonomy project in Siberia: A tribute to Nicolai Dmitrievich Ovodov, pioneering Siberia vertebrate paleontologist and cave archaeologist. *Alaska Journal of Anthropology* 8(1):87-105

-Vachula, R.S.; Huang, Y.; Longo, W.M.; Dee, S.D.; Daniels, W.C.; Russel, J.M. 2019. Evidence of Ice Age humans in Eastern Beringia suggests early migration to North America. *Quaternary Science Reviews* 205:35-44

-Vachula, R.S. 2020. Alaskan Lake sediment records and their implications for the Beringian Standstill hypothesis. *PaleoAmerica* 6(4):303-307

-Vachula, R.S.; Huang, Y.; Russel, J.M.; Abbott, M.B.; Finkenbinder, M.S.; O'Donnell, J.A. 2020. Sedimentary biomarkers reaffirm human impacts on northern Beringian ecosystems during the Last Glacial period. *Boreas* 49(3):514-525

-Van Andel, T.H.; Tjeerd, H.; Davies, W.; Weninger, B. 2003. The human presence in Europe during the last glacial period 1: Human migrations and the changing climate. In van Andel, T.H.(ed) Neanderthals and modern humans in the European landscape during the last glaciation: archaeological results of the Stage 3. Cambridge: McDonald Institute Monograph series (chapter. 4:31-57)

-van Leusen, M. 1999. Viewshed and cost surface analysis using GIS (Cartographic modelling in a cell-based GIS II). *BAR International Series* 757:215-224

-Vasil'ev, S.A. 1993. The Upper Palaeolithic of Northern Asia. *Current Anthropology* 34(1):82-92

-Vasil'ev, S.A. 2001. Man and mammoth in Pleistocene Siberia. *The World of Elephants International Congress* 1:363-366

-Vate, V. 2005. Maintaining cohesion through rituals: Chukchi herders and hunters, a People of the Siberian Arctic. *Senri Ethnological Studies* 69:45-68

-Vereshchagin, N.K.; Baryshnikov, G.F. 1982. Paleoecology of the mammoth fauna in the Eurasian Arctic. . In: Hopkins, D.M.; Matthews Jr., J.V.; Schweger, C.E.; Young, S.B. (eds) Paleoecology of Beringia. New York: Academia Press (p. 267-279)

-Vershinina, A.O.; Heintzman, P.D.; Froese, D.G.; Zazula, G.; Cassatt-Johnstone, M.; Dalén, L.; Der Sarkissian, C.; Dunn, S.G.; Ermini, L.; Gamba, C.; Groves, P.; Kapp, J.D.; Mann, D.H.; Seguin-Orlando, A.; Southon, J.; Stiller, M.; Wooller, M.J.; Baryshnikov, G.; Gimranov, D.; Scott, E.; Hall, E.; Hewitson, S.; Kirillova, I.; Kosintsev, P.; Shidlovsky, F.; Tong, H.-W.; Tiunov, M.P.; Vartanyan, S.; Orlando, L.; Corbett-Detig, R.; MacPhee, R.D.; Shapiro, B. 2021. Ancient horse genomes reveal the timing and extent of dispersals across the Bering Land Bridge. *Molecular Ecology* 30(23):6144-6161

-Vogelaar, C. 2017. Using GIS modelling as a tool to search for late Pleistocene and early Holocene archaeology on Quadra Island, British Columbia Doctoral dissertation: University of Victoria

-Volodko, N.V.; Starikovskaya, E.B.; Mazunin, I.O.; Eltsov, N.P.; Naidenko, P.V.; Wallace, D.C.; Sukernik, R.I. 2008. Mitochondrial genome diversity in Arctic Siberians, with particular reference to the evolutionary history of Beringia and Pleistocene peopling of the Americas. *The American Journal of Human Genetics* 82:1084-1100

-Wang, S.; Lewis Jr., C.M.; Jakobsson, M.; Ramachandran, S.; Ray, N.; Bedoya, G.; Rojas, W.; Parra, M.V.; Molina, J.A.; Gallo, C.; Mazzotti, G.; Poletti, G.; Hill, K.; Hurtado, A.M.; Labuda, D.; Klitz, W.; Barrantes, R.; Bortoloni, M.C.; Salzano, F.M.; Petzl-Erler, M.L.; Tsuneto, L.T.; Llop, E.; Rothhammer, F.; Excoffier, L.; Feldman, M.W.; Rosenberg, N.A.; Ruiz-Linares, A. 2007. Genetic variation and population structure in Native Americans. *PLoS ONE* 3(11):2049-2067

-Warren, R.E.; Asch, D.L. 2003. A Predictive Model of Archaeological Site location in the Eastern Prairie Peninsula. In: Wescott, K.L.; Brandon, R.J. (eds) Practical Applications of GIS for Archaeologists: A predictive modelling toolkit. London: Taylor & Francis (Chapter 2:6-36)

-Waters, M.R.; Stafford Jr., T.W. 2007. Redefining the age of Clovis: Implications for the peopling of the Americas. *Science* 315(5815):1122-1126

-Waters, M.R.; Stafforod Jr., T.W.; Carlson, D.L. 2020. The age of Clovis – 13.050 to 12.750 cal yr BP. *Science Advances* 6:eaaz0455 (1-12)

-Weitzel, N.; Hence, A.; Herzschuh, U.; Böhmer, T.; Cao, X.; Rehfeld, K. 2020. A spatial reconstruction of Siberian last Glacial Maximum climate from pollen data. *Climate Dynamics* Preprint (https://eartharxiv.org/repository/view/368/)

-Whickham-Jones, C.R. 2014. Coastal adaptations. In: Cummings, V.; Jordan, P.; Zvelebil, M. (eds) The Oxford Handbook of the Archaeology and Anthropology of hunter-gatherers. Oxford: Oxford University Press (chapter 31:694-711)

-White, J.M.; Mathewes, R.W.; Mathews, W.H. 1985. Late Pleistocene Chronology and Environment of the "Ice-Free Corridor" of Northwestern Alberta. *Quaternary Research* 24:173-186

-Willerslev, E.; Raghavan, M. 2013. Ancient Siberian genome reveals genetic origins of Native Americans. *Natural history museum of Denmark: Center for GeoGenetics*. URL: http://geogenetics.ku./dk/latest-news/malta

-Willerslev, E.; Meltzer, D.J. 2020. Peopling of the Americas as inferred from ancient genomics. *Nature* 594(7863):356-364

-Wilson, M.C. 1996. Late quaternary vertebrates and the opening of the ice-free corridor, with special reference to the genus *bison*. *Quaternary International* 32:97-105

-Wishart, R.P. 2014. 'We ate lots of wish back then': the forgotten importance of fishing in Gwich'in country. *Polar Records* 40:343-353

-Woodgate, R. 2013. Arctic Ocean circulation: Going around at the top of the world. *Nature Education Knowledge* 4(8):8 (1-15)

-Wren, C.D.; Xue, J.Z.; Costopoulos, A.; Burke, A. 2014. The role of spatial foresight in models of hominin dispersal. *Journal of Human Evolution* 69:70-78

-Wright, J. 2021. Prehistoric Mongolian Archaeology in the Early 21st Century: Developments in the Steppe and Beyond. *Journal of Archaeological Research* 29:431-479

-Yesner, D.R.; Pasch, A.D.; Crossen, J.K. 2019. Late Pleistocene marine resources from the Bering Glacier Foreland and human coastal migration in the northern Gulf of Alaska region. *Quaternary Research* :1-17 doi:10.1017/qua.2018.92

-Young, S.B. 1982. The vegetation of land-bridge Beringia. In: Hopkins, D.M.; Matthews Jr., J.V.; Schweger, C.E.; Young, S.B. (eds) Paleoecology of Beringia. New York: Academia Press (p. 179-191)

-Yue, J.-P.; Yang, S.-X.; Li, Y.-Q.; Storozum, M.; Hou, Y.-M.; Chang, Y.; Petraglai, M.D. 2021. Human adaptations during MIS 2: Evidence from microblade industries of Northeast China. *Palaeogeography, Palaeoclimatology, Palaeoecology* 567:110286 (1-14)

-Yurtsev, B.A. 2001. The Pleistocene "tundra-steppe" and the productivity paradox: the landscape approach. *Quaternary Science Reviews* 20:165-174

-Zazula, G.D.; Froese, D.G.; Schweger, C.E.; Mathewes, R.W.; Beaudoin, A.B.; Telka, A.M.; Harington, C.R.; Westgate, J.A. 2003. Ice-age steppe vegetation in east Beringia. *Nature* 423(6940):603

-Zazula, G.D.; Schweger, C.E.; Beaudoin, A.B.; McCourt, G.H. 2006. Macrofossil and pollen evidence for full-glacial steppe within an ecological mosaic along the Bluefish River, eastern Beringia. *Quaternary International* 142-143:2-19

-Zong, C. 2015. Late Pleistocene sea levels and resulting changes in global land distributions. Doctoral dissertation: University of Kansas

-Zwyns, N.; Gladyshev, S.A.; Gunchinsuren, B.; Bolordbat, T.; Flas, D.; Dogandzic, T.; Tabarev, A.V.; Gillam, J.C.; Khatsenovich, A.M.; McPherron, S.; Odsuren, D.; Paine, C.H.; Purevjal, K.-E.; Stewart, J.R. 2014. The open-air site of Tolbor 16 (Northern Mongolia): Preliminary results and perspectives. *Quaternary International* 347:53-65

Supplementary Data 1 – Model workflow

The workflow presented here is a summarised version of the step-by-step followed for the creation of this project's model. Although here we mention only the LGM data, the same workflow was followed for the overall MIS3 data, as well as the stadial and interstadial models.

A. Creation of river layer

1. Add dem layer (" *lgm_dem_proj* ")

2. Fill (Spatial Analyst) where *lgm_dem* is the input surface raster to create *lgm_fill* as the output surface raster; specify the environment settings with the output coordinate system is reinforced as "WGS_1984_EPSG_Arctic_Regional_zone_A5", the processing extent is the same as *lgm_dem_proj* and the raster analysis's cell size is the maximum of inputs, its projection method is CONVERT_UNITS and its mask is *lgm_dem_proj*

3. Flow Direction (Spatial Analyst) where *lgm_fill* is the input surface raster, the flow direction type is D8 to create *lgm_flowdir*. Specify the environment settings with the output coordinate system is reinforced as "WGS_1984_EPSG_Arctic_Regional_zone_A5", the processing extent is the same as *lgm_dem_proj* and the raster analysis's cell size is the maximum of inputs, its projection method is CENTER_OF_EXTENT and its mask is *lgm_dem_proj*

4. Flow Accumulation (Spatial Analyst) where *lgm_flowdir* is the flow direction raster, the output data type is FLOAT and the flow direction type is D8 to create *lgm_flowacc*. Specify the environment settings with the output coordinate system is reinforced as "WGS_1984_EPSG_Arctic_Regional_zone_A5", the processing extent is the same as *lgm_dem_proj* and the raster analysis's cell size is the maximum of inputs, its projection method is CENTER_OF_EXTENT and its mask is *lgm_dem_proj*

5. Con (Spatial Analyst) where *lgm_flowacc* is the conditional raster, *value>50000* is the SQL expression; the true raster or constant value is 1 whereas the false raster or constant value is left blank, in order to create *lgm_con*

6. Raster to Polyline (Conversion) with *lgm_con* as the input raster (field: VALUE and background value ZERO) to create *lgm_streams*

7. Stream Order (Spatial Analyst) with *lgm_con* as the stream raster and *lgm_flowdir* as the flow direction raster to create *lgm_stream_shr* for the SHREVE method of stream ordering and *lgm_stream_str* for the STRAHLER method of stream ordering

B. Creation of LCP

This LCP includes the river raster (*lgm_streams*) and modifies the weights of the raster when creating the cost raster (*weightedsum_R*), as these are required for the creation of our final model.

1. Add layers: *lgm_dem_proj, LGM_Sites_proj, LGM_icesheets_proj* and *LGM_streams*

2. Slope (Spatial Analyst) with *lgm_dem_proj* as the input raster, the output measurement as DEGREE and the method as PLANAR to create the *lgm_slope* raster. Specify the environment settings with the output coordinate system is reinforced as "WGS_1984_EPSG_Arctic_Regional_zone_A5", the processing extent is the same as *lgm_dem_proj* and the raster analysis's cell size is the maximum of inputs, its projection method is CENTER_OF_EXTENT and its mask is *lgm_dem_proj*

3. Euclidean Distance (Spatial Analyst) with *LGM_Sites_proj* as the feature source data, the input barrier as *LGM_icesheets_proj* and the distance method as PLANAR to create the distance-to-site *distance* raster. Specify the environment settings with the output coordinate system is reinforced as "WGS_1984_EPSG_Arctic_Regional_zone_A5", the processing extent is the same as *lgm_dem_proj* and the raster analysis's cell size is the maximum of inputs, its projection method is CENTER_OF_EXTENT and its mask is *lgm_dem_proj*

4. Euclidean Distance (Spatial Analyst) with *LGM_streams* as the feature source data, the input barrier as *LGM_icesheets_proj* and the distance method as PLANAR to create the distance-to-water *distance_R* raster. Specify the environment settings with the output coordinate system is reinforced as "WGS_1984_EPSG_Arctic_Regional_zone_A5", the processing extent is the same as *lgm_dem_proj* and the raster analysis's cell size is the maximum of inputs, its projection method is CENTER_OF_EXTENT and its mask is *lgm_dem_proj*

5. Weighted Sum (Spatial Analyst) where the rasters *lgm_slope*, *distance* and *distance_R* are inputted. The weights are modified to '29', '1' and '70', respectively, to create the *weightedsum_R* raster

6. Cost Connectivity (Spatial Analyst) with *LGM_Sites_proj* is the features region data and *weightedsum_R* is the cost raster in order to create *LGM_R_connectivity* and *LGM_R_neighbouring*. Specify the environment settings with the output coordinate system is reinforced as "WGS_1984_EPSG_Arctic_Regional_zone_A5", the processing extent is the same as *lgm_dem_proj* and the raster analysis's cell size is the maximum of inputs, its projection method is CENTER_OF_EXTENT and its mask is *lgm_dem_proj*.

For the experimental models, the workflow is the same, with the exception of:

- when creating the distance-to-site raster, the input raster is the isolated 'origin' site (e.g., *MIS2_Yana*)

- when creating the cost connectivity rasters, the features region data is the 'destinations' sites (e.g., *MIS2_YDestinations*)

C. Experimental *x* sites

1. Add layer *lgm_dem_proj*, *LGM_Icesheets_proj*, *LGM_Sites_proj*

2. Raster Calculator (Spatial Analyst) expression *lgm_dem_proj <=0* to create the *exp_subm* raster; the resulting raster value '1' equal the now-submerged landmass whereas the value '0' equal the now-exposed landmass

3. Reclassify (Spatial Analyst) with *exp_subm* as the input raster and reclass field VALUE. By manually reclassifying the new values where the old value '1' becomes '1' and the old value '0' becomes 'NoData' to create *exposed*. Repeat the same by reversing the values, where old value '1' becomes 'NoData' and old value '0' becomes '1' to create *submerged*

4. Raster to Polygon (Conversion) with *exposed* as the input raster (field VALUE) in order to create *LGM_exposed*. Do the same for *submerged* so it becomes *LGM_submerged*.

5. Dissolve (Data Management) by inputting *LGM_exposed* in order to created *Exposed_LGM* and then by repeating it by inputting *LGM_Submerged* in order to create *Submerged_lgm*.

6. Erase (Analysis) by making the *Submerged_lgm* as the input feature and the *LGM_Icesheets_proj* as the erase feature to create *Submerged_noIce*

7. Calculate the Area of the submerged landmass by firstly creating another column (type DOUBLE) in the layer's attribute table (*Area*) and then generating the calculate geometry (in sq km)

8. Create Random Points (Data Management) by specifying its location, then its name (*LGM_x*), the *Submerged_lgm* as its constraining feature, the number of points (min. 11 – LONG) and the minimum distance (100km – LINEAR UNIT)

9. Merge (Data Management) by adding *LGM_x* and *LGM_Sites_proj* in order to create *LGM_x_Sites*.

The merged sites are then used to replace *LGM_Sites_proj* in the workflow B in order to create an experimental LCP with the experimental sites.

Supplementary Data 2 - Project database, "*README"*

	SummaryData
siteID	number attributed to a given site (*n* = 1-92)
site_name	name of site
area	site area in accordance with the Beringian landscape: EB - Eastern Beringia (Alaska + Yukon east of Mackenzie River ; WB - Western Beringia (Siberia west of Verkhoyansk Mountain Range) ; OB - Outside Beringia (Siberia + Mongolia) ; PSHK - Palaeo-Sakhalin-Hokkaido Peninsula (+ Southeast Russia and Northeast China)
country	present-day country in which site is located
x_coord	site's longitude (degree decimal)
y_coord	site's latitude (degree decimal)
elevation(m)	site's elevation as meters above sea level
site_type	type of site: c (cave); o/a (open-air); p/e (palaeoenvironmental site); rs (rockshelter); s/c (part of site complex); l/c (lithic cache); s/m (shell midden); g/a (geoarchaeological site)
age_m	mean of the calibrated ages of the site (OxCal 4.4 IntCal 20)
n_dates	number of radiocarbon dates
temp_group	temporal group to which the site has been attributed to: 1 (35.000-23.000 cal yr BP) and 2 (22.000-18.000 cal yr BP)
ref_loc	reference pertaining to the site's location
	DetailedData
siteID	number attributed to a given site (*n* = 1-92)
site	name of site
area	site area in accordance with the Beringian landscape: EB - Eastern Beringia (Alaska + Yukon east of Mackenzie River ; WB - Western Beringia (Siberia west of Verkhoyansk Mountain Range) ; OB - Outside Beringia (Siberia + Mongolia) ; PSHK - Palaeo-Sakhalin-Hokkaido Peninsula (+ Southeast Russia and Northeast China)
country	present-day country in which site is located
level	stratigraphic layer dated material was found in
mat_type	type of dated material
mat_spec	specification on material
date_type	type of dating method
lab_code	laboratory code attributed to each date
spec_code	specification on code
age	uncalibrated radiocarbon age
s_dev	standard deviation of uncalibrated radiocarbon age
ref	reference
source	source
comments	comments by CILMC on a given date
Age_Cal	calibrated range of date
σ-error	sigma-error on calibrated age (95.4%)
Age_CalM	mean of calibrated age
Status	status of date - Accepted or Rejected
TempGroup	temporal group to which the site has been attributed to: 1 (35.000-23.000 cal yr BP) and 2 (22.000-18.000 cal yr BP)
grnlnd-stage	greenland stage correspondant to mean calibrated age

Supplementary Data 3 - Project database, '*SummaryData*'... continuation

siteID	site_name	area	country	x_coord	y_coord	elevation (m)	site_type	age_m	n_dates	temp_ group	ref_loc
1	Alekseevks-1	OB	Russia	108.37	57.83	407	o/a	24811	1	1_int	Vachula et al. 2019; Pitblado 2017; Kuzmin & Keates 2016; Madsen 2004
2	Ankarito 7	PSHK	Japan	141.70	42.84	21	u/k	19631	1	2	Vachula et al. 2019; Pitblado 2017
3	Arta 2	OB	Russia	112.40	51.25	55	o/a	27095	1	1_int	Kuzmin & Orlova 1998
4	Berelekh	WB	Russia	143.95	70.43	17	g/a; o/a	20840	1	2	Vachula et al. 2019; Pitblado 2017
5	Bibi 5	OB	Russia	89.57	42.77	20	u/k	18862	1	2	Vachula et al. 2019; Pitblado 2017
6	Bluefish Caves	EB	Canada	-140.75	67.15	250	c	26606	7	1_int	Bourgeon et al. 2017
6	Bluefish Caves	EB	Canada	-140.75	67.15	250	c	20501	8	2	Bourgeon et al. 2017
7	Buret	OB	Russia	103.50	52.97	454	o/a	23560	1	1_int	Vachula et al. 2019; Pitblado 2017; Michael 1984
8	Burial Lake	EB	US - Alaska	-159.17	68.43	460	o/a; p/e	30599	2	1_std	Vachula et al. 2020; Finkenbinder et al. 2016
8	Burial Lake	EB	US - Alaska	-159.17	68.43	460	o/a; p/e	34694	5	1_int	Vachula et al. 2020; Finkenbinder et al. 2016
8	Burial Lake	EB	US - Alaska	-159.17	68.43	460	o/a; p/e	19797	3	2	Vachula et al. 2020; Finkenbinder et al. 2017
9	Chikhen Agui	OB	Mongolia	99.07	44.78	1996	rs	27060	2	1_int	Vachula et al. 2019; Pitblado 2017
10	Chikhen-2	OB	Mongolia	99.07	44.78	1996	o/a	33126	1	1_int	Vachula et al. 2019; Pitblado 2017
11	Chitkan	OB	Mongolia	107.98	49.93	762	o/a	27729	1	1_std	Vachula et al. 2019; Pitblado 2017
11	Chitkan	OB	Mongolia	107.98	49.93	762	o/a	23636	1	1_int	Vachula et al. 2019; Pitblado 2017
12	Derbina V	OB	Russia	92.50	55.32	237	o/a; s/c	28933	6	1_int	Pitblado 2017; Vasil'ev et al. 2002
12	Derbina V	OB	Russia	92.50	55.32	237	o/a; s/c	21963	2	2	Pitblado 2017; Vasil'ev et al. 2002
13	Döröljˇ1	OB	Mongolia	103.57	49.43	859	o/a; g/a? p/e?	26865	3	1_int	Pitblado 2017
13	Döröljˇ1	OB	Mongolia	103.57	49.43	859	o/a; g/a? p/e?	34836	1	1_std	Pitblado 2017
14	Dvuglazka Cave	OB	Russia	90.95	54.13	600	c	29870	1	1_int	Vasili'ev et al. 2002; Turner et al. 2013
15	Dvuglazka Rockshelter	OB	Russia	90.95	54.13	600	rs	24863	1	1_int	Vasili'ev et al. 2002
15	Dvuglazka Rockshelter	OB	Russia	90.95	54.13	600	rs	28876	1	1_std	Vasili'ev et al. 2002
15	Dvuglazka Rockshelter	OB	Russia	90.95	54.13	600	rs	22135	2	2	Vasili'ev et al. 2002
16	Ezhantsy	OB	Russia	135.13	60.52	162	o/a	18900	1	2	Vachula et al. 2019; Pitblado 2017
17	Gosudarev Log 1	OB	Russia	93.23	56.05	50	o/a	25137	1	1_int	Vachula et al. 2019; Turner et al. 2013
18	Guanqhetun 1	PSHK	China	123.92	48.31	210	o/a; s/m	27534	1	1_int	Guan et al. 2021; Yue et al. 2021
18	Guanqhetun 1	PSHK	China	123.92	48.31	210	o/a; s/m	28624	1	1_std	Guan et al. 2021; Yue et al. 2021
19	Hattoridai 2	PSHK	Japan	143.13	43.87	449	o/a; l/c	19322	2	2	Vachula et al. 2019; Pitblado 2017
20	Hirosato 8	PSHK	Japan	143.81	43.75	110	u/k	26044	1	1_int	Vachula et al. 2019; Pitblado 2017
21	Hokuto	PSHK	Japan	144.33	43.07	14	u/k	19524	1	2	Vachula et al. 2019; Pitblado 2017
22	Ikhine I	OB	Russia	133.60	63.12	134	o/a	18158	1	2	Vachula et al. 2019; Pitblado 2017
23	Ikhine II	OB	Russia	133.62	63.12	151	o/a	28874	8	1_int	Vachula et al. 2019; Pitblado 2017
23	Ikhine II	OB	Russia	133.62	63.12	151	o/a	31219	2	1_std	Vachula et al. 2019; Pitblado 2017
23	Ikhine II	OB	Russia	133.62	63.12	151	o/a	21948	2	2	Vachula et al. 2019; Pitblado 2017
24	ISM-034	WB	Russia	140.70	70.80	18	o/a	25046	1	1_int	Pavlova & Pitulko 2020; Pitulko et al. 2017

Supplementary Data 3 - Project database, '*SummaryData*'... continuation

siteID	site_name	area	country	x_coord	y_coord	elevation (m)	site_type	age_m	n_dates	temp_ group	ref_loc
25	Kamenka	OB	Russia	108.33	51.77	589	o/a	30350	6	1_int	Vachula et al. 2019; Pitblado 2017; Turner et al. 2013
25	Kamenka	OB	Russia	108.33	51.77	589	o/a	31184	2	1_std	Vachula et al. 2019; Pitblado 2017; Turner et al. 2013
26	Kamiitaira	PSHK	Japan	143.23	42.72	150	o/a	28981	4	1_int	Vachula et al. 2019; Pitblado 2017
27	Kamishirataki 2	PSHK	Japan	143.14	43.87	443	s/c; o/a	19911	4	2	Vachula et al. 2019; Pitblado 2017
28	Kamishirataki 5	PSHK	Japan	143.15	43.87	443	s/c; o/a	20592	1	2	Vachula et al. 2019; Pitblado 2017
29	Kamishirataki 8	PSHK	Japan	143.14	43.87	416	s/c; o/a	25282	2	1_int	Vachula et al. 2019; Pitblado 2017
29	Kamishirataki 8	PSHK	Japan	143.14	43.87	416	s/c; o/a	20681	5	2	Vachula et al. 2019; Pitblado 2017
30	Kashiwadai 1	PSHK	Japan	141.68	42.82	17	o/a	25347	8	1_int	Vachula et al. 2019; Pitblado 2017
30	Kashiwadai 1	PSHK	Japan	141.68	42.82	17	o/a	22500	17	2	Vachula et al. 2019; Pitblado 2017
31	Kashtanka 1	OB	Russia	91.50	55.12	223	o/a	27087	6	1_int	Vachula et al. 2019; Pitblado 2017
32	Kawanishi-C	PSHK	Japan	143.19	42.88	68	o/a	25164	5	1_int	Vachula et al. 2019; Pitblado 2017
33	Khayrgas Cave	OB	Russia	117.35	59.99	155	c	23410	2	1_int	Vachula et al. 2019; Pitblado 2017
34	Khodulikha-2	PSHK	Russia	127.33	50.33	135	g/a	24747	1	1_int	Vachula et al. 2019; Pitblado 2017
35	Khotyk 3	OB	Russia	109.83	52.28	695	u/k	29341	4	1_int	Vachula et al. 2019; Pitblado 2017
36	Kiusu 5	PSHK	Japan	141.72	42.88	36	s/c; o/a	24722	1	1_int	Vachula et al. 2019; Pitblado 2017
36	Kiusu 5	PSHK	Japan	141.72	42.88	36	s/c; o/a	20531	2	2	Vachula et al. 2019; Pitblado 2017
37	Krasny Yar 1	OB	Russia	103.43	53.67	447	o/a; p/e	21307	1	2	Vachula et al. 2019; Pitblado 2017; Turner et al. 2013
38	Kukouminami A	PSHK	Japan	143.23	42.72	145	u/k	22294	1	2	Vachula et al. 2019; Pitblado 2017
39	Kurtak-3	OB	Russia	91.47	55.15	416	g/a;s/c	18659	1	2	Vachula et al. 2019; Pitblado 2017
40	Kurtak-4	OB	Russia	91.47	55.15	223	g/a;s/c	27514	10	1_int	Vachula et al. 2019; Pitblado 2017
40	Kurtak-4	OB	Russia	91.47	55.15	223	g/a;s/c	34744	1	1_std	Vachula et al. 2019; Pitblado 2017
40	Kurtak-4	OB	Russia	91.47	55.15	223	g/a;s/c	21264	2	2	Vachula et al. 2019; Pitblado 2017
41	Kuylug Khem-1	OB	Russia	51.69	92.58	10	c	26013	1	1_int	Graf 2008
42	Kyushiarataki 3	PSHK	Japan	143.22	43.91	323	u/k	27926	6	1_int	Vachula et al. 2019
42	Kyushiarataki 3	PSHK	Japan	143.22	43.91	323	u/k	30635	1	1_std	Vachula et al. 2019
42	Kyushiarataki 3	PSHK	Japan	143.22	43.91	323	u/k	20007	13	2	Vachula et al. 2019
43	Lagerny	WB	Russia	135.42	70.63	15	o/a	24264	1	1_int	Kuzmin & Keates 2016; Andreev et al. 2001
44	Lake E5	EB	US - Alaska	-149.45	68.64	798	o/a; p/e	20024	3	2	Longo et al. 2020; Vachula et al. 2019
44	Lake E5	EB	US - Alaska	-149.45	68.64	798	o/a; p/e	31377	4	1_int	Longo et al. 2020; Vachula et al. 2019
45	Listvenka	OB	Russia	92.37	55.93	558	o/a	19195	4	2	Vachula et al. 2019; Pitblado 2017
46	Maininskaia East	OB	Russia	91.45	52.97	390	o/a	18032	1	2	Pitblado 2017
47	Maininskaia West	OB	Russia	91.45	52.97	390	o/a	21300	1	2	Pitblado 2017
48	Malaya Syia	OB	Russia	89.45	54.42	35	o/a	29990	2	1_int	Pitblado 2017; Graf 2014; Turner et al. 2013; Vasili'ev et al. 2002
48	Malaya Syia	OB	Russia	89.45	54.42	35	o/a	22547	1	2	Pitblado 2017; Graf 2014; Turner et al. 2013; Vasili'ev et al. 2002
49	Mal'ta	OB	Russia	103.53	52.83	414	o/a	22290	3	2	Vachula et al. 2019; Pitblado 2017
49	Mal'ta	OB	Russia	103.53	52.83	414	o/a	23939	4	1_int	Vachula et al. 2019; Pitblado 2017
51	Masterov Kliych	OB	Russia	110.00	50.43	1112	o/a	32253	1	1_std	Vachula et al. 2019; Pitblado 2017
52	Minamimachi 2	PSHK	Japan	143.17	42.88	77	u/k	21647	1	2	Vachula et al. 2019; Pitblado 2017
52	Minamimachi 2	PSHK	Japan	143.17	42.88	77	u/k	23947	1	1_int	Vachula et al. 2019; Pitblado 2017

Supplementary Data 3 - Project database, '*SummaryData*'... continuation

siteID	site_name	area	country	x_coord	y_coord	elevation (m)	site_type	age_m	n_dates	temp_ group	ref_loc
53	Moil'tyn-am	OB	Mongolia	103.80	47.20	1332	o/a	21760	2	2	Pitblado 2017
54	Nakamoto	PSHK	Japan	143.88	43.81	85	o/a	21427	1	2	Vachula et al. 2019; Pitblado 2017
55	Nepa-1	OB	Russia	108.30	59.16	20	o/a	28515	1	1_int	Kuzmin 2017; Madsen 2004
56	Nitto	PSHK	Japan	142.80	43.84	362		18280	2	2	Vachula et al. 2019; Pitblado 2017
57	Nizhnii Idzhir-1	OB	Russia	92.35	52.08	622	o/a; l/c	18785	1	2	Vachula et al. 2019; Pitblado 2017; Graf 2008
58	Novoselovo-6	OB	Russia	90.97	55.03	365	o/a	20017	1	2	Vachula et al. 2019; Pitblado 2017
59	Ochiai	PSHK	Japan	143.18	42.90	64	u/k	20610	2	2	Vachula et al. 2019; Pitblado 2017
60	Ogonki 5	PSHK	Russia	142.43	46.78	39	o/a; p/e	20981	5	2	Vachula et al. 2019; Pitblado 2017
60	Ogonki 5	PSHK	Russia	142.43	46.78	39	o/a; p/e	33523	1	1_std	Vachula et al. 2019; Pitblado 2017
61	Okushirataki 1	PSHK	Japan	143.13	43.87	446	o/a	20396	3	2	Vachula et al. 2019; Pitblado 2017
62	Oribe 16	PSHK	Japan	143.37	43.22	263	u/k	25997	1	1_int	Vachula et al. 2019; Pitblado 2017
63	Orkhon-7	OB	Mongolia	102.83	47.56	1373	o/a	29827	2	1_int	UNESCO WH Nomination 2004
64	Pirika 1	PSHK	Japan	140.21	42.48	153	o/a	20791	5	2	Vachula et al. 2019; Pitblado 2017
64	Pirika 1	PSHK	Japan	140.21	42.48	153	o/a	23221	1	1_int	Vachula et al. 2019; Pitblado 2017
65	Podzvonkaya	OB	Russia	107.23	50.27	713	o/a	24698	1	1_int	Vachula et al. 2019; Pitblado 2017
65	Podzvonkaya	OB	Russia	107.23	50.27	713	o/a	28625	1	1_std	Vachula et al. 2019; Pitblado 2017
66	Priiskovoye	OB	Russia	108.55	50.18	765	p/e	28192	5	1_int	Vachula et al. 2019; Pitblado 2017
66	Priiskovoye	OB	Russia	108.55	50.18	765	p/e	32300	1	1_std	Vachula et al. 2019; Pitblado 2017
67	Shimaki	PSHK	Japan	143.30	43.23	290	o/a; g/a	26339	4	1_int	Vachula et al. 2019; Izuho 2014
67	Shimaki	PSHK	Japan	143.30	43.23	290	o/a; g/a	19988	5	2	Vachula et al. 2019; Izuho 2014
68	Shishkino 8	OB	Russia	105.67	54.02	600	o/a	23569	1	1_int	Vachula et al. 2019; Pitblado 2017
69	Shukubai-Kaso (Sankakuyama)	PSHK	Japan	141.67	42.83	27	o/a; l/c	29097	12	1_int	Morisaki et al. 2015
69	Shukubai-Kaso (Sankakuyama)	PSHK	Japan	141.67	42.83	27	o/a; l/c	27650	3	1_std	Morisaki et al. 2015
70	Sokhatino 4	OB	Russia	113.43	52.02	695	o/a	18497	2	2	Vachula et al. 2019; Pitblado 2017
71	Studenoe 1	OB	Russia	108.50	50.17	867	o/a	20489	1	2	Vachula et al. 2019; Pitblado 2017
72	Studenoe 2	OB	Russia	108.51	50.17	867	o/a	19866	15	2	Vachula et al. 2019; Pitblado 2017
73	Tesa	OB	Russia	112.50	57.50	336	o/a	22280	1	2	Vachula et al. 2019; Pitblado 2017
74	Tolbaga	OB	Russia	109.33	51.22	904	o/a	27557	1	1_std	Vachula et al. 2019; Pitblado 2017
74	Tolbaga	OB	Russia	109.33	51.22	904	o/a	27827	6	1_int	Vachula et al. 2019; Pitblado 2017
75	Tolbor-15	OB	Mongolia	102.97	49.27	1008	o/a	31743	1	1_int	Vachula et al. 2019; Pitblado 2017
75	Tolbor-15	OB	Mongolia	102.97	49.27	1008	o/a	30768	1	1_std	Vachula et al. 2019; Pitblado 2017
76	Tolbor-16	OB	Mongolia	102.92	49.23	1169	o/a	34355	5	1_int	Zwyns 2019
77	Tolbor-17	OB	Mongolia	102.97	49.27	11	o/a	31648	1	1_int	Pitblado 2017
78	Tolbor-4	OB	Mongolia	102.96	49.29	1044	o/a	31187	2	1_std	Derevianko et al. 2007
79	Tsagaan Agui	OB	Mongolia	101.17	44.71	1878	c	33414	1	1_std	Pitblado 2017
79	Tsagaan Agui	OB	Mongolia	101.17	44.71	1878	c	35860	1	1_int	Pitblado 2017
80	Tsatsyn-Ereg 2	OB	Mongolia	101.39	47.76	1700	o/a	26285	3	1_int	Simonet et al. 2011; Magail et al. 2006
80	Tsatsyn-Ereg 2	OB	Mongolia	101.39	47.76	1700	o/a	18681	1	2	Simonet et al. 2011; Magail et al. 2006
81	Ui 1	OB	Russia	91.43	52.97	532	o/a	25084	1	1_int	Vachula et al. 2019; Pitblado 2017
81	Ui 1	OB	Russia	91.43	52.97	532	o/a	19628	4	2	Vachula et al. 2019; Pitblado 2017
82	Ust'-Kova	OB	Russia	100.33	58.30	173	o/a	29446	6	1_int	Vachula et al. 2019; Pitblado 2017

Supplementary Data 3 - Project database, '*SummaryData*'... continuation

siteID	site_name	area	country	x_coord	y_coord	elevation (m)	site_type	age_m	n_dates	temp_ group	ref_loc
82	Ust'-Kova	OB	Russia	100.33	58.30	173	o/a	21814	3	2	Vachula et al. 2019; Pitblado 2017
85	Ust'-Menza 2	OB	Russia	108.37	50.15	987	o/a	19021	10	2	Vachula et al. 2019; Pitblado 2017
86	Ust'-Mil' II	OB	Russia	133.12	59.65	213	o/a	31388	3	1_int	Vachula et al. 2019; Pitblado 2017
87	Ust'-Ulma 1	PSHK	Russia	129.58	51.83	238	o/a	21441	1	2	Vachula et al. 2019; Pitblado 2017
88	Varvarina Gora	OB	Russia	108.17	51.63	657	o/a	33500	1	1_std	Vachula et al. 2019; Pitblado 2017
88	Varvarina Gora	OB	Russia	108.17	51.63	657	o/a	33220	1	1_int	Vachula et al. 2019; Pitblado 2017
88	Varvarina Gora	OB	Russia	108.17	51.63	657	o/a	18726	1	2	Vachula et al. 2019; Pitblado 2017
89	Verkhne-Troitskaya	OB	Russia	134.45	60.35	158	o/a	19892	2	2	Vachula et al. 2019; Pitblado 2017
90	Wakabanomori	PSHK	Japan	143.18	42.90	69	o/a ; g/a	27213	5	1_int	Vachula et al. 2019; Pitblado 2017
91	Wr-12 Exposure	WB	Russia	-179.75	71.16	200	o/a	24728	1	1_int	Kuzmin & Orlova 2004; Lozhkin et al. 2001
92	Yana Rino Horn Site (RHS)	WB	Russia	135.42	70.72	18	o/a; s/c; g/a	29140	50	1_int	Vachula et al. 2019; Pitblado 2017
92	Yana Rino Horn Site (RHS)	WB	Russia	135.42	70.72	18	o/a; s/c; g/a	30376	15	1_std	Vachula et al. 2019; Pitblado 2017
92	Yana Rino Horn Site (RHS)	WB	Russia	135.42	70.72	18	o/a; s/c; g/a	20666	7	2	Vachula et al. 2019; Pitblado 2017

siteID	site	area	country	level	mat_type	mat_spec	date_type	lab_code	spec_code	age	s_dev	ref	source	comments	Age_Cal	σ_error_%	Age_CalM	Status	TempGroup	grnInd_stage
1	Alekseevsk-1	OB	Russia	cult.lay	charcoal	wood	Conv 14C	LE-3931	N/A	22410	480	Pitul'ko & Pavlova 2016; Kuzmin et al. 2016	Dolukhanov et al. 2001; Kuzmin et al. 2011	N/A	25684-23938	95.4	24811	Accept	1_int	GI-2.2
2	Ankarito 7	PSHK	Japan	concentration 1	charcoal	N/A	AMS	IAAA-82669	N/A	17760	80	Buvit et al. 2016	HCBCP 2010	N/A	19958-19304	95.4	19631	Accept	2	GS-2.1
3	Arta-2	WB	Russia	3	charcoal	N/A	Conv 14C	LE-2966	N/A	23200	2000	Khenzykhenova et al. 2016	Kirilov & Kasparov 1990; Kuzmin & Tankersley 1996; Kuzmin & Orlova 1998	Standard deviation considerably big	32227-21832	95.4	27095	Accept	1_int	GI-2.2
4	Berelekh	WB	Russia	surface	tusk	assegai (spear)	AMS	Beta-243747	N/A	18920	80	Slobodin et al. 2017	Pitul'ko & Pavlova 2016	N/A	21059-20621	95.4	20840	Accept	2	GS-2.1
5	Bibi 5	PSHK	Japan	UpperPaleolithic	charcoal	N/A	AMS	Gak-7764	N/A	17090	520	Buvit et al. 2016	HCBCP 1979	N/A	20175-17550	95.4	18862	Accept	2	GS-2.1
6	Bluefish Caves	EB	Canada	MgVo-1	bone	horse metatarsal	Conv 14C	RIDDL-278	N/A	17440	220	Bourgeon et al. 2017	N/A	N/A	19847-18585	95.4	19216	Accept	2	GS-2.1
6	Bluefish Caves	EB	Canada	MgVo-1	bone	horse metatarsal	AMS	OxA-33775*	K.8.1.13	17610	100	Bourgeon et al. 2017	N/A	>same specimen as RIDDL-278 (*)	19766-19005	95.4	19385	Accept	2	GS-2.1
6	Bluefish Caves	EB	Canada	MgVo-1	bone	horse metatarsal	AMS	OxA-33774*	K8.1.13	17660	100	Bourgeon et al. 2017	N/A	>same specimen as RIDDL-278 (*)	19831-19051	95.4	19441	Accept	2	GS-2.1
6	Bluefish Caves	EB	Canada	MgVo-2	bone	mammoth scapula	Conv 14C	CRNL-1221	N/A	17880	330	Bourgeon et al. 2017	N/A	N/A	20481-18914	95.4	19697	Accept	2	GS-2.1
6	Bluefish Caves	EB	Canada	MgVo-2	bone	caribou coxal bone	AMS 14C	OxA-33777	I5.6.5	18570	110	Bourgeon et al. 2017	N/A	N/A	20924-20350	95.4	20637	Accept	2	GS-2.1
6	Bluefish Caves	EB	Canada	MgVo-2	bone	horse mandible	AMS 14C	OxA-33778	J7.8.17	19650	130	Bourgeon et al. 2017	N/A	N/A	21951-21285	95.4	21618	Accept	2	GS-2.1
6	Bluefish Caves	EB	Canada	MgVo-2	bone	mammoth scapula	Conv 14C	RIDDL-330	N/A	19640	170	Bourgeon et al. 2017	N/A	N/A	22063-21180	95.4	21621	Accept	2	GS-2.1
6	Bluefish Caves	EB	Canada	MgVo-2	bone	mammoth scapula	Conv 14C	RIDDL-223	N/A	20230	180	Bourgeon et al. 2017	N/A	N/A	22888-21901	95.4	22394	Accept	2	GS-2.1
6	Bluefish Caves	EB	Canada	MgVo-2	bone	caribou / sheep	Conv 14C	Beta-140679	N/A	21100	150	Bourgeon et al. 2017	N/A	N/A	23826-23171	95.4	23498	Accept	1_int	GI-2.2
6	Bluefish Caves	EB	Canada	MgVo-2	bone	mammoth limb bone	Conv 14C	CAMS-23470	N/A	22740	90	Bourgeon et al. 2017	N/A	N/A	25339-24546	95.4	24942	Accept	1_int	GI-2.2
6	Bluefish Caves	EB	Canada	MgVo-2	bone	hose limb bone	Conv 14C	CRNL-1237	N/A	22680	530	Bourgeon et al. 2017	Burke & Cinq Mars 1998	N/A	25928-23964	95.4	24946	Accept	1_int	GI-2.2
6	Bluefish Caves	EB	Canada	MgVo-2	bone	mammoth limb bone	Conv 14C	RIDDL-225	N/A	23200	250	Bourgeon et al. 2017	N/A	N/A	25886-25162	95.4	25524	Accept	1_int	GI-2.2
6	Bluefish Caves	EB	Canada	MgVo-2	bone	mammoth limb bone	Conv 14C	RIDDL-224	N/A	23910	200	Bourgeon et al. 2017	N/A	N/A	26651-25786	95.4	26218	Accept	1_int	GI-2.2
6	Bluefish Caves	EB	Canada	MgVo-2	bone	caribou tibia	Conv 14C	RIDDL-226	N/A	24820	115	Bourgeon et al. 2017	N/A	N/A	27271-26846	95.4	27058	Accept	1_int	GI-2.2
6	Bluefish Caves	EB	Canada	MgVo-2	bone	bison tibia	Conv 14C	CAMS-23469	N/A	31730	230	Bourgeon et al. 2017	N/A	N/A	34587-33532	95.4	34059	Accept	1_int	GI-6
7	Buret	OB	Russia	cult.lay	bone	animal	Conv 14C	SOAN-1680	N/A	21190	100	Kuzmin & Keates 2016	Orlova 1995; Kuzmin & Orlova 1998; Kuzmin et al. 2012	N/A	23816-23304	95.4	23560	Accept	1_int	GI-2.2
8	Burial Lake	EB	US-Alaska	core A-98 D1	macrofossil	N/A	AMS 14C	AA-35196	N/A	16900	270	Finkenbinder et al. 2015	Abbott et al. 2010	N/A	19088-17671	95.4	18380	Accept	2	GS-2.1
8	Burial Lake	EB	US-Alaska	core C-98 D3	macrofossil	N/A	AMS 14C	CAMS-73173	N/A	16740	520	Finkenbinder et al. 2015	Abbott et al. 2010	N/A	19778-17094	95.4	18436	Accept	2	GS-2.1
8	Burial Lake	EB	US-Alaska	core C-98 D4	macrofossil	N/A	AMS 14C	AA-35199	N/A	20330	560	Finkenbinder et al. 2015	Abbott et al. 2010	N/A	23852-21297	95.4	22575	Accept	2	GS-2.1
8	Burial Lake	EB	US-Alaska	core A-10 D7	seed	N/A	AMS 14C	UCIAMS#89201	N/A	25300	510	Finkenbinder et al. 2015	N/A	N/A	28842-26687	95.4	27765	Accept	1_std	GS-3
8	Burial Lake	EB	US-Alaska	core C-98 D4	wood sample	N/A	AMS 14C	OS-18368	N/A	30300	600	Finkenbinder et al. 2015	Abbott et al. 2010	N/A	34161-31772	95.4	32966	Accept	1_int	GI-5.2
8	Burial Lake	EB	US-Alaska	core C-10 D7	wood sample	N/A	AMS 14C	UCIAMS#89124	N/A	31090	210	Finkenbinder et al. 2015	N/A	N/A	34104-32961	95.4	33432	Accept	1_std	GS-6
8	Burial Lake	EB	US-Alaska	core C-98 D5	macrofossil	N/A	AMS 14C	CAMS-73174	N/A	31680	720	Finkenbinder et al. 2015	Abbott et al. 2010	N/A	36288-32645	95.4	34466	Accept	1_int	GI-6
8	Burial Lake	EB	US-Alaska	core A-10 D8	wood sample	N/A	AMS 14C	UCIAMS#89121	N/A	32150	240	Finkenbinder et al. 2015	N/A	N/A	35074-34119	95.4	34597	Accept	1_int	GI-6
8	Burial Lake	EB	US-Alaska	core C-98 D5	macrofossil	N/A	AMS 14C	OS-27279	N/A	32780	560	Finkenbinder et al. 2015	Abbott et al. 2010	N/A	37185-34253	95.4	35719	Accept	1_int	GI-7
8	Burial Lake	EB	US-Alaska	core C-98 D5	wood sample	N/A	AMS 14C	CAMS-73175	N/A	32770	940	Finkenbinder et al. 2015	Abbott et al. 2010	N/A	37960-33487	95.4	35724	Accept	1_int	GI-7
9	Chikhen Agui	OB	Mongolia	3	humates	N/A	AMS	AA-32207	N/A	21620	180	Gomez Coutouly 2018b; Rybin et al. 2018; Rybin et al. 2016	Derevianko et al. 2004; Rybin 2014	N/A	24399-23692	95.4	24045	Accept	1_int	GI-2.2
9	Chikhen Agui	OB	Mongolia	3	charcoal (hearth)	N/A	AMS	AA-26580	N/A	27432	872	Gomez Coutouly 2018b; Rybin et al. 2018; Rybin et al. 2016	Derevianko et al. 2004; Rybin 2014	N/A	31991-28157	95.4	30074	Accept	1_int	GI-4
10	Chikhen-2	OB	Mongolia	2.5	bone	N/A	AMS	AA-31870	N/A	30550	410	Gomez Coutouly 2018b; Rybin et al. 2016	Derevianko et al. 2004; Rybin 2014	N/A	33910-32342	95.4	33126	Accept	1_int	GI-5.2
11	Chitkan	OB	Mongolia	4	charcoal	N/A	AMS	AA-67828	N/A	21330	790	Buvit et al. 2016	Buvit 2008	N/A	25326-21946	95.4	23636	Accept	1_int	GI-2.2
11	Chitkan	OB	Mongolia	4	bone	N/A	AMS	AA-67827	N/A	25510	230	Buvit et al. 2016	Buvit et al. 2015	N/A	28194-27265	95.4	27729	Accept	1_std	GS-3
12	Derbina V	OB	Russia	cult.lay	charcoal	N/A	Conv 14C	SOAN-6007	N/A	18960	220	Malikov 2016	Kuzmin et al. 2011	N/A	21741-20454	95.4	21098	Accept	2	GS-2.1
12	Derbina V	OB	Russia	cult.lay	charcoal	N/A	Conv 14C	SOAN-4796	N/A	20460	465	Malikov 2016	Kuzmin et al. 2011	N/A	23869-21789	95.4	22829	Accept	2	GS-2.1
12	Derbina V	OB	Russia	cult.lay	charcoal	N/A	Conv 14C	SOAN-4346	N/A	21100	120	Malikov 2016	Kuzmin et al. 2011	N/A	23776-23224	95.4	23500	Accept	1_int	GI-2.2
12	Derbina V	OB	Russia	cult.lay	charcoal	N/A	Conv 14C	SOAN-4346a	N/A	21320	300	Malikov 2016	Kuzmin et al. 2011	N/A	24324-23054	95.4	23689	Accept	1_int	GI-2.2
12	Derbina V	OB	Russia	cult.lay	charcoal	N/A	Conv 14C	SOAN-4797	N/A	21440	450	Malikov 2016	Kuzmin et al. 2011	N/A	24956-22758	95.4	23857	Accept	1_int	GI-2.2
12	Derbina V	OB	Russia	cult.lay	charcoal	N/A	Conv 14C	SOAN-4202	N/A	31480	1650	Malikov 2016	Kuzmin et al. 2011	Standard deviation considerably big	39026-31154	95.4	35090	Accept	1_int	GI-7
12	Derbina V	OB	Russia	cult.lay	charcoal	N/A	Conv 14C	SOAN-4200	N/A	29230	940	Rybin 2014	Akimova et al. 2000b; Vasili'ev et al. 2002; Kuzmin et al. 2011	N/A	33754-29553	95.4	31654	Accept	1_int	GI-5.1
12	Derbina V	OB	Russia	cult.lay	charcoal	N/A	Conv 14C	SOAN-4201	N/A	32430	1540	Rybin 2014	Akimova et al. 2000b; Vasili'ev et al. 2002; Kuzmin et al. 2011	Standard deviation considerably big	39127-32487	95.4	35807	Accept	1_int	GI-7
13	Dörölj-1	OB	Mongolia	12-13	bone	N/A	AMS	GifA-99561	N/A	29540	390	Gladyshev et al. 2012	N/A	N/A	32820-31149	95.4	31985	Accept	1_int	GI-5.1
13	Dörölj-1	OB	Mongolia	12-13	eggshell	Struthio	AMS	GifA-11664	N/A	31880	800	Gladyshev et al. 2012	N/A	N/A	36893-32778	95.4	34836	Accept	1_std	GS-7
13	Dörölj-1	OB	Mongolia	7	eggshell	Struthio	AMS	GifA-102451	N/A	21820	190	Rybin et al. 2018	Gladyshev et al. 2012	N/A	24505-23822	95.4	24164	Accept	1_int	GI-2.2
13	Dörölj-1	OB	Mongolia	7	eggshell	Struthio	AMS	GifA-102453	N/A	22030	180	Rybin et al. 2018	Gladyshev et al. 2012	N/A	24932-23963	95.4	24448	Accept	1_int	GI-2.2
14	Dvuglazka Cave	OB	Russia	7	bone	N/A	Conv 14C	LE-4811	N/A	27200	800	Vasili'ev et al. 2002	Lisitsyn & Svezhentsev 1997	N/A	31668-28071	95.4	29870	Accept	1_int	GI-4
15	Dvuglazka Rockshelter	OB	Russia	4	bone	N/A	Conv 14C	LE-1433	N/A	19880	200	Vasili'ev et al. 2002	Arslanov et al. 1981	N/A	22536-21405	95.4	21971	Accept	2	GS-2.1
15	Dvuglazka Rockshelter	OB	Russia	4	bone	N/A	Conv 14C	LE-1433	N/A	20190	140	Vasili'ev et al. 2002	Arslanov et al. 1981	N/A	22686-21911	95.4	22299	Accept	2	GS-2.1
15	Dvuglazka Rockshelter	OB	Russia	4	bone	N/A	Conv 14C	LE-1433	N/A	22500	600	Vasili'ev et al. 2002	Arslanov et al. 1981	N/A	25980-23746	95.4	24863	Accept	1_int	GI-2.2
15	Dvuglazka Rockshelter	OB	Russia	4	bone	N/A	Conv 14C	LE-4808	N/A	26580	520	Vasili'ev et al. 2002	Lisitsyn 2000	N/A	29764-27987	95.4	28876	Accept	1_std	GS-4
16	Ezhantsy	WB	Russia	3	bone	N/A	Conv 14C	IM-459	N/A	17150	345	Pitulko & Pavlova 2016; Gomez Coutouly 2018b	Kostiukevich et al. 1980; Kashin 1991; Kuzmin & Orlova 1998	N/A	19853-17947	95.4	18900	Accept	2	GS-2.1
17	Gosudarev Log 1	OB	Russia	N/A	charcoal	N/A	Conv 14C	SOAN-4315	N/A	22870	380	Kuzmin & Keates 2016	Kuzmin et al. 2011	N/A	25856-24418	95.4	25137	Accept	1_int	GI-2.2
18	Guanghetun 1	PSHK	China	4	charcoal	N/A	AMS	Beta-469561	GHT0101	25150	100	Guan et al. 2021	N/A	N/A	27857-27211	95.4	27534	Accept	1_int	GI-2.2
19	Hattoridai 2	PSHK	Japan	Dense charcoal 7 Lithic concentration 15 Unit C-14	charcoal	N/A	AMS	Beta-150444	N/A	17270	110	Buvit et al. 2016	HCBCP 2007	N/A	19171-18572	95.4	18871	Accept	2	GS-2.1
19	Guanghetun 1	PSHK	China	4	charcoal	N/A	AMS	Beta-469562	GHT0102	26300	100	Guan et al. 2021	N/A	N/A	28930-28317	95.4	28624	Accept	1_std	GS-4
19	Hattoridai 2	PSHK	Japan	Dense charcoal 7 Lithic concentration 15 Unit C-14	charcoal	N/A	AMS	PLD-3315	N/A	17900	60	TBD	HCBCP 2007	N/A	20042-19502	95.4	19772	Accept	2	GS-2.1
20	Hirosato 8	PSHK	Japan	Upper Paleolithic	charcoal	N/A	AMS	Gak-11901	N/A	23320	1130	Buvit et al. 2016	Kitami City 1985	s_dev too big	28385-23703	95.4	26044	Accept	1_int	GI-2.2
22	Hokuto	PSHK	Japan	Upper Paleolithic	charcoal	N/A	AMS	Gak-17292	N/A	17690	310	Buvit et al. 2016	Kushiro Board of Education 1994	N/A	20313-18735	95.4	19524	Accept	2	GS-2.1
22	Ikhine I	WB	Russia	II	bone	N/A	Conv 14C	IM-452	N/A	16600	270	Pitulko & Pavlova 2016	Kashin 1991; Kuzmin & Orlova 1998; Kashin 2003	N/A	18816-17501	95.4	18158	Accept	2	GS-2.1
23	Ikhine II	OB	Russia	N/A	animal bone	N/A	Conv 14C	SOAN-3186	N/A	19695	100	Kuzmin & Keates 2016; Pitul'ko & Pavlova 2016	Kuzmin 2008	N/A	21958-21399	95.4	21678	Accept	2	GS-2.1
23	Ikhine II	OB	Russia	N/A	animal bone	N/A	Conv 14C	SOAN-3185	N/A	20080	150	Kuzmin & Keates 2016; Pitul'ko & Pavlova 2016	Kuzmin 2008	N/A	22576-21861	95.4	22218	Accept	2	GS-2.1
23	Ikhine II	WB	Russia	IIb	wood	N/A	Conv 14C	LE-1131	N/A	24330	200	Pitulko & Pavlova 2016	Mochanov 1977; Kuzmin & Orlova 1998	N/A	27068-25991	95.4	26529	Accept	1_int	GI-2.2
23	Ikhine II	WB	Russia	IIb	wood	N/A	Conv 14C	IM-203	N/A	24500	480	Pitulko & Pavlova 2016	Mochanov 1977; Kuzmin & Orlova 1998	N/A	27889-25846	95.4	26867	Accept	1_int	GI-2.2
23	Ikhine II	WB	Russia	IIb	wood	N/A	Conv 14C	IM-153	N/A	24600	380	Pitulko & Pavlova 2016	Mochanov 1977; Kuzmin & Orlova 1998	N/A	27821-25966	95.4	26893	Accept	1_int	GI-2.2
23	Ikhine II	WB	Russia	IIc	wood	N/A	Conv 14C	IM-202	N/A	26500	540	Pitulko & Pavlova 2016	Mochanov 1977; Kuzmin & Orlova 1998	N/A	29792-27853	95.4	28822	Accept	1_std	GS-4

Supplementary Data 4 - Project Database '*DetailedData*'... continuation

siteID	site	area	country	level	mat_type	mat_spec	date_type	lab_code	spec_code	age	s_dev	ref	source	comments	Age_Cal	σ_error_%	Age_CalM	Status	TempGroup	grnlnd_stage
23	Ikhine II	WB	Russia	IIc	wood	N/A	Conv 14C	IM-201	N/A	26600	900	Pitulko & Pavlova 2016	Mochanov 1977; Kuzmin & Orlova 1998	N/A	31262-27188	95.4	29225	Accept	1_int	GI-4
23	Ikhine II	WB	Russia	IIb	wood	N/A	Conv 14C	IM-205	N/A	27400	800	Pitulko & Pavlova 2016	Mochanov 1977; Kuzmin & Orlova 1998	N/A	31794-28192	95.4	29993	Accept	1_int	GI-4
23	Ikhine II	WB	Russia	IIb	wood	N/A	Conv 14C	GIN-1019	N/A	30200	300	Pitulko & Pavlova 2016	Mochanov 1977; Kuzmin & Orlova 1998	N/A	33331-32242	95.4	32786	Accept	1_int	GI-5.2
23	Ikhine II	WB	Russia	IIc	wood	N/A	Conv 14C	GIN-1020	N/A	31200	500	Pitulko & Pavlova 2016	Mochanov 1977; Kuzmin & Orlova 1998	N/A	34605-32627	95.4	33616	Accept	1_std	GS-6
23	Ikhine II	WB	Russia	IIv	wood	N/A	Conv 14C	IM-239	N/A	26030	200	Pitul'ko & Pavlova 2016	Mochanov 1977	N/A	28864-28040	95.4	28452	Accept	1_int	GI-3
23	Ikhine II	WB	Russia	IIg/IId	wood	N/A	Conv 14C	IM-206	N/A	27800	500	Pitulko & Pavlova 2017	Mochanov 1977	N/A	31378-29117	95.4	30247	Accept	1_int	GI-4
25	Kamenka	OB	Russia	component A	bone	N/A	Conv 14C	SOAN-3031	N/A	24625	190	Buvit et al. 2016	Orlova 1995; Kuzmin & Orlova 1998; Lbova 2000	N/A	27274-26527	95.4	26900	Accept	1_int	GI-2.1
25	Kamenka	OB	Russia	component A	bone	N/A	Conv 14C	SOAN-3355	N/A	25540	300	Buvit et al. 2016	Orlova 1995; Kuzmin & Orlova 1998; Lbova 2000	N/A	28425-27200	95.4	27812	Accept	1_int	GI-3
25	Kamenka	OB	Russia	component A		N/A	Conv 14C	SOAN-2903	N/A	28060	475	Buvit et al. 2016	Orlova 1995; Kuzmin & Orlova 1998; Lbova 2000	N/A	31589-29240	95.4	30414	Accept	1_int	GI-4
25	Kamenka	OB	Russia	component B	bone	N/A	Conv 14C	SOAN-3032	N/A	28815	150	Buvit et al. 2016	Lbova 2000	N/A	31877-30357	95.4	31117	Accept	1_int	GI-5.1
25	Kamenka	OB	Russia	component A	bone	N/A	Conv 14C	SOAN-3353	N/A	26760	265	Buvit et al. 2016; Rybin 2014	Orlova 1995; Kuzmin & Orlova 1998; Lbova 2000	N/A	29326-28381	95.4	28853	Accept	1_std	GS-4
25	Kamenka	OB	Russia	component A	bone	N/A	Conv 14C	SOAN-3354	N/A	30460	430	Kuzmin & Orlova 1998	Orlova 1998	N/A	33871-32246	95.4	33058	Accept	1_int	GI-5.2
25	Kamenka	OB	Russia	component A	bone	N/A	Conv 14C	SOAN-3133	N/A	31060	530	Kuzmin & Orlova 1998	Orlova 1998	N/A	34518-32512	95.4	33515	Accept	1_std	GS-6
25	Kamenka	OB	Russia	component C	bone	N/A	Conv 14C	SOAN-3052	N/A	30220	270	Orlova 1998	Kuzmin & Orlova 1998	N/A	33301-32295	95.4	32798	Accept	1_int	GI-5.2
25	ISM-034	WB	Russia	surface	bone	mammoth mandible	AMS 14C	LE-9506	N/A	22700	300	Pitulko et al. 2017			25672-24421	95.4	25046	Accept	1_int	GI-2.2
26	Kamiitaira	PSHK	Japan	Dense charcoal 1	charcoal	N/A	AMS	Gak-7079	N/A	22230	1440	Buvit et al. 2016	Obihiro Board of Education 1978	Standard deviation considerably big	28299-21814	95.4	25056	Accept	1_int	GI-2.2
26	Kamiitaira	PSHK	Japan	Cobble concentration 2	charcoal	dense charcoal	AMS	Beta-358835	N/A	23420	120	Buvit et al. 2016	Naobe & Kudo 2014	N/A	25850-25404	95.4	25627	Accept	1_int	GI-2.2
26	Kamiitaira	PSHK	Japan	Upper Paleolithic	charcoal	N/A	AMS	Gak-7078	N/A	25290	2080	Buvit et al. 2016	Obihiro Board of Education 1978	Standard deviation considerably big	34821-23932	95.4	29376	Accept	1_int	GI-4
26	Kamiitaira	PSHK	Japan	Upper Paleolithic	charcoal	N/A	AMS	Gak-7080	N/A	28750	1840	Buvit et al. 2016	Obihiro Board of Education 1978	Standard deviation considerably big	37196-28046	95.4	32621	Accept	1_int	GI-5.2
27	Kamishirataki 2	PSHK	Japan	Dense charcoal 2(1) lithic concentration 1 unit S25	charcoal	N/A	AMS	Beta-112885	N/A	17670	180	Buvit et al. 2016	HCBCP 2001	N/A	20011-18967	95.4	19489	Accept	2	GS-2.1
27	Kamishirataki 2	PSHK	Japan	Dense charcoal 6(1) Lithic concentration 8 Unit J38-39	charcoal	N/A	AMS	Beta-150432	N/A	17740	110	Buvit et al. 2016	HCBCP 2001	N/A	19974-19136	95.4	19555	Accept	2	GS-2.1
27	Kamishirataki 2	PSHK	Japan	Lithic concentration 8 Unit J38-39	charcoal	dense charcoal 6(3)	AMS	Beta-112888	N/A	18050	190	Buvit et al. 2016	HCBCP 2001	N/A	20416-19456	95.4	19936	Accept	2	GS-2.1
27	Kamishirataki 2	PSHK	Japan	Lithic concentration 3	charcoal	N/A	AMS	Beta-112889	N/A	18620	160	Buvit et al. 2016	HCBCP 2001	N/A	20992-20337	95.4	20664	Accept	2	GS-2.1
28	Kamishirataki 5	PSHK	Japan	Dense charcoal 17(3) Lithic concentration 85 Unit P35	charcoal	N/A	AMS	Beta-126158	N/A	18530	150	Buvit et al. 2016	HCBCP 2002	N/A	20948-20236	95.4	20592	Accept	2	GS-2.1
29	Kamishirataki 8	PSHK	Japan	Dense Charcoal 6(3) Lithic concentration 8 Unit J38-39	charcoal	N/A	AMS	Beta-101793	N/A	18510	270	Buvit et al. 2016	HCBCP 2006	N/A	21061-19942	95.4	20501	Accept	2	GS-2.1
29	Kamishirataki 8	PSHK	Japan	Lithic concentration 2	charcoal	dense charcoal	AMS	Beta-101788	N/A	18580	60	Buvit et al. 2016	HCBCP 2004	N/A	20784-20384	95.4	20584	Accept	2	GS-2.1
29	Kamishirataki 8	PSHK	Japan	Dense Charcoal 16	charcoal	N/A	AMS	Beta-112900	N/A	18770	170	Buvit et al. 2016	HCBCP 2004	N/A	21046-20436	95.4	20741	Accept	2	GS-2.1
29	Kamishirataki 8	PSHK	Japan	Lithic concentration 85 Unit P35	charcoal	Dense charcoal 17(1)	AMS	Beta-112906	N/A	18870	160	Buvit et al. 2016	HCBCP 2006	N/A	21100-20477	95.4	20788	Accept	2	GS-2.1
29	Kamishirataki 8	PSHK	Japan	Lithic concentration 6 Unit M42	charcoal	Dense charcoal 1	AMS	Beta-126159	N/A	18870	140	Buvit et al. 2016	HCBCP 2002	N/A	21070-20508	95.4	20789	Accept	2	GS-2.1
29	Kamishirataki 8	PSHK	Japan	Unit D-57	charcoal	N/A	AMS	Beta-112908	N/A	22230	110	Buvit et al. 2016	HCBCP 2006	N/A	24993-24159	95.4	24576	Accept	1_int	GI-2.2
29	Kamishirataki 8	PSHK	Japan	Lithic concentration 66 unit S35-36	charcoal	dense charcoal 18(3)	AMS	Beta-112907	N/A	23640	310	Buvit et al. 2016	HCBCP 2006	N/A	26621-25353	95.4	25987	Accept	1_int	GI-2.2
30	Kashiwadai 1	PSHK	Japan	Lithic concenration 9	charcoal	N/A	AMS	Beta-112914	N/A	20570	120	Buvit et al. 2016	HCBCP 1999	N/A	23169-22381	95.4	22775	Accept	2	GS-2.1
30	Kashiwadai 1	PSHK	Japan	Area F-64 Unit KD1-3	charcoal	N/A	AMS	Beta-112915	N/A	19660	130	Buvit et al. 2016	HCBCP 1999	N/A	21968-21289	95.4	21628	Accept	2	GS-2.1
30	Kashiwadai 1	PSHK	Japan	Dense charcoal 18	charcoal	N/A	AMS	Beta-112916	N/A	20320	150	Buvit et al. 2016	HCBCP 1999	N/A	22973-22048	95.4	22510	Accept	2	GS-2.1
30	Kashiwadai 1	PSHK	Japan	Dense charcoal 18	charcoal	N/A	AMS	Beta-120880	N/A	20390	70	Buvit et al. 2016	HCBCP 1999	N/A	22802-22264	95.4	22533	Accept	2	GS-2.1
30	Kashiwadai 1	PSHK	Japan	Lithic concentration 10 Unit I-63	charcoal	hearth	AMS	Beta-126178	N/A	20900	190	Buvit et al. 2016	HCBCP 1999	N/A	23746-22731	95.4	23238	Accept	2	GS-2.2
30	Kashiwadai 1	PSHK	Japan	Dense charcoal 7	charcoal	N/A	AMS	Beta-126174	N/A	21790	230	Buvit et al. 2016	HCBCP 1999	N/A	24848-23728	95.4	24288	Accept	1_int	GI-2.2
30	Kashiwadai 1	PSHK	Japan	Lithic concentration 11 Unit F-61	charcoal	hearth	AMS	Beta-126183	N/A	22200	170	Buvit et al. 2016	HCBCP 1999	N/A	25017-24054	95.4	24535	Accept	1_int	GI-2.2
30	Kashiwadai 1	PSHK	Japan	Lithic concentration 66 unit S35-36	charcoal	dense charcoal 18(3)	AMS	Beta-112913	N/A	22210	210	Buvit et al. 2016	HCBCP 1999	N/A	25081-24034	95.4	24557	Accept	1_int	GI-2.2
30	Kashiwadai 1	PSHK	Japan	Lithic concentration 7 Unit D-58	charcoal	hearth	AMS	Beta-126169	N/A	22300	180	Buvit et al. 2016	HCBCP 1999	N/A	25141-24132	95.4	24637	Accept	1_int	GI-2.2
30	Kashiwadai 1	PSHK	Japan	Lithic concentration 10 Unit I-63	charcoal	hearth	AMS	Beta-126173	N/A	22340	220	Buvit et al. 2016	HCBCP 1999	N/A	25211-24131	95.4	24671	Accept	1_int	GI-2.2
30	Kashiwadai 1	PSHK	Japan	Lithic cocentration 4a Unit H-58	charcoal	hearth	AMS	Beta-126168	N/A	22340	170	Buvit et al. 2016	HCBCP 1999	N/A	25198-24173	95.4	24685	Accept	1_int	GI-2.2
30	Kashiwadai 1	PSHK	Japan	Lithic concentration 9 Unit F-59	charcoal	hearth	AMS	Beta-126171	N/A	22550	180	Buvit et al. 2016	HCBCP 1999	N/A	25270-24475	95.4	24872	Accept	1_int	GI-2.2
30	Kashiwadai 1	PSHK	Japan	Unit 0-7	charcoal	N/A	AMS	Beta-112918	N/A	28200	480	Buvit et al. 2016	HCBCP 1999	N/A	31755-29316	95.4	30535	Accept	1_int	GI-4
30	Kashiwadai 1	PSHK	Japan	1	charcoal	N/A	AMS	Beta-112919	N/A	20200	120	Gomez Coutouly 2018b	Hokkaido Center for Buried Cultural Property 1999	N/A	22657-21947	95.4	22302	Accept	2	GS-2.1
30	Kashiwadai 1	PSHK	Japan	4	charcoal	N/A	AMS	Beta-112920	N/A	20510	160	Gomez Coutouly 2018b	Hokkaido Center for Buried Cultural Property 1999	N/A	23170-22281	95.4	22725	Accept	2	GS-2.1
30	Kashiwadai 1	PSHK	Japan	4-5	charcoal	N/A	AMS	Beta-112921	N/A	20500	130	Gomez Coutouly 2018b	Hokkaido Center for Buried Cultural Property 1999	N/A	23102-22303	95.4	22702	Accept	2	GS-2.1
30	Kashiwadai 1	PSHK	Japan	2-3	charcoal	N/A	AMS	Beta-112922	N/A	20700	210	Gomez Coutouly 2018b	Hokkaido Center for Buried Cultural Property 1999	N/A	23610-22342	95.4	22976	Accept	2	GS-2.1
30	Kashiwadai 1	PSHK	Japan	4	charcoal	N/A	AMS	Beta-120881	N/A	19840	70	Gomez Coutouly 2018b	Nakazawa et al. 2005	N/A	22133-21800	95.4	21966	Accept	2	GS-2.1
30	Kashiwadai 1	PSHK	Japan	4	charcoal	hearth	AMS	Beta-120883	N/A	20370	70	Gomez Coutouly 2018b	Nakazawa et al. 2005	N/A	22756-22255	95.4	22505	Accept	2	GS-2.1
30	Kashiwadai 1	PSHK	Japan	4	charcoal	N/A	AMS	Beta-126167	N/A	20570	160	Gomez Coutouly 2018b	Hokkaido Center for Buried Cultural Property 1999	N/A	23226-22326	95.4	22776	Accept	2	GS-2.1
30	Kashiwadai 1	PSHK	Japan	4	charcoal	hearth	AMS	Beta-126170	N/A	20130	150	Gomez Coutouly 2018b	Nakazawa et al. 2005	N/A	22632-21881	95.4	22257	Accept	2	GS-2.1
30	Kashiwadai 1	PSHK	Japan	4	charcoal	hearth	AMS	Beta-126175	N/A	20790	160	Gomez Coutouly 2018b	Nakazawa et al. 2005	N/A	23631-22658	95.4	23145	Accept	2	GS-2.1
30	Kashiwadai 1	PSHK	Japan	4	charcoal	hearth	AMS	Beta-126176	N/A	20700	150	Gomez Coutouly 2018b	Nakazawa et al. 2006	N/A	23362-22421	95.4	22891	Accept	2	GS-2.1

Supplementary Data 4 - Project Database '*DetailedData*'... continuation

siteID	site	area	country	level	mat_type	mat_spec	date_type	lab_code	spec_code	age	s_dev	ref	source	comments	Age_Cal	σ_error_%	Age_CalM	Status	TempGroup	grnlnd_stage
30	Kashiwadai 1	PSHK	Japan	4	charcoal	N/A	AMS	Beta-126177	N/A	18830	150	Gomez Coutouly 2018b	Nakazawa et al. 2005	N/A	21053-20485	95.4	20769	Accept	2	GS-2.1
30	Kashiwadai 1	PSHK	Japan	4	charcoal	hearth	AMS	Beta-126184	N/A	20610	160	Gomez Coutouly 2018b	Nakazawa et al. 2005	N/A	23262-22354	95.4	22808	Accept	2	GS-2.1
31	Kashtanka-1	OB	Russia	Str 9/ cult.lay	charcoal	dispersed	Conv 14C	IGAN-1049	N/A	21800	200	Graf 2009	Drozdov et al. 1990; Kuzmin & Orlova 1998	>table 1 - only keeping "accepted"	24510-23786	95.4	24148	Accept	1_int	GI-2.2
31	Kashtanka-1	OB	Russia	Str 9/ cult.lay	charcoal	hearth context	Conv 14C	GIN-6968	N/A	23470	200	Graf 2009	Drozdov et al. 1990; Kuzmin & Orlova 1998	>table 1 - only keeping "accepted"	26003-25333	95.4	25668	Accept	1_int	GI-2.2
31	Kashtanka-1	OB	Russia	1	charcoal	N/A	Conv 14C	IGAN-1050	N/A	23830	580	Malikov 2016	Kuzmin et al. 2011	N/A	27519-25107	95.4	26313	Accept	1_int	GI-2.2
31	Kashtanka-1	OB	Russia	1	charcoal	N/A	Conv 14C	SOAN-2853	N/A	24805	425	Malikov 2016	Kuzmin et al. 2011	N/A	28055-26135	95.4	27095	Accept	1_int	GI-2.2
31	Kashtanka-1	OB	Russia	1	charcoal	N/A	Conv 14C	IGAN-1048	N/A	24400	1500	Malikov 2016	Kuzmin et al. 2011	Standard deviation considerably big	30902-23994	95.4	27448	Accept	1_int	GI-2.2
31	Kashtanka-1	OB	Russia	2	charcoal	N/A	Conv 14C	GIN-6969	N/A	29400	400	Malikov 2016	Kuzmin et al. 2011	N/A	32767-30933	95.4	31850	Accept	1_int	GI-5.1
32	Kawanishi-C	PSHK	Japan	V	charcoal	scattered charcoal	AMS 14C	TKa-15536	N/A	27840	200	Buvit et al. 2016	Izuho et al. 2014; Izuho et al. 2013	N/A	30827-29286	95.4	30056	Accept	1_int	GI-5.1
32	Kawanishi-C	PSHK	Japan	VII	charcoal	burned soil	AMS 14C	Beta-106506	N/A	21420	190	Takakura 2021	Izuho et al. 2014; Kitazawa 1998	N/A	24060-23321	95.4	23690	Accept	1_int	GI-2.2
32	Kawanishi-C	PSHK	Japan	VII	charcoal	burned soil	AMS 14C	TKa-15537	N/A	21480	120	Takakura 2021	Izuho et al. 2014; Izuho et al. 2013	N/A	24043-23678	95.4	23860	Accept	1_int	GI-2.2
32	Kawanishi-C	PSHK	Japan	VII	charcoal	burned soil	AMS 14C	Beta-107731	N/A	21780	90	Takakura 2021	Izuho et al. 2014; Kitazawa 1998	N/A	24356-23916	95.4	24136	Accept	1_int	GI-2.2
32	Kawanishi-C	PSHK	Japan	VI	burned sediment	with lithic concentration	AMS 14C	NUTA2-7677	N/A	21710	70	Takakura 2021;Izuho et al. 2014	Nakamura 2005	N/A	24281-23875	95.4	24078	Accept	1_int	GI-2.2
33	Khayrgas Cave	OB	Russia	7	bone	N/A	Conv 14C	AA-79786	N/A	20720	320	Kuzmin et al. 2017		N/A	23784-22229	95.4	23007	Accept	1_int	GI-2.1
33	Khayrgas Cave	OB	Russia	7	bone (tool)	mammoth	Conv 14C	SOAN-4249	N/A	21500	775	Pitul'ko & Pavlova 2016; Kuzmin & Keates 2016	Stepanov et al. 2003	N/A	25487-22138	95.4	23813	Accept	1_int	GI-2.1
34	Khodulikha	PSHK	Russia	1	wood charcoal	N/A	Conv 14C	SNU03-365	N/A	22530	320	Pitblado 2017; Kuzmin & Keates 2016; Kuzmin et al. 2011	Kuzmin et al. 2005	N/A	25410-24085	95.4	24747	Accept	1_int	GI-2.2
35	Khotyk 3	OB	Russia	2	bone	N/A	Conv 14C	SOAN-5497	N/A	23750	650	Buvit et al. 2016	Kuzmin et al. 2011	N/A	27696-24596	95.4	26146	Accept	1_int	GI-2.2
35	Khotyk 3	OB	Russia	2	bone	N/A	AMS	AA-32669	N/A	26220	550	Buvit et al. 2016	Kuzmin et al. 2011	N/A	29344-27307	95.4	28325	Accept	1_int	GI-3
35	Khotyk 3	OB	Russia	3	bone	N/A	Conv 14C	SOAN-5082	N/A	28770	245	Buvit et al. 2016	Kuzmin et al. 2011	N/A	31951-30208	95.4	31079	Accept	1_int	GI-5.1
35	Khotyk 3	OB	Russia	3	bone	N/A	Conv 14C	SOAN-5495	N/A	29310	340	Buvit et al. 2016	Kuzmin et al. 2011	N/A	32567-31061	95.4	31814	Accept	1_int	GI-5.1
36	Kiusu 5	PSHK	Japan	Lithic concentration 2	charcoal	dense charcoal	AMS	IAAA-72131	N/A	18500	70	Buvit et al. 2016	HCBCP 2013	N/A	20593-20324	95.4	20458	Accept	2	GS-2.1
36	Kiusu 5	PSHK	Japan	Unit 3-1	charcoal	scattered charcoal	AMS	IAAA-72130	N/A	18570	80	Buvit et al. 2016	HCBCP 2013	N/A	20841-20367	95.4	20604	Accept	2	GS-2.1
36	Kiusu 5	PSHK	Japan	Dense charcoal 6 Lithic concentration 20 Unit N16	charcoal	N/A	AMS	IAAA-72132	N/A	22350	70	Buvit et al. 2016	HCBCP 2013	North of lithic concentration	24997-24447	95.4	24722	Accept	1_int	GI-2.2
37	Krasny Yar 1	OB	Russia	6	animal bone	N/A	Conv 14C	GIN-5330	N/A	19100	100	Gomez Coutouly 2018b	Kuzmin & Keates 2016 ; Kuzmin 2008	N/A	21719-20895	95.4	21307	Accept	2	GS-2.1
38	Kukouminami A	PSHK	Japan	Upper Paleolithic	charcoal	N/A	AMS	GaK-10746	N/A	19420	1770	Buvit et al. 2016	Tokachi Branch Office 1983	Standard deviation considerably big	26712-17876	95.4	22294	Accept	2	GS-2.1
40	Kurtak-3	OB	Russia	EB 1, cult. Lay	charcoal	hearth context	Conv 14C	GIN-2102	N/A	16900	700	Malikov 2016	Abramova et al. 1991; Vasili'ev et al. 2002; Graf 2009; Kuzmin et al. 2011	N/A	20333-16985	95.4	18659	Accept	2	GS-2.1
40	Kurtak-4	OB	Russia	Str 11	charcoal	N/A	Conv 14C	AA-68670	N/A	17740	120	Malikov 2016	Kuzmin et al. 2011	N/A	19987-19116	95.4	19552	Accept	2	GS-2.1
40	Kurtak-4	OB	Russia	Str 11	charcoal	N/A	Conv 14C	AA-72146	N/A	20690	240	Malikov 2016	Kuzmin et al. 2011	N/A	23636-22315	95.4	22976	Accept	2	GS-2.1
40	Kurtak-4	OB	Russia	Str 11	charcoal	N/A	Conv 14C	AA-72147	N/A	21270	160	Malikov 2016	Kuzmin et al. 2011	N/A	23942-23296	95.4	23619	Accept	1_int	GI-2.2
40	Kurtak-4	OB	Russia	Str 11	charcoal	N/A	Conv 14C	AA-68668	N/A	27770	310	Malikov 2016	Kuzmin et al. 2011	N/A	30906-29210	95.4	30058	Accept	1_int	GI-4
40	Kurtak-4	OB	Russia	K28-30/L28-29	charcoal	hearth context	AMS	AA-68669	N/A	25160	280	Malikov 2016	Svezhentsev et al. 1992; Vasili'ev et al. 2002; Graf 2009; Kuzmin et al. 2011	>table 2 - new AMS dates	28065-26937	95.4	27501	Accept	1_int	GI-2.2
40	Kurtak-4	OB	Russia	Str 11	charcoal	N/A	Conv 14C	GIN-3357	N/A	24800	670	Malikov 2016	Kuzmin et al. 2011	N/A	28732-25785	95.4	27259	Accept	1_int	GI-2.2
40	Kurtak-4	OB	Russia	Str 11/cult.lay 1	charcoal	hearth context	Conv 14C	GIN-5350	N/A	24800	400	Malikov 2016	Svezhentsev et al. 1992; Vasili'ev et al. 2002; Graf 2009; Kuzmin et al. 2011	>table 1 - only keeping "accepted"	28041-26194	95.4	27117	Accept	1_int	GI-2.2
40	Kurtak-4	OB	Russia	Str 11/cult.lay 1	charcoal	hearth context	Conv 14C	LE-2833	N/A	23470	200	Malikov 2016	Drozdov et al. 1990;Svezhentsev et al. 1992; Kuzmin & Orlova 1998; Vasili'ev et al. 2002; Graf 2009; Kuzmin et al. 2011	>table 1 - only keeping "accepted"	26003-25333	95.4	25668	Accept	1_int	GI-2.2
40	Kurtak-4	OB	Russia	Str 11/cult.lay 1	charcoal	hearth context	Conv 14C	LE-3351	N/A	24170	230	Malikov 2016	Svezhentsev et al. 1992; Vasili'ev et al. 2002; Graf 2009; Kuzmin et al. 2011	>table 1 - only keeping "accepted"	26880-25858	95.4	26369	Accept	1_int	GI-2.2
40	Kurtak-4	OB	Russia	Str 11/cult.lay 1	charcoal	hearth context	Conv 14C	LE-3357	N/A	24890	670	Malikov 2016	Svezhentsev et al. 1992; Vasiliev 1992; Kuzmin & Orlova 1998; Vasili'ev et al. 2002; Graf 2009; Kuzmin et al. 2011	>table 1 - only keeping "accepted"	28765-25838	95.4	27301	Accept	1_int	GI-2.2
40	Kurtak-4	OB	Russia	Str 11	bone	N/A	Conv 14C	LE-4155	N/A	23800	900	Malikov 2016	Svezhentsev et al. 1992; Vasiliev 1992; Vasili'ev et al. 2002; Graf 2009; Kuzmin et al. 2011	N/A	28140-24435	95.4	26287	Accept	1_int	GI-2.2
40	Kurtak-4	OB	Russia	Str 17	charcoal	N/A	Conv 14C	LE-3352	N/A	31560	520	Vasili'ev et al. 2002	Svezhentsev et al. 1992	N/A	35096-32831	95.4	33963	Accept	1_int	GI-6
40	Kurtak-4	OB	Russia	Str 17	bone	N/A	Conv 14C	LE-3638	N/A	32280	280	Vasili'ev et al. 2002	Svezhentsev et al. 1992	N/A	35340-34148	95.4	34744	Accept	1_std	GS-7
41	Kuylug Khem-1	OB	Russia	cult.lay 4	bone	N/A	Conv 14C	LE-6899	N/A	23600	400	Graf 2009	N/A	>table 1 - only keeping "accepted"	26766-25261	95.4	26013	Accept	1	GI-2.2
42	Kyushiarataki 3	PSHK	Japan	Dense charcoal 9(1)	charcoal	N/A	AMS	IAAA-82699	N/A	17910	80	Buvit et al. 2016	HCBCP 2015	N/A	20074-19491	95.4	19782	Accept	2	GS-2.1
42	Kyushiarataki 3	PSHK	Japan	Dense charcoal 13	charcoal	N/A	AMS	IAAA-82700	N/A	17660	80	Buvit et al. 2016	HCBCP 2015	N/A	19795-19079	95.4	19437	Accept	2	GS-2.1
42	Kyushiarataki 3	PSHK	Japan	Lithic concentration 10 Unit I-63	charcoal	N/A	AMS	IAAA-82701	N/A	20330	100	Buvit et al. 2016	HCBCP 2015	N/A	22822-22192	95.4	22507	Accept	2	GS-2.1
42	Kyushiarataki 3	PSHK	Japan	Lithic concentration 13 Unit K-65	charcoal	hearth	AMS	IAAA-82702	N/A	20390	100	Buvit et al. 2016	HCBCP 2015	N/A	22915-22251	95.4	22583	Accept	2	GS-2.1
42	Kyushiarataki 3	PSHK	Japan	Dense charcoal 4	charcoal	N/A	AMS	IAAA-82708	N/A	17170	80	Buvit et al. 2016	HCBCP 2015	N/A	18953-18576	95.4	18764	Accept	2	GS-2.1
42	Kyushiarataki 3	PSHK	Japan	Dense charcoal 4	charcoal	N/A	AMS	IAAA-82709	N/A	17380	80	Buvit et al. 2016	HCBCP 2015	N/A	19361-18841	95.4	19101	Accept	2	GS-2.1
42	Kyushiarataki 3	PSHK	Japan	Dense Charcoal 6	charcoal	N/A	AMS	IAAA-82710	N/A	16860	70	Buvit et al. 2016	HCBCP 2015	N/A	18587-18247	95.4	18417	Accept	2	GS-2.1
42	Kyushiarataki 3	PSHK	Japan	Dense Charcoal 11(1) Lithic concentration 51 Unit R51	charcoal	N/A	AMS	IAAA-82716	N/A	18790	90	Buvit et al. 2016	HCBCP 2015	N/A	20997-20526	95.4	20761	Accept	2	GS-2.1
42	Kyushiarataki 3	PSHK	Japan	Lithic concentration 15 Unit H-63	charcoal	hearth	AMS	IAAA-82717	N/A	18830	90	Buvit et al. 2016	HCBCP 2015	N/A	21017-20552	95.4	20784	Accept	2	GS-2.1
42	Kyushiarataki 3	PSHK	Japan	Dense charcoal 5	charcoal	N/A	AMS	IAAA-91779	N/A	17620	80	Buvit et al. 2016	HCBCP 2015	N/A	19760-19025	95.4	19392	Accept	2	GS-2.1
42	Kyushiarataki 3	PSHK	Japan	Dense charcoal 5	charcoal	N/A	AMS	IAAA-91780	N/A	17800	80	Buvit et al. 2016	HCBCP 2015	N/A	19984-19421	95.4	19702	Accept	2	GS-2.1
42	Kyushiarataki 3	PSHK	Japan	Dense charcoal 9	charcoal	N/A	AMS	IAAA-91782	N/A	17600	70	Buvit et al. 2016	HCBCP 2015	N/A	19691-19004	95.4	19347	Accept	2	GS-2.1
42	Kyushiarataki 3	PSHK	Japan	Dense charcoal 13	charcoal	N/A	AMS	IAAA-91785	N/A	17710	80	Buvit et al. 2016	HCBCP 2015	N/A	19872-19153	95.4	19512	Accept	2	GS-2.1
42	Kyushiarataki 3	PSHK	Japan	Cb-17	charcoal	N/A	AMS	IAAA-81786	N/A	26780	140	Buvit et al. 2016	HCBCP 2015	N/A	29226-28866	95.4	29046	Accept	1_int	GI-4
42	Kyushiarataki 3	PSHK	Japan	Dense charcoal 14	charcoal	N/A	AMS	IAAA-82694	N/A	24990	130	Buvit et al. 2016	HCBCP 2015	N/A	27776-26934	95.4	27355	Accept	1_int	GI-2.2
42	Kyushiarataki 3	PSHK	Japan	Dense charcoal 12	charcoal	N/A	AMS	IAAA-82695	N/A	24910	110	Buvit et al. 2016	HCBCP 2015	N/A	27361-26846	95.4	27103	Accept	1_int	GI-2.2
42	Kyushiarataki 3	PSHK	Japan	Dense charcoal 11	charcoal	N/A	AMS	IAAA-91783	N/A	27560	130	Buvit et al. 2016	HCBCP 2015	N/A	29801-29261	95.4	29531	Accept	1_int	GI-4
42	Kyushiarataki 3	PSHK	Japan	Dense charcoal 11	charcoal	N/A	AMS	IAAA-91784	N/A	28440	140	Buvit et al. 2016	HCBCP 2015	N/A	31194-30077	95.4	30635	Accept	1_std	GS-5.1
42	Kyushiarataki 3	PSHK	Japan	Dense charcoal 17	charcoal	N/A	AMS	IAAA-91786	N/A	25060	120	Buvit et al. 2016	HCBCP 2015	N/A	27856-27114	95.4	27485	Accept	1_int	GI-2.2
42	Kyushiarataki 3	PSHK	Japan	Dense charcoal 12	charcoal	N/A	AMS	IAAA-91787	N/A	24770	110	Buvit et al. 2016	HCBCP 2015	N/A	27244-26827	95.4	27035	Accept	1_int	GI-2.2
44	Lagerny	WB	Russia	surface	bone	ivory	AMS	BETA-362949	N/A	22040	100	Kuzmin & Keates 2016	Pitulko et al. 2015	N/A	24523-24006	95.4	24264	Accept	1	GI-2.2
44	Lake E5	EB	US-Alaska	254cm depth	plant parts	N/A	Conv 14C	OS-118250	N/A	16550	1200	Vachula et al. 2019		Standard deviation considerably big	21744-15525	95.4	18634	Accept	2	GS-2.1
44	Lake E5	EB	US-Alaska	283.5cm depth	plant parts	N/A	Conv 14C	OS-115834	N/A	18550	1200	Vachula et al. 2019		Standard deviation considerably big	23791-17941	95.4	20866	Accept	2	GS-2.1

Supplementary Data 4 - Project Database '*DetailedData*'... continuation

siteID	site	area	country	level	mat_type	mat_spec	date_type	lab_code	spec_code	age	s_dev	ref	source	comments	Age_Cal	σ_error_%	Age_CalM	Status	TempGroup	grnlnd_stage
44	Lake E5	EB	US-Alaska	409cm depth	plant parts	N/A	Conv 14C	OS-118653	N/A	23600	980	Vachula et al. 2019		N/A	28091-24072	95.4	26081	Accept	1_int	GI-2.2
44	Lake E5	EB	US-Alaska	209.5cm depth	plant & insect parts	N/A	Conv 14C	OS-123767	N/A	29200	740	Vachula et al. 2020		N/A	33243-29852	95.4	31548	Accept	1_int	GI-5.1
44	Lake E5	EB	US-Alaska	213.5cm depth	plant parts	N/A	Conv 14C	OS-123773	N/A	30600	800	Vachula et al. 2022		N/A	35007-31588	95.4	33298	Accept	1_int	GI-5.2
44	Lake E5	EB	US-Alaska	364.5cm depth	plant & insect parts	N/A	Conv 14C	OS-123781	N/A	18250	1200	Vachula et al. 2023		Standard deviation considerably big	23582-17559	95.4	20571	Accept	2	GS-2.1
45	Listvenka	OB	Russia	cult.lay 19	charcoal	dispersed	Conv 14C	SOAN-3734	N/A	16640	350	Graf 2009	N/A	>table 1 - only keeping "accepted"	18986-17276	95.4	18131	Accept	2	GS-2.1
45	Listvenka	OB	Russia	cult.lay15	charcoal	hearth context	Conv 14C	SOAN-3314	N/A	17080	485	Graf 2009	N/A	>table 1 - only keeping "accepted"	20079-17594	95.4	18836	Accept	2	GS-2.1
45	Listvenka	OB	Russia	cult.lay 19	bone	mammoth	Conv 14C	SOAN-5084	N/A	17200	230	Graf 2009	N/A	>table 1 - only keeping "accepted"	19476-18264	95.4	18870	Accept	2	GS-2.1
45	Lake E5	EB	US-Alaska	213.5cm depth	wood	N/A	Conv 14C	OS-123774	N/A	31300	1000	Vachula et al. 2021		Standard deviation considerably big	36987-32180	95.4	34584	Accept	1_int	GI-6
45	Listvenka	OB	Russia	cult.lay 12	charcoal	N/A	Conv 14C	Beta-58391	N/A	19000	60	Vasili'ev et al. 2002	Akimova 1998	N/A	21111-20776	95.4	20944	Accept	2	GS-2.1
46	Maininskaia East	OB	Russia	cult.lay 5 (eastern pit)	bone	N/A	Conv 14C	LE-2135	N/A	16540	170	Graf 2009	N/A	>table 1 - only keeping "accepted"	18453-17611	95.4	18032	Accept	2	GS-2.1
47	Maininskaia West	OB	Russia	cult.lay A3	bone	N/A	AMS 14C	AA-38055	N/A	19300	350	Graf 2009	N/A	N/A	22073-20528	95.4	21300	Accept	2	GS-2.1
48	Malaya Syia	OB	Russia	2	charcoal	N/A	Conv 14C	SOAN-1124	N/A	20300	350	Vasili'ev et al. 2002	Derevianko et al. 1992	N/A	23576-21518	95.4	22547	Accept	2	GS-2.1
48	Malaya Syia	OB	Russia	2	bone	N/A	Conv 14C	LE-4918	N/A	25250	1200	Vasili'ev et al. 2002	Lisitsyn 2000	standard deviation considerably big	30833-25326	95.4	28080	Accept	1_int	GI-3
48	Malaya Syia	OB	Russia	2	bone	N/A	Conv 14C	AA-8876	N/A	29450	420	Vasili'ev et al. 2002	Kuzmin & Orlova 1998	N/A	32889-30913	95.4	31901	Accept	1_int	GI-5.1
49	Mal'ta	OB	Russia	8	bone	N/A	Conv 14C	OxA-6192	N/A	20340	320	Gomez Coutouly 2018b	Medvedev et al. 1996; Vasil'ev et al. 2002	N/A	23324-21838	95.4	22581	Accept	2	GS-2.1
49	Mal'ta	OB	Russia	8	bone	N/A	AMS 14C	OxA-6193	N/A	21340	340	Gomez Coutouly 2018b	Medvedev et al. 1996; Vasil'ev et al. 2002	N/A	24433-22970	95.4	23701	Accept	1_int	GI-2.2
49	Mal'ta	OB	Russia	8	bone	N/A	Conv 14C	GIN-7708	N/A	21600	200	Gomez Coutouly 2018b	Medvedev et al. 1996; Vasil'ev et al. 2002	N/A	24433-23428	95.4	23930	Accept	1_int	GI-2.2
49	Mal'ta	OB	Russia	8	bone	N/A	Conv 14C	GIN-8475	N/A	21600	170	Gomez Coutouly 2018b	Medvedev et al. 1996; Vasil'ev et al. 2002	N/A	24369-23687	95.4	24028	Accept	1_int	GI-2.2
49	Mal'ta	OB	Russia	8	bone	N/A	AMS 14C	OxA-6191	N/A	21700	160	Gomez Coutouly 2018b	Medvedev et al. 1996; Vasil'ev et al. 2002	N/A	24399-23793	95.4	24096	Accept	1_int	GI-2.2
49	Mal'ta	OB	Russia	8	human bone	N/A	Conv 14C	OxA-7129	N/A	19880	160	Kuzmin & Keates 2016	Richards et al. 2001	N/A	22336-21451	95.4	21894	Accept	2	GS-2.1
49	Mal'ta	OB	Russia	8	human bone	N/A	Conv 14C	UCIAMS-79666	N/A	20240	60	Kuzmin & Keates 2016	Raghavan et al. 2013	N/A	22621-22171	95.4	22396	Accept	2	GS-2.1
50	Marukoyama	PSHK	Japan	Dense charcoal 9	charcoal	N/A	AMS	MTC-17450	N/A	22200	100	Buvit et al. 2016	Izuho et al. 2016	N/A	24961-24112	95.4	24536	Accept	1_int	GI-2.2
50	Marukoyama	PSHK	Japan	Dense charcoal 8	charcoal	N/A	AMS	MTC-17451	N/A	21830	90	Buvit et al. 2016	Izuho et al. 2016	N/A	24387-23946	95.4	24166	Accept	1_int	GI-2.2
50	Marukoyama	PSHK	Japan	Dense charcoal 4	charcoal	N/A	AMS	MTC-17452	N/A	22090	90	Buvit et al. 2016	Izuho et al. 2016	N/A	24805-24024	95.4	24414	Accept	1_int	GI-2.2
50	Marukoyama	PSHK	Japan	BE5	charcoal	lithic concentration	AMS	MTC-17453	N/A	21920	90	Buvit et al. 2016	Izuho et al. 2016	N/A	24428-23991	95.4	24209	Accept	1_int	GI-2.2
50	Marukoyama	PSHK	Japan	Lithic concentration 11 Unit F-61	charcoal	hearth	AMS	MTC-17454	Lithic concentration 11	21830	90	Buvit et al. 2016	Izuho et al. 2016	N/A	24387-23946	95.4	24166	Accept	1_int	GI-2.2
50	Marukoyama	PSHK	Japan	Lithic concentration 3 Unit 16-19	charcoal	burned soil	AMS	MTC-17455	Lithic concentration 3	21830	90	Buvit et al. 2016	Izuho et al. 2016	N/A	24387-23946	95.4	24166	Accept	1_int	GI-2.2
50	Marukoyama	PSHK	Japan	Dense charcoal 12	charcoal	N/A	AMS	MTC-17456	N/A	21980	90	Buvit et al. 2016	Izuho et al. 2016	N/A	24459-24013	95.4	24236	Accept	1_int	GI-2.2
50	Marukoyama	PSHK	Japan	Dense charcoal 10	charcoal	N/A	AMS	MTC-17457	N/A	22010	90	Buvit et al. 2016	Izuho et al. 2016	N/A	24478-24020	95.4	24249	Accept	1_int	GI-2.2
50	Marukoyama	PSHK	Japan	Dense charcoal 11	charcoal	N/A	AMS	MTC-17458	N/A	22150	90	Buvit et al. 2016	Izuho et al. 2016	N/A	24903-24055	95.4	24479	Accept	1_int	GI-2.2
50	Marukoyama	PSHK	Japan	Dense charcoal 5	charcoal	N/A	AMS	MTC-17459	N/A	21940	90	Buvit et al. 2016	Izuho et al. 2016	N/A	24437-23999	95.4	24218	Accept	1_int	GI-2.2
50	Marukoyama	PSHK	Japan	Dense charcoal 13	charcoal	N/A	AMS	MTC-17460	N/A	22080	90	Buvit et al. 2016	Izuho et al. 2016	N/A	24786-24020	95.4	24403	Accept	1_int	GI-2.2
50	Marukoyama	PSHK	Japan	Dense charcoal 17	charcoal	N/A	AMS	MTC-17461	N/A	21780	90	Buvit et al. 2016	Izuho et al. 2016	N/A	24356-23916	95.4	24136	Accept	1_int	GI-2.2
50	Marukoyama	PSHK	Japan	Dense charcoal 15	charcoal	N/A	AMS	MTC-17462	N/A	22130	90	Buvit et al. 2016	Izuho et al. 2016	N/A	24876-24043	95.4	24459	Accept	1_int	GI-2.2
50	Marukoyama	PSHK	Japan	Dense charcoal 2	charcoal	N/A	AMS	MTC-17463	N/A	21860	90	Buvit et al. 2016	Izuho et al. 2016	N/A	24403-23962	95.4	24182	Accept	1_int	GI-2.2
50	Marukoyama	PSHK	Japan	Lithic concentration 4 Unit 17-15	charcoal	N/A	AMS	MTC-17464	N/A	21740	90	Buvit et al. 2016	Izuho et al 2016	N/A	24321-23891	95.4	24106	Accept	1_int	GI-2.2
50	Marukoyama	PSHK	Japan	Lithic concentration 9 Unit F-59	charcoal	hearth	AMS	NUTA-2801	N/A	20940	250	Buvit et al. 2016	Chitose Board of Education 1994	N/A	23868-22654	95.4	23261	Accept	1_int	GI-2.2
51	Masterov Kliych	OB	Russia	component IV	bone	N/A	AMS	AA-8888	N/A	24360	270	Buvit et al. 2016	Goebel 1993; Kuzmin & Orlova 1998	N/A	27174-25953	95.4	26563	Accept	1_int	GI-2.2
51	Masterov Kliych	OB	Russia	II	bone	N/A	AMS	AA-23641	N/A	29860	1000	Buvit et al. 2016	Goebel etal. 2000	Standard deviation considerably big	34605-29901	95.4	32253	Accept	1_std	GS-5.2
52	Minamimachi 2	PSHK	Japan	Upper Paleolithic	charcoal	N/A	AMS	Gak-18248	N/A	19610	270	Buvit et al. 2016	Obihiro board of Education 1995	N/A	22242-21052	95.4	21647	Accept	2	GS-2.1
53	Minamimachi 2	PSHK	Japan	Lithic concentration 4	charcoal	N/A	AMS	NUTA2-7680	N/A	21610	70	Buvit et al. 2016	Nakamura 2005	N/A	24056-23838	95.4	23947	Accept	1_int	GI-2.2
53	Moil'tyn-am	OB	Mongolia	4	bone	N/A	AMS	SOAN-8156	N/A	18830	290	Rybin et al. 2016	N/A	N/A	21756-20251	95.4	21003	Accept	2	GS-2.2
53	Moil'tyn-am	OB	Mongolia	4	charcoal	N/A	AMS	GifA-10857	N/A	20240	300	Rybin et al. 2016	Bertran et al. 2003	N/A	23211-21821	95.4	22516	Accept	2	GS-2.2
54	Nakamoto	PSHK	Japan	Lithic concentration 1	charcoal	dense charcoal	AMS	Beta-111881	N/A	19360	190	Buvit et al. 2016	Izuho & Akai 2005	N/A	21822-21033	95.4	21427	Accept	2	GS-2.1
55	Nepa-1	OB	Russia	4	bone	cervid vertebra	Conv 14C	AA-8885	N/A	26065	300	Kuzmin 2017	Graf 2013; Goebel 2004	N/A	29067-27962	95.4	28515	Accept	1_int	GI-3
56	Nitto	PSHK	Japan	Dense charcoal 2 Lithic concentration 1 Unit P-25S	charcoal	N/A	AMS	Beta-136455	N/A	16560	120	Buvit et al. 2016	HCBCP 1999	N/A	18368-17661	95.4	18014	Accept	2	GS-2.1
56	Nitto	PSHK	Japan	Lithic	charcoal	N/A	AMS	Beta-136453	N/A	16940	80	Buvit et al. 2016	HCBCP 1999	N/A	18778-18314	95.4	18546	Accept	2	GS-2.1
57	Nizhnii Idzhir-1	OB	Russia	cult. lay	charcoal	hearth context	Conv 14C	LE-1984	N/A	17200	70	Graf 2009	Abramova et al. 1991	>table 1 - only keeping "accepted"	18966-18605	95.4	18785	Accept	2	GS-2.1
58	Novoselovo-6	OB	Russia	cult.lay	bone	reindeer	Conv 14C	LE-4807	N/A	18090	940	Malikov 2016	Graf 2009; Kuzmin et al. 2011	N/A	22361-17673	95.4	20017	Accept	2	GS-2.1
59	Ochiai	PSHK	Japan	Dense charcoal 1 lithic concentration 6 Unit M42	charcoal	N/A	AMS	TKa-15509	N/A	18540	90	Buvit et al. 2016	Izuho et al. 2013	N/A	20822-20321	95.4	20571	Accept	2	GS-2.1
59	Ochiai	PSHK	Japan	Dense charcoal 2(2) lithic concentration 53 Unit R48	charcoal	N/A	AMS	Beta-111832	N/A	18590	140	Buvit et al. 2016	Obihiro Board of Education 1999	N/A	20966-20332	95.4	20649	Accept	2	GS-2.1
60	Ogonki 5	PSHK	Russia	3	charcoal	N/A	AMS	AA-23137	N/A	17860	120	Gomez Coutouly 2018b	Vasilevski 2008	N/A	20127-19400	95.4	19763	Accept	2	GS-2.1
60	Ogonki 5	PSHK	Russia	Sq. C-22 Strat 2B Pit 1	charcoal	N/A	AMS	AA-25434	N/A	18920	150	Gomez Coutouly 2018b	Vasilevski 2003, 2008	Gomez Coutouly 2018b placed this date in layer 2B or 3	21146-20502	95.4	20824	Accept	2	GS-2.1
60	Ogonki 5	PSHK	Russia	3	charcoal	N/A	AMS	Beta-23138	N/A	31130	440	Gomez Coutouly 2018b	Vasilevski 2003	Gomez Coutouly 2018b rejected this date because it was considered too old in comparison with the site's other dates	34376-32671	95.4	33523	Accept	1_std	GS-6
60	Ogonki 5	PSHK	Russia	2B or 3	wood	N/A	AMS	AA-20864	N/A	19320	145	Gomez Coutouly 2018b; Vasilevskii 2008	Kuzmin & Keates 2016 ; Vasilevski 2003; Kuzmin 2008	N/A	21793-21036	95.4	21414	Accept	2	GS-2.1
60	Ogonki 5	PSHK	Russia	2B or 3	wood	N/A	AMS	Beta-115986	N/A	19380	190	Gomez Coutouly 2018b; Vasilevskii 2008	Kuzmin & Keates 2016 ; Vasilevski 2003; Kuzmin 2008	N/A	21827-21042	95.4	21434	Accept	2	GS-2.1
60	Ogonki 5	PSHK	Russia	2B or 3	wood	N/A	AMS	Beta-115987	N/A	19440	140	Gomez Coutouly 2018b; Vasilevskii 2008	Kuzmin & Keates 2016 ; Vasilevski 2003; Kuzmin 2008	N/A	21823-21120	95.4	21471	Accept	2	GS-2.1
61	Okushirataki 1	PSHK	Japan	Lithic concentration 4 Unit '23	charcoal	dense charcoal 18	AMS	Beta-112878	N/A	18250	190	Buvit et al. 2016	HCBCP 2002	North margin of lithic concentration	20611-19531	95.4	20071	Accept	2	GS-2.1
61	Okushirataki 1	PSHK	Japan	Lithic concentration 2	charcoal	dense charcoal	AMS	Beta-126156	N/A	18360	140	Buvit et al. 2016	HCBCP 2002	N/A	20591-20045	95.4	20318	Accept	2	GS-2.1
61	Okushirataki 1	PSHK	Japan	Lithic concentration 21 Unit M17	charcoal	N/A	AMS	Beta-126157	N/A	18890	140	Buvit et al. 2016	HCBCP 2002	East margin of lithic concentration	21086-20512	95.4	20799	Accept	2	GS-2.1
62	Oribe 16	PSHK	Japan	Upper Paleolithic	charcoal	N/A	Conv 14C	KSU-761	N/A	23600	700	Buvit et al. 2016	Kamishihoro Board of Education 1985	N/A	27532-24463	95.4	25997	Accept	1_int	GI-2.2

Supplementary Data 4 - Project Database '*DetailedData*'... continuation

siteID	site	area	country	level	mat_type	mat_spec	date_type	lab_code	spec_code	age	s_dev	ref	source	comments	Age_Cal	σ_error_%	Age_CalM	Status	TempGroup	grnlnd_stage
63	Orkhon-7	OB	Mongolia	trench 3, layer 2	bone	N/A	Conv 14C	SOAN-2883	N/A	23595	155	Khatsenovich et al. 2021	Astashkin et al. 1993	N/A	26103-25417	95.4	25760	Accept	1_int	GI-2.2
63	Orkhon-7	OB	Mongolia	trench 3, layer 5	bone	N/A	Conv 14C	SOAN-2879	N/A	31490	310	Khatsenovich et al. 2021	Derevianko & Petrin 1995	N/A	34483-33305	95.4	33894	Accept	1_int	GI-6
64	Pirika 1	PSHK	Japan	Upper Paleolithic	charcoal	N/A	AMS	KSU-688	N/A	17500	200	Buvit et al. 2016	HCBCP 1985	N/A	19878-18674	95.4	19276	Accept	2	GS-2.1
64	Pirika 1	PSHK	Japan	Upper Paleolithic	charcoal	N/A	Conv 14C	N-4936	N/A	18200	230	Buvit et al. 2016	HCBCP 1985	N/A	20627-19457	95.4	20042	Accept	2	GS-2.1
64	Pirika 1	PSHK	Japan	Unit 24G-(4)	charcoal	dense charcoal	AMS	Beta-164956	N/A	18420	120	Buvit et al. 2016	Imakane Board of Education 2002	N/A	20622-20126	95.4	20374	Accept	2	GS-2.1
64	Pirika 1	PSHK	Japan	2	charcoal	N/A	AMS	KSU-687	N/A	19800	380	Gomez Coutouly 2018b	Naganuma 1985; Ono et al. 2002	N/A	22890-21038	95.4	21964	Accept	2	GS-2.1
64	Pirika 1	PSHK	Japan	1	charcoal	N/A	Conv 14C	N-4937	N/A	20100	335	Gomez Coutouly 2018b	Naganuma 1985; Ono et al. 2002	N/A	23189-21407	95.4	22298	Accept	2	GS-2.1
64	Pirika 1	PSHK	Japan	1	charcoal	N/A	Conv 14C	KSU-689	N/A	20900	260	Gomez Coutouly 2018b	Naganuma 1985; Ono et al. 2002	N/A	23872-22570	95.4	23221	Accept	1_int	GI-2.1
65	Podzvonkaya	OB	Russia	2/3	bone	N/A	Conv 14C	SOAN-3350	N/A	22675	265	Buvit et al. 2016	Orlova 1995; Kuzmin & Orlova 1998	N/A	25525-24412	95.4	24698	Accept	1_int	GI-2.2
65	Podzvonkaya	OB	Russia	1/2	bone	N/A	Conv 14C	SOAN-3404	N/A	26000	920	Buvit et al. 2016	Tashak 1996; Orlova 1998; Kuzmin & Orlova 1998	N/A	30841-26409	95.4	28625	Accept	1_std	GS-4
66	Priiskovoye	OB	Russia	2	charcoal	N/A	AMS	AA-67830	N/A	21080	190	Buvit et al. 2016	Buvit 2008	N/A	23876-23057	95.4	23466	Accept	1_int	GI-2.2
66	Priiskovoye	OB	Russia	2	bone	N/A	AMS	AA-8891	N/A	25825	290	Buvit et al. 2016	Goebel 1993; Kuzmin & Orlova 1998	N/A	28874-27373	95.4	28123	Accept	1_int	GI-3
66	Priiskovoye	OB	Russia	2	bone	N/A	AMS	UCIAMS-143228	N/A	27320	240	Buvit et al. 2016	N/A	N/A	29793-29120	95.4	29456	Accept	1_int	GI-5
66	Priiskovoye	OB	Russia	2	bone	N/A	AMS	UCIAMS-143230	N/A	27340	380	Buvit et al. 2016	N/A	N/A	30797-28863	95.4	29830	Accept	1_int	GI-5
66	Priiskovoye	OB	Russia	2	bone	N/A	AMS	UCIAMS-143227	N/A	27840	300	Buvit et al. 2016	N/A	N/A	30910-29257	95.4	30083	Accept	1_int	GI-5
66	Priiskovoye	OB	Russia	2	bone	N/A	AMS	AA-27383	N/A	29900	1000	Buvit et al. 2016	Buvit 2008	Standard deviation considerably big	34667-29934	95.4	32300	Accept	1_std	GS-5.2
67	Shimaki	PSHK	Japan	IV S2	obsidian artifact	N/A	OH	B1-2896	N/A	17200	800	Buvit et al. 2014	N/A	N/A	20953-17139	95.4	19046	Accept	2	GS-2.1
67	Shimaki	PSHK	Japan	IV S2	obsidian artifact	N/A	OH	B3-80	N/A	17500	900	Buvit et al. 2014	N/A	N/A	21761-17216	95.4	19489	Accept	2	GS-2.1
67	Shimaki	PSHK	Japan	IV S2	obsidian artifact	N/A	OH	A1-137	N/A	18200	500	Buvit et al. 2014	N/A	N/A	21267-18864	95.4	20066	Accept	2	GS-2.1
67	Shimaki	PSHK	Japan	IV S2	obsidian artifact	N/A	OH	B1-43	N/A	18200	700	Buvit et al. 2014	N/A	N/A	21836-18520	95.4	20178	Accept	2	GS-2.1
67	Shimaki	PSHK	Japan	IV S2	obsidian artifact	N/A	OH	BS.A1-26	N/A	19000	800	Buvit et al. 2014	N/A	N/A	23150-19178	95.4	21164	Accept	2	GS-2.1
67	Shimaki	PSHK	Japan	IV S2	obsidian artifact	N/A	FT	BS.A-51	N/A	21700	1800	Buvit et al. 2014	N/A	N/A	29130-20503	95.4	24817	Accept	1_int	GI-2.2
67	Shimaki	PSHK	Japan	IV S2	charcoal	N/A	Conv 14C	Tka-15543	N/A	25630	380	Buvit et al. 2014	N/A	N/A	28839-27211	95.4	28025	Accept	1_int	GI-3
67	Shimaki	PSHK	Japan	IV S2 (dense charcoal 16)	charcoal	N/A	Conv 14C	D-AMS-4466	N/A	21875	90	Buvit et al. 2016	Buvit et al. 2014	N/A	24408-23971	95.4	24189	Accept	1_int	GI-2.2
67	Shimaki	PSHK	Japan	Upper Paleolithic	charcoal	N/A	AMS	Gak-3262	N/A	25500	1200	Buvit et al. 2016	Kosaka & Nogawa 1972	N/A	30990-25661	95.4	28325	Accept	1_int	GI-3
68	Shishkino 8	OB	Russia	cult.lay	animal bone	N/A	Conv 14C	AA-8882	N/A	21190	175	Kuzmin & Keates 2016; Pitul'ko & Pavlova 2016	Goebel 1993; Kuzmin & Orlova 1998; Kuzmin et al. 2011	N/A	23918-23220	95.4	23569	Accept	1_int	GI-2.2
69	Shukubai-Kaso (Sankakuyama)	PSHK	Japan	Dense charcoal 30 Unit Y-14	charcoal	N/A	AMS	Gak-4346	N/A	21450	750	Buvit et al. 2014	Chitose Board of Education 1974	N/A	25386-22146	95.4	23766	Accept	1_int	GI-2.2
69	Shukubai-Kaso (Sankakuyama)	PSHK	Japan	III	charcoal	N/A	AMS	MTC-17812	SKS01	24830	180	Izuho et al. 2018	N/A	N/A	27601-26732	95.4	27167	Accept	1_int	GI-2.2
69	Shukubai-Kaso (Sankakuyama)	PSHK	Japan	III	charcoal	N/A	AMS	MTC-17813	SKS02	25080	190	Izuho et al. 2018	N/A	N/A	27965-27009	95.4	27487	Accept	1_int	GI-2.2
69	Shukubai-Kaso (Sankakuyama)	PSHK	Japan	V	charcoal	N/A	AMS	MTC-17814	SKS03	31420	290	Izuho et al. 2018	N/A	N/A	34381-33297	95.4	33839	Accept	1_int	GI-6
69	Shukubai-Kaso (Sankakuyama)	PSHK	Japan	V	charcoal	N/A	AMS	MTC-17815	SKS04	31500	270	Izuho et al. 2018	N/A	N/A	34390-33370	95.4	33880	Accept	1_int	GI-6
69	Shukubai-Kaso (Sankakuyama)	PSHK	Japan	III	charcoal	N/A	AMS	MTC-17816	SKS05	31710	290	Izuho et al. 2018	N/A	N/A	34709-33450	95.4	34080	Accept	1_int	GI-6
69	Shukubai-Kaso (Sankakuyama)	PSHK	Japan	V	charcoal	N/A	AMS	MTC-17817	SKS06	31530	290	Izuho et al. 2018	N/A	N/A	34462-33354	95.4	33908	Accept	1_int	GI-6
69	Shukubai-Kaso (Sankakuyama)	PSHK	Japan	III	charcoal	N/A	AMS	MTC-17818	SKS07	25300	200	Izuho et al. 2018	N/A	N/A	28037-27232	95.4	27635	Accept	1_std	GS-3
69	Shukubai-Kaso (Sankakuyama)	PSHK	Japan	III	charcoal	N/A	AMS	MTC-17819	SKS08	25430	190	Izuho et al. 2018	N/A	N/A	28089-27286	95.4	27688	Accept	1_std	GS-3
69	Shukubai-Kaso (Sankakuyama)	PSHK	Japan	III	charcoal	N/A	AMS	MTC-17820	SKS09	24780	180	Izuho et al. 2018	N/A	N/A	27516-26679	95.4	27098	Accept	1_int	GI-2.2
69	Shukubai-Kaso (Sankakuyama)	PSHK	Japan	III	charcoal	N/A	AMS	MTC-17821	SKS10	24700	190	Izuho et al. 2018	N/A	N/A	27313-26611	95.4	26962	Accept	1_int	GI-2.2
69	Shukubai-Kaso (Sankakuyama)	PSHK	Japan	III	charcoal	N/A	AMS	MTC-17822	SKS11	25040	210	Izuho et al. 2018	N/A	N/A	27945-26910	95.4	27428	Accept	1_int	GI-2.2
69	Shukubai-Kaso (Sankakuyama)	PSHK	Japan	III	charcoal	N/A	AMS	MTC-17823	SKS12	24440	190	Izuho et al. 2018	N/A	N/A	27186-26176	95.4	26681	Accept	1_int	GI-2.2
69	Shukubai-Kaso (Sankakuyama)	PSHK	Japan	III	charcoal	N/A	AMS	MTC-17824	SKS13	25280	200	Izuho et al. 2018	N/A	N/A	28031-27222	95.4	27627	Accept	1_int	GS-3
69	Shukubai-Kaso (Sankakuyama)	PSHK	Japan	III	charcoal	N/A	AMS	MTC-17825	SKS14	24600	190	Izuho et al. 2018	N/A	N/A	27260-26480	95.4	26870	Accept	1_std	GI-2.2
70	Sokhatino 4	OB	Russia	7	charcoal	N/A	Conv 14C	LE-3647	N/A	16810	390	Buvit et al. 2016	Kuzmin et al. 2011	N/A	19456-17431	95.4	18443	Accept	2	GS-2.1
70	Sokhatino 4	OB	Russia	8	charcoal	N/A	Conv 14C	LE-3653	N/A	16970	300	Buvit et al. 2016	Kuzmin et al. 2011	N/A	19412-17690	95.4	18551	Accept	2	GS-2.1
71	Studenoe 1	OB	Russia	cult.hor 19/1 unit V	charcoal	N/A	Conv 14C	GIN-6133	N/A	18550	35	Buvit et al. 2016; Tsydenova & Piezonka 2015	Konstantinov 2000; Buvit 2003	excluded from Buvit et al. 2003 analysis	20576-20402	95.4	20489	Accept	2	GS-2.1
72	Studenoe 2	OB	Russia	4/5	charcoal	N/A	AMS	AA-37962	N/A	16950	180	Buvit et al. 2016	Konstantinov 2001	N/A	18956-18089	95.4	18522	Accept	2	GS-2.1
72	Studenoe 2	OB	Russia	4/5	charcoal	N/A	AMS	AA-67845	N/A	18020	230	Gomez Coutouly 2017b; Buvit et al. 2016	Buvit 2008	N/A	20464-19265	95.4	19864	Accept	2	GS-2.1
72	Studenoe 2	OB	Russia	4/5	charcoal	N/A	AMS	AA-37963	N/A	17840	110	Gomez Coutouly 2018b	Konstantinov 2001; Buvit et al. 2016	N/A	20091-19402	95.4	19746	Accept	2	GS-2.1
72	Studenoe 2	OB	Russia	4/5	charcoal	N/A	AMS	AA-37964	N/A	17550	90	Gomez Coutouly 2018b	Konstantinov 2001; Buvit et al. 2016	N/A	19495-18960	95.4	19227	Accept	2	GS-2.1
72	Studenoe 2	OB	Russia	4/5	charcoal	N/A	AMS	AA-67842	N/A	18540	140	Gomez Coutouly 2018b	Buvit 2008; Buvit et al. 2016	N/A	20945-20266	95.4	20605	Accept	2	GS-2.1
72	Studenoe 2	OB	Russia	4/5	bone	N/A	AMS	Beta-241403	N/A	18680	80	Gomez Coutouly 2018b	Buvit et al. 2016	N/A	20941-20461	95.4	20701	Accept	2	GS-2.1
72	Studenoe 2	OB	Russia	4/5	bone	N/A	AMS	Beta-241404	N/A	18700	80	Gomez Coutouly 2018b	Buvit et al. 2016	N/A	20952-20474	95.4	20713	Accept	2	GS-2.1
72	Studenoe 2	OB	Russia	cult.hor 4/5 unit II	charcoal	N/A	AMS	AA-23653	N/A	17885	120	Gomez Coutouly 2018b; Buvit et al. 2016	Goebel etal. 2000; Buvit et al. 2003	hearth context	20132-19429	95.4	19780	Accept	2	GS-2.1
72	Studenoe 2	OB	Russia	cult.hor 4/5 unit II	charcoal	N/A	AMS	AA-23655	N/A	17228	115	Gomez Coutouly 2018b; Buvit et al. 2016	Goebel etal. 2000; Buvit et al. 2003	hearth context	19091-18546	95.4	18818	Accept	2	GS-2.1
72	Studenoe 2	OB	Russia	cult.hor 5 unit II	charcoal	N/A	AMS	AA-23657	N/A	17165	115	Gomez Coutouly 2018b; Buvit et al. 2016;	Goebel etal. 2000; Buvit et al. 2003	dwelling context	19004-18521	95.4	18762	Accept	2	GS-2.1
72	Studenoe 2	OB	Russia	4/5 unit II	bone	N/A	AMS	AA-26739	N/A	18830	300	Gomez Coutouly 2018b; Buvit et al. 2016; Tsydenova & Piezonka 2015	Goebel et al. 2000; Buvit et al. 2003	dwelling context	21763-20235	95.4	20999	Accept	2	GS-2.1
72	Studenoe 2	OB	Russia	Layer 8	charcoal	N/A	Conv 14C	CAMS-90971	N/A	20620	90	Kuzmin & Keates 2016	Buvit et al. 2004	N/A	23196-22610	95.4	22903	Accept	2	GS-2.1
72	Studenoe 2	OB	Russia	Layer 4/5	charcoal	N/A	AMS	AA-26653	N/A	17885	120	Tsydenova & Piezonka 2015	Goebel 2000	hearth 1	20132-19429	95.4	19780	Accept	2	GS-2.1
72	Studenoe 2	OB	Russia	Layer 4/5	charcoal	N/A	AMS	AA-26655	N/A	17225	115	Tsydenova & Piezonka 2015	Goebel 2000	hearth 2	19084-18546	95.4	18815	Accept	2	GS-2.1
72	Studenoe 2	OB	Russia	Layer 5	charcoal	N/A	AMS	AA-26657	N/A	17165	115	Tsydenova & Piezonka 2015	Goebel 2000	hearth 1	19004-18521	95.4	18762	Accept	2	GS-2.1
73	Tarachikha	OB	Russia	surface	bone	mammoth	Conv 14C	LE-3834	N/A	18930	320	Malikov 2016	Lisitsyn 2000; Vasili'ev et al. 2002; Graf 2009; Kuzmin et al. 2011	N/A	21792-20358	95.4	21075	Accept	2	GS-2.1
73	Tarachikha	OB	Russia	surface	bone	reindeer	Conv 14C	LE-3821	N/A	19850	180	Malikov 2016	Lisitsyn 2000; Vasili'ev et al. 2002; Graf 2009; Kuzmin et al. 2011	N/A	22355-21396	95.4	21875	Accept	2	GS-2.1
74	Tesa	OB	Russia	cult.lay	animal bone	N/A	Conv 14C	SOAN-4419	N/A	20040	765	Kuzmin & Keates 2016	Kuzmin 2008	N/A	23963-20597	95.4	22280	Accept	2	GS-2.1
75	Tolbaga	OB	Russia	4	bone	N/A	AMS	UCIAMSS-143218	N/A	21760	120	Buvit et al. 2016	N/A	N/A	24386-23885	95.4	24135	Accept	1_int	GI-2.2
75	Tolbaga	OB	Russia	4	bone	Bison	AMS	UCIAMS-143239	N/A	24070	150	Buvit et al. 2016	N/A	N/A	26687-25892	95.4	26289	Accept	1_int	GI-2.2
75	Tolbaga	OB	Russia	4	bone	Rangifer	AMS	Beta-344456	N/A	24410	120	Buvit et al. 2016	Buvit et al. 2015	N/A	27050-26344	95.4	26697	Accept	1_int	GI-2.2

Supplementary Data 4 - Project Database '*DetailedData* '... continuation

siteID	site	area	country	level	mat_type	mat_spec	date_type	lab_code	spec_code	age	s_dev	ref	source	comments	Age_Cal	σ_error_%	Age_CalM	Status	TempGroup	grnlnd_stage
75	Tolbaga	OB	Russia	4	bone	N/A	Conv 14C	SOAN-1523	N/A	27210	300	Buvit et al. 2016	Bazarov et al. 1982; Konstantinov 1994; Kuzmin & Orlova 1998	N/A	29861-28956	95.4	29408	Accept	1_int	GI-4
75	Tolbaga	OB	Russia	4	bone	N/A	AMS	AA-8874	N/A	25200	260	Buvit et al. 2016; Rybin 2014	Goebel 1993; Kuzmin & Orlova 1998	N/A	28077-27037	95.4	27557	Accept	1_std	GS-3
75	Tolbaga	OB	Russia	3	bone	N/A	AMS	AA-26740	N/A	29000	1000	Buvit et al. 2016; Rybin 2014	Goebel & Waters 2000	Standard deviation considerably big	33538-29262	95.4	31400	Accept	1_int	GI-5.1
75	Tolbaga	OB	Russia	4	bone	N/A	Conv 14C	SOAN-3078	N/A	26900	225	Orlova 1998; Kuzmin & Orlova 1998	N/A	N/A	29551-28509	95.4	29030	Accept	1_int	GI-4
77	Tolbor-16	OB	Mongolia	Pit 2-Unit 3	bone	N/A	AMS	AA-93135	N/A	29230	930	Zwyns et al. 2014			33726-29571	95.4	31649	Accept	1_int	GI-5.1
77	Tolbor-16	OB	Mongolia	Pit 4-Unit 2/3a	bone	N/A	AMS	MAMS-31815	R-EVA-1899	31920	130	Zwyns et al. 2019			34635-34041	95.4	34338	Accept	1_int	GI-6
77	Tolbor-16	OB	Mongolia	Pit 4-Unit 2/3a	bone	N/A	AMS	MAMS-24090	S-EVA-31446	32360	110	Zwyns et al. 2019			35026-34386	95.4	34706	Accept	1_int	GI-6
77	Tolbor-16	OB	Mongolia	Pit 1-Unit 3a	bone	N/A	AMS	MAMS-20980	S-EVA-28443	32910	160	Zwyns et al. 2019			36153-34865	95.4	35509	Accept	1_int	GI-7
77	Tolbor-16	OB	Mongolia	Pit 4-Unit 2/3a	bone	N/A	AMS	MAMS-24089	S-EVA-31445	32970	140	Zwyns et al. 2019			36164-34984	95.4	35574	Accept	1_int	GI-7
78	Tolbor-17	OB	Mongolia	Test pit 2, level 3	bone	N/A	AMS	AA-93135	N/A	29230	930	Rybin et al. 2016	Zwyns et al. 2014	N/A	33726-29571	95.4	31648	Accept	1_int	GI-5.1
79	Tolbor-15	OB	Mongolia	5	eggshell	ostrich (struthio)	AMS	AA-84137	N/A	28460	310	Gomez Coutouly 2018b	Derevianko et al. 2013; Gladyshev et al. 2010	N/A	31696-29843	95.4	30768	Accept	1_std	GS-5.1
79	Tolbor-4	OB	Mongolia	Arch.horiz. 4	eggshell (bead)	ostrich	AMS	AA-84135	N/A	26700	300	Rybin 2014	Derevianko et al. 2013	N/A	29326-28280	95.4	28803	Accept	1_std	GS-4
79	Tolbor-4	OB	Mongolia	Arch.horiz. 6-5	eggshell	ostrich	AMS	AA-93140	N/A	31210	410	Rybin 2014	Derevianko et al. 2013	N/A	34391-32751	95.4	33571	Accept	1_std	GS-6
79	Tolbor-15	OB	Mongolia	7	eggshell	ostrich (struthio)	AMS	AA-84138	N/A	29150	200	Rybin et al. 2016; Rybin 2014	Gladyshev et al. 2010	N/A	32266-31220	95.4	31743	Accept	1_int	GI-5.1
80	Tsagaan-agui	OB	Mongolia	3	charcoal	N/A	AMS	AA-26589	N/A	30942	478	Rybin et al. 2016	Derevianko et al. 2000	N/A	34297-32532	95.4	33414	Accept	1_std	GS-6
80	Tsagaan-agui	OB	Mongolia	3	bone	N/A	AMS	AA-23159	N/A	32960	670	Rybin et al. 2016	Derevianko et al. 2000	N/A	37491-34229	95.4	35860	Accept	1_int	GI-7
81	Tsatsyn-Ereg 2	OB	Mongolia	2	bone	N/A	AMS	BETA-?	N/A	17050	70	Rybin et al. 2016	Simonet et al. 2011	No lab code	18870-18492	95.4	18681	Accept	2	GS-2.1
81	Tsatsyn-Ereg 2	OB	Mongolia	2	bone	N/A	AMS	BETA-?	N/A	21130	90	Rybin et al. 2016	Simonet et al. 2011	No lab code	23755-23282	95.4	23519	Accept	1_int	GI-2.2
81	Tsatsyn-Ereg 2	OB	Mongolia	2	bone	N/A	AMS	BETA-?	N/A	23500	130	Rybin et al. 2016	Simonet et al. 2011	No lab code	25906-25425	95.4	25666	Accept	1_int	GI-2.2
81	Tsatsyn-Ereg 2	OB	Mongolia	2	bone	N/A	AMS	BETA-?	N/A	27750	120	Rybin et al. 2016	Simonet et al. 2011	No lab code	29978-29366	95.4	29672	Accept	1_int	GI-4
82	Ui-1	OB	Russia	cult.lay 2	bone	N/A	Conv 14C	LE-3358	N/A	16760	120	Graf 2009	Vasiliev 1992; Kuzmin & Orlova 1998	N/A	18570-17979	95.4	18274	Accept	2	GS-2.1
82	Ui-1	OB	Russia	cult.lay 2	bone	N/A	Conv 14C	LE-3359	N/A	17520	130	Graf 2009	Vasiliev 1992; Kuzmin & Orlova 1998	N/A	19758-18893	95.4	19325	Accept	2	GS-2.1
82	Ui-1	OB	Russia	cul.lay 2	bone	N/A	AMS 14C	AA-38054	N/A	17690	210	Graf 2009	N/A	N/A	20087-18944	95.4	19515	Accept	2	GS-2.1
82	Ui-1	OB	Russia	cult.lay 2	bone	N/A	Conv 14C	LE-4257	N/A	19280	200	Graf 2009	Vasiliev 1992; Kuzmin & Orlova 1998	>table 1 - only keeping "accepted"	21826-20967	95.4	21396	Accept	2	GS-2.1
82	Ui-1	OB	Russia	cult.lay 2	charcoal	dispersed	Conv 14C	LE-4189	N/A	22830	530	Graf 2009	Drozdov et al. 1990; Kuzmin & Orlova 1998	>table 1 - only keeping "accepted"	26153-24015	95.4	25084	Accept	1	GI-2.2
83	Ust'-Kova	OB	Russia	middle complex	wood charcoal	N/A	Conv 14C	SOAN-1900	N/A	19540	90	Kuzmin & Keates 2016	Drozdov et al. 1990; Kuzmin & Orlova 1998; Kuzmin 2008	N/A	21844-21303	95.4	21573	Accept	2	GS-2.1
83	Ust'-Kova	OB	Russia	middle complex	wood	N/A	Conv 14C	SOAN-7746	N/A	19790	190	Lbova et al. 2020	Medvedev et al. 2014	N/A	22306-21329	95.4	21871	Accept	2	GS-2.1
83	Ust'-Kova	OB	Russia	middle complex	wood	N/A	Conv 14C	NSKA-620	N/A	19676	648	Lbova et al. 2020	N/A	N/A	23559-20437	95.4	21998	Accept	2	GS-2.1
83	Ust'-Kova	OB	Russia	middle complex	wood	N/A	Conv 14C	NSKA-621	N/A	22448	774	Lbova et al. 2020	N/A	N/A	26531-23324	95.4	24927	Accept	1_int	GI-2.2
83	Ust'-Kova	OB	Russia	middle complex	wood charcoal	N/A	Conv 14C	KRIL-381	N/A	23920	310	Lbova et al. 2020	Laukhin et la. 1980; Vasilievsky et al. 1988; Drozdov et al. 1990; Kuzmin & Orlova 1998	N/A	26862-25546	95.4	26204	Accept	1_int	GI-2.2
83	Ust'-Kova	OB	Russia	middle complex	wood	N/A	Conv 14C	NSKA-619	N/A	23929	855	Lbova et al. 2020	Akimova et al. 2014	N/A	28138-24522	95.4	26330	Accept	1_int	GI-2.2
83	Ust'-Kova	OB	Russia	lower complex	wood	N/A	Conv 14C	SOAN-1875	N/A	28050	670	Lbova et al. 2020	Drozdov et al. 1990; Kuzmin & Orlova 1998	N/A	32039-29153	95.4	30596	Accept	1_int	GI-4
83	Ust'-Kova	OB	Russia	lower complex	wood	N/A	Conv 14C	GIN-1741	N/A	30100	310	Lbova et al. 2020	Drozdov et al. 1990; Kuzmin & Orlova 1998	N/A	33303-32139	95.4	32721	Accept	1_int	GI-5.2
83	Ust'-Kova	OB	Russia	lower complex	wood	N/A	Conv 14C	SOAN-7543	N/A	33150	150	Lbova et al. 2020	Drozdov et al. 1990; Kuzmin & Orlova 1998	N/A	36660-35139	95.4	35899	Accept	1_int	GI-7
85	Ust'-Menza 2	OB	Russia	20	charcoal	N/A	AMS	AA-67834	N/A	17770	130	Buvit et al. 2016	Buvit 2008	N/A	20041-19145	95.4	19593	Accept	2	GS-2.1
85	Ust'-Menza 2	OB	Russia	16	charcoal	N/A	AMS	AA-67836	N/A	16800	100	Buvit et al. 2016	Buvit 2008	N/A	18586-18077	95.4	18331	Accept	2	GS-2.1
85	Ust'-Menza 2	OB	Russia	21	charcoal	N/A	AMS	AA-67837	N/A	17080	120	Buvit et al. 2016	Buvit 2008	N/A	18956-18427	95.4	18691	Accept	2	GS-2.1
85	Ust'-Menza 2	OB	Russia	20	charcoal	N/A	AMS	AA-67838	N/A	17900	100	Buvit et al. 2016	Buvit 2008	N/A	20095-19467	95.4	19781	Accept	2	GS-2.1
85	Ust'-Menza 2	OB	Russia	24	charcoal	N/A	Conv 14C	GIN-5463	N/A	16560	300	Buvit et al. 2016	Konstantinov 1994; Kuzmin & Orlova 1998	N/A	18841-17354	95.4	18097	Accept	2	GS-2.1
85	Ust'-Menza 2	OB	Russia	21	charcoal	N/A	Conv 14C	GIN-5464	N/A	17600	250	Buvit et al. 2016	Konstantinov 1994; Kuzmin & Orlova 1998	N/A	20108-18739	95.4	19423	Accept	2	GS-2.1
85	Ust'-Menza 2	OB	Russia	21	charcoal	N/A	Conv 14C	GIN-5464a	N/A	17190	120	Buvit et al. 2016	Konstantinov 1994; Kuzmin & Orlova 1998	N/A	19046-18521	95.4	18783	Accept	2	GS-2.1
85	Ust'-Menza 2	OB	Russia	20	charcoal	N/A	Conv 14C	GIN-5465	N/A	16980	150	Buvit et al. 2016	Konstantinov 1994; Kuzmin & Orlova 1998	N/A	18932-18218	95.4	18575	Accept	2	GS-2.1
85	Ust'-Menza 2	OB	Russia	17	charcoal	N/A	Conv 14C	GIN-6117	N/A	16900	500	Buvit et al. 2016	Konstantinov 1994; Kuzmin & Orlova 1998	N/A	19941-17321	95.4	18631	Accept	2	GS-2.1
85	Ust'-Menza 2	OB	Russia	UpperPaleolithic	bone	N/A	AMS	UCIAMS-143232	N/A	18310	80	Buvit et al. 2016	N/A	N/A	20466-20136	95.4	20301	Accept	2	GS-2.1
86	Ust'-Mil' II	WB	Russia	C	wood	N/A	Conv 14C	LE-1000	N/A	33000	500	Kuzmin & Orlova 1998	Mochanov 1977	N/A	3726-34481	95.4	35853	Accept	1_int	GI-7
86	Ust'-Mil' II	WB	Russia	B (~1.9-1.95)	wood	N/A	Conv 14C	LE-999	N/A	23500	500	Pitul'ko & Pavlova 2016	Mochanov 1977 ; Kuzmin & Orlova 1998	N/A	27015-24601	95.4	25808	Accept	1_int	GI-2.2
86	Ust'-Mil' II	WB	Russia	C (~2.5m)	wood	N/A	Conv 14C	LE-1001	N/A	30000	500	Pitul'ko & Pavlova 2016	Mochanov 1977 ; Kuzmin & Orlova 1999	N/A	33551-31456	95.4	32503	Accept	1_int	GI-5.2
87	Ust'-Ulma 1	PSHK	Russia	2b	wood	N/A	Conv 14C	SOAN-2619	N/A	19360	65	Kuzmin & Keates 2016	Orlova 1995; Kuzmin & Orlova 1998; Kuzmin 2008	N/A	21782-21101	95.4	21441	Accept	2	GS-2.1
88	Varvarina Gora	OB	Russia	1	bone	N/A	Conv 14C	SOAN-3053	N/A	17035	400	Buvit et al. 2016	Kuzmin 1994; Kuzmin & Orlova 1998	N/A	19807-17645	95.4	18726	Accept	2	GS-2.1
88	Varvarina Gora	OB	Russia	2	bone	N/A	Conv 14C	SOAN-3054	N/A	29900	1790	Buvit et al. 2016; Rybin 2014	Orlova 1998; Kuzmin & Orlova 1998; Lbova 2000	Standard deviation considerably big	37855-29146	95.4	33500	Accept	1_std	GS-6
88	Varvarina Gora	OB	Russia	2	bone	N/A	Conv 14C	SOAN-850	N/A	30600	500	Kuzmin & Orlova 1998	Orlova 1995	N/A	34134-32307	95.4	33220	Accept	1_int	GI-5.2
89	Verkhne-Troitskaya	WB	Russia	6	wood	N/A	Conv 14C	LE-906	N/A	17680	250	Gomez Coutouly 2018b	Mochanov & Fedosseva 1996; Pitul'ko & Pavlova 2015	N/A	20185-18867	95.4	19526	Accept	2	GS-2.1
89	Verkhne-Troitskaya	WB	Russia	6	wood	N/A	Conv 14C	LE-905	N/A	18300	180	Gomez Coutouly 2018b	Mochanov & Fedosseva 1996; Kuzmin & Orlova 1998; Pitul'ko & Pavlova 2016	N/A	20686-19830	95.4	20258	Accept	2	GS-2.1
90	Wakabanomori	PSHK	Japan	Lithic concentration 1	charcoal	N/A	AMS	Beta-162683	N/A	23930	220	Buvit et al. 2016	Obihiro Board of Education 2004	N/A	26694-25784	95.4	26239	Accept	1_int	GI-2.2
90	Wakabanomori	PSHK	Japan	North of lithic concentration 1	charcoal	burned soil	AMS	Beta-162682	N/A	24410	240	Buvit et al. 2016	Obihiro Board of Education 2004	N/A	27191-26030	95.4	26610	Accept	1_int	GI-2.2
90	Wakabanomori	PSHK	Japan	North of lithic concentration 4	charcoal	burned soil	AMS	Beta-174962	N/A	24410	220	Buvit et al. 2016	Obihiro Board of Education 2004	N/A	27179-26066	95.4	26622	Accept	1_int	GI-2.2
90	Wakabanomori	PSHK	Japan	Dense charcoal 14	charcoal	N/A	AMS	Beta-174961	N/A	24670	230	Buvit et al. 2016	Obihiro Board of Education 2004	N/A	27543-26358	95.4	26950	Accept	1_int	GI-2.2
90	Wakabanomori	PSHK	Japan	Unit P-4	charcoal	burned soil	AMS	Beta-174960	N/A	27640	230	Buvit et al. 2016	Obihiro Board of Education 2004	N/A	30075-29209	95.4	29642	Accept	1_int	GI-4
91	Wr-12 exposure	WB	Russia	surface	bone	mammoth scapula (human mod.)	Conv 14C	GIN-8257	P-44, SR-2, SR-43, ARP-3	22400	200	Pitulko et al. 2020; Pitulko et al. 2017; Kuzmin & Orlova 2004	Sulerzhitsky & Romanenkov 1999	N/A	25270-24186	95.4	24728	Accept	1_int	GI-2.2
92	Yana RHS	WB	Russia	floodplain	collagen	rhinoceros horn foreshaft	Conv 14C	Beta-162233	N/A	27440	210	Pitul'ko & Pavlova 2016	Pitulko et al. 2004	Northern Point	29817-29176	95.4	29496	Accept	1_int	GI-4
92	Yana RHS	WB	Russia	floodplain	collagen	ivory foreshaft	Conv 14C	Beta-173064	Y02FS	28250	170	Pitul'ko & Pavlova 2016	Pitulko et al. 2004	Northern Point	31061-29851	95.4	30456	Accept	1_int	GI-4
92	Yana RHS	WB	Russia	cult.lay	collagen	N/A	Conv 14C	Beta-191321	1259	27140	180	Pitul'ko & Pavlova 2016	Pitulko et al. 2004	Northern Point	29632-29076	95.4	29354	Accept	1_int	GI-4
92	Yana RHS	WB	Russia	12.761m	collagen	N/A	Conv 14C	Beta-191322	1241	28570	300	Pitul'ko & Pavlova 2016	Pitulko et al. 2004	Northern Point	31798-29941	95.4	30869	Accept	1_int	GI-5.1
92	Yana RHS	WB	Russia	19.027m	collagen	N/A	Conv 14C	Beta-191323	ARA 799	27910	280	Pitul'ko & Pavlova 2016	Pitulko et al. 2004	Yana B	30944-29311	95.4	30127	Accept	1_int	GI-4
92	Yana RHS	WB	Russia	12.489m	collagen	N/A	Conv 14C	Beta-191326	K1093	28500	200	Pitul'ko & Pavlova 2016	Pitulko et al. 2004	Northern Point	31416-29991	95.4	30703	Accept	1_std	GS-5.1
92	Yana RHS	WB	Russia	12.995m	collagen	N/A	Conv 14C	Beta-191327	1150	28090	200	Pitul'ko & Pavlova 2016	Pitulko et al. 2004	Northern Point	30992-29677	95.4	30334	Accept	1_int	GI-4
92	Yana RHS	WB	Russia	13.0m	plant macroremains	N/A	Conv 14C	Beta-191328	907	27820	190	Pitul'ko & Pavlova 2016	Pitulko et al. 2004	Northern Point	30763-29277	95.4	30020	Accept	1_int	GI-4
92	Yana RHS	WB	Russia	12.64m	plant macroremains	N/A	Conv 14C	Beta-191329	977	28000	190	Pitul'ko & Pavlova 2016	Pitulko et al. 2004	Northern Point	30915-29585	95.4	30250	Accept	1_int	GI-4
92	Yana RHS	WB	Russia	below cult.lay	plant macroremains	N/A	Conv 14C	Beta-191331	1412	26450	160	Pitul'ko & Pavlova 2016	Pitulko et al. 2004	Northern Point	29103-28374	95.4	28738	Accept	1_std	GS-4
92	Yana RHS	WB	Russia	12.887m	plant macroremains	N/A	Conv 14C	Beta-191332	1411	27510	180	Pitul'ko & Pavlova 2016	Pitulko et al. 2004	Northern Point	29822-29214	95.4	29518	Accept	1_int	GI-4
92	Yana RHS	WB	Russia	12.243m	hearth	N/A	Conv 14C	Beta-191333	1386-1	27900	200	Pitul'ko & Pavlova 2016	Pitulko et al. 2004	Northern Point	30883-29334	95.4	30108	Accept	1_int	GI-4
92	Yana RHS	WB	Russia	cult.lay	collagen	burned bone	Conv 14C	Beta-191334	1386-2	26680	160	Pitul'ko & Pavlova 2016	Pitulko et al. 2004	Northern Point	29209-28486	95.4	28847	Accept	1_std	GS-4
92	Yana RHS	WB	Russia	12.238m	plant macroremains	N/A	Conv 14C	Beta-191335	1385	27890	190	Pitul'ko & Pavlova 2016	Pitulko et al. 2004	Northern Point	30862-29334	95.4	30098	Accept	1_int	GI-4
92	Yana RHS	WB	Russia	13.0m	humic acids	silt	Conv 14C	Beta-191594	907	28520	200	Pitul'ko & Pavlova 2016	Pitulko et al. 2004	N/A	31466-30011	95.4	30738	Accept	1_std	GS-5.1

Supplementary Data 4 - Project Database '*DetailedData*'... continuation

siteID	site	area	country	level	mat_type	mat_spec	date_type	lab_code	spec_code	age	s_dev	ref	source	comments	Age_Cal	σ_error_%	Age_CalM	Status	TempGroup	grnlnd_stage
92	Yana RHS	WB	Russia	12.64m	humic acids	silt	Conv 14C	Beta-191595	977	31050	300	Pitul'ko & Pavlova 2016	Pitulko et al. 2004	N/A	34147-32798	95.4	33472	Accept	1_std	GS-6
92	Yana RHS	WB	Russia	13.118m	humic acids	silt	Conv 14C	Beta-191597	1412	29540	220	Pitul'ko & Pavlova 2016	Pitulko et al. 2004	N/A	32566-31657	95.4	32111	Accept	1_std	GS-5.2
92	Yana RHS	WB	Russia	12.887m	humic acids	silt	Conv 14C	Beta-191598	1411	29810	230	Pitul'ko & Pavlova 2016	Pitulko et al. 2004	N/A	32742-31923	95.4	32332	Accept	1_std	GS-5.2
92	Yana RHS	WB	Russia	12.243m	humic acids	silt	Conv 14C	Beta-191599	1386-1	31300	280	Pitul'ko & Pavlova 2016	Pitulko et al. 2004	N/A	34326-33206	95.4	33766	Accept	1_int	GI-6
92	Yana RHS	WB	Russia	12.238m	humic acids	silt	Conv 14C	Beta-191600	1385	29660	230	Pitul'ko & Pavlova 2016	Pitulko et al. 2004	N/A	32636-31782	95.4	32209	Accept	1_std	GS-5.2
92	Yana RHS	WB	Russia	13.38m	collagen	N/A	Conv 14C	Beta-204863	LY04-NP/W-ES/F16/15b	27620	240	Pitul'ko & Pavlova 2016	Pitulko et al. 2004	Northern Point	30081-29197	95.4	29639	Accept	1_int	GI-4
92	Yana RHS	WB	Russia	13.29-13.31m	soot	N/A	AMS	Beta-204864	LY04-NP/W-ES/F16/10	29130	410	Pitul'ko & Pavlova 2016	Pitulko et al. 2004	Northern Point	32476-30303	95.4	31389	Accept	1_int	GI-5.1
92	Yana RHS	WB	Russia	cult.lay	collagen	N/A	Conv 14C	Beta-204881	33BJ2/1	28350	250	Pitul'ko & Pavlova 2016	Pitulko et al. 2004	Yana B	31321-29806	95.4	30563	Accept	1_int	GI-4
92	Yana RHS	WB	Russia	cult.lay	charcoal	N/A	Conv 14C	Beta-223413	LY06-L23/2FP/8	27250	230	Pitul'ko & Pavlova 2016	Pitulko et al. 2004	Northern Point	29748-29098	95.4	29423	Accept	1_int	GI-4
92	Yana RHS	WB	Russia	15.57m	collagen	N/A	Conv 14C	Beta-250633	38670-YB	28250	200	Pitul'ko & Pavlova 2016	Pitulko et al. 2004	Yana B	31111-29816	95.4	30463	Accept	1_int	GI-4
92	Yana RHS	WB	Russia	14.51m	collagen	N/A	Conv 14C	Beta-250634	40275-YB	27670	210	Pitul'ko & Pavlova 2016	Pitulko et al. 2004	Yana B	30059-29233	95.4	29646	Accept	1_int	GI-4
92	Yana RHS	WB	Russia	13.52m	collagen	N/A	Conv 14C	Beta-250635	40345-YB	28210	200	Pitul'ko & Pavlova 2016	Pitulko et al. 2004	Yana B	31077-29783	95.4	30430	Accept	1_int	GI-4
92	Yana RHS	WB	Russia	cult.lay	collagen	mammoth mandible	Conv 14C	GIN-11466	2001/3	27400	600	Pitul'ko & Pavlova 2016	Pitulko et al. 2004	YMAM & SP	31256-28416	95.4	29836	Accept	1_int	GI-4
92	Yana RHS	WB	Russia	cult.lay	charcoal	N/A	Conv 14C	LE-7668	YA06/3W17/FP	27200	2400	Pitul'ko & Pavlova 2016	Pitulko et al. 2004	Northern Point; Standard deviation considerably big	38808-25411	95.4	32109	Accept	1_std	GS-5.2
92	Yana RHS	WB	Russia	7.5m a.w.l.	bone	horse mandible	AMS	Beta-173067	N/A	27300	270	Pitul'ko & Pavlova 2016; Pitulko et al 2014	Pitulko et al 2004	TUMS 1	29844-29084	95.4	29464	Accept	1_int	GI-4
92	Yana RHS	WB	Russia	below cult.lay	plant macroremains	N/A	Conv 14C	Beta-191330	978	29610	230	Pitul'ko & Pavlova 2016; Pitulko et al. 2014	Pitulko et al. 2004; Pitulko et al. 2007	Northern Point	32611-31730	95.4	32170	Accept	1_std	GS-5.2
92	Yana RHS	WB	Russia	cult.lay	collagen	mammoth tusk fragment (burnt)	Conv 14C	GIN-11464	N/A	27800	500	Pitul'ko & Pavlova 2016; Pitulko et al. 2014	Pitulko et al. 2004; Pitulko & Pavlova 2010	YMAM & SP	31378-29117	95.4	30248	Accept	1_int	GI-4
92	Yana RHS	WB	Russia	cult.lay	collagen	burnt piece of mammoth ivory	Conv 14C	GIN-11465	2001/3	25800	600	Pitul'ko & Pavlova 2016; Pitulko et al. 2014	Pitulko et al. 2004	YMAM & SP	29197-27017	95.4	28107	Accept	1_int	GI-3
92	Yana RHS	WB	Russia	6.75m a.w.l.	plant material	filiform rootlets	Conv 14C	LE-6443	N/A	26500	600	Pitulko et al 2004	N/A	TUMS 1	29889-27401	95.4	28645	Accept	1_std	GS-4
92	Yana RHS	WB	Russia	8.3m a.w.l.	plant remains	twigs	Conv 14C	LE-6445	N/A	18100	340	Pitulko et al 2014	Pitulko et al 2004	TUMS 1	20806-19054	95.4	19930	Accept	2	GS-2.1
92	Yana RHS	WB	Russia	7.5m a.w.l.	plant remains	N/A	Conv 14C	LE-6444	N/A	25900	750	Pitulko et al 2014	Pitulko et al 2004	TUMS 1	29651-26785	95.4	28218	Accept	1_int	GI-3
92	Yana RHS	WB	Russia	9.6m a.w.l.	plant remains	filiform rootlets	Conv 14C	LE-6446	N/A	22400	300	Pitulko et al 2014	Pitulko et al 2004	TUMS 1	25298-24082	95.4	24690	Accept	1_int	GI-2.2
92	Yana RHS	WB	Russia	cult.lay	collagen	woolly rhinoceros humerus	Conv 14C	LU-5968	N/A	17710	140	Pitulko et al. 2014	Basilyan et al. 2011	YMAM	19981-19047	95.4	19514	Accept	2	GS-2.1
92	Yana RHS	WB	Russia	below cult.lay	plant remains	N/A	Conv 14C	Beta-243116	N/A	17970	100	Pitulko et al. 2014	Pitulko & Pavlova 2010	Northern Point	20169-19498	95.4	19834	Accept	2	GS-2.1
92	Yana RHS	WB	Russia	cult.lay	collagen	mammoth scapula	Conv 14C	LE-8492	N/A	18550	180	Pitulko et al. 2014	Basilyan et al. 2011	YMAM	20980-20211	95.4	20596	Accept	2	GS-2.1
92	Yana RHS	WB	Russia	cult.lay	plant remains	N/A	Conv 14C	Beta-250677	N/A	18750	100	Pitulko et al. 2014	Basilyan et al. 2011	YMAM	20984-20493	95.4	20739	Accept	2	GS-2.1
92	Yana RHS	WB	Russia	below cult.lay	plant remains	N/A	Conv 14C	Beta-243117	N/A	19770	100	Pitulko et al. 2014	Pitulko & Pavlova 2010	Northern Point	22137-21447	95.4	21792	Accept	2	GS-2.1
92	Yana RHS	WB	Russia	cult.lay	plant remains	N/A	Conv 14C	Beta-250676	N/A	20150	120	Pitulko et al. 2014	Basilyan et al. 2011	YMAM	22600-21916	95.4	22258	Accept	2	GS-2.1
92	Yana RHS	WB	Russia	below cult.lay	plant remains	N/A	Conv 14C	Beta-204858	N/A	22290	150	Pitulko et al. 2014	Pitulko & Pavlova 2010	Northern Point	25102-24156	95.4	24629	Accept	1_int	GI-2.2
92	Yana RHS	WB	Russia	cult.lay	collagen	reindeer mandible	Conv 14C	Beta-250636	N/A	28030	160	Pitulko et al. 2014	Basilyan et al. 2011	between SP and Yana B	30908-29638	95.4	30273	Accept	1_int	GI-4
92	Yana RHS	WB	Russia	cult.lay	collagen	Pleistocene bison metacarpal	Conv 14C	Beta-250637	N/A	28060	210	Pitulko et al. 2014	Basilyan et al. 2011	Yana B	30995-29630	95.4	30313	Accept	1_int	GI-4
92	Yana RHS	WB	Russia	cult.lay	collagen	mammoth rib	Conv 14C	Beta-250638	N/A	27970	210	Pitulko et al. 2014	Basilyan et al. 2011	between SP and Yana B	30922-29485	95.4	30204	Accept	1_int	GI-4
92	Yana RHS	WB	Russia	cult.lay	collagen	caribou antler	Conv 14C	Beta-250639	N/A	23450	160	Pitulko et al. 2014	Basilyan et al. 2011	YMAM	25895-25378	95.4	25637	Accept	1_int	GI-2.2
92	Yana RHS	WB	Russia	cult.lay	collagen	Pleistocene bison vertebra	Conv 14C	Beta-250640	N/A	23330	150	Pitulko et al. 2014	Basilyan et al. 2011	YMAM	25823-25352	95.4	25588	Accept	1_int	GI-2.2
92	Yana RHS	WB	Russia	cult.lay	plant remains	grass	Conv 14C	Beta-250661	N/A	21220	100	Pitulko et al. 2014	Basilyan et al. 2011	YMAM	23845-23320	95.4	23583	Accept	1_int	GI-2.2
92	Yana RHS	WB	Russia	cult.lay	plant remains	grass	Conv 14C	Beta-250662	N/A	23230	110	Pitulko et al. 2014	Basilyan et al. 2011	YMAM	25759-25335	95.4	25547	Accept	1_int	GI-2.2
92	Yana RHS	WB	Russia	cult.lay	plant remains	grass	Conv 14C	Beta-250663	N/A	22400	110	Pitulko et al. 2014	Basilyan et al. 2011	YMAM	25092-24445	95.4	24769	Accept	1_int	GI-2.2
92	Yana RHS	WB	Russia	cult.lay	plant remains	grass	Conv 14C	Beta-250664	N/A	21570	100	Pitulko et al. 2014	Basilyan et al. 2011	YMAM	24055-23775	95.4	23915	Accept	1_int	GI-2.2
92	Yana RHS	WB	Russia	cult.lay	collagen	woolly rhinoceros horn	Conv 14C	Beta-250672	N/A	26650	200	Pitulko et al. 2014	N/A	YMAM & SP	29199-28450	95.4	28825	Accept	1_std	GS-4
92	Yana RHS	WB	Russia	cult.lay	collagen	brown bear	Conv 14C	Beta-258535	N/A	28470	210	Pitulko et al. 2014	Basilyan et al. 2011	YMAM & SP	31390-29950	95.4	30670	Accept	1_std	GS-5.1
92	Yana RHS	WB	Russia	cult.lay	bone	horse (w/ flake embedded)	Conv 14C	GIN-11467	N/A	27600	500	Pitulko et al. 2014	Pitulko et al 2004	N/A	31223-28994	95.4	30108	Accept	1_int	GI-4
92	Yana RHS	WB	Russia	cult.lay	collagen	mammoth	Conv 14C	LE-8471	N/A	27500	350	Pitulko et al. 2014	Basilyan et al. 2011	between SP and Yana B	30841-29068	95.4	29955	Accept	1_int	GI-4
92	Yana RHS	WB	Russia	below cult.lay	organic material	peat	Conv 14C	LE-8498	N/A	31500	500	Pitulko et al. 2014	Basilyan et al. 2011	YMAM	34986-32841	95.4	33914	Accept	1_int	GI-6
92	Yana RHS	WB	Russia	cult.lay	plant remains	grass	Conv 14C	LE-8502	N/A	21010	500	Pitulko et al. 2014	Basilyan et al. 2011	YMAM	24411-22156	95.4	23284	Accept	1_std	GS-2.2
92	Yana RHS	WB	Russia	cult.lay	plant remains	grass	Conv 14C	LE-8508	N/A	27740	200	Pitulko et al. 2014	Basilyan et al. 2011	YMAM & SP	30146-29259	95.4	29703	Accept	1_int	GI-4
92	Yana RHS	WB	Russia	cult.lay	plant remains	grass	Conv 14C	LE-8509	N/A	21580	400	Pitulko et al. 2014	Basilyan et al. 2011	YMAM	24970-23145	95.4	24058	Accept	1_int	GI-2.2
92	Yana RHS	WB	Russia	cult.lay	plant remains	grass	Conv 14C	LE-8510	N/A	21640	250	Pitulko et al. 2014	Basilyan et al. 2011	YMAM	24480-23397	95.4	23939	Accept	1_int	GI-2.2
92	Yana RHS	WB	Russia	cult.lay	collagen	mammoth mandible	Conv 14C	LE-8565	N/A	28400	430	Pitulko et al. 2014	Basilyan et al. 2011	YMAM & SP	31931-29635	95.4	30783	Accept	1_std	GS-5.1
92	Yana RHS	WB	Russia	cult.lay	collagen	mammoth mandible	Conv 14C	LE-8568	N/A	28200	400	Pitulko et al. 2014	Basilyan et al. 2011	YMAM & SP	31605-29401	95.4	30503	Accept	1_int	GI-4
92	Yana RHS	WB	Russia	cult.lay	collagen	mammoth mandible	Conv 14C	LE-8569	N/A	31200	1200	Pitulko et al. 2014	Basilyan et al. 2011	YMAM & SP ; Standard deviation considerably big	37446-31603	95.4	34525	Accept	1_int	GI-6
92	Yana RHS	WB	Russia	cult.lay	collagen	mammoth mandible	Conv 14C	LE-8572	N/A	27200	1200	Pitulko et al. 2014	Basilyan et al. 2011	YMAM & SP ; Standard deviation considerably big	32516-27283	95.4	29900	Accept	1_int	GI-4
92	Yana RHS	WB	Russia	cult.lay	collagen	mammoth mandible	Conv 14C	LE-8573	N/A	28900	900	Pitulko et al. 2014	Basilyan et al. 2011	YMAM & SP	33226-29351	95.4	31289	Accept	1_int	GI-5.1
92	Yana RHS	WB	Russia	cult.lay	collagen	mammoth mandible	Conv 14C	LE-8574	N/A	28600	800	Pitulko et al. 2014	Basilyan et al. 2011	YMAM & SP	32600-29265	95.4	30933	Accept	1_int	GI-5.1
92	Yana RHS	WB	Russia	cult.lay	collagen	mammoth mandible	Conv 14C	LE-8644	N/A	25100	1000	Pitulko et al. 2014	Basilyan et al. 2011	YMAM & SP ; Standard deviation considerably big	29402-25479	95.4	27441	Accept	1_int	GI-2.2
92	Yana RHS	WB	Russia	cult.lay	collagen	mammoth mandible	Conv 14C	LE-8650	N/A	27600	600	Pitulko et al. 2014	Basilyan et al. 2011	YMAM & SP	31651-28844	95.4	30248	Accept	1_int	GI-4
92	Yana RHS	WB	Russia	cult.lay	ivory	N/A	Conv 14C	LE-8808	N/A	27700	270	Pitulko et al. 2014	Basilyan et al. 2011	between SP and Yana B	30826-29185	95.4	30006	Accept	1_int	GI-4